Holocene Relative Sea-Level Changes along the Northwest Cumbrian Coastline

Dayang Siti Maryam Binti Mohd Hanan

PhD

University of York

Environment and Geography

June 2018

ABSTRACT

Holocene relative sea-level (RSL) changes from four sites along the Cumbrian coastline have been reconstructed. A multiproxy approach including lithostratigraphical, biostratigraphical combined with radiocarbon dating, enabled the production of ten sea-level index points (SLIPs). The SLIPs constrained Holocene RSL changes in the region between 8324 cal BP and 6018 cal BP. All four sites appear to have recorded the Main Postglacial Transgression, with Allonby, Cowgate Farm and Pelutho potentially also recording the earlier glacial Lake Agassiz-Ojibway flood event. All SLIPs were corrected for post-depositional lowering using a geotechnical model. The ten SLIPs produced in this study have refined the trend of Holocene RSL changes for the coastal region situated between the southern Solway Firth and central Cumbria, a region where only four SLIPs were available prior to this study. Changes in the palaeo-tidal range in the Solway Firth were also modelled for the last 10000 year and corrections were applied to the SLIPs produced in this study, as well as for the 88 existing SLIPs from the Solway Firth allowing a comparison of these data to glacio-isostatic adjustment model predictions. Examination of the data from the northern and southern shores of the Solway Firth indicated that differential isostatic uplift had occurred in this region.

Pollen analysis was undertaken at Cowgate Farm and Herd Hill, to provide a record on vegetation and coastal changes and act as a chronostratigraphic marker when compared to the published pollen records of the region. In addition, a local, foraminifera-based transfer function was developed from three contemporary saltmarshes located on the southern Solway Firth to aid in the reconstruction of sea-level changes. However, the lack of preservation of calcareous foraminiferal species at the four study sites led to a bias in the species assemblage of the fossil data and therefore, the transfer function was deemed unreliable.

TABLE OF CONTENTS

CHAPTER 11 DISCUSSION

CHAPTER 12 CONCLUSION

LIST OF FIGURES

LIST OF TABLES

ACKNOWLEDGEMENTS

It would not have been possible for me to complete this study without the support of the many kind people around me. First and foremost, I would like to extend my sincerest gratitude to my supervisor, Dr Katherine Selby, for the continuous support, guidance and insightful comments throughout my PhD journey in York. Her guidance has helped me tremendously, both in the field and in the department.

I would also like to thank Dr Jon Hill, for his advice and encouragement, and for his contribution with the palaeo-tidal modelling. Many thanks are also extended to Dr Matthew Brain (post-depositional lowering modelling), Professor Ian Shennan (geotechnical model predictions data), Professor David Smith, Professor Robert Marchant and Associate Professor Natasha Barlow for their advice and suggestions on the research. Thank you to Laura and Lucy for proofreading the thesis, and friends who had helped with various part of the research.

To all my friends and colleagues who have braved the infamous English weather with me in the field over the years, unlucky. It is over now, although the mystery of the red knife will forever haunt us in our sleep. Their help in the field was invaluable for me. Thank you for always being so patient and good natured in the field, even at those times when everything seemed to go wrong. I would also like to extend my gratitude to the staff, colleagues and friends in the Department of Environment and Geography and in York that have helped and advised me in completing this study, and for their support rendered throughout the duration of this study. A special mention to the ladies of ENV128, we will always be the best. Thank you for all the fun and for your friendship.

And last but not least, my deepest appreciation goes out to my dearest family member for their continuous encouragement, advice and moral support which have kept me motivated throughout. I would not have made it to the end without you being on my side.

AUTHOR'S DECLARATION

I declare that the work contained and presented in this thesis is of my own original work, and I am the sole author. This work has not previously been presented for an award at this, or any other university. All sources and data obtained from other authors had been appropriately acknowledged and are listed in the references.

CHAPTER 1

CONTEXT OF THE RESEARCH

1.0 Introduction

Cumbria is located on the northwest coast of England, bordered to the north by Dumfries and Galloway in Scotland, to the west by the Irish Sea, to the south by Lancashire, to the southeast by North Yorkshire and the east by County Durham and Northumberland (Figure 1.1). The northwest region of Cumbria consists of farmed and coastal landscapes, including raised beaches, e.g. the oldest marine deposit observed adjacent to the Black Dub north of Allonby, dated at 10151-9009 cal BP (Eastwood *et al.*, 1968), lowland raised mires and bogs (e.g. Bowness Common, Wedholme Flow and Drumburgh Moss, Glasson Moss, Salta Moss), sand dunes, saltmarshes and intertidal flats at the Solway Firth and Moricambe Bay. Grune Point is the western limit of the intertidal flats and saltmarshes located in Moricambe Bay and along the southern Solway Firth. The coastal areas between Grune Point and Maryport are directly exposed to the Irish Sea, subjected to a northerly longshore drift and characterised by high energy wave and tidal activities. Sand dune systems can be found along the northwest Cumbrian coastline from Grune Point to Maryport, with the most extensive and undisturbed sand dune system situated between Wolsty Bank and Dubmill Point (Solway Coast AONB, 2010).

1.1 Climate

The coastline of northwest Cumbria located on the southern Solway Firth experiences a temperate maritime climate. The mean annual temperature varies dependent on the altitude and to some extent the proximity of the location to the coast. The low-lying areas of the Solway Lowlands and Carlisle recorded a mean annual temperature of approximately 9 °C, with an approximate 0.5 °C temperature decrease with every 100 metres increase in altitude (Met Office, 2018). Temperature in the study region located in northwest of Cumbria shows both diurnal and seasonal variation, with February the coldest month with an average minimum temperature of 0.9 °C, and the warmest month July with an average maximum temperature of 19.1 °C. The

annual rainfall recorded at Carlisle (the nearest weather station to the study area) was 1318.9 mm a^{-1}, with the highest average annual rainfall of 148.6 mm a^{-1} recorded in October, and the lowest average annual rainfall recorded in May with 77 mm a^{-1} (Met Office, 2018).

1.2 Vegetation

Areas of saltmarshes, along with relatively small but important areas of dune grasslands and heaths, cover the majority of the coastal margin of northwest Cumbria. Salt-resistant grasses including marram (*Ammophila* spp.) and sand couch (*Elymus farctus*) are common on the sand dunes, with sea spurge (*Euphorbia paralias*) and sea holly (*Eryngium maritimum*) also present, more commonly on the sheltered leeward zone. A distinct zonation is observed in the saltmarshes, with the upper marsh almost devoid of halophytic species (Walker, 1966). Most of the saltmarshes in the region have been heavily grazed by domestic livestock, which has limited the presence of the natural vegetation communities. The presence of gorse (*Ulex* spp.) is also common in the region, and is usually present at the uppermost extent of the saltmarshes.

The vegetation of the raised peat bogs is one of the only near-natural plant communities that remain in the region, although most of the raised bogs and mires have been subjected to drainage associated with agriculture or through peat cutting for fuel (Walker, 1966; Solway Coast AONB, 2010). The bogs are associated with the presence of cotton grass (*Eriophorum angustifolium*) and bog rosemary (*Andromeda polifolia*), with moss (*Sphagnum* spp.), cross-leaved heath (*Erica tetralix*), heather (*Calluna vulgaris*) and purple moor grass (*Molinia caerulea*) also noted in the drier part of the bogs forming part of the regenerating communities (Walker, 1966; Solway Coast AONB, 2010). The wetter part of the raised bogs has developed an outer margin comprised of wet birch scrub (*Betula* spp.) and willow carr (*Salix* spp.), e.g. at Glasson Moss and Bowness Common.

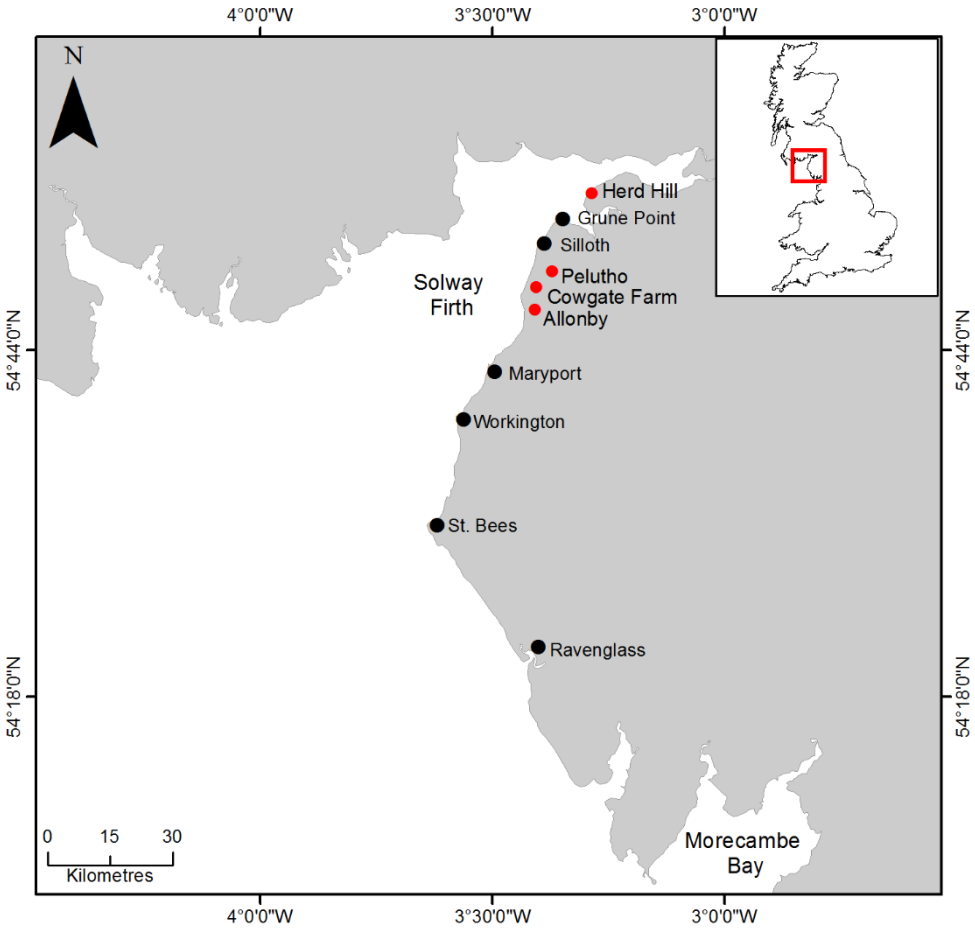

Figure 1.1: Location map of Cumbria, England with the study sites marked in red

1.3 Geology

Most of the southern Solway Firth, in particular the inner estuary, is surrounded by coastal lowlands which are comprised of unconsolidated sediments of Devensian and Holocene origins (Lloyd *et al.*, 1999; British Geological Survey, 2018). The bedrock geology along the southern Solway Firth and the northwest Cumbrian coastline is mainly made up of mudstone, siltstone, sandstone and occasional interbedded conglomerate of Permo-Triassic age (British Geological Survey, 2018). The relatively subdued relief for the areas in the inner Solway Firth is partly attributed to the underlying bedrock comprising of New Red Sandstone. In comparison, the western part of north Solway Firth is comprised of more resistant Carboniferous rocks, resulting in a rugged cliffed coastline (British Geological Survey, 2018). Glaciofluvial outwash from the Devensian ice sheet is usually present overlying the bedrock, which is then overlain by Holocene sediments (Walker, 1966; Lloyd *et al.*, 1999; British

Geological Survey, 2018). The bedrock geology for the study region and surrounding areas is shown in Figure 1.2.

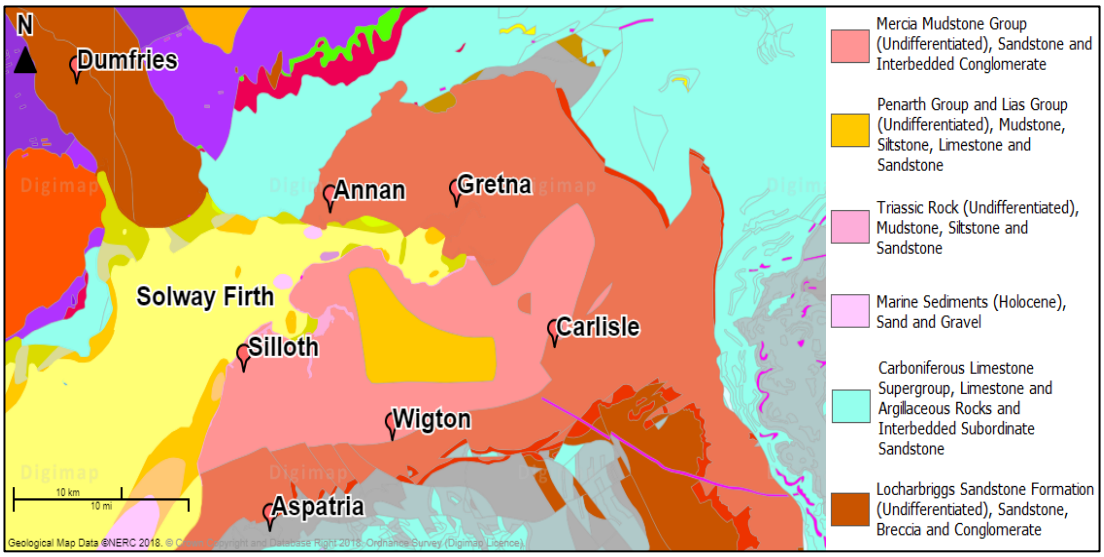

Figure 1.2: Bedrock geology of the study region and surrounding areas. Full geological key available at: http://digimap.edina.ac.uk/roam/geology. Image and key modified and adapted from Digimap (2018) (Service Layer Credit: Geological Map Data, BGS) © Crown Copyright and Database Right (2018) Ordnance Survey (Digimap Licence)

The superficial geology overlying the bedrock in the areas located close to the shores of Morecambe Bay and Solway Firth is mainly comprised of raised marine deposits of silt, clay and sand, with sand and gravel forming the sand dunes located along the coastline between Grune Point and Maryport. In some areas, peat has developed upon the glaciofluvial deposits and bedrock (British Geological Survey, 2018), as shown in Figure 1.3. Extensive saltmarshes are present on the coast of Morecambe Bay and the southern Solway Firth, with occasional relict sand bars observed in areas located behind the saltmarshes. Raised freshwater mires and bogs are also abundant on the southern shore of the Solway Firth, and this includes Bowness Common, Drumburgh Moss, Glasson Moss and Wedholme Flow.

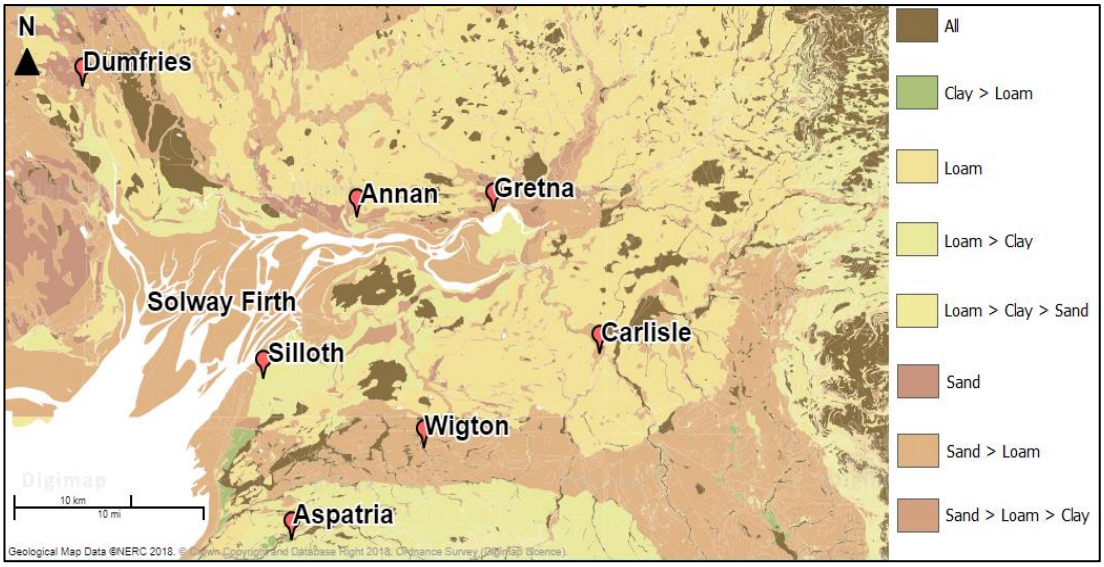

Figure 1.3: Superficial deposits of the study region and surrounding areas. Image and key modified and adapted from Digimap (2018) (Service Layer Credit: Geological Map Data, BGS) © Crown Copyright and Database Right (2018) Ordnance Survey (Digimap Licence)

1.4 Justification of the Research

Despite being one of the largest macrotidal estuarine systems in the United Kingdom, the Solway Firth, in particular its southern shore, is still relatively understudied with respect to Holocene sea-level reconstruction. Holocene relative sea-level reconstruction has been undertaken at several sites on the southern shore of the Solway Firth, namely Drumburgh Moss and Boustead Hill (Lloyd *et al.*, 1999), the raised bog of Bowness Common and Wedholme Flow (Walker, 1966; Tooley, 1974; 1978; Huddart *et al.*, 1977) and at Crosscanonby (Huddart *et al.*, 1977). The reconstruction of Late Devensian and Holocene sea level was also undertaken in the Ravenglass Estuary and sites in central Cumbria by Huddart *et al.* (1977); Tooley (1985); Auton *et al.* (1998); Balson (2010) and Lloyd *et al.* (2013). Further south in Morecambe Bay, extensive studies on the history of Late Devensian and Holocene sea level were undertaken, and these include those of Smith (1959); Oldfield (1960a, b); Oldfield and Statham (1963); Barnes (1975); Birks (1982); Tooley (1987) and Zong & Tooley (1996). However limited data is available on Holocene relative sea-level change for the area located between the southern shore of the Solway Firth and central Cumbria in particular. The only sites studied to date are Wedholme Flow and

Crosscanonby, which provided records of Holocene marine transgression and regression, and two sea-level index points from Wedholme Flow.

The Holocene sea-level record in the Solway Firth is a result of the combined effects of eustatic and isostatic changes. The region was affected by the British and Irish Ice Sheet (BIIS) during the Last Glacial Maximum (LGM) as well as the subsequent local ice re-advances centred in Scotland (Bradley *et al.*, 2011), resulting in isostatic re-adjustment and land uplift following decay of the ice mass. The relative sea-level record for the region located south of the Solway Firth in northwest Cumbria may potentially be further complicated due to the effect of the local Lake District ice mass. Therefore, different records of relative sea level between sites located on the northern and southern Solway Firth may be observed.

Previously, the study undertaken by Lloyd *et al.* (1999) have highlighted the potential differential crustal movement between the northern and southern Solway Firth, which resulted in different records of relative sea-level change between the two localities. However, the southern Solway Firth at present is still understudied compared to the northern side, particularly for the region located between the southern shore of the Solway Firth and central Cumbria, and previous research was focused on the inner part of the estuary and the raised bogs (e.g. Lloyd *et al.*, 1999). As a comparison, there are 75 sea-level index points (SLIPs) presently available along the northern coastline of the Solway Firth, with only 13 SLIPs available for the southern shore of the Solway Firth. The clear difference in number of data points available at each location may potentially lead to bias in the data when testing the variation in changes of relative sea-level between the two localities. The lack of data from a particular region may also contribute to the existing mismatch between geological field data and relative sea-level predictions produced from glacio-isostatic adjustment (GIA) models e.g. Bradley *et al.* (2011), Kuchar *et al.* (2012) and Shennan *et al.* (2018) (Edwards *et al.*, 2017).

To ascribe an indicative meaning for the calculation of SLIPs, contemporary data which acts as a representation of the fossil samples are needed. The indicative meaning of a sea-level proxy describes its relationship to elevations within the tidal frame and is comprised of a tidal datum midpoint (the reference water level) and a vertical range (the indicative range) (Horton & Edwards, 2006; Horton *et al.*, 2013).

To date, there is only one set of contemporary data available from the Solway Firth. This was obtained from the Nith Estuary located on the northern Solway Firth, which comprised of 13 contemporary samples (Horton & Edwards, 2006). No contemporary data is available from the southern Solway Firth. To enable the development of a local transfer function and also to ascribe the indicative meaning of the fossil samples obtained in this study from sites located on the southern Solway Firth, a survey of the contemporary saltmarshes located near to the palaeo study sites is crucial.

In addition, the effect of changes in palaeo-tidal range in the Solway Firth throughout the Holocene was not previously taken into consideration when calculating most of the existing 88 sea-level index points from sites located on the northern and southern coastline of the Solway Firth. If tidal range at the study sites was greater in the past, the reference water level assigned to the SLIPs would also be greater, resulting in a lower relative sea level than calculated by the SLIPs. Failing to account for the changes or increase in tidal range through time would therefore lead to an underestimation of the altitude of relative sea level during the study period (Horton *et al*., 2013). The development of numerical palaeotidal models, e.g. Hill *et al*. (2011); for the Caribbean Sea, Gulf of Mexico and western Atlantic and Hall *et al*. (2013); for Delaware Bay, USA, has resulted in the prediction of temporal tidal-range changes throughout the Holocene in the respective studies. For the United Kingdom, palaeotidal changes have been modelled for the Humber Estuary (Shennan *et al*., 2003) and the western North Sea region (Shennan *et al*., 2000). These have, and will enable, the refinement of the reference water level and the indicative range ascribed to the SLIPs produced, resulting in more precise data.

The other significant vertical uncertainties that should be quantified is the effect of post-depositional lowering of sediments. SLIPs obtained from intercalated samples are most likely to have been subjected to post-depositional compaction, and this should be quantified to provide the most accurate sea-level reconstruction (Shennan & Horton, 2002; Edwards, 2006; Massey *et al*., 2006; Horton & Shennan, 2009; Brain *et al*., 2011; 2012; 2015; Horton *et al*., 2013; Barlow *et al*., 2013; Brain, 2016).

The overall aim of this research is therefore to reconstruct Holocene relative sea-level changes obtained through detailed lithostratigraphical and biostratigraphical analyses and interpretation of data obtained from four sites located on the currently

understudied southern shore of the Solway Firth. The correction of changes in the palaeo-tidal range in the Solway Firth will also be incorporated in the calculation of SLIPs produced in this study, along with the presently available SLIPs from the region. This will ultimately contribute and lead to the improvement of the whole dataset available for the region, and allow investigation of the variation in relative sea-level changes between the northern and southern Solway Firth and therefore the drivers of these changes.

1.5 Objectives of the Research

Several objectives were identified in this study:

1. To generate SLIPs from sites located along the currently understudied southern shore of the Solway Firth

2. To define the timing of sea-level and broader environmental changes recorded at each site using microfossil analyses and radiocarbon dating

3. To establish the contemporary distribution of foraminifera from three saltmarshes located in the study region

4. To examine, and correct for palaeo-tidal changes of the SLIPs produced in this study, and the ones that currently exist for the northern and southern Solway Firth

5. To compare the corrected SLIPs with relative sea-level values produced from glacio-isostatic models

1.6 Location of the Study Sites

Three coastal sites at Allonby (NY 0949 4410), Cowgate Farm (NY 0967 4737), Pelutho (NY 1202 4920), and one inner estuary site at Herd Hill (NY 1794 6010) were investigated in this study (Figure 1.1). Pasture House (NY 1861 6030) was included to provide additional geomorphological information of the area around Herd Hill. Several other sites were also visited and sampled, however after initial analyses these

sites were deemed unsuitable for further study (discussed in Chapter 3; Section 3.1.1). The selection of the coastal and inner estuary sites was intended to identify and compare different coastal settings as well as Holocene relative sea-level changes.

1.7 Structure of the Thesis

Chapter 1 presents an introduction to the environment in the study region located on the southern shore of the Solway Firth and outlines the main hypothesis and objectives of the research. **Chapter 2** is a literature review which summarises the glacial history and relative sea level changes in the study region. An overview of the regional vegetation history, along with the methods and techniques used for the reconstruction of relative sea level are also presented. **Chapter 3** outlines the specific methods and techniques used in this study.

The research on the contemporary foraminifera and saltmarsh environment located along the coast of Moricambe Bay and southern Solway Firth is presented in **Chapter 4**. The main aim of this chapter is to define the distribution of modern foraminifera from contemporary intertidal and saltmarsh environments, which can then be used to aid in the interpretation of the fossil records observed at each site.

The findings and results obtained from each of the sites investigated in this study are presented in **Chapter 5** (Allonby), **Chapter 6** (Cowgate Farm), **Chapter 7** (Pelutho), **Chapter 8** (Herd Hill) and **Chapter 9** (Pasture House). The results presented include lithostratigraphical work, altitudinal data from the boreholes records and from the sample cores, loss on ignition and particle size analyses, microfossil analyses and interpretation, the chronology and the development of the SLIPs. Post-depositional correction for each SLIPs are also presented in each of the result chapters.

All SLIPs produced in this study, along with the existing SLIPs available from the northern and southern Solway Firth are corrected for palaeotidal changes in **Chapter 10**.

Chapter 11 presents a critique of the methods used to reconstruct sea-level changes including an assessment of the contemporary foraminiferal and saltmarsh

environments investigated. A review of the methods and techniques used to reconstruct Holocene relative sea-level changes in the study area are also discussed. This chapter also combines the results obtained from the four main sites and summarises the Holocene relative sea-level changes of the region. The SLIPs prior to, and after, the correction of changes in palaeo-tidal changes plotted separately against relative sea-level predictions obtained from different geophysical models, to highlight the importance of correcting for palaeo-tidal changes are then presented. Data produced in this study along with the existing SLIPs from the southern Solway Firth was compared to reconstructions from the northern Solway Firth, enabling the identification of variations of relative sea-level records between the two localities. A review on the palaeogeography of the Solway Firth from 10 ka BP to 1 ka BP is also presented in this chapter.

The main conclusions of this study are outlined in **Chapter 12**, highlighting the contributions and wider implications of this research. Recommendations for potential future work on Holocene relative sea level in the area is also considered.

1.8 Summary

This chapter introduced the background and justification of the research, along with the identification of the research aims and objectives. A summary of the thesis structure was also presented.

CHAPTER 2

LITERATURE REVIEW

2.0 Introduction

This chapter summarises the glacial and relative sea-level history of the United Kingdom and specifically that of the study region in Cumbria. An overview of the Holocene relative sea-level changes in the Solway Firth is presented, and set within the broader context of Holocene relative sea-level changes along the coast of England. The Solway Firth coastline was affected by ice growth and decay during the Devensian that resulted in relative sea-level changes in the region. A summary of the available literature on the vegetation history of Cumbria for the Devensian and Holocene is also presented in this chapter. Finally, the methods and techniques that can be utilised in the reconstruction and interpretation of relative sea-level changes are described.

2.1 Summary of the Glacial History of the United Kingdom

The British and Irish Ice Sheet (BIIS) was a long-lived feature that existed throughout most of the last glacial period, with records of glacial advances evidenced through dating of glacial boulders and glaciated surfaces, covering most of the British Isles and the surrounding continental shelf (Clark *et al.*, 2018). The most recent glacial advance, the Devensian, reached its maximum at approximately 23 to 21 ka BP (Clark *et al.*, 2018; Figure 2.1) and was reported to have lasted until approximately 13 ka BP in Scotland (Bradley *et al.*, 2011) as shown in Figure 2.2.

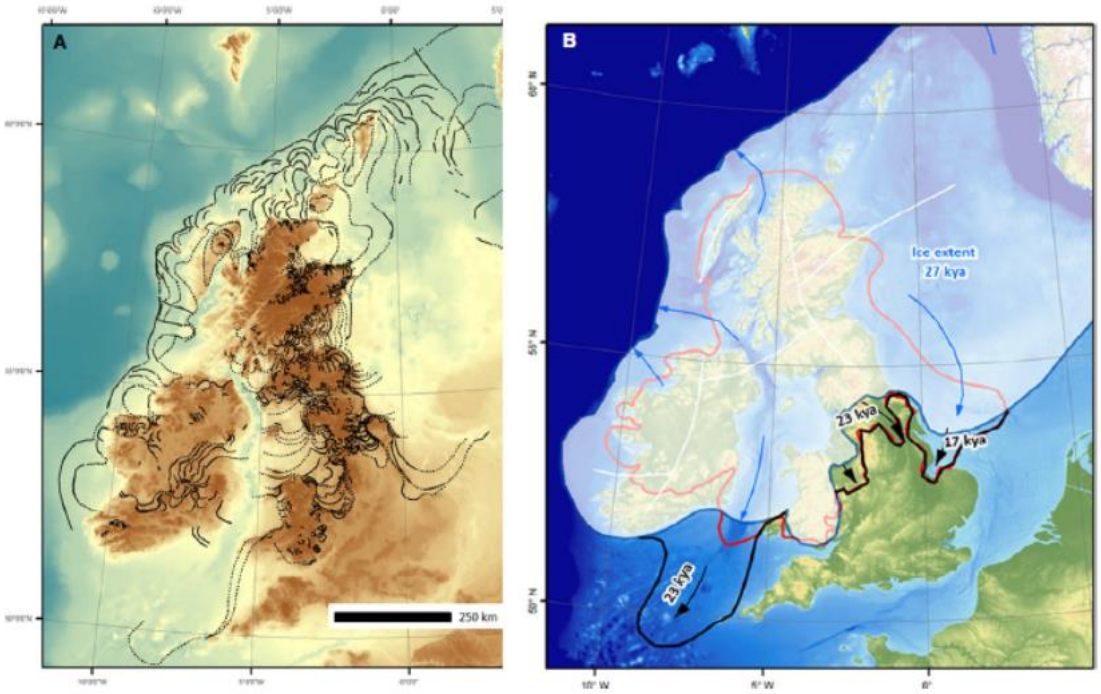

(a) (b)

Figure 2.1: (a) Reconstructions of the retreat pattern of the BIIS adapted from Clark *et al*. (2012) in Clark *et al*. (2018) which includes meltwater channels, eskers, moraines and subglacial bedforms (b) Maximum extent of the different sectors of BIIS with dates adapted from Clark *et al*. (2012). Red line is the long-standing view of a more restricted extent of the ice mass, white-shaded area is the extent at 27 ka BP and black lines are the subsequent advances in the southern margin of the BIIS (Clark *et al*., 2018)

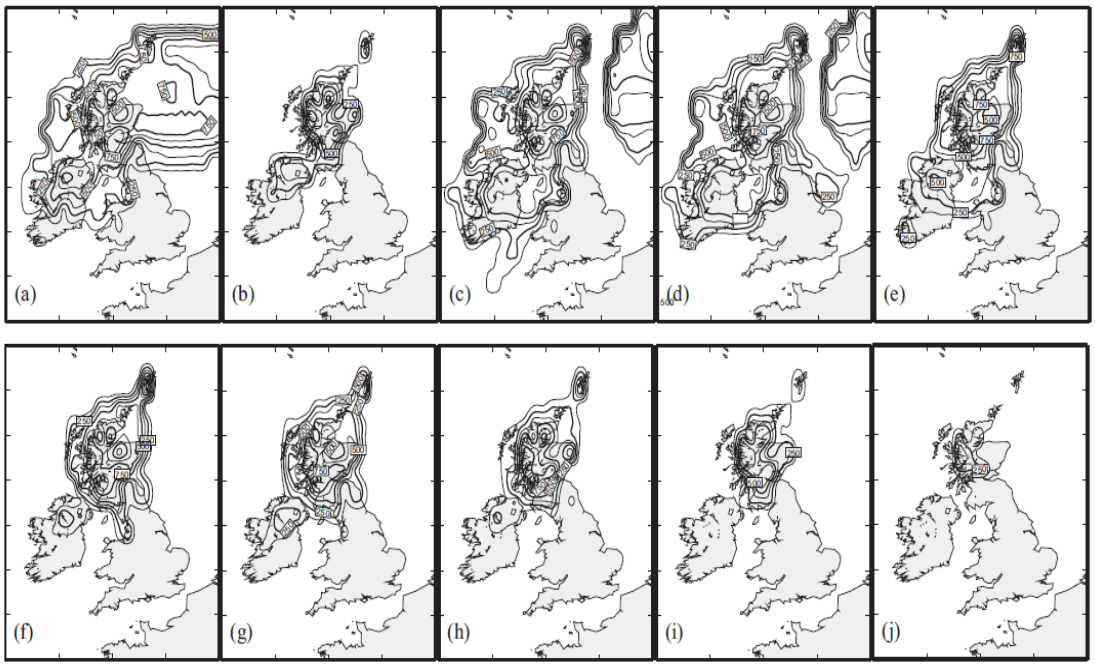

Figure 2.2: Maps showing the extent and thickness of the BIIS model (Bradley *et al.*, 2011). (a) 32 ka BP (b) 26 ka BP (c) 24 ka BP (d) 21 ka BP (e) 20 ka BP (f) 19 ka BP (g) 18 ka BP (h) 17 ka BP (i) 16 ka BP and (j) 13 ka BP

It was inferred that the BIIS and Scandinavian Ice Sheet (SIS) were confluent at least on two occasions in the North Sea during the Devensian, with the period of maximum confluence occurring at approximately 34.2 to 29.3 ka BP. This was later followed by an extensive period of large ice sheet reorganisation (Ehlers and Wingfield, 1991; Bowen *et al.*, 2002; Carr *et al.*, 2006). Bradwell *et al.* (2008) concluded that the zone of contact between BIIS and SIS probably occurred across the north of the Orkney Islands, Scotland, and that the SIS was reported to have confined the BIIS during the Dimlington Stadial in the Late Devensian (Davies, 2008). At 22 ka BP, the BIIS and SIS were no longer in contact with each other (Bowen *et al.*, 2002), and this is in agreement with the model developed by Bradley *et al.* (2011) which illustrated that the BIIS and the SIS were confluent between 32 to 27 ka BP.

An initial pulse of deglaciation of the BIIS was recorded at approximately 22.7 ka BP and the collapse of the BIIS across northern Britain started at approximately 20.6 ka BP (Bowen *et al.*, 2002; Clark *et al.*, 2012). This was followed by an extensive deglaciation at approximately 17.8 ka BP (Bowen *et al.*, 2002) although Bradley *et al.* (2011) modelled the deglaciation to have started at approximately 20 ka BP, with a

rapid thinning and retreat of the Irish Ice sheet starting at 19 ka BP (Figure 2.2). The Irish Ice Sheet re-advanced across Northern Ireland to record the 'Killard point stadial' starting from approximately 17 ka BP, with complete ice retreat from Ireland recorded by approximately 16.5 to 16 ka BP (Bradley *et al*., 2011, Finlayson *et al*., 2014).

Retreat of the BIIS occurred from a number of different and separate ice caps, rather than reduction from a single mass (Clark *et al*., 2012; 2018). At 27.5 ka BP, the ice sheet retreated along the northern boundaries of the BIIS. At the same time the southern margins began to expand, including transient ice streaming down the Irish Sea and expansion of ice domes in the Vale of York, Cheshire Basin and east coast of England. At 23.1 ka BP, the BIIS deteriorated with major and widespread loss of marine based ice, especially in the Irish Sea and North Sea. At 20.6 ka BP, the final collapse of all marine based ice occurred, and most marine margins started to retreat onshore. Although not confirmed, the North Sea 'ice bridge' that connected Britain and Norway was speculated to disintegrate at approximately 20.6 ka BP (Clark *et al*., 2012), however this bridge was already absent at 26 ka BP in the model developed by Bradley *et al*. (2011). At 19.5 ka BP, the Irish Sea and North Channel ice streams cleaved the ice sheet into two separate sheets comprising the Irish ice sheet and Scottish ice sheet (Clark *et al*., 2012).

Several smaller scale ice growths and re-advances have been recorded in Scotland. This includes the Perth re-advance and the Wester Ross re-advance that occurred approximately between 15 to 13 ka BP during the Late Glacial (Sissons *et al*., 1966; Sissons, 1967; Robinson & Ballantyne, 1979; Ballantyne, 1986; Everest *et al*., 2006; Ballantyne & Stone, 2009; Ballantyne, 2010). The ice re-advance during the Loch Lomond Stadial was also localised and occurred between 15.4 to 13.4 ka BP, e.g. at sites studied in the Outer Hebrides, the North-West Highlands, Orkney, Caithness and Buchan (Wilson *et al*., 2002; Ballantyne, 2010), with the final deglaciation occurring sometime after 11.7 ka BP when climate warmed at the start of the Holocene (Lowe *et al*., 2008; Walker *et al*., 2009).

2.2 Summary of the Glacial History of Cumbria

During the Devensian maximum that occurred approximately 23 to 21 ka BP, the northwest of England was covered in ice originating from the Lake District and Scotland (Delaney, 2003; Bradley *et al*., 2011; Clark *et al*., 2012; 2018). The Solway Lowlands, Stainmore, Vale of Eden and the Tyne Gap regions were located at the centre of the BIIS, and therefore were highly affected by the complex interactions between several upland ice dispersal centres, such as the Lake District, north Pennines and Southern Uplands. The Solway Lowlands in Cumbria were also affected by ice divides, and the migration and impact of the Irish Sea and Tyne Gap ice streams (Livingston *et al*., 2008; 2012) (Figure 2.3).

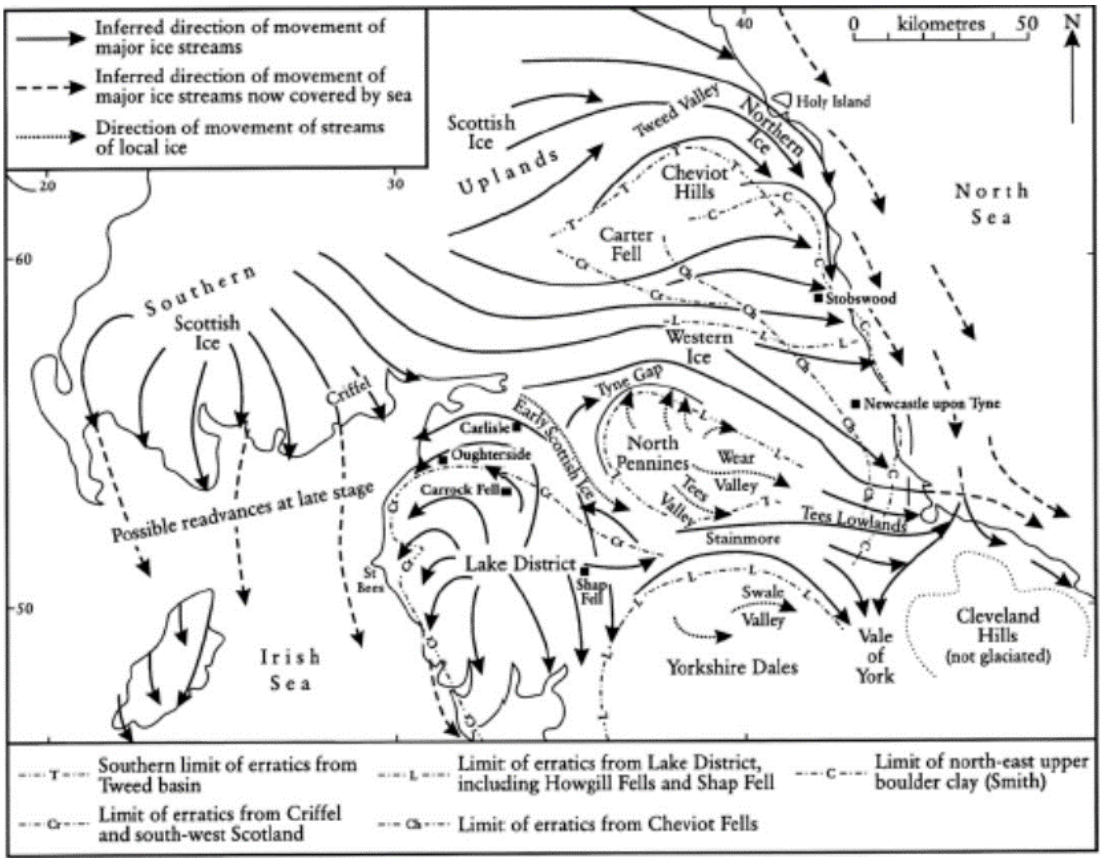

Figure 2.3: Map showing generalised ice flow directions in northern England and southern Scotland (from Livingstone *et al*., 2012)

Research undertaken on Scottish ice re-advances in the Solway Lowlands was summarised in Livingstone *et al*. (2010), and is described briefly here. Site locations mentioned in this section are shown in Figure 2.4 The first evidence to support a

glacial re-advance into the Solway Lowlands comprising of a thin upper till horizon overlying a series of sands and laminated clays horizons was presented by Trotter (1922; 1923; 1929). These minerogenic units were comprised of the Scottish erratics identified in Dixon *et al*. (1926) and Trotter & Hollingworth (1932). Several eskers which were believed to have flowed in a northwest to southeast direction were identified at Thursby, Cummertrees and Gretna (Figure 2.3), with outwash deltas deposited in association with the esker formation at Gretna further supporting a Scottish glacial re-advance into the area (Dixon *et al*., 1926; Charlesworth, 1926; Trotter, 1929).

The ice limit from the Scottish re-advance reached as far as Lanercost, Brampton and Cumwhitton in the east and Foulbridge and Bolton Low Houses in the south (Trotter, 1929). At the maximum extent of the Scottish re-advance, Lake Carlisle and Lake Lyne formed against the reverse slope of the Tyne Gap, and water drained in an eastward direction via the Gilsland meltwater channel. When ice retreated westwards, Lake Caldew formed initially, followed by the development of Lake Wigton. Meltwater escaped westwards as ice retreated via overspill channels which flowed into the lakes, depositing a series of deltas (Trotter, 1929).

Re-evaluation of the Scottish ice re-advance into the Solway Lowlands was undertaken by Huddart (1970; 1971a; 1971b; 1991; 1994), Huddart & Tooley (1972), Huddart *et al*., (1977) and Huddart & Glasser (2002). Huddart (1970) stated that the Scottish ice did not extend far beyond Carlisle, and most of the stratigraphic evidence previously presented by Trotter (1922; 1923; 1929) was patchy or could instead be re-interpreted as debris flow deposits. Huddart (1970; 1991; 1994) also stated that the Scottish re-advance limits were most likely defined by the esker deposits at Thursby, a thin upper till located west of Carlisle and a major glaciofluvial deltaic complex found at Holme St Cuthbert. The St Bees push moraine situated on the west Cumbrian coastline was attributed to have originated from the Scottish re-advance as reported by Huddart (1994) and Merritt & Auton (2000).

Fluctuations of small radially flowing ice caps occurred before 34.2 ka BP in the Lake District. At approximately 23.6 ka BP the Lake District ice sheet grew, producing a triangular and elongated dome over northwest England and southwest Scotland during the Devensian. During the recession which happened after 22.5 ka BP, a

complex pattern of significant ice flow developed, switching directions over a relatively short period (Evans *et al.*, 2009). The central sector of the BIIS became a major dispersal centre for the duration of 2500 years after the Devensian. The ice sheet that developed over Cumbria had no stable or steady state, and was made up mainly of constantly moving ice divides and dispersal centres. The subglacial streamlining that occurred was also completed over a short period of time, with flow reversals happening in less than 300 years (Evans *et al.*, 2009).

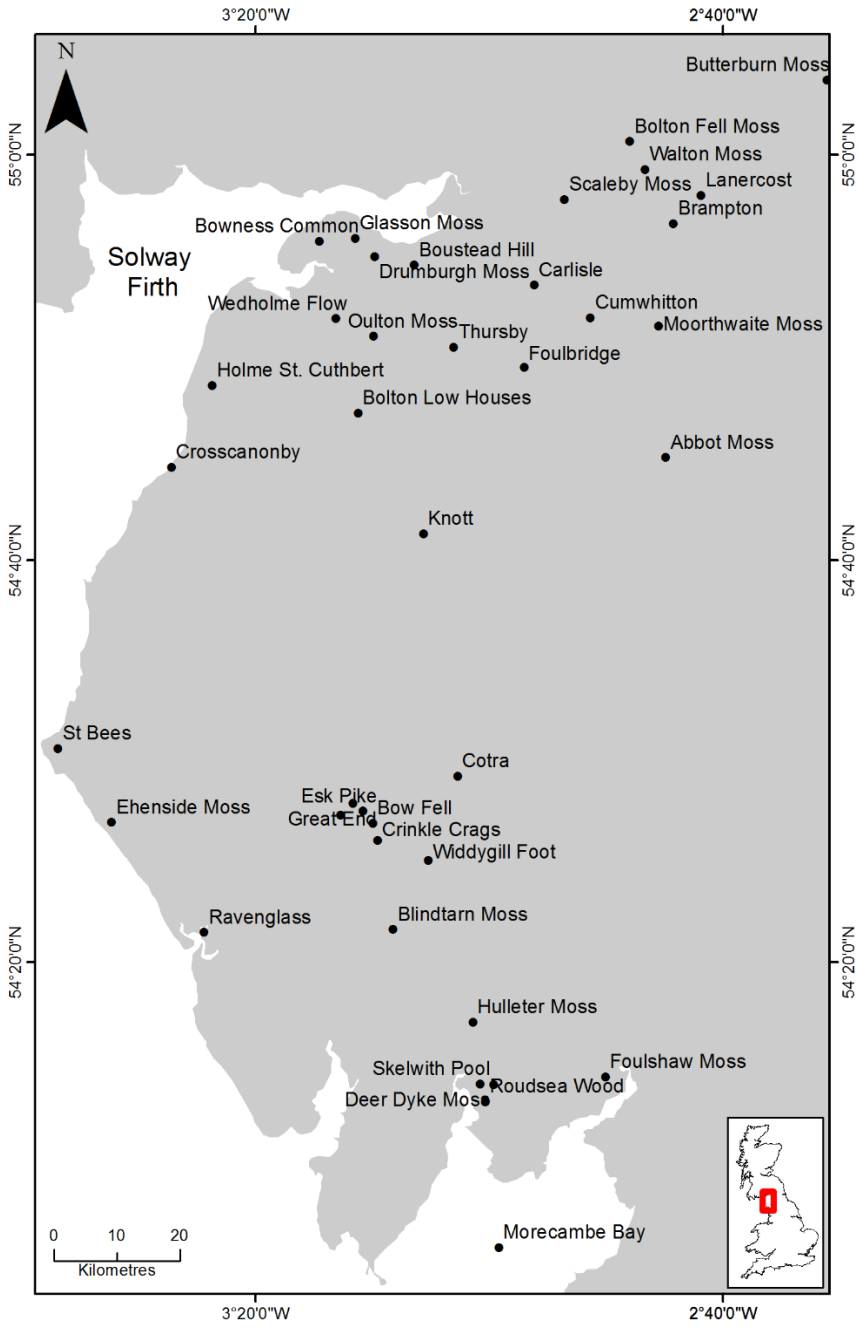

Figure 2.4: Location map of areas in Cumbria mentioned in the text

Ballantyne *et al*. (2009) suggested that an independent ice dispersal centre formed in the Lake District during the Devensian, based on the distribution of Borrowdale Volcanic erratics, absence of allochthonous erratics and the orientation of striae in the Lake District's mountains. Based on the evidence, it was suggested that the Lake District ice dome deflected ice moving south from Scotland towards two areas: further south into the Irish Sea basin and eastward into northern England (Ballantyne *et al*., 2009; Livingstone *et al*., 2012), as illustrated in Figure 2.3.

Cosmogenic ^{36}Cl exposure dating showed that the summit plateau of Scafell Pike (at 978 metres above sea level) in the southwest of Lake District escaped ice erosion during the Devensian. Ice moulded bedrock on an adjacent col (at 750-765 metres, exposure age of 24 to 18.6 ka BP) confirmed erosion and over-riding of bedrock by warm based Devensian ice, consistent with other high-level sites in the British Isles (Ballantyne *et al*., 2009). This suggests substantial (although not complete) retreat of the BIIS at approximately 20.6 ka BP. Ballantyne *et al*. (2009) also suggested that the final stage of local glaciation in the Lake District occurred during the Loch Lomond Stadial at approximately 15.6-13.6 ka BP, based on an exposure age of 17.3 to 13.0 ka BP which was obtained from a glacially transported rockfall boulder within the limits of later corrie glaciation.

The glacial geomorphology of the southwest Lake District was mapped by Brown *et al*. (2011; 2013). It was assumed that Upper Eskdale located in the southwest Lake District, did not nourish ice during the Younger Dryas prior to the mapping done by Brown *et al*. (2011). The authors however concluded that this was unlikely to be true as Upper Eskdale is one of the highest elevation cirques (valley formed by glacial erosion). The eastern part of the Scafell Pike range in the Lake District was inundated by ice during the Younger Dryas, which then supplied ice to the major part of the Upper Eskdale valley. This would therefore explain the lack of moraines within and around the Upper Eskdale, which would have been more evident when ice was confined within the cirques themselves rather than spread down-valley from Scafell Pike (Brown *et al*., 2011; 2013).

Lamb and Ballantyne (1998) suggested that Late Devensian glacial ice crossed the high ridges linking Crinkle Crags (859 metres), Esk Pike (885 metres), Great End (910 metres) and Bow Fell (902 metres). Only small areas around Bow Fell, Esk Pike and

Great End were free of evidence of Late Devensian glaciation. The high-level striae and roches mountonnées in these areas confirmed that the lower zones of peaks and cols were over-run by ice that moved westwards or south-westwards, which is consistent with the movement of ice away from the ice-free domes located in the central Lake District (Lamb and Ballantyne, 1998). Clark (1999) echoed the findings of Lamb and Ballantyne (1998) and stated that the area around Great End was free from ice cover, including the top of Scafell Pike. The top of Great Gable (height of 899 metres) was also identified to have escaped ice cover during the Devensian. It was also concluded that the ice in Lake District moved west and southwest during its retreat (Clark, 1999, Clark *et al.*, 2018).

Lamb and Ballantyne (1998) reported that the mountains in the southwest of the Lake District have a high weathering limit separating the upper zone of shattered blockfields, bedrock and tors from the lower zone of bedrock moulded by glaciers, with the weathering limit declining from approximately 870 metres (on the eastern side) and approximately 800-830 metres (on the north-western side). The weathering limit represents the approximate altitude of the last BIIS surface at its maximum thickness. The maximum BIIS surface altitude based on these ridges is estimated to be approximately 870 m OD adjacent to the Bow Fell summit, and about approximately 830 m OD near Scafell Pike (Clark, 1999).

At Widdygill Foot, Blindtarn Moss and Cotra which are located in the south-central Lake District, moraine ridges and mounds have been mapped and based on their location and morphology, were found to have been formed during the Loch Lomond Stadial. Patterns of moraines at all sites showed that the Lake District glaciers underwent active retreat of 0.2-0.8 km occurring approximately between 19.5 to 16.8 ka BP, suggesting that glaciation during the subsequent Loch Lomond Stadial in the Lake District was more extensive than previously accepted (Wilson, 2002; 2004). Although the moraines were not dated, patterns of moraine ridges show that ice-removal from the valley during the Loch Lomond Stadial involved active retreat or stillstands and possible re-advances rather than in-situ decay (Wilson, 2004; Livingston *et al.*, 2012).

McDougall (2001) also presented evidence of the development of plateau icefields in the central fells of the Lake District during the Loch Lomond Stadial, which occurred at approximately 15.4 to 13.4 ka BP (Wilson *et al.*, 2002; Ballantyne, 2010). The largest was centred on High Raise and covered an area of approximately 55 km^2 including the outlet glaciers. To the west of High Raise fell, smaller plateau icefields were found on Grey Knotts/Brandreth and Dale Head, covering 7 km^2 and 3 km^2 respectively. Debris that accumulated in the hills at the centre of Knott in the northern Lake District resulted from glacial deposition during the Loch Lomond Stadial (Wilson and Clark, 1999).

More recently, Livingstone *et al.* (2012) suggested that there were six stages of glacial advance in the central sector of the last BIIS, affecting the areas in Cumbria. These consisted of: (i) eastward flow through the north Pennines; (ii) termination of Stainmore ice flow pathway and migration of the North Irish Sea basin ice divide; (iii) cessation and retreat of Tyne Gap ice stream; (iv) Blackhall Wood-Gosforth Oscillation which occurred at approximately 23.7 ka BP; (v) Solway Lowland ice deglaciation; (vi) the re-advance of Scottish ice, prior to the final retreat of ice out of the central sector of BIIS. The last phase of ice deglaciation then occurred between approximately 16.5 ka BP to 8.2 ka BP (Bradley *et al.*, 2011).

2.3 Sea-Level Change

Relative sea-level change is a result of various contributing factors at a global, regional and local spatial scales, which can be driven by either variations in volume of the ocean (i.e. eustatic changes) or through changes of the land with respect to the surface of the sea (i.e. isostatic changes) at varying temporal scales (Gehrels & Long, 2008; Rovere *et al.*, 2016). Factors contributing to changes in sea level include melting of land-based ice (e.g. polar ice sheets, ice caps and mountain glaciers), thermal expansion or contraction of the upper layer of the ocean, ocean siphoning (where equatorial ocean water flows towards the collapsing forebulges of the mid and high latitudes) and continental levering (rebound of the coast as a result of water loading in continental shelf) (Gehrels & Long, 2008; Mitrovica & Milne, 2003).

More local factors contributing to sea-level change includes changes in tidal range in an area (i.e. which may lead to changes in height and impact of storm waves, storm

surges and height of high tides), sediment compaction, tectonic processes (e.g. earthquakes; Hamilton and Shennan (2005)) and the vertical land movement in response to unloading of ice masses, referred to as glacio-isostatic adjustment (GIA) of the land (Gehrels & Long, 2008; Shennan *et al.*, 2012).

Relative sea level can be defined as the change in sea relative to the land at a given location, as a result of the combined eustatic, isostatic, tectonic and other local factors (Shennan *et al.*, 2012). Shennan *et al.* (2012) expressed the change in relative sea level (ΔRSL) of a specific geographical location (ϕ), at time t, where t is the time relative to present, as:

$$\Delta RSL = \Delta EUS(t) + \Delta ISO(\phi,t) + \Delta TECT(\phi,t) + \Delta LOCAL(\phi,t) + \Delta UNSP(\phi,t)$$

Where $\Delta EUS(t)$ is the time-dependent eustatic sea level as a result of meltwater distribution; $\Delta ISO(\phi,t)$ is the total isostatic effect (glacio-isostatic and hydro-isostatic) and rotational contributions of ocean mass redistribution; $\Delta TECT(\phi,t)$ is the tectonic effect (although deemed negligible in the British Isles during the Holocene); $\Delta LOCAL(\phi,t)$ is the total effect of local processes within the coastal system of the location (a combined effect of changes in tidal regime, $\Delta TIDE(\phi,t)$ and sediment elevation, $\Delta SED(\phi,t)$); and $\Delta UNSP(\phi,t)$ is the total unspecified factors (Shennan *et al.*, 2012).

2.3.1 Abrupt Eustatic Sea-Level Rise and the 8.2 ka Event

Eustatic sea-level changes occur at a global scale and are caused by processes that alter the volume or mass of the world's ocean (Fleming *et al.*, 1998; Shennan *et al.*, 2012; Rovere *et al.*, 2016). The mass of the ocean can change due to the melting or accumulation of continental ice sheets over time (glacio-eustasy) and as a result of water moving between different reservoirs (hydro-eustasy). Changes in volume of the world ocean are due to variations in ocean water density and changes in salinity. Changes in the volume of ocean basins can also cause eustatic sea-level changes (e.g. tectono-eustasy). Eustatic sea-level changes can vary temporally and although usually defined as the change in sea level that has occurred in a uniform manner globally, the loading and unloading of water mass and volume over time leads to deformation, gravitational and rotational disturbances of the solid Earth leading to spatial variations in eustatic sea-level changes (Rovere *et al.*, 2016).

At approximately 21 ka BP, during the Devensian glaciation eustatic sea-level minimum of approximately 130-135 m was recorded as ice cover was at its maximum (Fleming *et al.*, 1998; Peltier, 2002; Clark *et al.*, 2018). A rapid rate of sea-level rise followed the Devensian deglaciation, with two episodes of further sea-level rise accelerations recorded at approximately 14 and 11.5 ka BP, which were assumed to reflect the increased rates of global ice melt during those periods. The event at 14 ka BP is known as the meltwater pulse (MWP) 1a, with the less pronounced sea-level rise acceleration at 11.5 ka BP associated with the MWP 1b (Alley *et al.*, 2005; Peltier, 2005).

The rate of Holocene eustatic sea-level rise then decreased significantly after 5 ka BP, as continental ice sheets have melted to small residuals remnants. Eustatic sea-level then broadly stabilised between the periods of 3 to 2 ka BP (IPCC, 2007). During the late Holocene, eustatic sea-level may have fallen slightly as a result of ocean siphoning, but the process has been reversed in more recent centuries, where sea level rose again from the early 1800s as a result of anthropogenic activities. Data from the east coast of the USA provided evidence of an eustatic sea-level rise of approximately 1.7 mm a^{-1} in the twentieth century (Gehrels *et al.*, 2004; 2006; Engelhart *et al.*, 2011).

Sea-level fingerprinting can be defined as the attribution of past episodes of sea-level rise to meltwater sources that were constrained spatially (Kendall *et al.*, 2008; Törnqvist & Hijma, 2012). As an ice sheet melts, the meltwater is distributed in a distinct pattern known as a 'fingerprint' (Kendall *et al.*, 2008; Törnqvist & Hijma, 2012). This unique signature results from the gravitational pull that ice sheets and glaciers have on the water that surrounds them, increasing sea level on the peripheries. Upon deglaciation, the gravitational pull decreases and sea level falls. This change in the gravitational field of the earth results in a movement of water away from the ice sheets and the sea-level rise caused by this movement is known as the sea-level fingerprint (Hay *et al.*, 2017), e.g. the input of freshwater following the decay of the glacial Lakes Agassiz-Ojibway in North America.

A brief and rapid episode of marine transgression and increased relative sea level as a result of the discharge of Lakes Agassiz-Ojibway in North America due to the collapse of the Laurentide Ice Sheet (LIS), has been increasingly recognised in stratigraphic sequences from a number of locations. It was reported that the collapse of the LIS discharged more than 10^{14} m^3 of fresh water into the Labrador Sea, resulting in a significant reduction in the sea surface salinity and temperature (Barber *et al.*, 1999; Li *et al.*, 2012). This event occurred at approximately 8470 to 8000 cal BP (Barber *et al.*, 1999; Törnqvist & Hijma, 2012), and the massive input of freshwater altered the ocean's circulation and led to a cooling event at 8200 BP with a significant drop in temperature recorded in Greenland and the North Atlantic Ocean (Barber *et al.*, 1999).

Several researches have potentially recorded the marine transgression resulting from the drainage of Lakes Agassiz-Ojibway (e.g. Long *et al.*, 2006; Turney & Brown, 2007; Yu *et al.*, 2007; Kendall *et al.*, 2008; Hijma & Cohen, 2010; Li *et al.*, 2012; Törnqvist & Hijma, 2012; Selby & Smith, 2016). An increase in sea level occurring between 8310 to 8180 cal BP in the Mississippi Delta attributed to the final drainage of proglacial Lake Agassiz–Ojibway was documented by Li *et al.* (2012), and Yu *et al.* (2007) reported a later increased sea level at approximately 7600 cal BP on the southeastern Swedish Baltic coast, also attributed to the collapse of the ice sheet. At Talisker Bay, Isle of Skye, a marine transgression was recorded between 8373 to 7793 cal BP, and was suggested to have potentially resulted from the Lake Agassiz-Ojibway flood (Selby & Smith, 2016).

Jennings *et al*. (2015) developed a detailed history of the timing of ice-sheet discharge events from the Hudson Strait outlet of the LIS throughout the Holocene, which included events associated with the drainage of Lake Agassiz-Ojibway. Based on the stratigraphic evidence and the modelled ages of Hudson Strait/Bay deglaciation events, the authors identified three separate episodes associated with the 8.2 ka cooling, the retreat of Hudson Strait ice stream, the opening of the Tyrell Sea and the drainage of the glacial lakes Agassiz and Ojibway, which have been combined in previous estimates (Jennings *et al*., 2015).

Research undertaken by Hijma & Cohen (2010) in the Rhine-Meuse Delta, Netherlands, Li *et al*. (2012) in the Mississippi Delta, USA and by Smith *et al*. (2013) in the Ythan Estuary, United Kingdom provides three well-dated relative sea-level records (through dating of basal peat samples) which have captured the sea-level jump prior to the 8.2 ka event. An eustatic sea-level jump of 3.0 ± 1.5 m at 8590-8350 cal BP and 1.2 ± 0.2 m at 8310-8180 cal BP was recorded at Rhine-Meuse Delta (Hijma & Cohen, 2010) and Mississippi Delta (Li *et al*., 2012) respectively. Based on the differences in timing and magnitude at the two sites, it was suggested that the Rhine-Meuse Delta sea-level jump contained two separate events while the data from Mississippi Delta captured only a final event relating to the lake drainage (Hijma & Cohen, 2010; Li *et al*., 2012). In the Ythan Estuary a single jump between 2.56 m and 4.77 m was recorded, dated between 8366-8177 cal BP and 8637-8445 cal BP (2σ ranges) (Smith *et al*., 2013).

The studies in the Rhine-Meuse Delta, Mississippi Delta and Ythan Estuary therefore lacked lithostratigraphic and biostratigraphic evidence of more than one sea-level jump in a continuous stratigraphic sequence. The data obtained from these three studies are unable to illustrate and test the three-stage meltwater model presented in Jennings *et al*. (2015) associated with the drainage of the glacial lakes and the other two events (Lawrence *et al*., 2016).

Evidence of abrupt sea-level rise as a result of the Lake Agassiz-Ojibway drainage was obtained from the Cree Estuary, located in southwest Scotland on the northern shore of the Solway Firth (Lawrence *et al*., 2016). The authors presented a stratigraphically continuous record of relative sea level in the Cree Estuary, which was not evidenced in the studies undertaken by Hijma & Cohen (2010), Li *et al*. (2012)

and Smith *et al*. (2013). The study in the Cree Estuary recorded three accelerations in the rate of relative sea-level rise based on lithostratigraphic and biostratigraphic evidence, which occurred between 8760-8640 cal BP (sea-level jump of 0.24 to 0.45 m), between 8595-8465 cal BP (0.67 to 0.73 m) and a final event recorded between 8320-8235 cal BP (0.37 to 0.43 m) (Lawrence *et al*., 2016).

It is possible that the sites studied in this research may have the potential to record a sea-level rise associated with the Lake Agassiz-Ojibway drainage based on the study conducted in the Cree Estuary (Lawrence *et al*., 2016).

2.4 Relative Sea-Level History of the United Kingdom

The United Kingdom has been the focus of much Quaternary sea-level research over the years, resulting in many reconstructions of Late Devensian and Holocene relative sea-level changes. The relative sea-level history of the United Kingdom in the Late Devensian and Holocene is highly complex and variable due to the differences in isostatic rebound associated with the spatial and temporal changes of the Devensian glaciation (Peltier, 1998; Shennan & Horton, 2002; Shennan *et al*., 2000; 2006; 2012; Lowe & Walker, 2015). The variation in glacial and hydro isostasy experienced along the coastline of United Kingdom was attributed mainly to the presence of ice centred in the north, with most of southern Britain ice free during the Devensian (Evans *et al*., 2009; Clark *et al*., 2012; Bradley *et al*., 2011). Areas located closer to the centre of the ice mass across Scotland would have generally experienced relative land uplift, with land areas further away from the centre of the ice mass experiencing subsidence (Figure 2.5), as shown by field evidence and GIA models (e.g. Shennan *et al*., 2012; 2018). The GIA model of Shennan *et al*. (2012) included two key inputs, which comprised of a Late Quaternary ice model from approximately 120 ka BP and an Earth model that was utilised to reproduce the solid Earth deformation that had resulted from surface mass redistribution between the ocean and ice sheets, resulting in the prediction of relative sea-level changes.

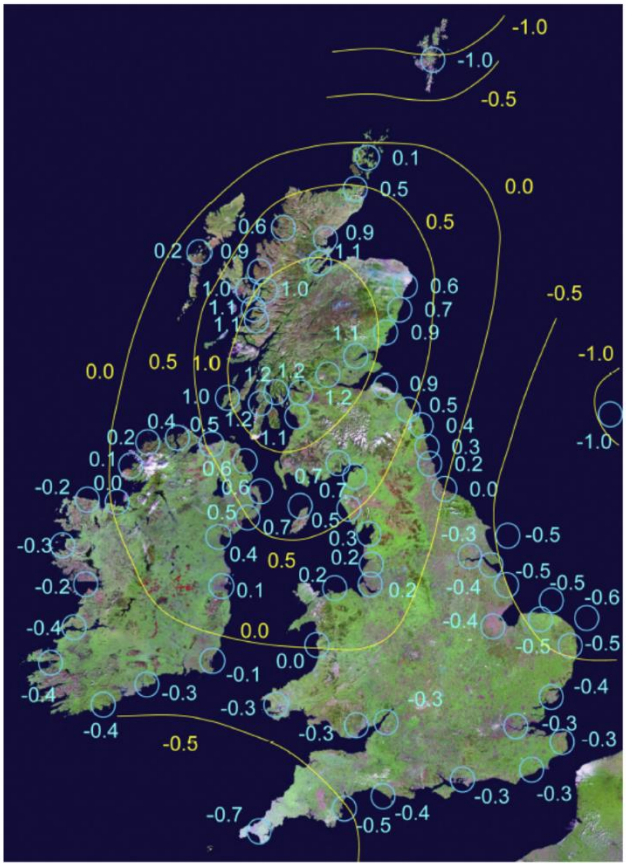

Figure 2.5: Rate of relative land-level change (mm a^{-1}) from 1000 BP to the present day for the United Kingdom. Relative land uplift is marked as positive and relative subsidence is marked as negative (Shennan *et al.*, 2012)

Models have been developed to predict changes in relative sea level (e.g. Bradley *et al.*, 2011; Shennan *et al.*, 2012; Shennan *et al.*, 2018), as well as numerous studies undertaken to reconstruct past relative sea-level changes along the coast of Britain (e.g. Firth & Haggart, 1989; Haggart, 1989; Shennan *et al.*, 1994; Long & Tooley, 1995; Long *et al.*, 1996; Long *et al.*, 1999; Plater *et al.*, 2000; Edwards, 2001; Waller & Long, 2003; Shennan *et al.*, 2005; Massey & Taylor, 2007; Selby & Smith, 2007; Massey *et al.*, 2008; Gehrels *et al.*, 2011; Smith *et al.*, 2012; Selby & Smith, 2016). The relative sea-level changes recorded around the coast of United Kingdom reflect the variation of isostatic and eustatic changes in sea level (Figure 2.6).

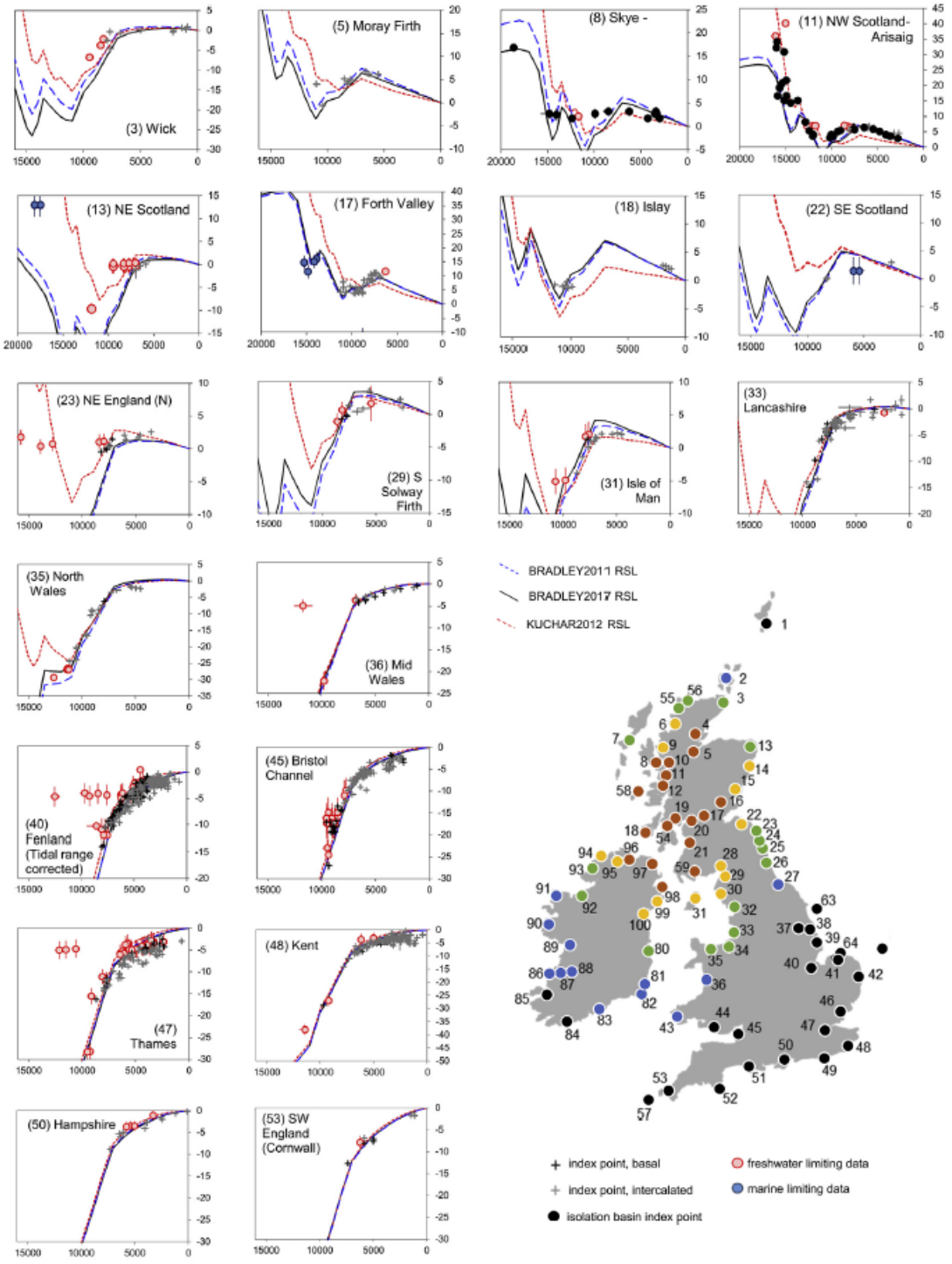

Figure 2.6: Reconstructions and model predictions of relative sea level around the United Kingdom. Figures modified and adapted from Shennan *et al.* (2018)

The relative sea-level predictions of Shennan *et al.* (2012) were based on three different ice models comprised of the Shennan *et al.* (2006) thin ice model, Shennan *et al.* (2006) thick ice model and Bradley *et al.* (2011) as shown in Figure 2.7a. More recently, Shennan *et al.* (2018) provided an updated prediction for relative sea-level

changes in the United Kingdom which included in excess of 2100 data points from 86 regions across the United Kingdom and new data points from Ireland. The relative sea-level predictions in Shennan *et al*. (2018) utilised three different GIA models: BRADLEY2011; the final version of the model developed in Bradley *et al*. (2011), KUCHAR2012; the first model that used quantitative models of climate-driven glaciological processes for the reconstruction of the Celtic ice sheet (Kuchar *et al*., 2012) and BRADLEY2017; an updated BRADLEY2011 model with higher grid resolution than the previous one (of ~70 km) to ~35 km (Shennan *et al*., 2018). The relative sea-level changes based on the model predictions were plotted against the available geological records for the respective regions, and the predicted patterns of relative sea-level changes are consistent and in good agreement with the field data for relative sea level (Shennan *et al*., 2012; 2018).

The trend of relative sea-level changes of sites located in northern England in particular varied from those located in southern England. In Scotland, variation in the pattern of relative sea level was also observed, for example between the Shetland Islands and sites located on the west coast of Scotland (Figure 2.7). This can be attributed mainly to the re-advances of the ice sheet in Scotland, and in part to the effects of the Celtic ice sheet in Ireland during the Devensian (Shennan *et al*., 2018). Several episodes of alternating increase and decrease in relative sea level were observed through studies undertaken in Scotland (e.g. Sissons, 1966; Firth & Haggart, 1989; Shennan *et al*., 1994; Dawson & Smith, 1997; Shennan *et al*., 2005; Selby & Smith, 2007; 2016). A decrease in relative sea level at sites located in Scotland was observed at approximately 12 ka BP, and this was attributed to the formation of the more localised ice sheet during the Loch Lomond Stadial, which led to disturbance and variation in the GIA of the land and the resultant change in relative sea level, although spatial variability between the sites was also present as evidenced by the studies undertaken.

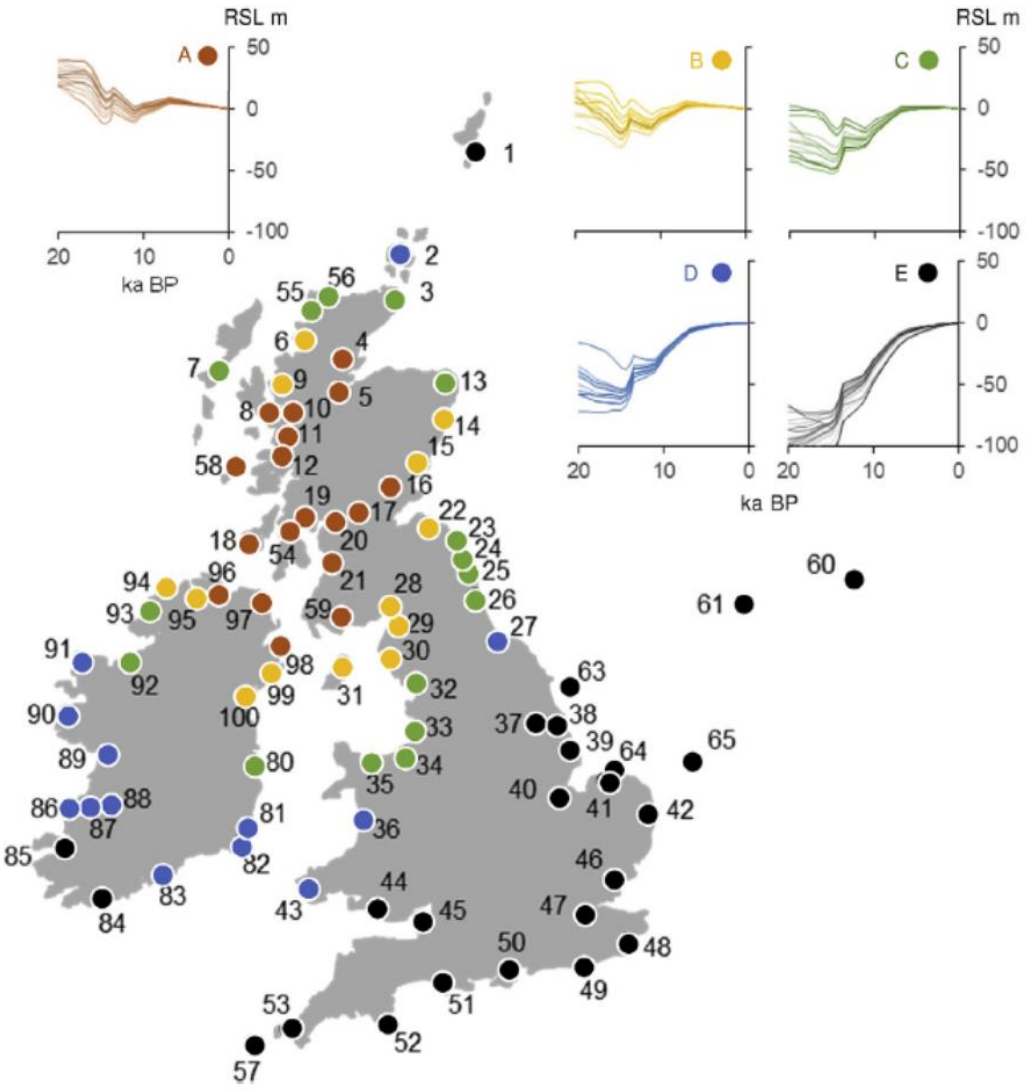

Figure 2.7: The spatial variability of relative sea level across the United Kingdom. The numbered sites were divided into five groups A to E, based on the broad pattern of predicted relative sea level change using the BRADLEY2011 model (from Shennan *et al.*, 2018)

During the Main Postglacial Transgression which occurred in the early to middle Holocene at approximately 8000 to 6000 BP, a general increase in relative sea level was observed at sites studied along the coast of United Kingdom, although fluctuations and regressions in relative sea level were observed in some parts of Scotland (Figure 2.6; e.g. graph B and C). After this increase in relative sea level, relative sea level fell to present level in areas experiencing land uplift, while relative sea level continued to increase until present day level for areas experiencing land subsidence in southern England. An increased relative sea level was also recorded at several sites in Scotland and England in the late Holocene (e.g. Wells, 1997; Zong &

Tooley, 1996; Long *et al.*, 1996; 1999; Plater *et al.*, 2000; Edwards, 2001; Smith *et al.*, 2002; Selby & Smith, 2007; 2016).

Records of more recent and contemporary (from approximately the last 200 years until present day) relative sea-level changes can be obtained through instrumental data obtained from tide gauges (e.g. Shennan & Woodworth, 1992; Woodworth *et al.*, 1999; Woodworth *et al.*, 2009; Gehrels & Woodworth, 2013; Ezer *et al.*, 2015). For the past 150 years, eustatic sea level in the United Kingdom and western Europe has risen at a rate of approximately 0.012±0.004 mm a^{-1} (Ezer *et al.*, 2015). However, spatial variability in the sea level recorded from tide gauges is evident, as well as variations on inter-annual and decadal timescales (Woodworth *et al.*, 2009).

2.5 Relative Sea-Level History of Cumbria

Studies of relative sea-level changes in the inner part of southern Solway Firth in Cumbria have been carried out previously at Boustead Hill and Drumburgh Moss (Lloyd *et al.*, 1999). Holocene relative sea-level changes were also recorded from two raised bog sites, Wedholme Flow and Bowness Common (Walker, 1966; Huddart *et al.*, 1977), and a site at Crosscanonby investigated by Huddart *et al.* (1977) also revealed a brief episode of marine transgression. In central Cumbria, studies on Holocene relative sea-level changes were undertaken by Huddart *et al.* (1977), Tooley (1985), Auton *et al.* (1998), Balson (2010) and are summarised in Lloyd *et al.* (2013). In southern Cumbria, in particular Morecambe Bay, a record of Holocene relative sea-level changes was presented by Zong & Tooley (1996), including previous work undertaken by Tooley (1987), Smith (1959), Barnes (1975), Oldfield & Statham (1963), Oldfield (1960a; b) and Birks (1982).

The oldest marine deposit identified along the northwest Cumbrian coastline was recorded adjacent to the Black Dub, north of Allonby (NY 0813 4324). Alternating bands of peat, clay and sand are exposed beneath the surface of the ~7.6 metres raised beach identified by Eastwood *et al.* (1968). Pollen analysis undertaken on the peat unit revealed a halophile-rich assemblage suggesting an early Holocene sand dune system dated at 10151-9009 cal BP. It is probable that the organic lenses are fossil dune slacks resulting from an episode of increased relative sea level (Jelgersma *et al.*, 1970).

At Drumburgh Moss (NY 2551 5863), a limiting basal date of 8545 cal BP was obtained at 4.44 m OD, a transgressive overlap was dated at 8125 cal BP at 4.55 m OD, and a regressive overlap at 6.85 m OD at 2428 cal BP. At Boustead Hill (NY 2913 5780) located east of Drumburgh Moss, a limiting basal date of 8065 cal BP was obtained at 6.19 m OD, a transgressive overlap was dated at 7394 cal BP at 6.68 m OD, and a regressive overlap was dated at 7090 cal BP (7.16 m OD) (Lloyd *et al.*, 1999). At Bowness Common (NY 2050 6011) and Wedholme Flow (NY 2187 5301), marine transgressions were dated at 7634 cal BP (4.73 m OD) and 7647 cal BP (4.66 m OD) respectively, while marine regressions at Bowness Common and Wedholme Flow were dated at 6722 cal BP (5.95 m OD) and 6189 cal BP (6.17 m OD) respectively (Huddart *et al.*, 1977).

A marine transgression recorded at 7678 cal BP at 3.71 m OD was also revealed at Crosscanonby (NY 0655 3971) (Huddart *et al.*, 1977). It was suggested that during the period of increased relative sea level correlated with the Main Postglacial Transgression, the seaward part of the drumlin of Swarthy Hill (NY 0644 3978) which protected the inter-drumlin depression where the sample was collected, was eroded. The lowest point of the drumlin was then breached as sea level continued to increase, inundating the freshwater lagoon, and this was evidenced by the presence of silts, clays, sands and shingle from the borehole taken at Crosscanonby. The marine transgression at Crosscanonby which ended at 7402 cal BP at an altitude of 4.44 m OD was brief (lasting for 276 years), and this was attributed to the accumulation of sand and shingle at Swarthy Hill which ultimately sealed the initial breach point (Huddart *et al.*, 1977).

The evidence from the Ravenglass estuary (SD 0867 9676) showed a clear Late Devensian relative sea-level highstand at approximately 2.3 m OD at 17 to 15 ka cal BP, which was followed by a rapid relative sea-level fall to below -5 m OD at approximately 10.5 ka cal BP. Relative sea level in the Ravenglass estuary then rose rapidly again during the early Holocence from below 7 m OD at approximately 8500 cal BP, to approximately 1.2 m OD at 8000 to 7800 cal BP as a result of ice melt. This culminated in a highstand during the mid-Holocene of approximately 1 m OD at approximately 6000 cal BP. Since then, relative sea level in the area has been gradually falling until the present day (Lloyd *et al.*, 2013).

Relative sea level in Skelwith Pool (SD 3407 8227), Morecambe Bay, rose rapidly at approximately 8847 cal BP until 8567 cal BP, with a maximum rate of increase of +36.7 mm a^{-1} (although this may have been exaggerated by the issue of old carbon contamination and changes in palaeo-tidal range, and varied between -8 mm a^{-1} and +12 mm a^{-1} subsequently. The effect of isostatic uplift can be observed evidenced by the change in biostratigraphy (diatoms assemblages) at the site at approximately 8567 cal BP but reduced soon after this, as glacio-isostatic recovery of the area was minimal from approximately 5767 cal BP. Crustal movements and uplift in Morecambe Bay area have been minimal since 5767 cal BP (Zong & Tooley, 1996). For Skelwith Pool, a rate of approximately +4 mm a^{-1} of relative sea-level change was found to be the critical threshold for retreat of the coastline, and rates greater than +4 mm a^{-1} may have resulted in extensive inundation over the coastal lowlands. A rise of sea level at a rate lower than 2 mm a^{-1} was not likely to have caused widespread inundation as intertidal deposition and saltmarsh accretion would have kept pace (Zong & Tooley, 1996).

A reduced rate of sea-level rise at approximately 8567 cal BP to 8091 cal BP was observed at Roudsea Wood (SD 3455 8067), Leven Estuary following the rapid rise of sea level that occurred before 8567 cal BP (Zong & Tooley, 1996; Zong, 1998). A period of sea-level fall was then recorded between 6887 cal BP to 5721 cal BP (3.43 to 3.99 m OD) based on the variation in diatom assemblages. This is in contrast to the sea-level trend in the area which predicted a sea-level increase at that particular time. This reversal in sea level was attributed to the enclosure of a sand barrier across the mouth of the valley causing the valley to dry out (Zong, 1998). There were also periodic inputs of sand-mudflat diatoms that were interpreted as signatures of storm tides which washed over the sand barrier and brought in marine and brackish diatoms to the study site. After approximately 5721 cal BP (2.99 m OD), relative sea level became stable and then started to fall. At approximately 5316 cal BP (4.18 m OD), a rise in sea level of approximately 1 m OD was recorded and was followed by a gradual fall in sea level, with another increase in relative sea level recorded at approximately 2516 cal BP (5.16 m OD). From approximately 1500 cal BP sea level fell slightly or has been stable until it attained present day level (Zong, 1998). The relative sea-level curve and reconstruction from the Solway Firth, central Cumbria and Morecambe Bay respectively are shown in Figure 2.8 below.

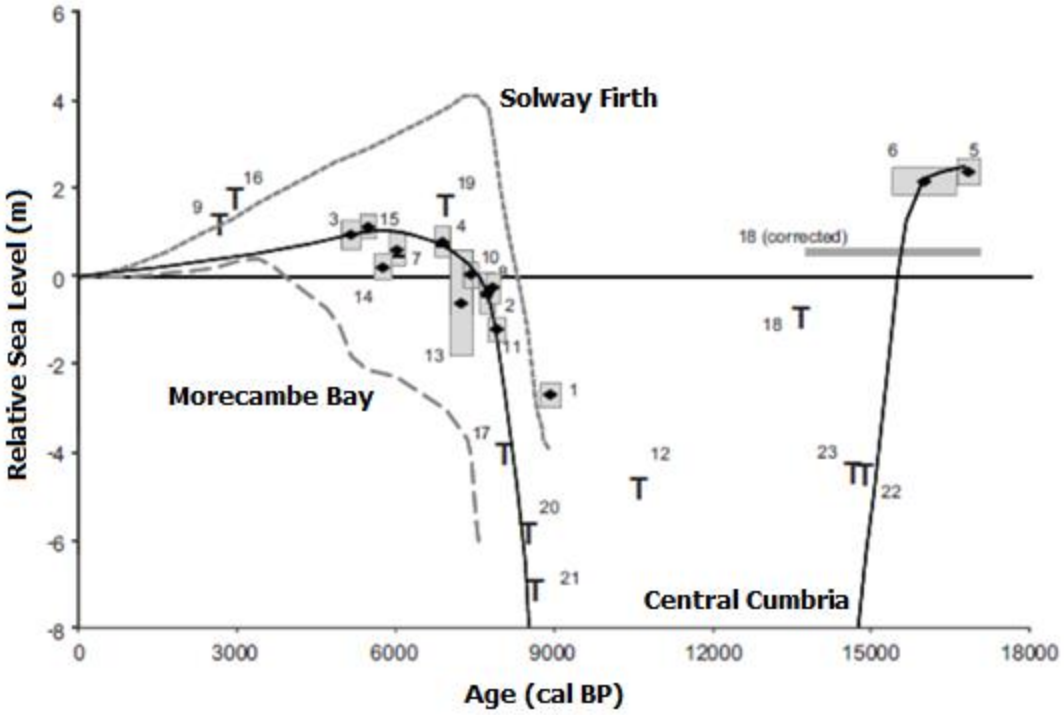

Figure 2.8: Relative sea-level curves from the Solway Firth, central Cumbria and Morecambe Bay (from Lloyd *et al.*, 2013)

The effects of differential GIA along the Cumbrian coastline is possible, as the evidence for a marine transgression in the late Holocene was mainly recorded at sites located in southern Cumbria. It is therefore possible that the land uplift at the northern sites which are closer to the centre of land uplift in Scotland had outpaced the increase in eustatic sea level that occurred during the late Holocene. This differential effect has been previously noted in the Solway Firth by Lloyd *et al.* (1999), who demonstrated that different rates of isostatic rebound exist between the shores located to the north and south of the Solway Firth.

To test whether differential GIA had occurred, a third order polynomial best fit line was drawn through the complete datasets and sea-level index points for the study sites on the north and south of the Solway Firth by Lloyd *et al.* (1999). If there was no variation in crustal movements between the north and south, a random scatter of values would have been observed, with some positives and negatives for each dataset. However, it was clear that there was a distinction between the two sets of data with all data points from the southern Solway Firth recording negative residuals and falling below the best fit line. Most of the northern Solway Firth datasets plotted above the best fit line (Figure 2.9). The negative residuals from the northern Solway

Firth before 8000 cal BP demonstrated the inadequacy of the best fit line at a period when only datasets from the north are available (Lloyd *et al.*, 1999).

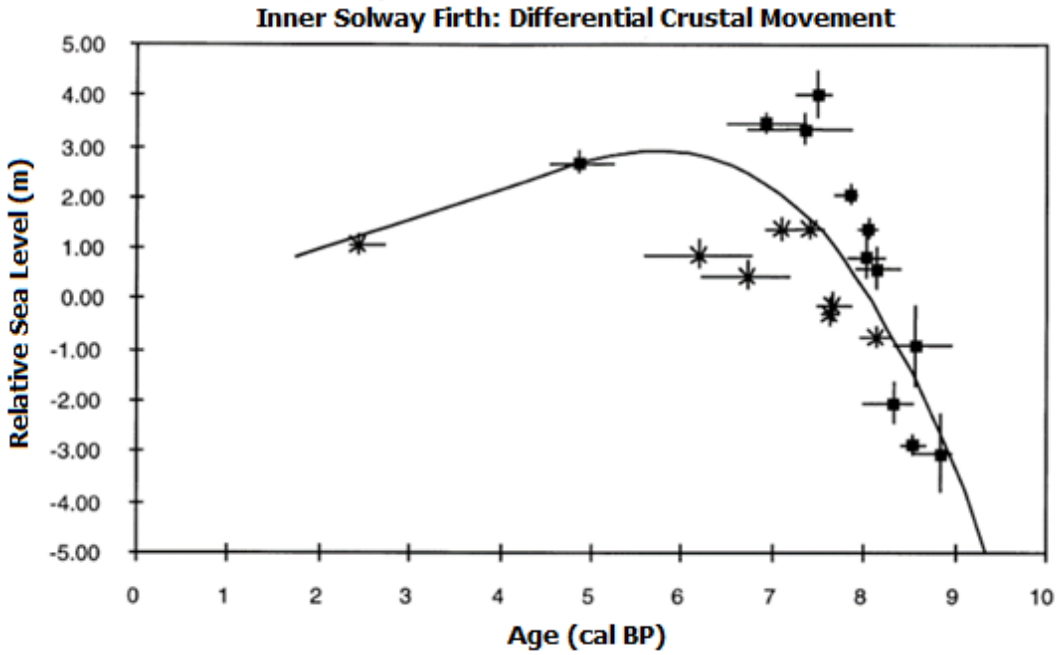

Figure 2.9: Differential crustal movement between the north and south Solway Firth. Black line is the third order polynomial best fit line for the dataset. Data from north Solway Firth shown by ■, data from south Solway Firth are marked by x (from Lloyd *et al.*, 1999)

2.6 Vegetation History of Cumbria

Pollen grains that have accumulated over time are representative of past vegetation in the area, and are commonly found in in stratigraphic sequence in peats and lake sediments (Turner, 1979). Analysis of the pollen grain in combination with radiocarbon dating alloqs a geographical and chronological pattern of vegetation changes to be established. During the late Quaternary the northern region of Cumbria consisted of various topographic zones including coastal and estuarine areas, undulating glaciated lowlands, major river catchments, piedmont zones and uplands (McCarthy, 1995). This significant variation in topography resulted in a great variety of habitats, settlement density and land use at different periods during the Late Devensian and Holocene.

The vegetation history of the Cumberland Lowlands in Cumbria has been extensively studied by Walker (1966) including sites at Scaleby Moss, Oulton Moss, Abbot Moss, Moorthwaite Moss, Ehenside Tarn, St. Bees, Glasson Moss and Bowness Common. The sites were selected as they may have been affected by the re-advance of Scottish ice sheet (Scaleby Moss and Oulton Moss), the Main Lakeland Glaciation (Abbot Moss and Moorthwaite Moss), coastal sites (Ehenside Tarn and St. Bees) and because they had the potential to illustrate the relationship between relative sea-level changes and land uplift (Bowness Common and Glasson Moss). A brief summary of the findings by Walker (1966) are presented here.

The occurrence of pioneer vegetation in the Cumberland Lowlands occurred between the onset of deglaciation in the area and prior to the start of the establishment of thermophilous woodland, which was preceded by the major expansion of *Corylus avellana* (Walker, 1966). Between the Devensian deglaciation and the onset of the Scottish Re-advance into the area, the basins at some of the sites investigated had accumulated silt and clay with very low organic content and little coarse-grained inorganic material. This suggests that there was little vegetation development around the periglacial lakes formed during this period, with the vegetation dominated by herbaceous pollen sedges and grass, and the presence of *Sphagnum*, *Filipendula*, *Artemisia*, with low frequencies of tree pollen. The presence of aquatic pollen (e.g. *Myriophyllum alterniflorum*) was also common (Walker, 1966).

The post-glacial woodland was characterised by the rapid expansion of *Corylus* into the woodland previously dominated by *Betula* at approximately 9000 BP, followed by the expansion of *Ulmus* and *Quercus*. The expansion of the mixed woodland dominated by *Betula* came to an end soon after approximately 7000 BP as woodland cover decreased, although the expansion of *Alnus* was observed at some of the sites during episodes of increased relative sea level due to alder's ability to grow on poor, waterlogged soils (Walker, 1966). *Pinus* was observed at Bowness Common, on the beaches and spits composed of sand and gravel as the coastline provided a habitat where *Pinus* had a competitive advantage over the other tree species (Walker, 1966).

The period of decreased woodland cover in the Cumberland Lowland was recorded from approximately 6000 BP at the coastal sites, and at approximately 5000 BP at sites located further inland. Early woodland clearances as a result of anthropogenic activities resulted in regional vegetation changes, which accentuated the natural decline of *Ulmus*, and resulted in the increased dominance of *Betula* and *Corylus* as well as the establishment of *Quercus* (Walker, 1966). The effect of human settlement in the area was not significant until approximately 3800 BP, and intensive until 3400 BP evidenced by the occurrence of polished stone axes from the late Neolithic. Extensive woodland clearance occurred during the Neolithic, and was suggested to have ceased soon after the Romans withdrew from the area (Walker, 1966).

Evidence from sites located in the Lake District, Cumbria also suggest a strong indication of the extension of early post-glacial woodland up to an altitude of 550 metres (Pennington, 1964). An *Ulmus* decline was observed in the sites investigated at approximately 5000 BP, with a later decline of *Ulmus* during the early Neolithic more evident at sites close to the stone-axe factories. Further woodland clearances during the Bronze Age were also observed, corresponding to human settlement and anthropogenic activities in the area (Pennington, 1964).

Bolton Fell Moss and Walton Moss in northern Cumbria were studied to reconstruct Holocene vegetation history, and particularly the time from the Bronze Age to the present day (Dumayne-Peaty and Barber, 1998). The pollen records between the two sites are broadly similar, however there were some notable differences especially during the Iron Age and Medieval times. At both sites during the Bronze Age and Early Iron Age (2800 to 2100 BP) notable changes in *Corylus* and *Avena/Triticum* (oats and wheat) were recorded, showing that there were pastoral or arable agriculture practices in the areas. In the late and pre-Roman Iron Age (2100 to 1900 BP), there was rapid deforestation at Walton Moss represented by the decrease of arboreal pollen and replacement by sedges. These data suggest that woodland clearances had occurred close to the sites, and/or that there was an increase in population growth and settlement in the area. At Bolton Fell Moss, only a gradual decrease in arboreal pollen was observed within the same time period. The impact of the Roman invasion (1900 to 1730 BP) was less pronounced at Bolton Fell Moss as opposed to Walton Moss, due to its location which lies approximately 3.5 kilometres further away from the Stanegate frontier. Deforestation at both sites continued

throughout the Roman occupation, with woodland regeneration noted following the Roman withdrawal (Dumayne-Peaty and Barber, 1998).

The pollen analysis from Foulshaw Moss, southern Cumbria showed a series of small-scale but significant woodland clearance episodes throughout the Bronze Age, which were later followed by a reduced clearance activity during the early Iron Age (Wimble *et al.*, 2000). The first major woodland clearance was recorded in the late Iron Age (corresponding to the Roman occupation in the region), and was succeeded by woodland regeneration in the post-Roman/early Medieval periods. In the late Medieval period, woodland clearances were more significant, resulting in large areas of permanently open landscape (Wimble *et al.*, 2000).

The reconstruction of vegetation and land use history from the late Neolithic (5200 BP) to the present was undertaken at Butterburn Flow, Cumbria (Yeloff *et al.*, 2006). Three late Neolithic/Bronze Age woodland clearances were identified, with the first commencing at approximately 4300 BP indicating pastoral activities and limited arable agriculture. At approximately 4300 BP an intensified woodland clearance was observed, which culminated at approximately 2000 BP. Farmlands were then abandoned coinciding with the Roman occupation in the region (approximately 1900 to 1500 BP), with a resurgence of agricultural activities following the Roman withdrawal. A later decline in agricultural practices can be accounted for by climatic deterioration, political instability and disease in the region (Yeloff *et al.*, 2006).

Coombes *et al.* (2009) reported that the most substantial periods of deforestation had occurred in the late Neolithic/early Bronze Age period and then in the middle Iron Age, creating a patchwork of woodland, heather moorland, pasture and arable land during the Roman period based on sites studied at Deer Dyke Moss and Hulleter Moss in southern Cumbria. The main changes recorded in the Roman period were a decline in the extent of *Betula* woodland and the local introduction of *Secale cereale* cultivation in the region. A shift into pastoral land-use and abandonment of less favourable agricultural land were minor effects that could be related to the end of the Roman period, but the later shifts in land use could be better related to climate variability of the region (Coombes *et al.*, 2009).

2.7 Reconstruction of Palaeo Relative Sea Level

The methods and techniques employed in this research to reconstruct sea level are summarised below. Traditionally geomorphological and field evidence have been used to reconstruct sea-level changes, including features such as sand dunes, raised beaches and shorelines (Tooley, 1974; Tooley, 1976; Huddart *et al*., 1977; Horton & Edwards, 2005). Lithostratigraphy has also been relied upon to reconstruct past sea levels as the alternation between organic and inorganic sediments observed in a sediment sequence has the potential of recording the changes from terrestrial to marine environment related to fluctuations in sea level. However the reliance solely on the lithostratigraphic changes can significantly restrict the resolution of the potential changes that can be examined (Horton & Edwards, 2005).

A marine transgression results in the landward expansion of marine conditions and saltmarsh environment at the site, and is reflected in the lithostratigraphy and biostratigraphy of the sediments. A succession of sediment from terrestrial origin, to fen or reedswamp peats and intertidal or marine sediments may be recorded therefore in a transgressive overlap. A reverse in the sequence may be observed when there is reduced marine influence at the site, resulting in a regressive overlap (Tooley, 1978; Shennan, 1986).

Accommodation is defined as the space available for potential sediment accumulation and deposition (Schlager, 1993). The rate of change of accommodation on the shoreline and the rate of sediment supply are the two primary factors that determine the recording of transgressions and regressions in a stratigraphic sequence, and therefore the retreat and advance of a coastal depositional system (Muto & Steel, 1997). Falling sea level does not create the inland accommodation space for sea-level archives to be preserved well compared to that of increased sea level, resulting in a lack of regressive data points in comparison to the records of transgressive data points.

The high resolution reconstruction of palaeo sea-level changes based on geomorphological and lithostratigraphical changes at a site may not be feasible due to the slow accumulation of sediment and response times of the coastal feature, and the variation in the spatial or temporal distribution of the sediment and

geomorphological features (Edwards & Horton, 2000). The reduced accumulation of organic materials in the late Holocene has also prevented attempts to reconstruct sea-level changes in some coastal regions in the United Kingdom (Edwards, 2001; Horton & Edwards, 2005). The development of laboratory analyses which combine both lithostratigraphical and biostratigraphical changes (e.g. foraminifera and diatoms) observed in sediment sequences therefore increases the quality of data for high resolution relative sea-level reconstruction, in addition to the information obtained based on lithostratigraphic changes.

2.7.1 Foraminifera as Sea-Level Proxies

Foraminifera are unicellular testate organisms that are found only in brackish and marine environments. Foraminifera occupy almost every marine habitat, from the high water level mark to the deep ocean and comprise of benthic and planktonic species. Foraminifera are a useful proxy in the reconstruction of past sea levels, and commonly preserve well in the fossil record (Scott *et al.*, 2001).

Saltmarsh foraminifera are widely acknowledged as a useful proxy for the reconstruction of Holocene sea-level changes. Foraminifera have a distinct vertical zonation related to the elevation they occupy within the tidal frame (Scott, 1976). The duration and length of intertidal exposure is said to be the most significant controlling factor of foraminiferal distribution. By studying the relationship of these parameters to the foraminiferal assemblages in contemporary samples, it is possible to use this information as an analogue to reconstruct past sea-level changes (e.g. Gehrels, 1994; 1999; Gehrels *et al.*, 2001; Edwards, 2001; Horton and Edwards, 2006; Kemp *et al.*, 2009; 2013; Stephan *et al.*, 2015; Barnett *et al.*, 2016). Saltmarsh and intertidal foraminiferal species commonly occur in relatively high abundances with low species diversity, and are therefore a useful proxy for the reconstruction of high resolution sea-level records. The vertical zonation of saltmarsh in relation to the tidal datum has been demonstrated to show the strongest relationship with the variation in foraminiferal assemblages, although other environmental factors such as pH and salinity may also influence the species variation (Horton *et al.*, 1999; Horton & Edwards, 2006).

2.7.2 Transfer Functions

Most Quaternary palaeo-ecological research aims to reconstruct the past environment based on the preserved microfossil assemblage (i.e. foraminifera, diatoms, pollens, ostracods) in sediments, lakes or bogs. In the early studies, although these fossil assemblages were studied quantitatively, the resultant environmental reconstructions were however mostly qualitative and only presented in terms such as temperate, cool, moist and dry (Birks, 1995). A procedure to quantitatively reconstruct palaeo-environment parameters based on the fossil assemblages utilising transfer functions was first presented by Imbrie and Kipp (1971). The variation of marine foraminifera was explained based on their relation to ocean salinity and surface temperature (Imbrie & Kipp, 1971). Since that time the approach of quantitative palaeo-environmental reconstruction has been adopted (Birks, 1995).

The purpose of a transfer function is to express the value of an environmental parameter (e.g. pH or salinity) as a function of the biological data (i.e. foraminiferal assemblages), also known as the environmental proxy data. This is achieved through two stages; regression calculations that are utilised to model the response of the contemporary microfossil species as a function of the environmental parameter and a calibration procedure which then applies this response function to predict the past environmental parameter based on the fossil counterpart of the utilised microfossil (Birks, 1995).

The response function through the regression calculations can either result in a linear or unimodal response model (Birks, 1995; Horton & Edwards, 2006). Normalised clustering around the environmental parameter is assumed in a unimodal response model, with the optimum value of the environmental parameter represented by the highest abundance of the foraminiferal species (Birks, 1995). A unimodal distribution of microfossil assemblages would have been recorded previously (e.g. Zong & Horton, 1999; Horton & Edwards, 2006), and the statistical technique commonly employed to produce a unimodal response model is the weighted-averaging partial-least-squares (WA-PLS). The application of the WA-PLS technique in the development of a transfer function is detailed in Chapter 3 (Section 3.7.2).

Other techniques for sea-level reconstruction include the utilisation of a locally weighted model and Bayesian modelling (Kemp *et al.*, 2015). The locally weighted model or transfer function utilises the training set dynamically to generate specific model for an individual fossil sample. This results in a balance between the precise, small and local dataset in sea-level reconstruction and the wide range of the modern analogues available in a larger regional training set (Kemp *et al.*, 2015). The Bayesian modelling presents an alternative and new approach in the development and application of transfer functions for sea-level reconstructions. This approach is based on probability modelling associated with the fossil data, environmental parameters and all model parameters. Bayesian modelling involves forward modelling of the relationship between the model taxa and the environmental parameter of interest (e.g. elevation), and a backward modelling that then generates the relationship consistent with the fossil data (Kemp *et al.*, 2015).

Several assumptions are made in the utilisation of transfer functions. Firstly, it is assumed that the environmental parameter of interest for the reconstruction consistently explains the variation in species assemblages, with other environmental parameters not having any influence on the distribution (Birks, 1995; Horton & Edwards, 2006). The second assumption is that the distribution of the fossil assemblages is represented by their contemporary counterparts (Birks, 1995). The composition of the contemporary assemblages therefore can have implications on the precision and accuracy of the resultant transfer function (Gehrels *et al.*, 2001; Horton & Edwards, 2006). The practicality of both assumptions must therefore be assessed in the evaluation of the reliability of the developed transfer functions and the resultant reconstruction. The development and utilisation of a local, regional or national transfer function may also affect the accuracy and precision of the sea-level reconstructions (Gehrels *et al.*, 2001), e.g. as the inclusion of regional and national data may cover a bigger tidal range than the local transfer function developed as well as including a greater range or environmental parameters, which is more applicable to a greater range of palaeoenvironments (Shennan *et al.*, 2015).

2.8 Sea-Level Index Points

Sea-level index points (SLIPs) are individual sea-level reconstructions based on quantified ages and vertical uncertainties. They are an estimation of the relative sea-level position in space and time. SLIPs can be used to describe the overall trends and patterns of relative sea level in the region (Horton *et al.*, 2013). They are established through the combination of lithostratigraphic, chronostratigraphic and biostratigraphic data (Edwards, 2006). To establish a SLIP, information on the sample's location, age, altitude, tendency and indicative meaning are needed (Preuss, 1979; Devoy, 1982; Heyworth and Kidson, 1982; Shennan, 1982; Gehrels *et al.*, 1996; Shennan *et al.*, 2000; Massey *et al.*, 2008; Horton & Edwards, 2006; Barlow *et al.*, 2013; van de Plassche, 2013). The lithostratigraphical approach is mainly restricted to establishing SLIPs at the point of contacts between organic (i.e. terrestrial peat) and minerogenic (i.e. marine silt, clay and sand) sediments, which occur around the elevation of mean high water of spring tides (Edwards & Horton, 2006). SLIPs that are obtained at these point of contacts are therefore representative of the marine transgressions and regressions that occurred at the site (Gehrels, 2007).

A multi-proxy approach that employs radiocarbon dated lithostratigraphic and biostratigraphic sea-level proxies is now widely used, as this provides a more detailed and higher resolution reconstruction as microfossils respond rapidly to changes in sea level (Edwards & Horton, 2000; Gehrels, 2007). Relative sea-level reconstructions are based on sea-level proxies and their indicative meaning, derived from analogous modern counterparts. The indicative meaning of the sea-level proxies describe their relationship to respective elevations in the tidal frame, comprised of a tidal datum midpoint (the reference water level) and a vertical range (the indicative range). Indicative range is therefore defined as the altitudinal range over which the index point's proxy could have formed (Horton & Edwards, 2006; Horton *et al.*, 2013). Several sources of error should be taken into consideration when calculating SLIPs, including altitude, core collection and sampling errors (Chapter 3; Section 3.9).

2.9 Summary

This chapter has summarised the glacial, relative sea-level and vegetation history of Cumbria in particular, and more broadly for other sites located in the United Kingdom. A summary of the global, regional and local processes driving the changes in sea level was also presented. Variation in the patterns of relative sea level in particular are observed between sites located closer to the centre of isostatic uplift across Scotland and those located further away. An overview of the techniques and proxies utilised to reconstruct relative sea-level changes in this study was also described.

CHAPTER 3

METHODOLOGY

3.0 Introduction

This chapter describes the methods and techniques used in this research to reconstruct Holocene sea-level and environmental changes including fieldwork, laboratory techniques and microfossil analyses.

3.1 Selection of Palaeo Study Sites

Several key criteria were taken into consideration when looking for and selecting suitable sites to reconstruct Holocene sea-level changes. Isobase models from Sissons (1983), Firth *et al*. (1993), Smith *et al*. (2000) and Smith *et al*. (2012) and glacial isostatic adjustment (GIA) models from Peltier *et al*. (2002), Shennan *et al*. (2002), Shennan *et al*. (2006) and Bradley *et al*. (2011), along with relative sea-level predictions from Shennan *et al*. (2012; 2018) were referred to in order to identify at what altitude Holocene shorelines were likely to occur. As a result, sites with an altitude below 10 m relative to Ordnance Datum (OD) were sought for Holocene sea-level reconstruction.

A literature review was undertaken focused on the southern shore of the Solway Firth to identify potential new sites for investigation that contained a preserved record of Holocene sea-level and environmental changes. Information about the altitudes, stratigraphy and microfossils found at the studied sites, was used to identify potential areas. The study locations needed to be conducive to the preservation of microfossils, as they are a key proxy used in the reconstruction of past sea levels. Areas such as peat bogs that have anaerobic conditions, and thus low microbial activity which results in better microfossil preservation were therefore sought.

Borehole records from the British Geological Survey (2018), Ordnance Survey (OS) maps and Google Earth maps of the region were also accessed during the process of identification of potential sites, as they provide additional stratigraphical data, altitude

and topographical information about the area. For example, Google Earth provided information on possible contemporary marsh sites in the area, where different marsh zonation could be observed through satellite imagery and aerial photography. The historic OS maps (Seventh series, from the 1960s), provided information on former lowlands or marsh areas before any land reclamation occurred.

Potential sites (Section 3.1.1) were subsequently visited and initial coring undertaken to identify the stratigraphy of the area. Spot samples were also taken back to the laboratory to undertake a preliminary assessment of the microfossils at the site. Fifteen potential sites in the region were investigated (Section 3.1.1) and four sites (Allonby, Pelutho, Cowgate Farm and Herd Hill) were chosen subsequently and deemed the most suitable for reconstruction of Holocene sea level of the region.

3.1.1 Selection Criteria for Palaeo Study Sites

The selection of sites where Holocene sediment sequences are well preserved and undisturbed is crucial in studies attempting to reconstruct past environmental changes. The inner part of the Solway Firth estuary has been studied previously (e.g. Drumburgh Moss and Boustead Hill; Lloyd *et al.*, 1999), as well as the raised bog (e.g. Bowness Common and Wedholme Flow; Huddart *et al.*, 1977). Eleven other potential sites were investigated in the area (Figure 3.1; marked in black), and this resulted in four palaeo study sites (marked in red), which were investigated further for the reconstruction of Holocene sea-level and environmental changes.

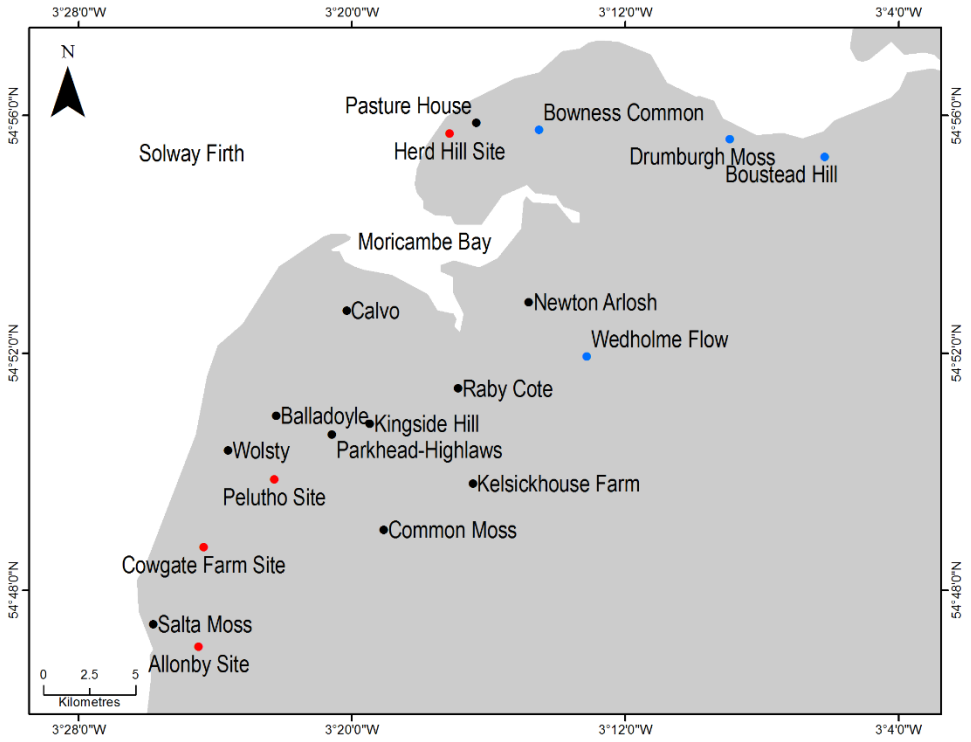

Figure 3.1: All sites investigated in this study, with the four main sites marked in red

In the field, the alternation between organic and inorganic sediments was sought as this has the potential to represent changes from terrestrial to marine environments related to fluctuations in relative sea level. Microfossils preserved in the cores were then used to identify the origin of the sediment deposited, based on the environmental preferences of the microfossil species. The microfossils present were also used as a proxy to provide an estimate of past sea level through the development of transfer function.

The main issues encountered when investigating potential sites in the area was the lack of well-preserved and suitable sediment sequences, and the high sand content within the sediment units which led to poor preservation of microfossils. Most of the low lying areas (below 10 m OD) are presently utilised as farmland, and the construction of roads connecting the villages and farmland may have disturbed the upper sections of the sediment. The sites located closer to the Moricambe Bay estuary (e.g. Calvo, Raby Cote, Newton Arlosh) may have experienced erosional, increased turbidity and sediment reworking when relative sea level was higher in the past, resulting in a lack of preserved sediment and high sand content within the minerogenic units.

Four palaeo sites (Allonby, Cowgate Farm, Pelutho and Herd Hill) with generally good preservation of microfossil and sediment sequences, were successfully identified and utilised in this study. All the other sites investigated were eliminated, apart from Pasture House, which was included to provide additional geomorphological context of the area around Herd Hill. A summary of the sediment description at the sites not utilised in this study are summarised in Table 3.1. Past sea-level and environmental changes along the Cumbrian coastline of the four selected sites were then reconstructed through detailed lithostratigraphical and biostratigraphical analyses in combination with radiocarbon dating undertaken on representative cores from each site.

Table 3.1: Summary of sediment description for all the other sites investigated

Site	Summary of Sediment Description
Raby Cote (NY 1783 5207)	Dense, very sandy brown and blue/grey silt-clay with mottling, overlain by top soil
Calvo (NY 1439 5457)	Brown silty sand, overlain by grey silty sand and top soil
Newton Arlosh (NY 2009 5473)	Dense, very sandy brown silt-clay with mottling, overlain by top soil
Balladoyle (NY 1212 5133)	Dense, very sandy brown silt-clay with mottling, overlain by top soil
Wolsty (NY 1058 5028)	Dense, very sandy brown and blue/grey silt-clay with mottling, some gravel, overlain by top soil
Parkhead-Highlaws (NY 1385 5070)	Dense, very sandy brown silt-clay with mottling, overlain by top soil
Kingside Hill (NY 1504 5103)	Red sand and gravel overlain by very sandy brown and blue/grey silt-clay with mottling, overlain by top soil
Kelsickhouse Farm (NY 1825 4909)	Basal gravel unit, overlain by sandy grey silt-clay with gravel, peat and top soil
Common Moss (NY 15422 47700)	Pink/brown clay overlain by very sandy grey silt-clay, organic brown silt-clay, peat and top soil.
Salta Moss (NY 0813 4488)	Silty grey sand with gravel overlain by brown sand with gravel and some shell fragments, peat and top soil. In some boreholes, the alternation between the sand and peat unit

	was observed, possibly indicating the presence of relict sand dunes.

3.1.2 Selection Criteria for Contemporary Saltmarsh Study Sites

Three contemporary saltmarsh sites (Skinburness, Cardurnock and Bowness Point) were selected for contemporary surface sample collection. Saltmarshes located in different parts of Moricambe Bay and the southern Solway Firth nearest to the palaeo study sites were selected, to provide the best representation of the fossil samples.

3.2 Fieldwork

Field investigations were undertaken at each site to determine the lithostratigraphy of the area and to collect representative sample cores. Detailed surveying was also undertaken at each site.

3.2.1 Determining the Stratigraphy and Sampling of the Palaeo Sites

A 1 metre long, 2 cm diameter Eijelkamp gouge was used to test the stratigraphy of the site. A grid system with an interval of 30, 60, 90 and 120 m was established for the sites depending on the size of the site investigated, with closer spaced boreholes undertaken where the stratigraphy was seen to be variable. The stratigraphy of all the boreholes cored at each site was described following the Tröels-Smith (1955) classification system. The stratigraphy was drawn up using TILIA 2.0.41 and TILIA*Graph (Grimm, 1991; 2004).

A 50 cm long, 5 cm diameter Russian corer was used to extract a representative sample core, in order to obtain the most complete stratigraphical record of environmental changes. Two parallel boreholes were cored using the Russian corer to provide an overlapping sequence and to minimise any loss, contamination or compression of the sediment. Sample cores were transferred into P.V.C pipes, wrapped in plastic cling film and aluminium foil and carefully labelled. The cores were stored in the cold storage room (temperature below 5 ºC) at the University of York

until required. Freezing was avoided as it is known to cause damage to foraminiferal tests.

3.2.2 Collection of Contemporary Surface Samples

Contemporary surface samples were collected from three saltmarshes along transects that covered the entire sub-environments, from high marsh areas to tidal flats (Barlow *et al.*, 2013; Horton and Edwards, 2006). For Skinburness Marsh, samples were taken at 30 metre intervals (with the last point located 5 metres away from the previous one). For Cardurnock and Bownes Point marshes, samples were taken along transects at 5 metre intervals. Samples were taken at larger intervals at Skinburness Marsh as the marsh spans a longer transect length (~750 metres) compared to Cardurnock Marsh and Bowness Marsh (both covering ~150 metres). Samples were collected at equal distances along the transect to cover the entire environmental range present within the saltmarsh (i.e. high saltmarsh to intertidal mudflat). Samples were also collected from sub-environment present within the saltmarsh (i.e. tidal creeks), where possible. The upper ~1 cm of surface sediments from the marsh were collected by carefully removing the sediment with a serrated knife and placing it into plastic sample jars for foraminifera, loss on ignition and particle size analyses. A pH measurement (using CyberScan pH 310 hand-held pH/mV/Temperature meter) on each sample was undertaken in the field. The pH value for surface sediment at all contemporary marshes was obtained by mixing a small amount of the surface sample with deionised water in a plastic centrifuge tube and placing the pH probe in the tube. The measurement was recorded when the reading on the meter had stabilised. The pH probe was cleaned with deionised water after each measurement and the pH meter was calibrated every day prior to using it in the field. The pH data were plotted against altitude (m OD) for each site. Once sampled, sediments in their respective plastic sample jars were labelled and refrigerated (while still at fieldwork site) and stored in the cold storage room (temperature below 5 ºC) upon return to University of York.

3.2.3 Surveying

All boreholes, sample cores, contemporary sample points and geomorphological features at the study sites were first marked using plastic marker flags and the locations of each were noted using a handheld global positioning system (GPS) device. Each site was then surveyed using a Trimble (Model R8 GNSS/R6/5800) differential global positioning system (δGPS) to obtain the precise coordinate and elevation of the boreholes, sample cores, contemporary sample points and any geomorphological features related to m OD.

3.2.4 Tidal Measurements at Contemporary Saltmarsh Study Sites

The funnel shape and macrotidal characteristic of the Solway Firth results in a significant tidal level variations between the sites located along the estuary. On the southern shore of the Solway Firth and for the northwest Cumbrian region, the nearest publicly accessible tidal gauge station is located at Workington. To relate the contemporary samples elevations recorded at the Skinburness Marsh, Cardurnock Marsh and Bowness Marsh to a reference tidal frame, repeated measurements of the high tide limit at each contemporary sites was made. Each high tide level measurement recoded at the three contemporary sites was levelled relative to OD using a Trimble (Model R8 GNSS/R6/5800) differential global positioning system (δGPS). The measurements of the local high tides at each contemporary sites were then compared to the same high tide level on the same day measured at the tide gauge station in Workington, which had been verified and corrected for atmospheric pressure, available approximately a month after the data were recorded (NTSLF, 2018). The tidal measurements taken at each contemporary saltmarsh site allow the surface samples collected to be related to a standardised tide level, and also highlight the spatial variation in tidal range along the Solway Firth and Moricambe Bay.

3.3 Laboratory Analyses

A multi-proxy approach was adapted to reconstruct Holocene sea-level changes and environmental changes of the study sites. A combination of loss on ignition, particle size and foraminiferal analyses were undertaken on sample cores from Allonby, Cowgate Farm, Pelutho and Herd Hill. Pollen analysis was undertaken on samples

from Cowgate Farm and Herd Hill to provide additional information on the vegetation and environmental changes for the region. Loss on ignition, particle size and foraminiferal analyses were also undertaken on all 72 contemporary surface samples collected from Skinburness Marsh, Cardurnock Marsh and Bowness Marsh to define the contemporary foraminiferal distribution in the region, and for the development of a transfer function.

3.3.1 Loss on Ignition

Loss on ignition (LOI) is a simple, common and widely used method to estimate the organic and carbonate content in sediments, using the linear relationship between LOI values and organic and inorganic carbon content (Heiri *et al.*, 2001; Santisteban *et al.*, 2004). In the first reaction, organic matter was oxidised at 550 °C to carbon dioxide and ash. In the second reaction, carbon dioxide was evolved from carbonate at 950 °C, leaving oxide. The weight loss during the reactions was measured by weighing the samples before and after each burn and these values were correlated to the organic matter and carbonate content of the sediment (Heiri *et al.*, 2001).

3.3.1.1 Preparation for Loss on Ignition

Samples were prepared using the method described by Heiri *et al.* (2001). After oven-drying of the sediment to constant weight (usually 12–24 hours at approximately 105 °C) organic matter was combusted in the first step to ash and carbon dioxide at a temperature of 550 °C for approximately four hours. Organic matter begins to ignite at about 200 °C and is completely depleted at about 550 °C (Santisteban *et al.*, 2004). The LOI was then calculated using the following equation:

$$\text{LOI 550} = [((\text{DW105-CW}) - (\text{DW550-CW}))/(\text{DW105-CW})]*100$$

Where LOI 550 represents LOI at 550 °C (as a percentage), DW105 represents the dry weight of the sample before combustion and DW550 the dry weight of the sample after heating to 550 °C.

In the second step, the residual samples were combusted at 950 °C as most carbonate minerals are destroyed at higher temperatures; calcite between 800 and 850 °C and dolomite between 700 and 750 °C (Santisteban *et al.*, 2004). Carbon dioxide is evolved from carbonate, leaving oxide and the LOI was calculated as:

$$LOI\ 950 = [((DW550\text{-}CW) - (DW950\text{-}CW))/DW105\text{-}CW)]*100$$

Where LOI 950 is the LOI at 950 °C (as a percentage), DW550 is the dry weight of the sample after combustion of organic matter at 550 °C, DW950 represents the dry weight of the sample after heating to 950 °C, and DW105 is the initial dry weight of the sample before the organic carbon combustion.

Assuming a respective weight of 44 g mol^{-1} for carbon dioxide and 60 g mol^{-1} for carbonate (CO_3^{2-}), the weight loss by LOI at 950 °C multiplied by 1.36 should then theoretically equal the weight of the carbonate in the original sample. This implies that inorganic carbon (IC) = 0.273 x LOI950 (Heiri *et al.*, 2001; Santisteban *et al.*, 2004). The LOI data were plotted against altitude (m OD) for both fossil and contemporary samples using TILIA 2.0.41 and TILIA*Graph (Grimm, 1991; 2004), C2 Version 1.7.7 (Juggins, 2007) and PAST Version 3.17 (Hammer *et al.*, 2001).

3.3.2 Particle Size Analysis

Samples were also analysed to determine their particle size composition, to enable a more complete description of the lithostratigraphy and to better understand the depositional processes acting upon the sediment within the study area. Particle size, along with organic content (LOI 550) analyses can also provide additional information when assessing the preservation and distribution of foraminifera (Zong & Horton, 1999; Edward & Horton, 2006).

3.3.2.1 Preparation for Particle Size Analysis

Approximately 1 g of sediment was treated with 30% hydrogen peroxide (H_2O_2) and heated on a hotplate to remove any organic material. H_2O_2 was continually added in small volumes to the samples until the reaction stopped, indicating that all the organic material had been oxidised. Samples were then washed with distilled water and

transferred into test tubes for analysis. All samples were then analysed using the Malvern Mastersizer Hydro 2000 laser granulometer, following the standard operating procedures of the equipment. Prior to analysing the samples, the granulometer was calibrated with standard sand (0.152-0.422 mm in size) to confirm the consistency and reliability of the granulometer. Each sample was also sonicated for five seconds to obtain an even dispersion before analysis. Measurements for each sample were undertaken in triplicates and averaged from the values. The data was then subdivided into clay, silt and sand fractions (Wentworth, 1922; Friedman & Sanders, 1978), and plotted against altitude (m OD) for both fossil and contemporary samples using TILIA 2.0.41 and TILIA*Graph (Grimm, 1991; 2004), C2 Version 1.7.7 (Juggins, 2007) and PAST Version 3.17 (Hammer *et al.*, 2001).

3.3.3 Foraminiferal Analysis

The following sections summarise the techniques used for foraminiferal analysis, including the sample preparation, counting and identification.

3.3.3.1 Preparation of Foraminiferal Samples

Foraminiferal samples preparation followed standard techniques (e.g. Scott & Medioli, 1980; Gehrels *et al.*, 2001 and Horton & Edwards, 2006). Samples with a volume of 2 cm^3 (measured through water displacement) were sub-sampled from the cores and sieved through a 250 µm sieve above a 63 µm sieve. The material collected in the 250 µm sieve was discarded, and that collected in the 63 µm sieve was washed with distilled water and transferred into a 250 ml beaker for analysis. Samples were stored in test tubes with two drops of 30% ethanol to prevent any fungal growth. If the abundance of foraminifera per sample was deemed to be too high, a wet splitter was used to divide the sample into eight smaller parts to avoid errors in counting and identification.

Contemporary surface samples were prepared for analysis within several days of returning from fieldwork to preserve the living and dead assemblages. 2 cm^3 of the contemporary surface sample (consistent with the fossil samples analysed) was prepared. Two drops of 30% ethanol were added to the samples to prevent any fungal growth and a few drops of Rose Bengal solution added to stain the living

foraminifera. Only the dead foraminiferal counts were used in the data analysis as they reduce the effect of seasonal fluctuations which may affect the final assemblage distributions (Edward & Horton, 2006).

3.3.3.2 Counting and Identification of Foraminiferal Samples

Foraminiferal samples were wet counted using a spiral counting tray under a low-powered microscope (magnification between 32x and 120x) with adjustable magnification (ZEISS AxioZoom V16). A minimum count of 200 specimens, where possible, was undertaken for each sample. Foraminiferal individuals of interest were picked out and placed on a glued slide to assist in further identification or for photographic purposes. Foraminiferal species were identified following the taxonomy in Murray (1971; 2000) and Horton & Edwards (2006).

3.3.4 Pollen and Spore Analysis

Pollen and spore analyses were used in this research to investigate past vegetation changes of the study sites, providing an environmental context and general chronology for the time the sediments were deposited. Pollen grains that have accumulated over time are representative of past vegetation in the area and can often be found in peat in stratigraphic sequence. Combined with radiocarbon dating, geographical patterns of vegetation change can then be established and this can be related to broader environmental changes in the area.

3.3.4.1 Preparation of Pollen and Spore Samples

Samples were prepared using the procedures described by Moore *et al*. (1991). One *Lycopodium* tablet was added into each test tube and dissolved with 5 ml of distilled water. Approximately 1 cm^3 of sediment (measured through water displacement) was added into each test tube. Samples were centrifuged and excess liquid was decanted off. 5 ml of 10% potassium hydroxide was added into each test tube, heated in a boiling water bath for 20 minutes and stirred occasionally to prevent clumping. After cooling, the samples were centrifuged and excess liquid was decanted. Samples were sieved through a 180 µm and 10 µm mesh, discarding the residual in the 180 µm sieve and retaining any material collected in the 10 µm mesh. Samples were washed

with a small amount of 10% hydrochloric acid (HCl) to remove any carbonates present. Samples were then washed with distilled water and poured back into their respective test tubes.

Samples were centrifuged and excess liquid was decanted. 5 ml of glacial acetic acid was added into each test tube to rehydrate the samples and the samples were then centrifuged and decanted again. A mixture of acetic anhydride and concentrated sulphuric acid in a 9:1 ratio was added into each test tube and placed in a boiling water bath for a maximum of 3 minutes. Samples were centrifuged, decanted and washed with 5 ml glacial acetic acid. The centrifuging and decanting process with the glacial acetic acid was repeated to remove any residual acid. Samples were then washed, centrifuged and decanted with distilled water for a further three times.

For very minerogenic samples, density separation was undertaken. 5 ml of a 1.95 mL^{-1} low toxicity sodium heteropolytungstate dissolved in water was measured into each sample and agitated with a vortex mixer. Samples were centrifuged at 1800 rpm for 20 minutes and the supernatant (pollen sample) decanted carefully into another labelled test tube. Both samples and residue were washed three times with distilled water and centrifuged. To aid counting, samples were stained with one drop of saffranine and centrifuged and decanted to remove excess liquid. Samples were then pipetted into epindorfs and liquid glycerol added to cover the sample. The pollen sample was then mounted onto a slide for counting.

3.3.4.2 Counting and Identification of Pollen and Spore Samples

Pollen grains and spores were counted using a high powered microscope with x400 magnification (Olympus BX43). A total of 300 pollen grains and spores were counted and identification of pollen grains followed Faegri & Iversen (1989) and Moore *et al*. (1991).

3.4 Fossil Foraminiferal and Pollen Data Analyses

Foraminiferal and pollen distribution plots for each palaeo site were drawn using C2 Version 1.7.7 (Juggins, 2007) and TILIA 2.0.41 and TILIA*Graph (Grimm, 1991; 2004). For both foraminifera and pollen, only species that exceeded 5% and 3% abundance respectively in at least one sample were included in the final analysis to avoid effects of insignificant species on the statistics (Horton & Edward, 2006). For foraminifera, samples with fewer than 40 individuals were also excluded from data analysis for both fossil and contemporary samples to avoid the effects of the low counts on the statistical analysis undertaken, as they may not be fully representative of the assemblage composition of the area (Horton & Edwards 2006).

The zonation of the pollen assemblages was calculated using Constrained Incremental Sum of Squares (CONISS) cluster analysis using TILIA 2.0.41 and TILIA*Graph (Grimm, 1991; 2004). CONISS divides the microfossil assemblages stratigraphically and statistically into zones, eliminating any subjectivity (Bennett, 1999). CONISS analyses were undertaken using no data transformation (Euclidean distance) for the data transformation/dissimilarity coefficient. CONISS analyses undertaken on fossil microfossil data were constrained by sample depths which divided the assemblages into zones throughout the core.

3.5 Radiocarbon Dating

Radiocarbon dating was used to develop a chronology for the reconstruction of Holocene sea-level and environmental changes at the study sites. Samples for radiocarbon dating were selected mainly based on biostratigraphical and lithostratigraphical changes. All samples submitted for radiocarbon dating were in the form of bulk sediment, obtained from ~1 cm thick slices and ~2 g in wet weight of the sediment apart from sample CGF-136/141 which was dated on a piece of wood present in the sediment. Radiocarbon ages were analysed at DirectAMS Radiocarbon Dating Service in Washington, USA using accelerator mass spectrometers (AMS) designed specifically for radiocarbon. Radiocarbon ages obtained were then calibrated using OxCal v.4.3 (Ramsey, 2009) and the IntCal13 atmospheric curve (Reimer *et al.*, 2013). All dates were calibrated to cal BP.

Chronologies and age-depth models for each palaeo site were established based upon the dated samples in respective sediment cores using the software package Bacon v.2.3.4 in R. Bacon is a Bayesian age-depth model that uses the Bayesian statistical method for the reconstruction of accumulation history of the sediment core and its age estimates (Blaauw & Christen, 2011). As opposed to linear or polynomial regression and weighted splines provided by software such as Clam (Blaauw, 2010), Bayesian age-depth modelling is considered to be a more detailed approach which takes into consideration the changes in sedimentation.

Markov Chain Monte-Carlo (MCMC) methods computed by Bacon provide analysis of the age-depth model (Blaauw & Christen, 2011). For all the palaeo sites investigated, the age-depth models were only established between dated horizons, and did not extend to the uppermost date and the core surface due to the unknown deposition rates as no age information is available for the core surface as there is the potential for erosion or reworking of the land surface.

3.5.1 Sources of Errors in Radiocarbon Dating

Lowe & Walker (2015) identified several possible sources of error when utilising radiocarbon as a dating method which include: temporal variation in ^{14}C production, circulation of marine carbon and contamination.

The most important assumption in radiocarbon dating is that the concentration of ^{14}C carbon in the atmosphere is consistent (or changed minimally) over time. However, this is untrue as previously evidenced by the age comparison of dating methods between radiocarbon and dendrochronology and it has been found that concentrations of ^{14}C in the atmospheric have fluctuated during the Holocene (Reimer *et al.*, 2004). Therefore, it is necessary to differentiate between 'radiocarbon years' and 'calendar years' when explaining the age of a sample, and ultimately calibrating the radiocarbon ages is required.

The marine reservoir effect occurs when samples from the deeper part of the ocean have an older date compared to those on or near the surface. ^{14}C is transferred from the atmosphere into the ocean through the ocean's surface, and mixing between warm, surface water and cold, deeper water is very slow. This causes the ^{14}C in the

deeper part of the ocean to decay without replenishment (Lowe & Walker, 2015). Therefore, terrestrial and marine samples must not be compared directly without first correcting for the marine reservoir effect.

Factors such as glacial melt and the hardwater effect may also contribute to contamination of older carbon during radiocarbon dating resulting in ages older than they actually are. Contamination of younger radiocarbon ages are also possible through, for example, roots penetrating into deeper sediments, infiltration of younger humic acid through sediment horizons and bioturbation (Törnqvist, 1992; Lowe & Walker, 2015).

For organic rich sediments (e.g. peat), dating bulk samples have been shown to produce less accurate ages with larger uncertainties when compared to the dating of plant macrofossils (Törnqvist, 1992; Björck *et al*., 1998; Nilsson *et al*., 2001). Fluvial input of older and reworked organic debris into siliciclastic material at the site investigated may also result in an aging effect of the dated sample (Törnqvist, 1992). For comparison in the accuracy between the dating of organic rich bulk samples and macrofossils, Hu (2010) conducted statistical analyses on the ^{14}C ages obtained from bulk samples and macrofossils in Törnqvist (1992). Based on the result obtained by Hu (2010), an additional error of ±100 ^{14}C was applied to organic rich bulk samples from Törnqvist (1992), in order to account for uncertainties associated with various types of samples contamination has been recorded previously (Lowe & Walker, 2015).

3.6 Contemporary Foraminiferal Distribution

Transfer functions are a quantitative approach that estimate the optimum value of a fossil sample against an environmental variable, by comparison of the same variable against a contemporary sample collected from the present day environment. To reconstruct Holocene sea-level changes at each palaeo study site in this study, a foraminifera-based transfer function was developed to provide the palaeo marsh surface elevation (PMSE) of the fossil samples based on the sample's contemporary counterpart obtained from three saltmarshes located near to the palaeo study sites. A series of statistical analyses were undertaken on the contemporary surface data prior to the development of foraminiferal transfer function.

3.6.1 Vertical Distribution of Contemporary Foraminiferal Samples

Multivariate methods of unconstrained cluster analysis based on unweighted Euclidean distance, using no transformation or standardisation of the percentage data was undertaken to describe and classify the vertical distribution of foraminifera at each of the modern marsh sites based on the species assemblage (i.e. classifying the foraminiferal distribution into high saltmarsh environment, low saltmarsh environment or intertidal mudflat/tidal flats environment). The unconstrained cluster analysis classifies the contemporary foraminiferal samples into clusters or zones along each transect (e.g. Avnaim-Katav *et al.*, 2017). Cluster analysis was undertaken using TILIA 2.0.41 and TILIA*Graph (Grimm, 1991; 2004).

3.6.2 Influence of Elevation on Foraminiferal Assemblages

Canonical Correspondence Analysis (CCA) and partial CCA were undertaken on the contemporary surface samples with their respective environmental variables which included elevation, LOI 550, silt and sand fractions (particle size) and pH (in line with Horton & Edwards, 2006; Zong & Horton, 1999). CCA is a multivariate analysis method used to explain and measure the relationships between the foraminiferal species assemblages and their measured environmental variables (ter Braak, 2014). The ordination axes produced are a linear combination of the environmental variables and the species' assemblages variations are directly related to changes in these environmental variables (Horton & Edwards, 2006). The lengths and positions of the arrows in a CCA biplot provide information on the relationship between the original environmental variables and the derived axes. Arrows that are parallel to an axis indicate a correlation and the length of the arrow shows the strength of that correlation. CCA was also undertaken to show the total percentage of variation within the foraminiferal species assemblages that can be explained by the measured environmental variables.

A series of partial CCAs were then undertaken to divide the total variation of contemporary data into three components: contribution of individual measured environmental variables; the intercorrelation between the measured environmental variables and the unexplained variance (Edwards & Horton, 2006). Intercorrelation between the measured environmental variables is represented by the remainder

variance after the cumulative variance (explained from individual measured environmental variables) was extracted from the total explained variations. CCA and partial CCAs were undertaken using CANOCO 5 (ter Braak and Smilauer, 2002).

3.6.3 Determination between Linear or Unimodal Methods

Foraminiferal taxa or assemblages that exhibit a unimodal response have a Gaussian distribution along an environmental gradient, with peaked abundance at a preferred or optimum environmental variable, while those exhibiting a linear response show that the foraminiferal abundance increases or decreases with the environmental gradient. It is therefore crucial to select the appropriate model which best describes the distribution of foraminifera within the training sets (contemporary data that are used to develop a transfer function).

Detrended canonical correspondence analysis (DCCA) was used to provide information on how species assemblage composition changes along the environmental gradient. The detrending by segments and using nonlinear rescaling, resulted in length of resulting DCCA axis one as an estimate of gradient length expressed in standard deviation (SD) units. If the gradient length of axis one is more than two standard deviations, a unimodal response method or model are deemed the most appropriate method to describe the training sets (Birks, 1995; Horton & Edwards, 2006; Barlow *et al.*, 2013).

DCCA analysis was undertaken using the CANOCO 5 software (ter Braak and Smilauer, 2003), with elevation as the only environmental variable (Birks, 1995; Horton & Edwards, 2006). For DCCA analysis and the resulting development of the transfer function (Section 3.7), the only environmental variable considered was elevation. This is because foraminiferal assemblages are ultimately related to elevation, a proxy of the frequency of tidal flooding in the area. All other environmental variables (e.g. salinity, pH, organic content and particle size) that determine the distribution of foraminifera are essentially related to tidal submergence of the area (Horton & Edwards, 2006), and are therefore also partially correlated with the elevation of the marsh. The distribution of foraminifera in a saltmarsh can be identified in different vertical zones, which depends on the dominant species assemblages found at each zone identified at respective marsh.

Transfer function regression and calibration as well as the assessment of modern analogue were then undertaken using the software C2 Version 1.7.7 (Juggins, 2007) to establish a numerical value of the variable in question (elevation for this study), based on the elevation optima of foraminifera found in the three contemporary saltmarshes.

3.7 Development of Transfer Function

The transfer function used in this study was developed using C2 Version 1.7.7 (Juggins, 2007). A local training set was developed from the contemporary samples collected in this study, obtained from Skinburness Marsh, Cardurnock Marsh and Bowness Marsh. A summary of the steps in the development of the transfer function (explained further in the following Section 3.7.1) is shown in Figure 3.2 below:

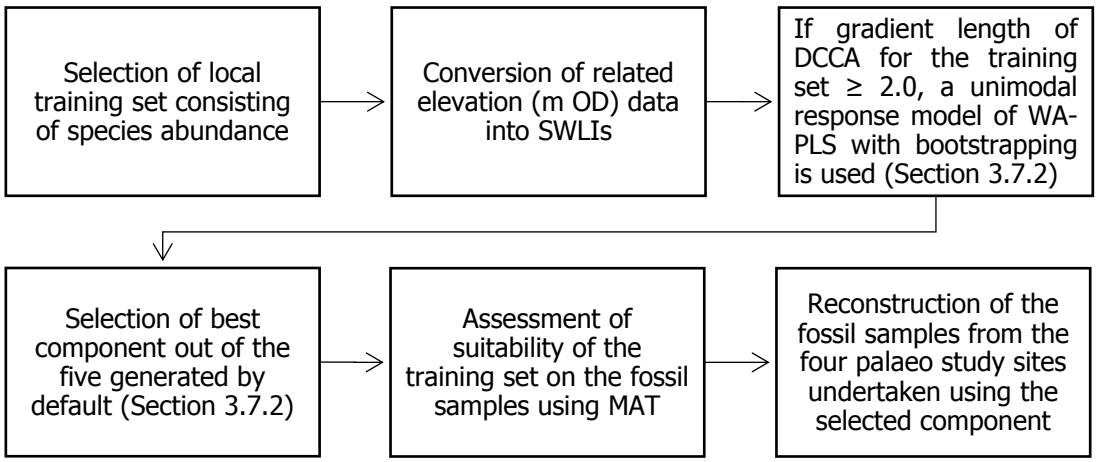

Figure 3.2: Summary of steps in the development of the transfer function. Abbreviations: SWLI = standardised water level index, DCCA = detrended canonical correspondence analysis, WA-PLS = weighted-averaging partial-least-squares, MAT = modern analogue technique

3.7.1 Considerations for Transfer Function

It was important when combining the datasets to be taxonomically consistent (using the complete taxonomic name for each species). Initial data screening was undertaken to remove samples with low counts (samples with fewer than 40 individuals), insignificant species (species that occur fewer than 5% in at least one sample) and shelf species (not agglutinated or calcareous saltmarsh species) that can be deposited into the marsh area by tidal wash and therefore wrongly classified as marsh species.

The different tidal ranges measured at the three contemporary saltmarshes were converted into sea water level index (SWLI) thus eliminating the variation in tidal range between the different locations. The SWLI equation used in this study followed Zong & Horton (1999):

$$SWLI_{ab} = [((A_{ab} - MTL_b) / (MHWST_b - MTL_b) \times 100) + 200]$$

Where $SWLI_{ab}$ is the SWLI of sample *a* at site *b*; A is the altitude (m OD) of sample *a* at site *b*; MTL_b is the mean tide level of site *b* (m OD); $MHWST_b$ is the mean high water spring tide value at site *b* (m OD). The addition of the constant (200) is to ensure that all SWLI calculated are positive. Using this equation, if altitude of the sample point is equal to MTL and MHWST, the SWLIs value will be 200 and 300 respectively. This SWLI equation was used in this study as it produced all positive SWLI values when combining tidal values from all the sites, as opposed to those in Horton & Edwards (2006) and Barlow *et al*. (2013). The relationship of the different tidal level is shown in Figure 3.3 below.

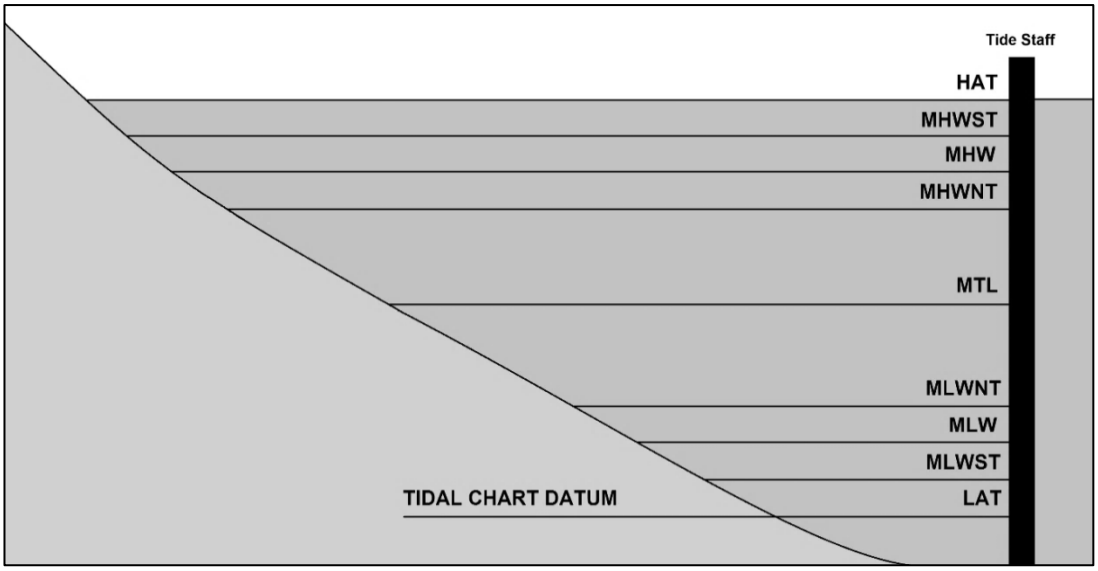

Figure 3.3: Tidal-level definitions used in this study. Abbreviations: HAT = highest astronomical tide, MHWST = mean high water spring tide, MHW = mean high water, MHWNT = mean high water neap tide, MTL = mean tide level (calculated as average of MHWST, MLWST, MLWNT and MLWST), MLWNT = mean low water neap tide, MLW = mean low water, MLWST = mean low water spring tide and LAT = lowest astronomical tide

3.7.2 Response Model and Transfer Function Selection

Based on the results of DCCA gradient length of > 2.0 obtained in this study (Table 3.2), a unimodal response model was selected for the development of all of the transfer functions in this study. The technique used to develop the transfer functions was weighted-averaging partial-least-squares (WA-PLS) with bootstrapping. The local Solway training set was used to develop the transfer function for this study, consisting of foraminiferal and elevation data from the three contemporary saltmarshes.

Table 3.2: Results of DCCA analysis for individual and the complete training set

Training Set	DCCA Axis 1 Length
Skinburness Marsh	2.25
Cardurnock Marsh	2.23
Bowness Marsh	2.52
Solway Training Set	2.60

The basic concept of the weighted-averaging method is that individual species will have their highest distribution at points where the environmental condition is optimum and lowest where the environmental condition is unfavourable. The optimum value is calculated as the average of the environmental variable's value where each individual species occurs, based or weighted by the species abundance. Weighted averaging method has previously been employed to develop foraminifera-based transfer functions for sea-level studies in Britain (Horton *et al.*, 1999; Edwards & Horton, 2000; Gehrels *et al.*, 2001; Horton & Edwards, 2006).

However, some correlations remain between the observed and predicted environmental values which will not be taken into consideration when using the weighted-averaging (WA) method. When a different environmental variable, pH for example, has an influence on foraminiferal species distribution, scatter will occur when the observed SWLI is plotted against the predicted SWLI, as opposed to an ideal linear relationship. This departure from the linear relationship between observed and predicted SWLI is termed the prediction residual (Horton & Edwards, 2006). The partial-least-squares (PLS) method uses these residuals to improve the correlation between the environmental variable and species abundance (Shennan *et al.*, 2015).

The coefficient of determination (r^2) and the root mean squared error (RMSE) utilises the whole dataset when developing the transfer function and when testing its performance. Bootstrapping (1000 cycles) is employed to assess the predictive abilities of the transfer functions developed by using the cross validation resampling method. Bootstrapping cross validation produces root-mean-square error of prediction (RMSEP) values, which are the predicted vertical errors for individual samples (Barlow *et al.*, 2013). The model outputs were therefore firstly assessed to determine the best performing component out of the first five components produced in C2 Version 1.7.7 (Juggins, 2007).

Improved performance between the components can generally be defined as a reduction of 5% in root-mean-square error of prediction (RMSEP) values and an increase in the bootstrapped coefficient of determination (r^2_{boot}). The bootstrapped r^2 value is considered to improve confidence in the value as it is based upon 1000 cycles of pseudo-replicate datasets (Barlow *et al.*, 2013). Each transfer function developed would ideally consist of the component with the lowest RMSEP value (which suggest

improved model performance) and the highest bootstrapped coefficient of determination (r^2_{boot}) values for the most accurate estimation of SWLIs.

The training set data can be screened again if desired to improve the model performance by removing samples that may cause less accurate reconstructions. Some samples may show a poor relationship with SWLI for several reasons including stronger effects of other environmental variables (e.g. pH or LOI) on the assemblage's distribution (Horton & Edwards, 2006). Samples with a poor fit with absolute residual SWLI (observed SWLI minus predicted SWLI) values greater than the standard deviation of all SWLI in the training set may also be removed from the training set (Edwards *et al.*, 2004; Gehrels *et al.*, 2005; Horton & Edwards, 2006).

3.8 Modern Analogue Technique

Values of RMSEP and r^2_{boot} are used to measure the performance of components and the transfer function developed. These values do not confirm or explain how reliable or realistic the estimated PMSE produced for each sample are (Horton & Edwards, 2006). Reconstruction of the estimated PMSE for fossil samples can be done within the transfer function, derived from the measured elevation of the training set (by comparing the fossil assemblages' distribution and the training set assemblages' distribution). It is therefore important to assess how suitable the estimated fossil PMSE values are.

The greater the dissimilarity between the fossil sample's species distribution to the training set's species distribution, the greater the error in the resultant estimated PMSE for the fossil sample will be, as the transfer function was forced to extrapolate more of the training set data. In this study for example, all the calcareous species in the fossil samples were dissolved by the acidic pore waters (leaving only the test linings behind), making identification impossible. The lack of calcareous species in the fossil samples therefore might have resulted in a larger extrapolation of the training set data to provide an estimate of PMSE for the fossil samples. The resulting PMSE estimates should therefore be treated with caution (Edwards & Horton, 2000; Horton & Edwards, 2006).

Dissimilarity between the fossil samples and the contemporary foraminiferal samples were calculated using the Modern Analogue Technique (MAT) using C2 Version 1.7.7 (Juggins, 2007). In this study, MAT was used to calculate the dissimilarity between the fossil sample and the ten most similar modern samples using the squared chord distance method as the dissimilarity coefficient. The squared chord method was used as it maximises the signal to noise ratio when used with percentage data (Birks, 1995; Edwards & Horton, 2000; Horton & Edwards, 2006). Samples with coefficient values below the 10th percentile were considered to have good modern analogues, those with coefficient values below the 20th percentile were considered to have close modern analogues, and those with coefficient values above the 20th percentile were considered to have poor modern analogues (Edwards & Horton, 2000; Horton & Edwards, 2006; Shennan *et al.*, 2015).

3.9 Sea-Level Index Points

Sea-level index points (SLIPs) are individual sea-level reconstructions based on quantified age and vertical uncertainties. They are an estimation of the relative sea-level (RSL) positions in space and time. SLIPs can be used to describe the overall trends and patterns of RSL in a region (Horton *et al.*, 2013) and are established through a combination of lithostratigraphic, chronostratigraphic and biostratigraphic data (Edwards, 2006).

RSL reconstructions are based on sea-level proxies (foraminiferal distribution and lithology for this study) and their indicative meaning can be derived from modern analogues within a transfer function or through the combined information on lithostratigraphy and biostratigraphy of a sample. The indicative meanings of the sea-level proxies describe their relationship to elevation within the tidal frame. The indicative meaning is comprised of a tidal datum midpoint (the reference water level) and a vertical range (the indicative range). Indicative range is the altitudinal range over which the index point's proxy could have occurred (Lloyd *et al.*, 1999; Horton *et al.*, 2013).

Samples used to calculate SLIPs in this study are based on either the presence, absence or changes in the distribution of the saltmarsh foraminiferal species observed in the fossil core, combined with the lithology observed in the core. If the predicted

reference water level and indicative range produced from the transfer function are deemed not suitable (e.g. high number of samples with poor modern analogues in the training set), the reference water level and indicative meaning for the sample can be estimated based on the zonation of foraminiferal assemblages with reference to tidal submergence of the respective contemporary sites combined with the changes in lithostratigraphy related to the respective sample. A general schematic representation of the indicative meaning is shown in Figure 3.4 (based on Engelhart & Horton, 2012).

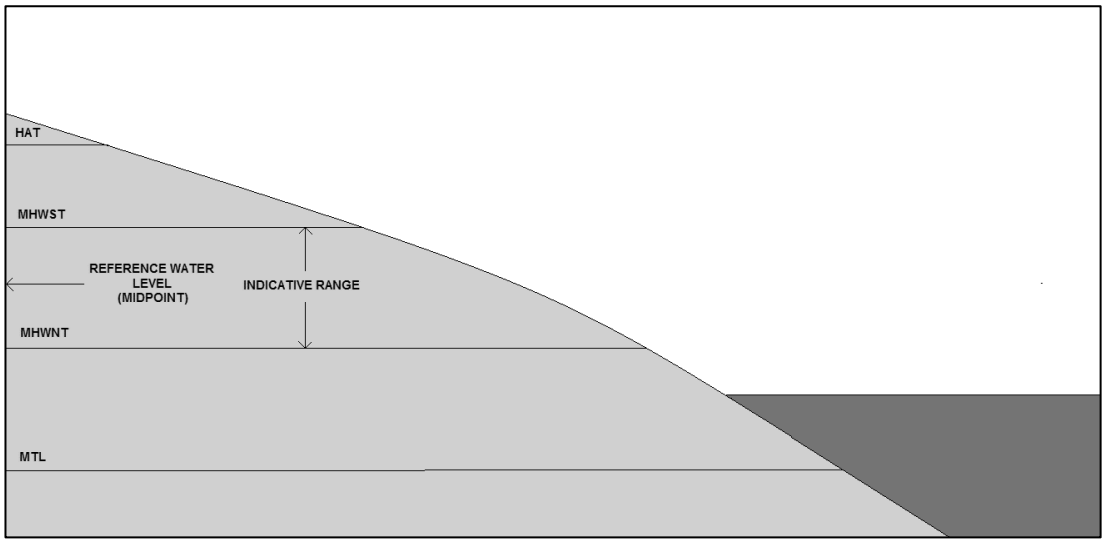

Figure 3.4: Schematic representation of the indicative meaning of foraminiferal species found at different marsh zones. Abbreviations: MHWST=Mean high water spring tide; MHWNT =Mean high water neap tide; MTL=Mean tide level; HAT=Highest astronomical tide

SLIPs are calculated following the equation in Horton *et al*. (2013):

$$RSL\ (m) = H\ (m\ OD) - RWL\ (m\ OD)$$

Where H is the altitude of the sample (subtracted from surface altitude of the core, based on depth of the sample down the core) and RWL is the altitude of reference water level of the sample (mid-point of the indicative range).

Several sources of error need to be taken into consideration when calculating the SLIP of a sample. Barlow *et al*. (2013) summarised the possible errors: surveying; angle of the borehole; measuring sample depth; overlying sediment compaction; core compaction; extrapolating tidal range estimates over large distances or in an area with a large tidal range; changes in the water table; uncertainty in identifying the correct tidal datum for the indicator of interest and changes in tidal regime and change in vegetation types over time. Some of the vertical errors are not relevant when calculating SLIPs from only one saltmarsh (e.g. tidal range correction). However, if SLIPs from several study sites, or from sites located within an estuary or different regions with varying tidal range are plotted on a single sea-level curve, vertical errors needs to be considered to avoid misinterpretation of RSL change, to provide consistency and to allow correlation between sites (Barlow *et al*., 2013).

The total error is calculated using the equation:

$$E = (e_1^2 + e_2^2 + e_3^2 + e_n^2)^{1/2},$$

Where E is the total error for a sample, and e_1-e_n are individual sources of errors for the sample (Barlow *et al*., 2013; Engelhart & Horton, 2012). Each SLIP in this study was calculated including the errors shown in Table 3.3 (based on Barlow *et al*., 2013; Engelhart & Horton, 2012; Lloyd *et al*., 1999).

Table 3.3: Sources of vertical error for the SLIPs in this study

Source of Error	**Example**	**Magnitude**
Altitude	High precision surveying (e.g. total station)	± 0.05 m
Core collection	Angle of borehole	± 1% overburden
	Sampling error	± 0.01 m
	Compaction due to coring (for Russian hand corer)	± 0.01 m
Sample	Thickness of sample	Half of sample thickness

3.9.1 Correction for Post-Depositional Lowering of Sediments

Post-depositional lowering caused by the compression of sediments under their own weight (when samples are obtained from unconsolidated peat sequences) is also an important vertical error that needs to be considered. SLIPs that are affected by compaction are displaced and lowered from their original altitude, consequently lowering the RSL reconstruction and overestimating the rate of increased RSL (Edwards, 2006; Tornqvist *et al*., 2008; Horton & Shennan, 2009; Horton *et al*., 2013; Brain *et al*., 2011; 2012 and 2015). Discrepancies between geological reconstructions and model estimations of RSL can be explained by the effect of sediment compaction on the SLIPs (Shennan *et al*., 2000; Shennan & Horton, 2002; Edwards, 2006). Sediment compaction is more common for intercalated samples from organic sediment that is easily compressible and enclosed between two clastic units. Basal samples from organic sediment sequences that overlay an incompressible substrate (i.e. bedrock) have minor or negligible effect of sediment compaction (Brain *et al*., 2017). Methods to estimate and potentially correct sediment compaction require quantitative information about the sediment type overlying and underlying the dated sample, which was not available for other SLIPs in the region. Post-depositional lowering corrections are therefore only applied to SLIPs produced in this study when plotted against the other available SLIPs in the region.

To correct for errors resulting from sediment compaction, this study employed the geotechnical modelling framework developed by Brain *et al*. (2011, 2012) to provide estimates of compaction-induced post-depositional lowering (PDL) downcore. The geotechnical decompaction approach employed here used the relationships between LOI and sediment compression properties reported by Brain *et al*. (2012) for three saltmarsh sites in the United Kingdom. On the basis of downcore measurements (0.02 m layer thickness) of LOI, it is possible to assign compression properties to each layer in the core and, subsequently, run decompaction algorithms to provide depth-specific estimates of PDL, which is the height correction that is added to the *in situ* elevation of each sample used to reconstruct RSL. The modelling employs a Monte-Carlo framework (5000 model runs) and specified uncertainties in input parameters to determine errors in each of these model outputs. LOI of each layer in each model run was sampled from a uniform probability distribution defined by the median value in each lithostratigraphic unit observed in the core; uncertainty was expressed as ± half

the range of observed values in each unit. Yield stress in each layer in each model run was sampled from a triangular probability distribution using values reported for Roudsea Marsh, UK, by Brain *et al*. (2012), since this site is geographically located close to the sites studied here. The specific gravity, G_s, in each modelled layer was estimated using the relationship with LOI provided by Hobbs (1986) (Brain, personal communication 23rd May 2018).

3.9.2 Correction for Changes in Palaeo-Tidal Range

If tidal range at the study sites was greater in the past, the reference water level assigned to the sea-level index points would also be greater, resulting in a lower relative sea-level of the calculated SLIPs. Failing to account for the changes or increase in tidal range through time would therefore lead to an underestimation of the altitude of relative sea level during the study period (Horton *et al*., 2013).

Palaeo-tidal data for the study area was predicted using the Fluidity model, a highly flexible finite element or control volume modelling framework which allows for the numerical solution of a number of equation sets (Piggott *et al*., 2008). Fluidity was used to model the tidal range using a palaeobathymetry constructed from General Bathymetric Chart of the Ocean (GEBCO) modern bathymetry/topographic data and accounting for relative sea-level change using the GIA model of Bradley *et al*. (2011), following Hill *et al*. (2014). Tides were calculated for the selected locations along the coastline of the Solway Firth and northwest Cumbrian region, in time slices at 1000 year intervals from 10 to 1 ka BP and the model forced at the continental shelf boundary using modern tidal data. Model simulations were spun-up for 30 days and then tidal range calculated using a further 30 days simulation time (Hill, personal communication 8th May 2018).

All SLIPs produced in this study were corrected for palaeo-tidal changes from the model developed by Hill (Personal communication 8th May 2018). The existing SLIPs from the northern and southern shore of the Solway Firth (from Shennan *et al*., 2018) were also corrected for palaeo-tidal change throughout the Holocene, to refine the RSL data observed and to highlight the importance of quantifying the change in tidal range over time (Chapter 10).

3.10 Summary

This chapter has summarised the methods and techniques employed in this study, including the selection of the study sites, field, laboratory and microfossil analyses. Methods for the reconstruction of Holocene relative sea level through the development of transfer function and calculation of sea-level index points were also presented.

CHAPTER 4

CONTEMPORARY FORAMINIFERAL DISTRIBUTION

4.0 Introduction

This chapter details the foraminiferal distribution and the environmental parameters of the surface samples collected from contemporary saltmarshes located near to the palaeo study sites. The saltmarshes studied were Skinburness Marsh, Cardurnock Marsh and Bowness Marsh. A total of 72 contemporary surface samples were collected from the three marshes, with eight major species of foraminifera identified.

4.1 Contemporary Marshes in the Solway Region

In the Solway Firth region, saltmarshes extend along the coastline from Grune Point at the mouth of Moricambe Bay to Gretna, located at the most inner point of the Solway Firth. The marshes along this coastline include Skinburness Marsh, Calvo Marsh, Newton Marsh, Anthorn Marsh, Cardurnock Marsh, Bowness Marsh, Burgh Marsh and Rockcliffe Marsh (Figure 4.1). Most of these marshes are grazed by cattle during spring and summer to manage the vegetation.

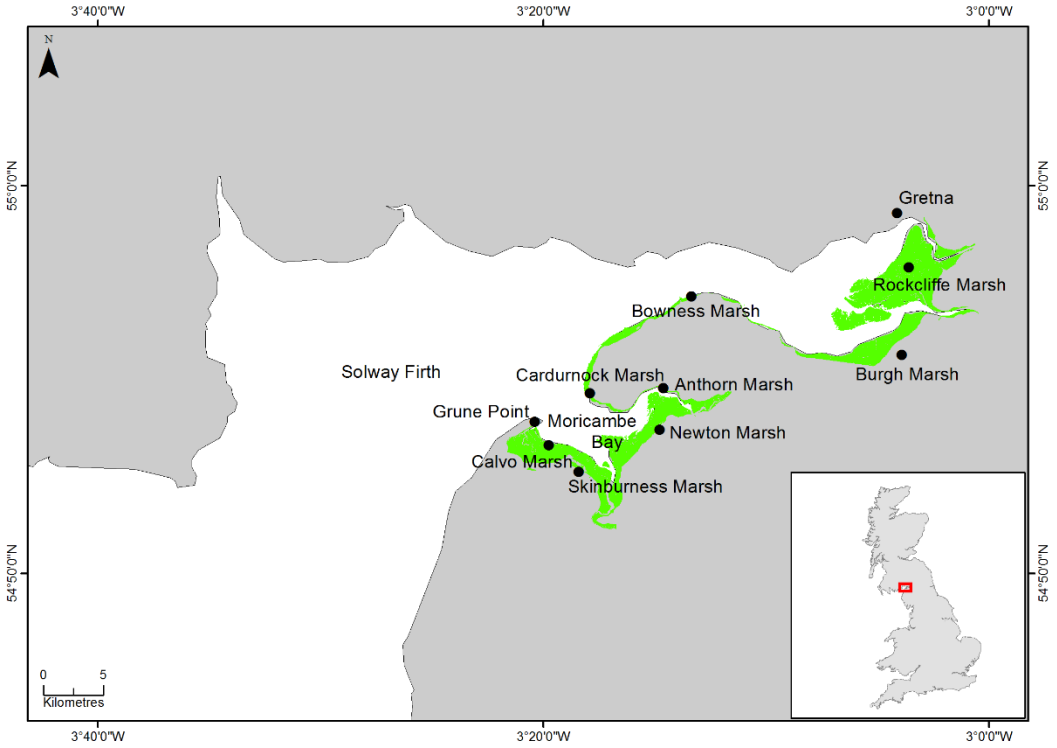

Figure 4.1: The green shaded areas are the estimated cover of contemporary saltmarsh in the region, along the coastline of Moricambe Bay and the southern Solway Firth (Source: © Environment Agency copyright and/or database right 2015. All rights reserved. Available at https://data.gov.uk)

4.1.1 Skinburness Marsh (NY 1630 5517)

Skinburness Marsh is one of the largest areas of saltmarsh located on the southern bank of Moricambe Bay, spanning from Grune Point (NY 1411 5651) on the outer estuary to Brownrigg (NY 1764 5271) at the mouth of the River Waver (Figure 4.2). The origins of Skinburness Marsh can be dated to the early 19th century and possibly formed as early as the 14th century. In 1870-1872 John Marius Wilson's Imperial Gazetteer of England and Wales (GB Historical GIS / University of Portsmouth, 2018) described Skinburness Marsh as:

"Skinburness, a village in Holme-Cultram parish, Cumberland; on the coast, 1¾ mile northern northeast of Silloth railway station. It was anciently an important place, destroyed by an irruption of the sea about the beginning of the 14th century; and is now a sea-bathing resort, and a place of herring-fishery".

Figure 4.2: The three contemporary marshes in this study: Skinburness Marsh (blue), Cardurnock Marsh (red) and Bowness Marsh (purple). Black symbol are the sample points at each site (Source: © Environment Agency copyright and/or database right 2015. All rights reserved. Available at https://data.gov.uk)

Skinburness Marsh covers an area of approximately 2.745 km^2, including a complete and undisturbed marsh sequence from tidal flats to high marsh environment with the presence of tidal creeks. The transect sampled across Skinburness Marsh site covered the distance of approximately 650 metres from the back of the marsh towards the unvegetated tidal flats environment (Figure 4.3). Skinburness Marsh is characterised by a generally flat profile throughout the high to the lower marsh, ranging from 5.7 m OD at the high marsh to 4.6 m OD at the lower marsh and 3.7 m OD at the tidal flats. A total of 24 contemporary samples were collected across Skinburness Marsh.

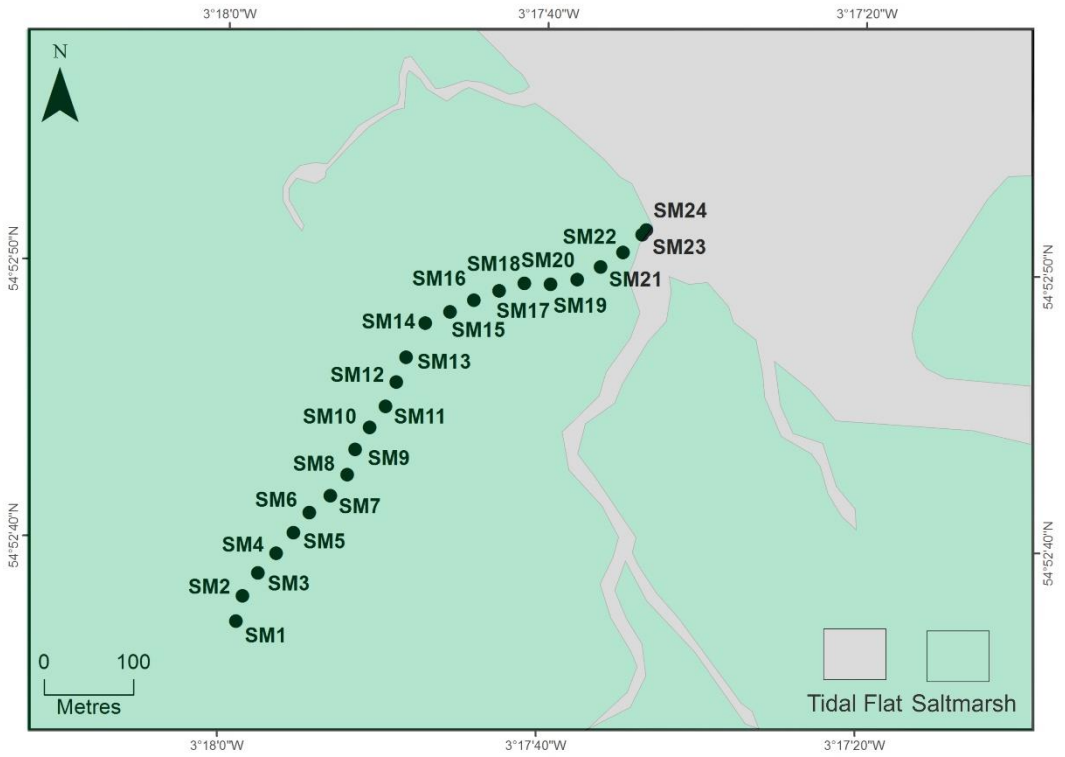

Figure 4.3: Skinburness Marsh transect with location of modern sample points indicated

The back marsh is bordered by *Ulex europaeus* (Gorse bush) towards the terrestrial area and most of the marsh area is dominated by *Puccinellia maritima* (Saltmarsh Grass), *Spartina anglica* (Common Cord Grass) and *Juncus maritimus* (Sea Rush), with patchy presence of *Sphagnum sp*. (Peat Moss), *Cochlearia officinalis* (Common Scurvy Grass), *Plantago maritima* (Sea Plaintain) and *Triglochin maritima* (Sea Arrow Grass). In the tidal creeks, *Cochlearia officinalis* (Common Scurvy Grass) and *Spergularia marina* (Lesser Sea Spurrey) can be found. The lowest vegetated saltmarsh zone is dominated mainly by *Suaeda maritima* (Sea Blite), *Tripolium pannonicum* (Sea Aster) and *P. maritima* (Sea Plaintain). In the mainly unvegetated tidal flats environment, patches of *Salicornia spp.* (Glasswort and Sea Asparagus) can be found.

4.1.2 Cardurnock Marsh (NY 1765 5759)

Cardurnock Marsh site is located on the northern bank of Moricambe Bay (Figure 4.2), covering an area of approximately 0.753 km^2 from Cardurnock (NY 1721 5880) to the mouth of the River Wampool in the inner Moricambe Bay estuary (NY 1894 5752).

The marsh is bordered by the construction of embankments and roads but a complete marsh sequence from high marsh to tidal flats is present.

The transect sampled across Cardurnock Marsh covered a distance of approximately 150 metres, from the high marsh to the mainly unvegetated tidal flats environments (Figure 4.4). Distinct elevation changes between areas along the saltmarsh and the tidal flats were observed, with the elevation decreasing south towards the estuary. Tidal creeks and waterlogged areas were present in the high marsh zone. The high marsh zone recorded an average elevation of 5 m OD, decreasing to 4 m OD in the mid/low marsh and 3 m OD in the tidal flats.

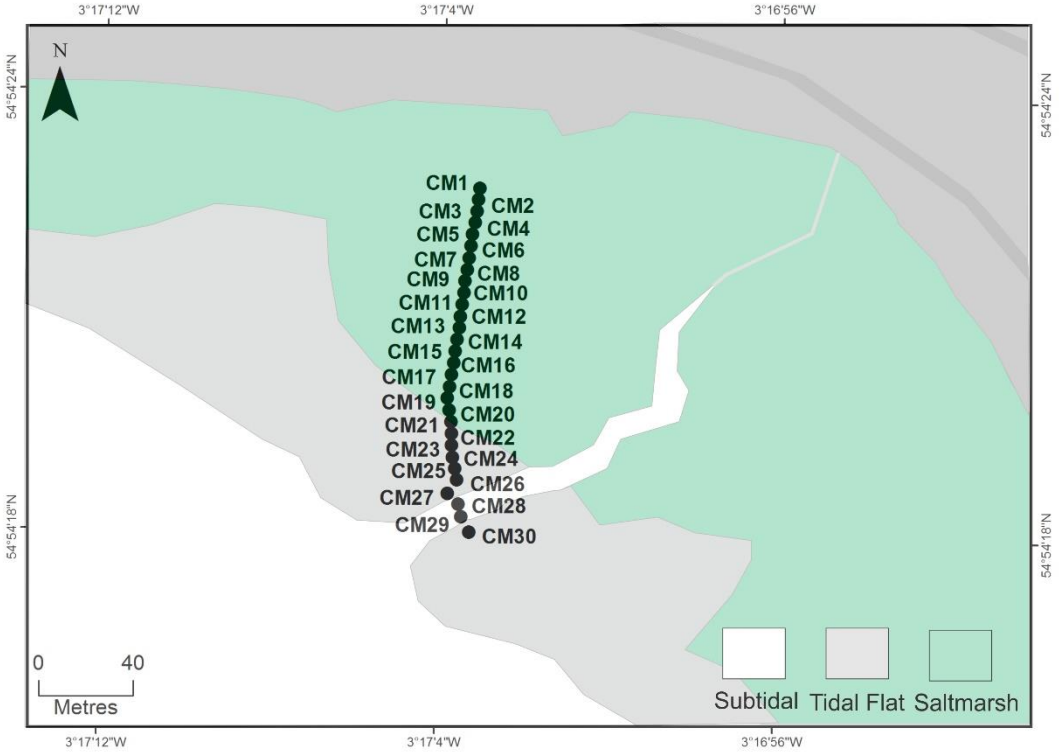

Figure 4.4: Cardurnock Marsh transect with location of modern sample points indicated

The back marsh is bordered by *U. europaeus* (Gorse bush) towards the land area and the high marsh zone is dominated by *P. maritima* (Saltmarsh Grass) and *J. maritimus* (Sea Rush). Moving down the transect from north to south, *C. officinalis* (Common Scurvy Grass), and *Aster tripolium* (Sea Aster) can be found, with *Glaux maritima* (Sea Milkwort) also present. This transitioned into a zone dominated mainly by *A. tripolium* (Sea Aster), *P. maritima* (Saltmarsh Grass) and *G. maritima* (Sea Milkwort). The presence of *A. tripolium* (Sea Aster), *S. anglica* (Cord Grass), *P. maritima*

(Saltmarsh Grass), *G. maritima* (Sea Milkwort) were then observed and an abundance of *C. officinalis* (Common Scurvy Grass) was noted in the tidal creeks. In the lowest zone of the marsh, the presence of *S. anglica* (Cord Grass) and patches of *Zostera noltii* (Dwarf Eelgrass) and *Enteromorpha intestinalis* (Gut Weed) were observed. In the mainly unvegetated tidal flats environment, patches of *Salicornia spp.* (Glasswort and Sea Asparagus) were also found.

4.1.3 Bowness Marsh (NY 2161 6258)

Bowness Marsh is located on the southern shore of the Solway Firth (Figure 4.2), spanning the area from North Plain (NY 1970 6167) to Bowness-on-Solway (NY 2226 6272). The marsh is separated into two by the now abandoned and dismantled railway track at Herdhill Scar (NY 2123 6266), with Campfield Marsh located west of the dismantled railway track. Bowness Marsh covers an area of approximately 0.262 km^2. Most of the marsh area is now bordered by an embankment and roads.

The transect sampled across the site at Bowness Marsh covers a distance of approximately 150 metres, from the high marsh zone towards the tidal flats (Figure 4.5). The rear of the marsh is bordered by an embankment and a road. A gently sloping hill is found on the opposite side of the road. The marsh has minimal elevation changes from the high to the lower marsh zones, ranging from 6.0 m OD at the high marsh to 4.0 m OD at the tidal flats.

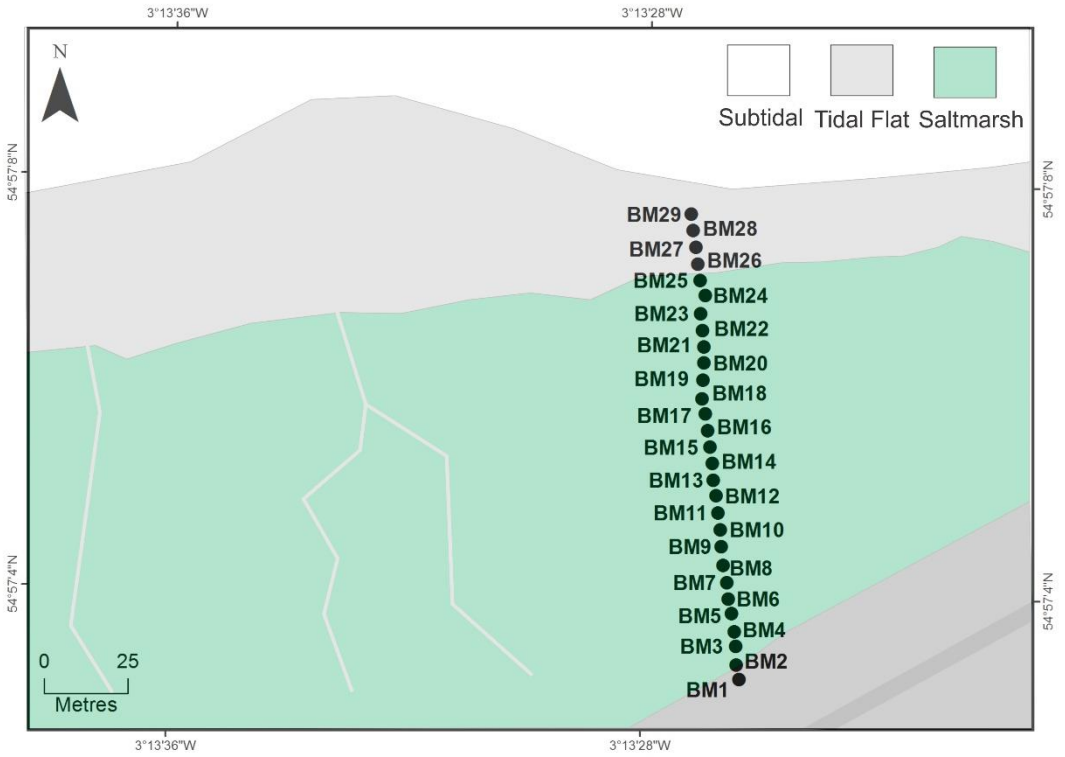

Figure 4.5: Bowness Marsh transect with location of modern sample points indicated

The rear of the marsh is bordered by *U. europaeus* (Gorse bush) towards the embankment area. The rear marsh is waterlogged, with species such as *P. maritima* (Saltmarsh Grass), *C. officinalis* (Common Scurvy Grass), *Festuca rubra* (Red Fescue), *T. maritima* (Sea Arrow Grass) and *J. maritimus* (Sea Rush) present. Moving along the transect from north to south, *P. maritima* (Sea Plaintain), *G. maritima* (Sea Milkwort) and *A. tripolium* (Sea Aster) were also observed. Patches of *Salicornia spp.* (Glasswort and Sea Asparagus) were also found in the mainly unvegetated tidal flats.

4.2 Tidal Measurements

High tide was recorded on three occasions at Skinburness Marsh and on four occasions at Cardurnock Marsh and Bowness Marsh. The highest point of the same high tide at each of the contemporary sites and from the Workington tide gauge data obtained from National Tidal and Sea Level Facility (NTSLF, 2018) on the same day were taken for calculation. This enabled the calculation of the highest astronomical tide (HAT), mean high water spring tide (MHWST), mean high water neap tide (MHWNT) and mean tide level (MTL) at each of the contemporary sites studied, using

the best fit regression equation shown in each graph and based on the value of the respective tidal datum recorded at Workington (Figure 4.6).

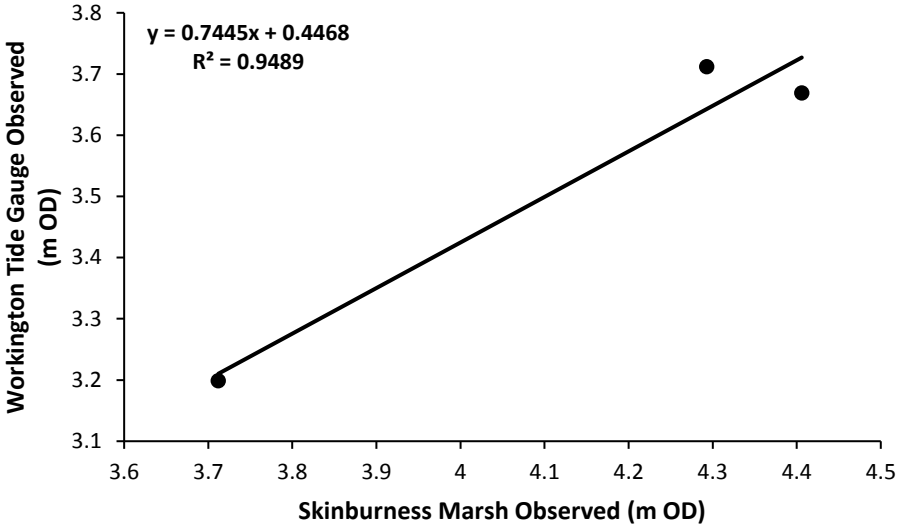

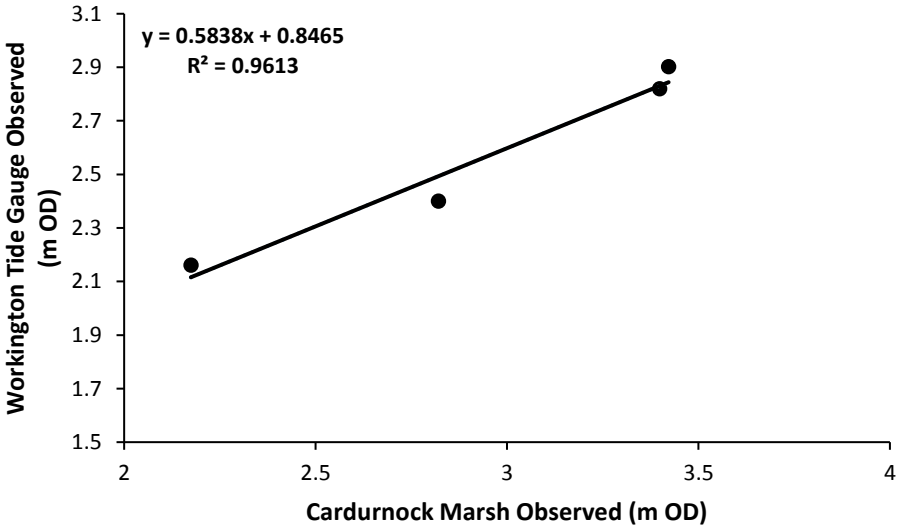

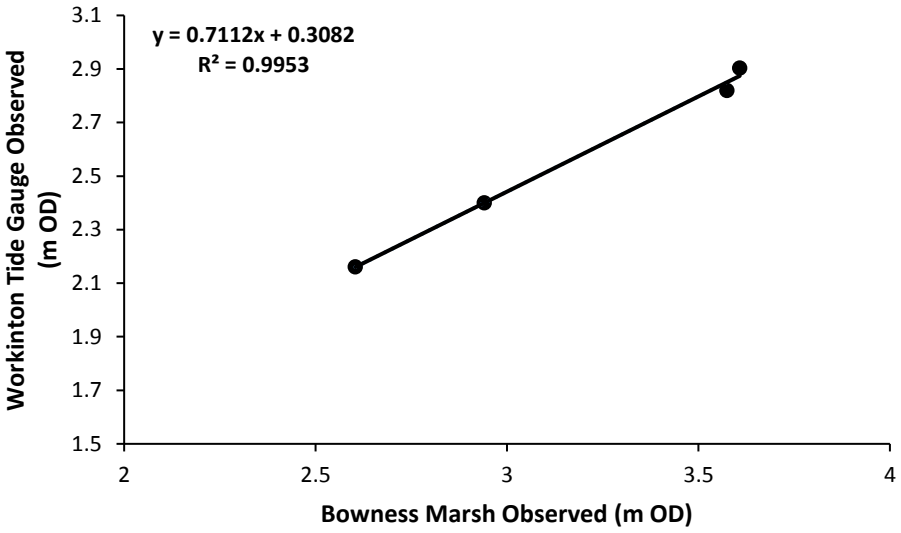

Figure 4.6: Tidal observations (m OD) at Skinburness Marsh, Cardurnock Marsh and Bowness Marsh compared to the verified data from Workington tide gauge (NTSLF, 2018)

The high tide elevation surveyed at all three contemporary saltmarshes showed a good fit with the verified Workington tide gauge data. It also revealed an amplification of the tide level from the outer estuary into the inner estuary, as Moricambe Bay and the Solway Firth narrow, and dampening tidal effects at Skinburness Marsh. Table 4.1 shows the elevation of tidal datum at Workington tide gauge, Maryport tide gauge and the Silloth tide gauge based on the information obtained through the Admiralty Tide Table (2016), along with the calculated tidal elevations at Skinburness Marsh, Cardurnock Marsh and Bowness Marsh. Tide levels at Maryport and Silloth were included to illustrate the amplification and dampening of the tide levels along the Solway Firth and Moricambe Bay (Figure 4.7).

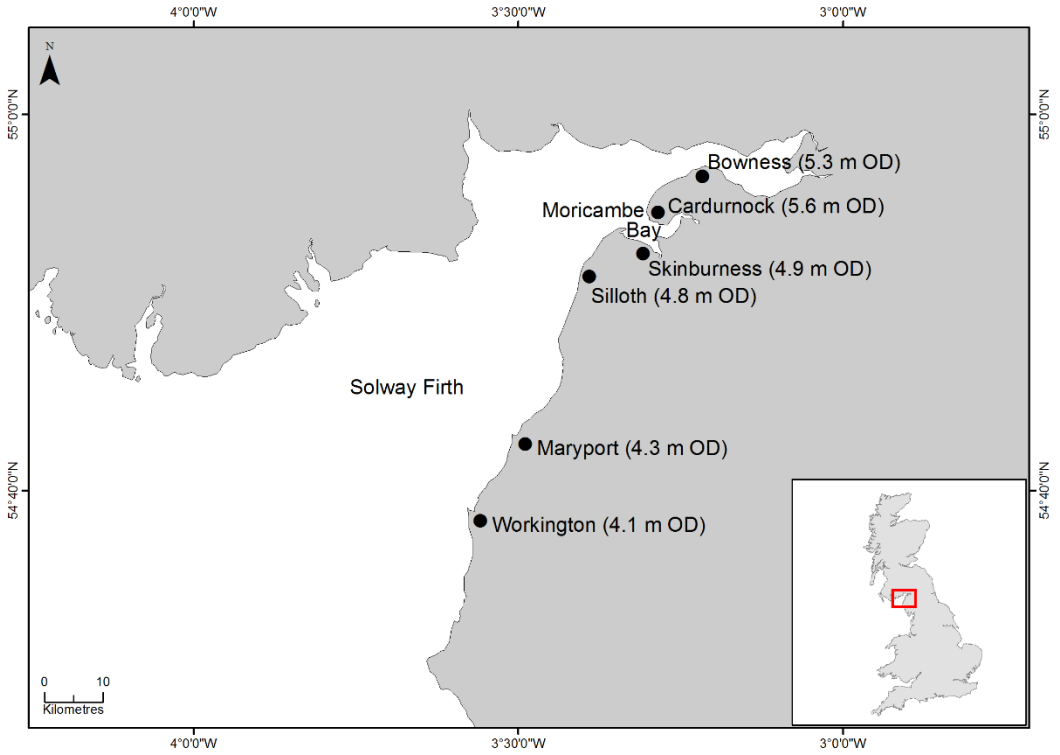

Figure 4.7: Tidal amplification and dampening along the Solway Firth and Moricambe Bay. Values are MHWST at each location (NTSLF, 2018)

Table 4.1: Tidal datum (m OD) at Workington, Maryport and Silloth tide gauges (Admiralty Tide Table, 2016; NTSLF, 2018) and the calculated tidal datum for Skinburness Marsh, Cardurnock Marsh and Bowness Marsh based on the best fit regression equations

Site	HAT (m OD)	MHWST (m OD)	MHWNT (m OD)	MTL (m OD)
Workington Tide Gauge	5.1	4.1	2.2	0.4
Maryport Tide Gauge	5.3	4.3	2.3	0.4
Silloth Tide Gauge	5.9	4.8	2.7	0.5
Skinburness Marsh	6.3	4.9	2.4	-0.1
Cardurnock Marsh	7.3	5.6	2.3	-0.8
Bowness Marsh	6.7	5.3	2.7	0.1

These data were then used for the calculation of sea-water level index (SWLI; calculated using equation in Section 3.7.1) values for the contemporary samples obtained at the sites, and for the reconstructed water level at each of the palaeo sites investigated.

4.3 Vertical Distribution of Contemporary Foraminiferal Assemblages

The results of the cluster analysis and detrended correspondence analysis (DCA) on the samples from Skinburness, Cardurnock and Bowness marshes are shown in Sections 4.3.1, 4.3.2 and 4.3.3 respectively and illustrated in Figures 4.8 to 4.13.

4.3.1 Vertical Distribution of Contemporary Foraminiferal Assemblages: Skinburnes Marsh

A total of six main foraminiferal species were identified from the 24 samples from Skinburness Marsh (Figure 4.8). The species of foraminifera identified consisted mainly of the agglutinated species *Jadammina macrescens* and *Miliammina fusca* in the high marsh environment (HAT of 6.3 m OD and MHWST of 4.9 m OD), and the calcareous species *Haynesina germanica* and *Elphidium williamsoni* (with the presence of *Ammonia beccarii*) in the lower marsh and tidal flats (MHWNT of 2.4 m OD).

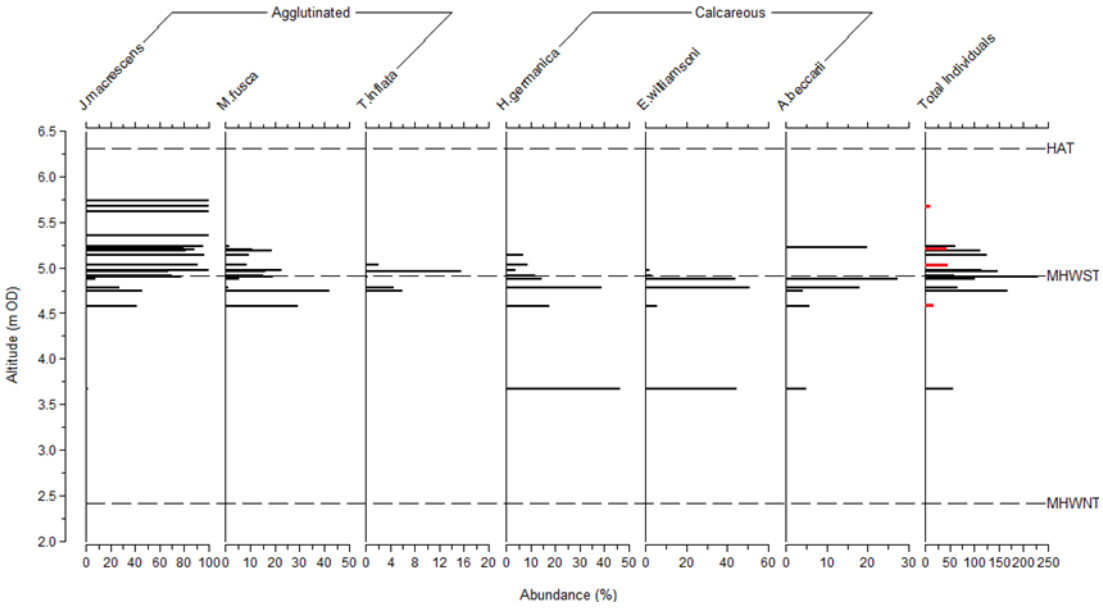

Figure 4.8: Foraminiferal assemblages of Skinburness Marsh contemporary samples. Samples with less than 40 individuals are marked with red lines. Species that contribute less than 5% of the dead assemblage were excluded

Based on the results of the unconstrained cluster analysis on samples from Skinburness Marsh, two main vertical zones were identified: SM-1 and SM-2 (Figure 4.9). Zone SM-1 corresponds to a high saltmarsh environment and is dominated

mainly by agglutinated species, in particular *J. macrescens* and *M. fusca*, with *T. inflata* and very low frequencies of the calcareous species *H. germanica* also present. Zone SM-2 corresponds to a lower marsh to a tidal flats environment and is dominated by the calcareous species *H. germanica*, *E. williamsoni* and *A. beccarii*.

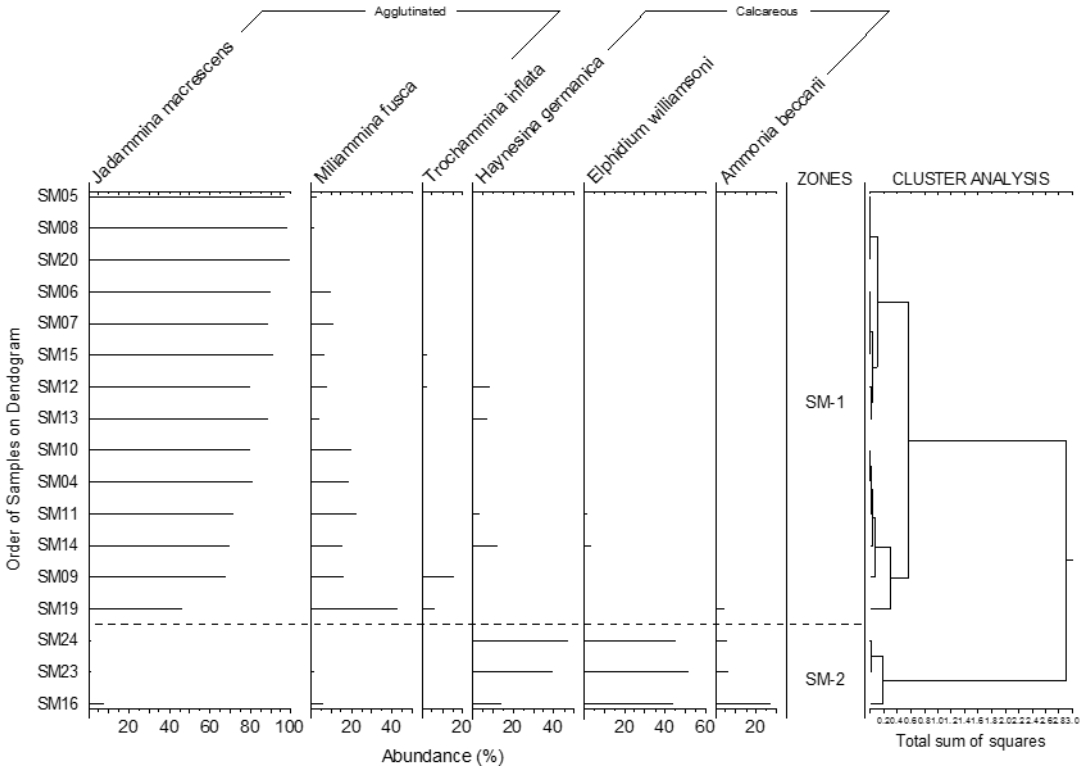

Figure 4.9: Unconstrained cluster analysis based on unweighted Euclidean distance for samples collected from Skinburness Marsh. Samples with fewer than 40 individuals and species that contribute less than 5% of the dead assemblage were excluded

4.3.2 Vertical Distribution of Contemporary Foraminiferal Assemblages: Cardurnock Marsh

A total of eight main species of foraminifera were identified from 30 samples collected from Cardurnock Marsh (Figure 4.10). All samples collected from Cardurnock Marsh occurred between MHWST (5.6 m OD) and MHWNT (2.3 m OD), with the HAT at Cardurnock Marsh calculated at 7.3 m OD. The marsh zone located at the higher elevation is dominated mainly by the agglutinated species *J. macrescens*, while the lower marsh and tidal flats environments are dominated mainly by the calcareous species *A. beccarii* with the presence of *H. germanica* and *E. williamsoni*.

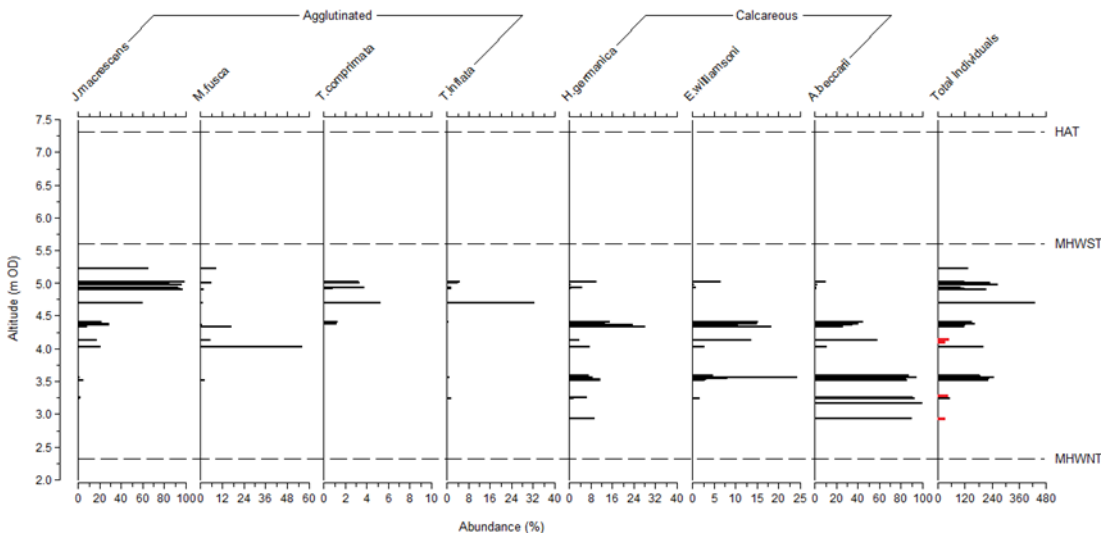

Figure 4.10: Foraminiferal assemblages of Cardurnock Marsh contemporary samples. Samples with less than 40 individuals are marked with red lines. Species that contribute less than 5% of the dead assemblage were excluded

Four zones were identified at Cardurnock Marsh based on the results of the unconstrained cluster analysis (Figure 4.11). Zone CM-1 is dominated mainly by the agglutinated species *J. macrescens* and therefore corresponds to a high saltmarsh environment, although falling below MHWST (5.6 m OD). The second zone CM-2 is dominated by the calcareous species *H. germanica*, *E. williamsoni* and *A. beccarii* corresponds to a lower saltmarsh and tidal flats environment. The third zone identified, CM-3 exhibits a similar foraminiferal assemblage to zone CM-2, although presence of the agglutinated species *J. macrescens* and *M. fusca* were also noted therefore also corresponding to a lower saltmarsh and tidal flats environment.

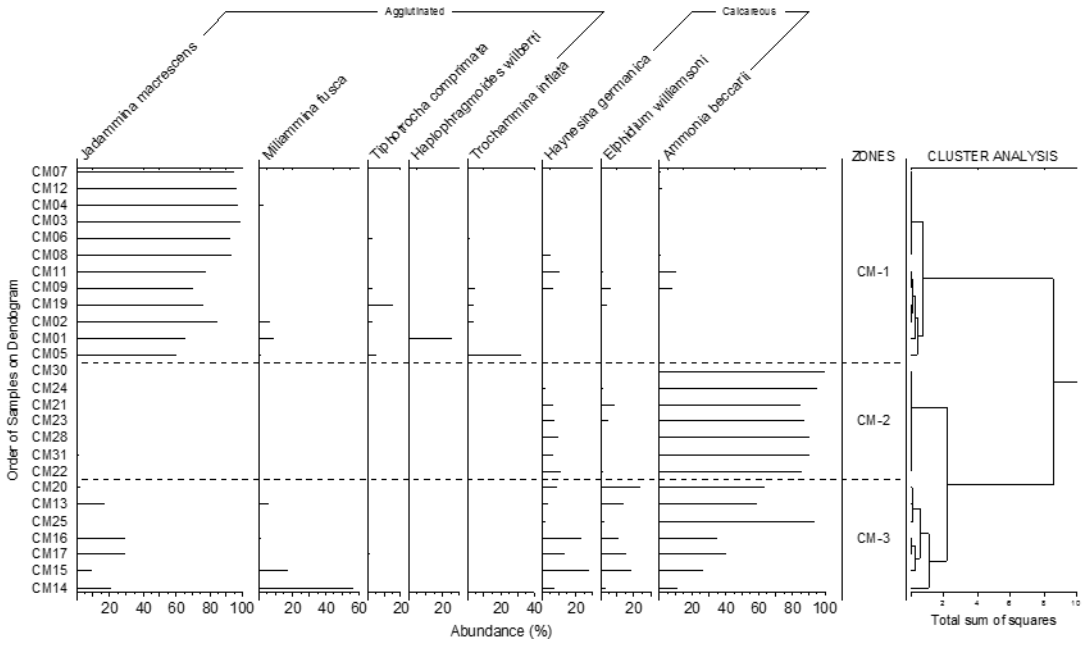

Figure 4.11: Unconstrained cluster analysis based on unweighted Euclidean distance for samples collected from Cardurnock Marsh. Samples with fewer than 40 individuals and species that contribute less than 5% of the dead assemblage were excluded

4.3.3 Vertical Distribution of Contemporary Foraminiferal Assemblages: Bowness Marsh

Six species of foraminifera were identified from 28 samples collected at Bowness Marsh, dominated mainly by the agglutinated species *J. macrescens* and *M. fusca* in the high marsh environment; HAT of 6.7 m OD and MHWST of 5.3 m OD (with increased presence of *Haplophragmoides wilberti* in the waterlogged marsh areas). The lower marsh and tidal flats environments that lie between the MHWST and MHWNT (5.3 and 2.7 m OD respectively) were dominated mainly by the calcareous species *H. germanica*, *E. williamsoni* and *A. beccarii* (Figure 4.12).

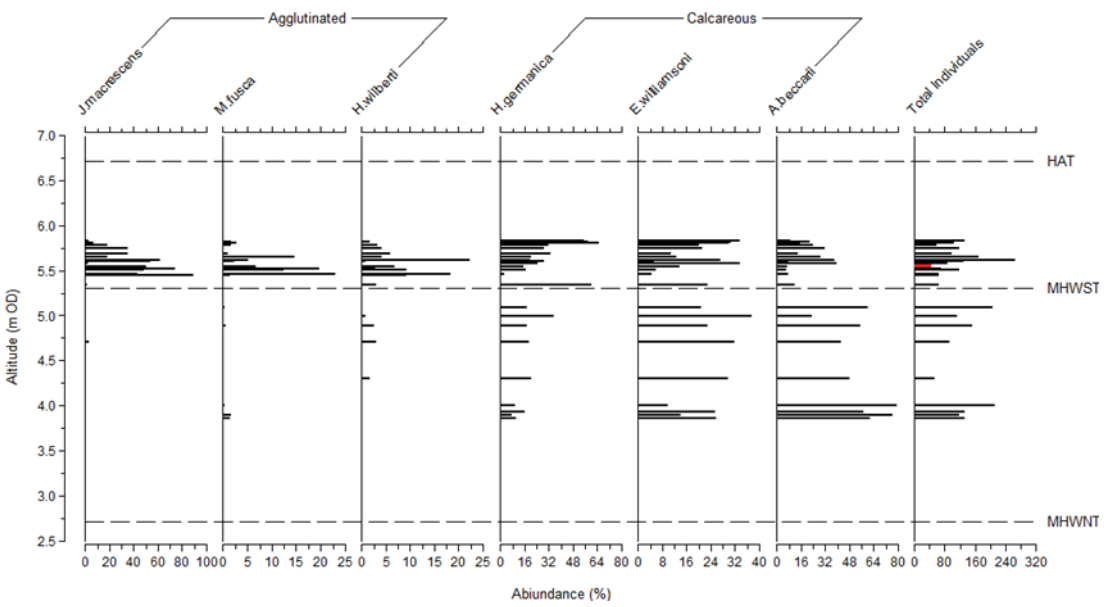

Figure 4.12: Foraminiferal assemblages of Bowness Marsh contemporary samples. Samples with less than 40 individuals are marked with red lines. Species that contribute less than 5% of the dead assemblage were excluded

Four zones were identified for the surface samples collected from Bowness Marsh (Figure 4.13). Zone BM-1 is located in the vegetated marsh zone above MHWST of 5.3 m OD. The high marsh zone BM-1 is dominated by the agglutinated species *J. macrescens*, with *M. fusca* and *H. wilberti* also present. Zone BM-2 is dominated by the calcareous species *H. germanica*, *E. williamsoni* and *A. beccarii* corresponds to a lower saltmarsh and tidal flats environment. Zone BM-3 is dominated mainly by the calcareous species *H. germanica, E. williamsoni* and *A. beccarii* similar to zone BM-2, with increased presence of *J. macrescens*. Zone BM-4 is dominated mainly by *A. beccarii*, followed by *E. williamsoni* and *H. germanica* and are mainly made up of samples that lie between MHWST and MHWNT at Bowness Marsh.

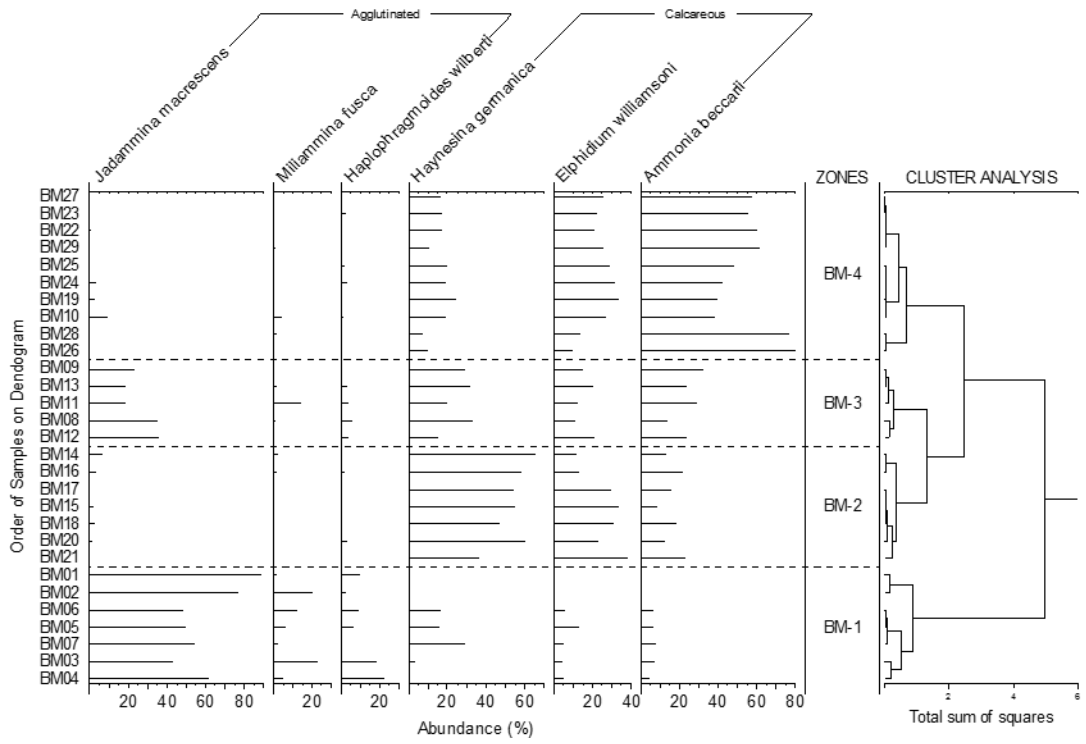

Figure 4.13: Unconstrained cluster analysis based on unweighted Euclidean distance for samples collected from Bowness Marsh. Samples with fewer than 40 individuals and species that contribute less than 5% of the dead assemblage were excluded

All three contemporary marshes in this study show a vertical zonation based on their foraminiferal assemblages and tidal datum levels recorded. The less distinct assemblage variations between the agglutinated and calcareous species from Skinburness Marsh are attributed to the presence of only one tidal flats sample from the site, due to the nature of the site which prevented collection of more samples from the tidal flats environment. The three marshes studied consists of two environments: a vegetated high marsh environment dominated mainly by the agglutinated species *J. macrescens* and a lower marsh and tidal flats environment (which falls above MHWNT at all contemporary sites) dominated mainly by the calcareous foraminiferal species *A. beccarii*. At Cardurnock Marsh, the agglutinated species *J. macrescens* is also present in the lower marsh and tidal flats environment, showing similar assemblages patterns to those of Nith Estuary located on the northern shore of the Solway Firth (Horton & Edwards, 2006). At Bowness Marsh, notable presence of the calcareous species *H. germanica* and *E. williamsoni* were also observed in the samples collected between MHWST and HAT correlating to a high saltmarsh environment.

4.4 Environmental Properties of Contemporary Samples

The pH of the surface sediments at the three contemporary saltmarshes were measured in-situ and samples were collected and analysed for organic carbon content (LOI 550), carbonate content (LOI 950) and particle size.

4.4.1 Environmental Properties: Skinburness Marsh

The organic content of sediments is highest at the back marsh, and decreases along the transect towards the tidal flats environment. The carbonate content is generally very low across the whole transect (less than 3%). The pH along the transect ranged between 7.07 and 8.79. High silt content was recorded in the samples collected along the transect, with increased sand content in the sample collected from the tidal flats environment (Figure 4.14).

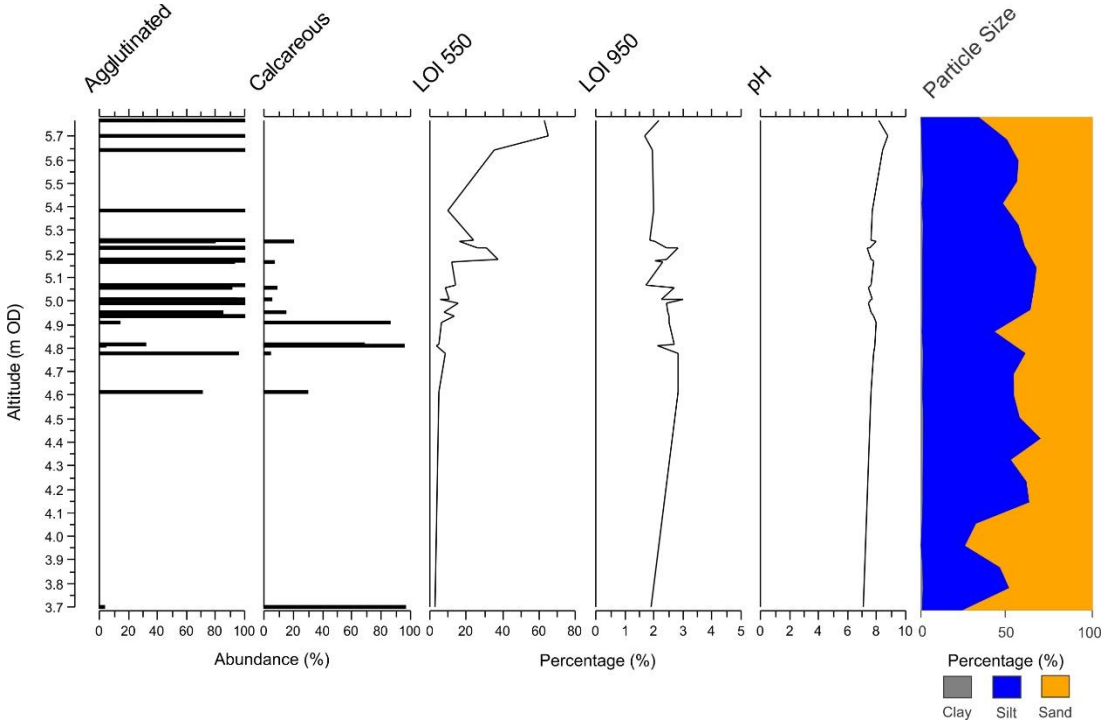

Figure 4.14: Summary plots of the analyses of contemporary surface samples from Skinburness Marsh including elevation, summary of foraminiferal assemblages, loss-on-ignition and particle size analyses

4.4.2 Environmental Properties: Cardurnock Marsh

The organic content of the sediments at Cardurnock Marsh shows a general decreasing trend along the transect towards the tidal flats, with the highest and lowest organic sediment content recorded as 17% and 3% respectively. The carbonate carbon content is relatively low throughout the transect sampled, with the highest value of 3% recorded. The minimum pH recorded was 6.51 while the highest level recorded was 8.42. The particle size of the surface sediments varied, with increased sand content observed along the transect towards the tidal flats environment (Figure 4.15).

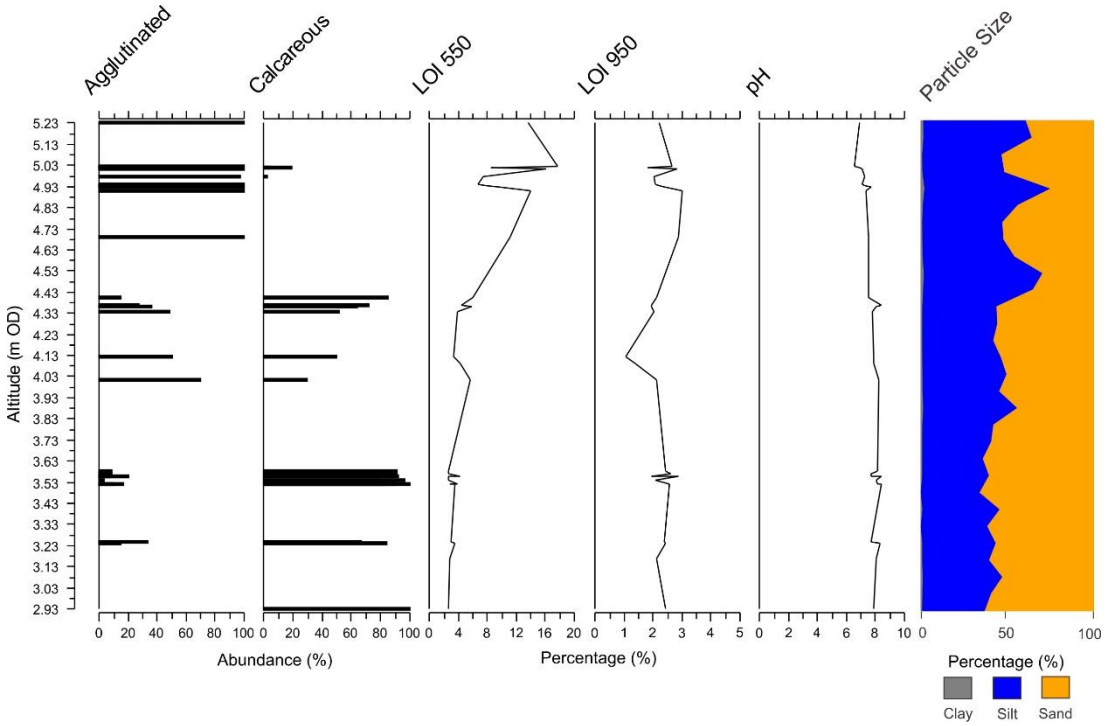

Figure 4.15: Summary plots of the analyses of contemporary surface samples from Cardurnock Marsh including elevation, summary of foraminiferal assemblages, loss-on-ignition and particle size analyses

4.4.3 Environmental Properties: Bowness Marsh

The organic carbon content showed a general decreasing trend along the transect from high marsh to the tidal flats, while the carbonate content remained relatively low across the transect. The pH at Bowness Marsh ranged between 5.90 and 8.85. The particle size of the sediments collected at Bowness Marsh is dominated by sand (Figure 4.16).

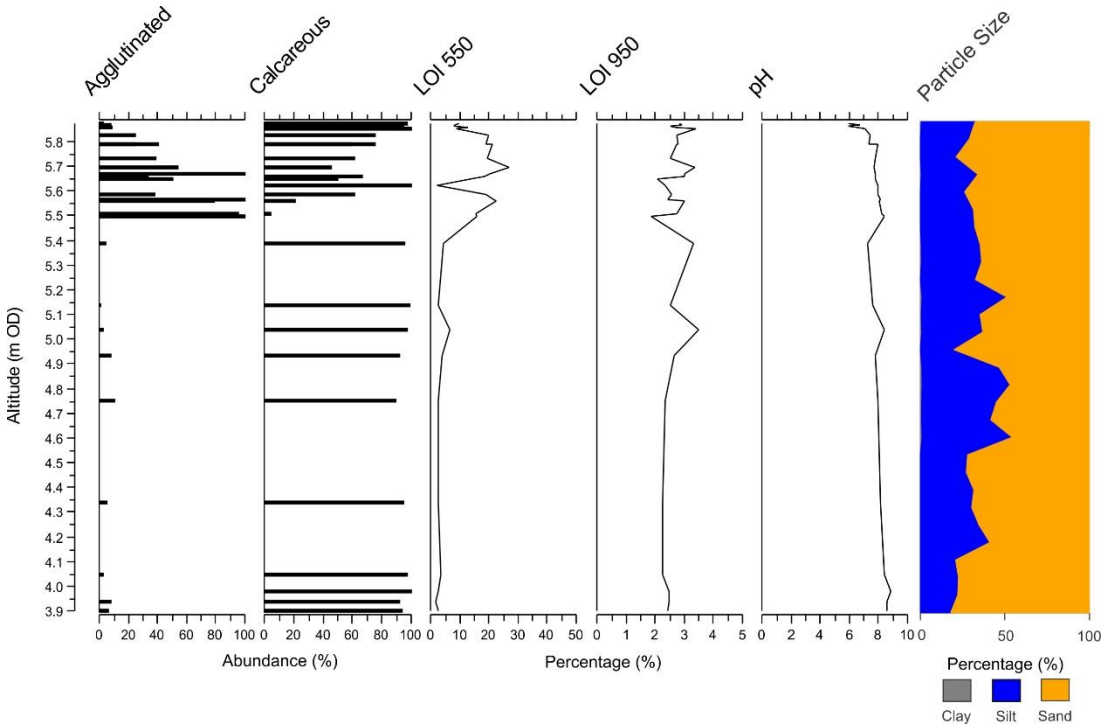

Figure 4.16: Summary plots of the analyses of contemporary surface samples from Bowness Marsh including summary of foraminiferal assemblages, loss-on-ignition, pH and particle size analyses

4.5 Influence of Environmental Parameters on Foraminiferal Assemblages

The canonical correspondence analysis (CCA) sample-environment and species-environment biplots for Skinburness Marsh, Cardurnock Marsh, Bowness Marsh and the Solway training set are described in Sections 4.5.1, 4.5.2, 4.5.3 and 4.5.4, and illustrated in Figures 4.17, 4.18, 4.19 and 4.20 respectively. The lengths of the environmental variables' arrow illustrates the variable's individual importance in explaining the variation in the foraminiferal data, while the orientation of the arrows illustrates the approximate correlation of the variables to ordination axes one and two, as well as individual correlation to other variables.

4.5.1 Influence of Environmental Parameters on Foraminiferal Assemblages: Skinburness Marsh

For Skinburness Marsh, the CCA axes one and two explain 64% of the total variation in the foraminiferal data. Correlations of the environmental variables with axes one

and two show that the elevation and LOI (organic content) are strongly correlated with axis one, pH is strongly correlated with axis two and the silt and sand fractions show a joint correlation between both the axes (Figure 4.17a). Axis one can therefore be deemed to reflect the major gradient change from a high marsh environment on the left of the graph, where high values are observed for elevation, LOI, and silt fraction, and low values for the sand fraction. The right of the graph therefore reflects the low marsh and tidal flats environment, with the opposite observed: high values of the sand fraction and low values of elevation, LOI and silt fraction. The pH gradient in Skinburness Marsh showed an increase in pH from tidal flats environment to high marsh environment.

For Skinburness Marsh (Figure 4.17b), the agglutinated species *J. macrescens*, *M. fusca* and *T. inflata* show a preference for a high and middle marsh environment located on the left side of the graph (high elevation, LOI and silt fraction, low sand fraction) while the calcareous species *H. germanica*, *E. williamsoni* and *A. beccarii* show a preference for a low marsh and tidal flats environment located on the right of the graph (high sand fraction, low elevation, LOI and silt fraction). The distribution of *T. inflata* has the strongest correlation with the LOI and silt fraction composition in Skinburness Marsh.

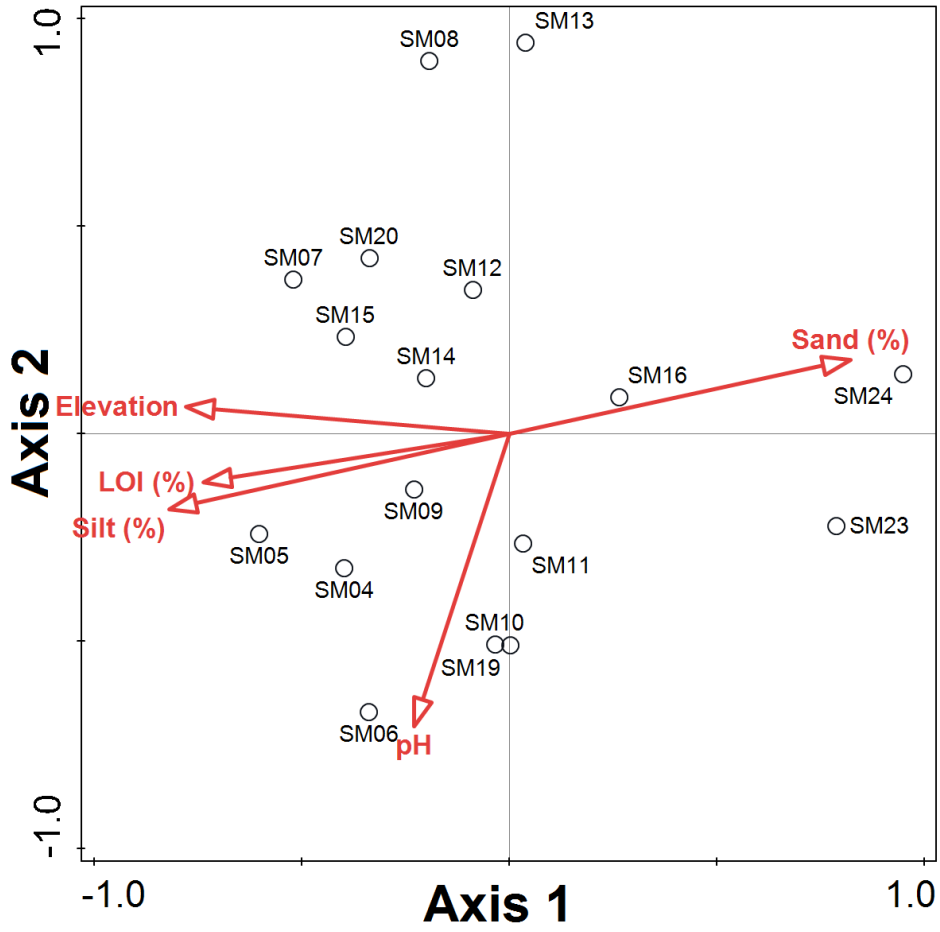
1.0
-1.0
Axis 2
-1.0
Axis 1
1.0
SM08
SM13
SM20
SM07
SM12
SM15
SM14
SM16
SM24
Sand (%)
Elevation
LOI (%)
Silt (%)
SM09
SM23
SM05
SM11
SM04
SM10
SM19
SM06
pH

(a)

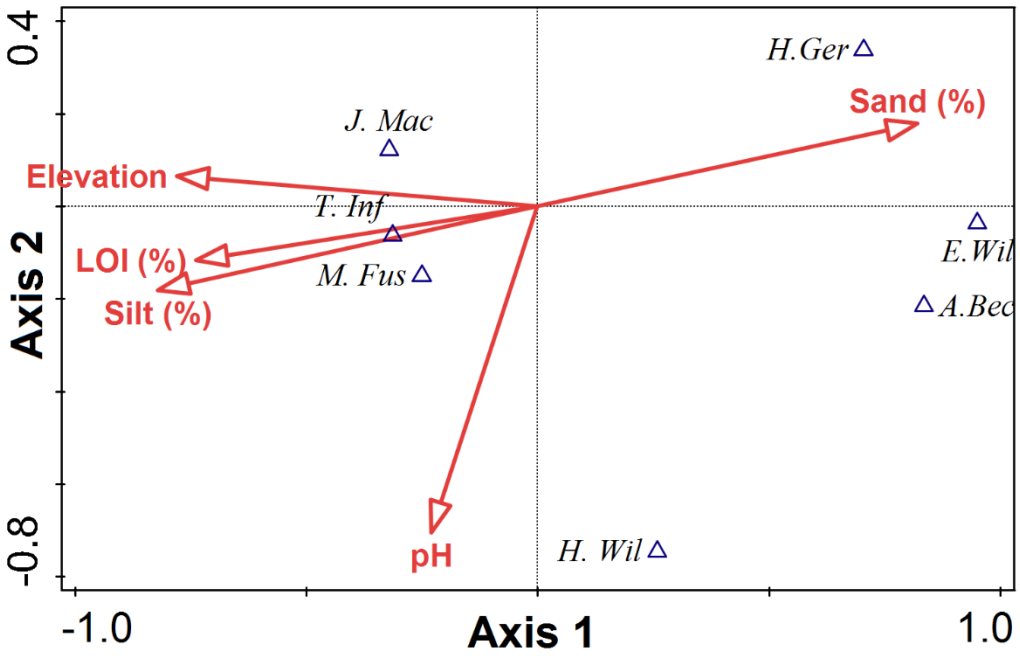
0.4
-0.8
Axis 2
-1.0
Axis 1
1.0
H.Ger
Sand (%)
J. Mac
Elevation
T. Inf
E.Wil
LOI (%)
M. Fus
A.Bec
Silt (%)
pH
H. Wil

(b)

Figure 4.17: Canonical Correspondence Analysis biplots of (a) sample-environment and (b) foraminiferal species-environment from Skinburness Marsh. Species abbreviations: A.Bec = *Ammonia beccarii*; E.Wil = *Elphidium williamsoni*; H.Ger = *Haynesina germanica*; H.Wil = *Haplophragmoides wilberti*; J.Mac = *Jadammina macrescens*; M.Fus = *Miliammina fusca*; T.Com = *Tipotrocha comprimata* and T.Inf = *Trochammina inflata*. Environmental abbreviations: LOI = loss on ignition. Samples with fewer than 40 individuals and species that contribute less than 5% of the dead assemblage were excluded

4.5.2 Influence of Environmental Parameters on Foraminiferal Assemblages: Cardurnock Marsh

For Cardurnock Marsh, the CCA axes one and two explain less than half (43%) of the total variation in the foraminiferal data. Correlations of the environmental variables with axes one and two show that the pH and LOI (organic content) are strongly correlated with axis one and elevation, silt fraction and sand fraction show a joint correlation between both the axes (Figure 4.18a). Axis one is therefore deemed to reflect the gradient changes from a high marsh environment on the right of the graph, where high values are observed for elevation, LOI, and silt fraction, and low values of sand fraction and pH. The left of the graph therefore reflects the low marsh and tidal flats environment, where the opposite is observed: high values of the sand fraction and pH with low values of elevation, LOI and silt fraction.

For the species-environment biplot (Figure 4.18b) of Cardurnock Marsh, the agglutinated species *J. macrescens*, *M. fusca*, *H. wilberti*, *T. comprimata* and *T. inflata* show a preference for a high and middle marsh environment located on the right of the graph (high elevation, LOI and silt fraction, low pH and sand fraction) while the calcareous species *H. germanica*, *E. williamsoni* and *A. beccarii* show a preference for a low marsh and tidal flats environment located on the left side of the marsh (high pH and sand fraction, low elevation, LOI and silt fraction). The agglutinated species *J. macrescens* show a stronger correlation with elevation and *H. wilberti* and *T. comprimata* show a stronger correlation with elevation and LOI. *M. fusca* and *T. inflata* show a stronger correlation with the silt fraction. The calcareous species, *A. beccarii* show a stronger correlation with pH, while *H. germanica* and *E. williamsoni* are correlated with both the pH and sand fraction.

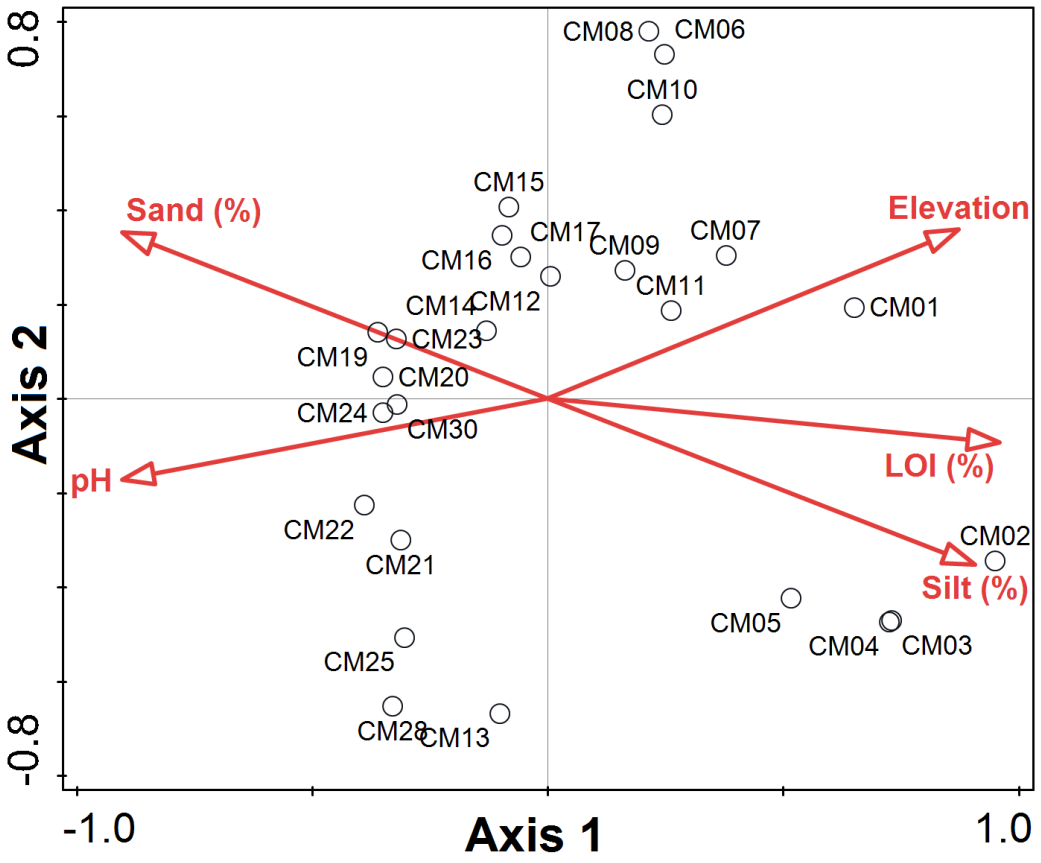

(a)

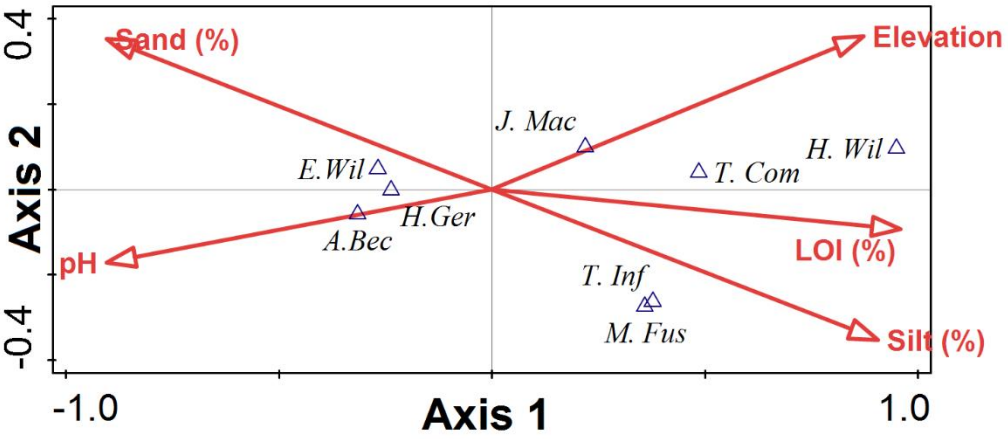

(b)

Figure 4.18: Canonical Correspondence Analysis biplots of (a) sample-environment and (b) foraminiferal species-environment from Cardurnock Marsh. Samples with fewer than 40 individuals and species that contribute less than 5% of the dead assemblage were excluded

4.5.3 Influence of Environmental Parameters on Foraminiferal Assemblages: Bowness Marsh

For Bowness Marsh, the CCA axes one and two explain approximately half (52%) of the total variation in the foraminiferal data. Correlations of the environmental variables with axes one and two show that the pH and silt fraction are strongly correlated with axis one, elevation is strongly correlated with axis two and the LOI and sand fraction show a joint correlation between both the axes (Figure 4.19a). Axis one is therefore deemed to reflect the gradient changes from a high marsh environment on the right of the graph, where high values are observed for elevation, LOI, and silt fraction, and low values for the sand fraction and pH. The left of the graph therefore reflects the low marsh and tidal flats environment, where the opposite is observed: high values of the sand fraction and pH with low values of elevation, LOI and silt fraction observed.

For the species-environment biplot (Figure 4.19b) at Bowness Marsh, the agglutinated species *J. macrescens*, *M. fusca* and *H. wilberti* show a preference for a high and middle marsh environment located on the right of the graph (high elevation, LOI and silt fraction, low pH and sand fraction) while the calcareous species *H. germanica*, *E. williamsoni* and *A. beccarii* show an opposite preference for a low marsh and tidal flats environment located on the left side of the graph (high pH and sand fraction, low elevation, LOI and silt fraction). The agglutinated species *J. macrescens* and *H. wilberti* show a stronger correlation with the LOI and silt fraction. The calcareous species *H. germanica* show the strongest correlation with pH, and *E. williamsoni* is most strongly correlated with the sand fraction.

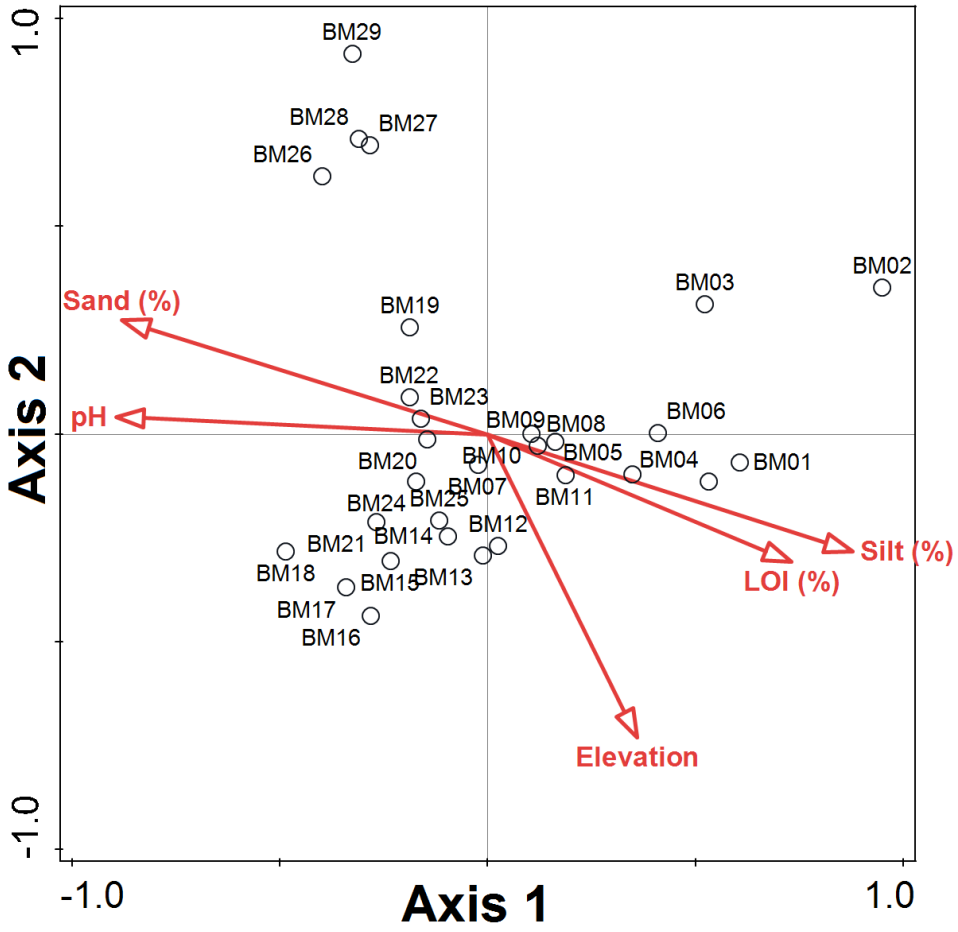
1.0
-1.0
Axis 2
-1.0
Axis 1
1.0
BM29
BM28
BM27
BM26
BM03
BM02
Sand (%)
BM19
BM22
BM23
pH
BM09
BM08
BM06
BM20
BM10
BM05
BM04
BM01
BM07
BM11
BM24
BM25
BM12
BM21
BM14
Silt (%)
BM18
BM15
BM13
LOI (%)
BM17
BM16
Elevation

(a)

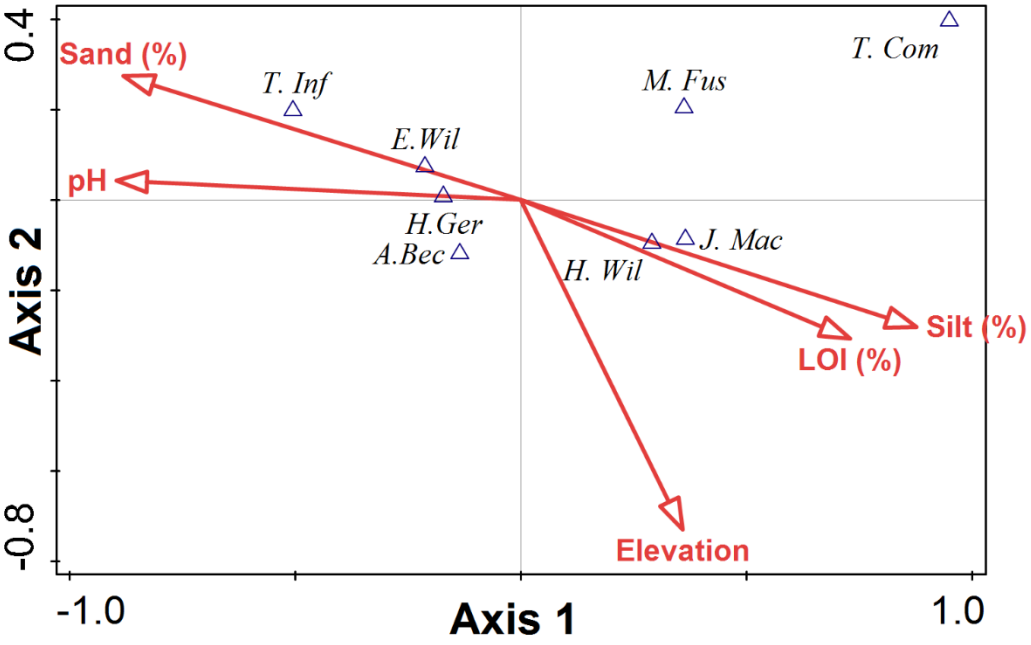
0.4
-0.8
Axis 2
-1.0
Axis 1
1.0
Sand (%)
T. Com
T. Inf
M. Fus
E.Wil
pH
H.Ger
A.Bec
J. Mac
H. Wil
Silt (%)
LOI (%)
Elevation

(b)

Figure 4.19: Canonical Correspondence Analysis biplots of (a) sample-environment and (b) foraminiferal species-environment from Bowness Marsh. Samples with fewer than 40 individuals and species that contribute less than 5% of the dead assemblage were excluded

4.5.4 Influence of Environmental Parameters on Foraminiferal Assemblages: Solway Training Set

When the data from all three contemporary marshes are combined as the Solway training set, CCA axes one and two explain 40% of the total variation in the foraminiferal data, the lowest when compared to the individual marshes. A general trend of high to middle marsh environment (high elevation, LOI and silt fraction, low pH and sand fraction) on the right side of the graph and a lower marsh and tidal flats environment illustrated on the left side of the graph (high pH and sand fraction, low elevation, LOI and silt fraction) is observed. All agglutinated species are also shown to have a preference for the high to middle marsh environment, while the calcareous species are restricted to the low marsh and tidal flats environments (Figure 4.20).

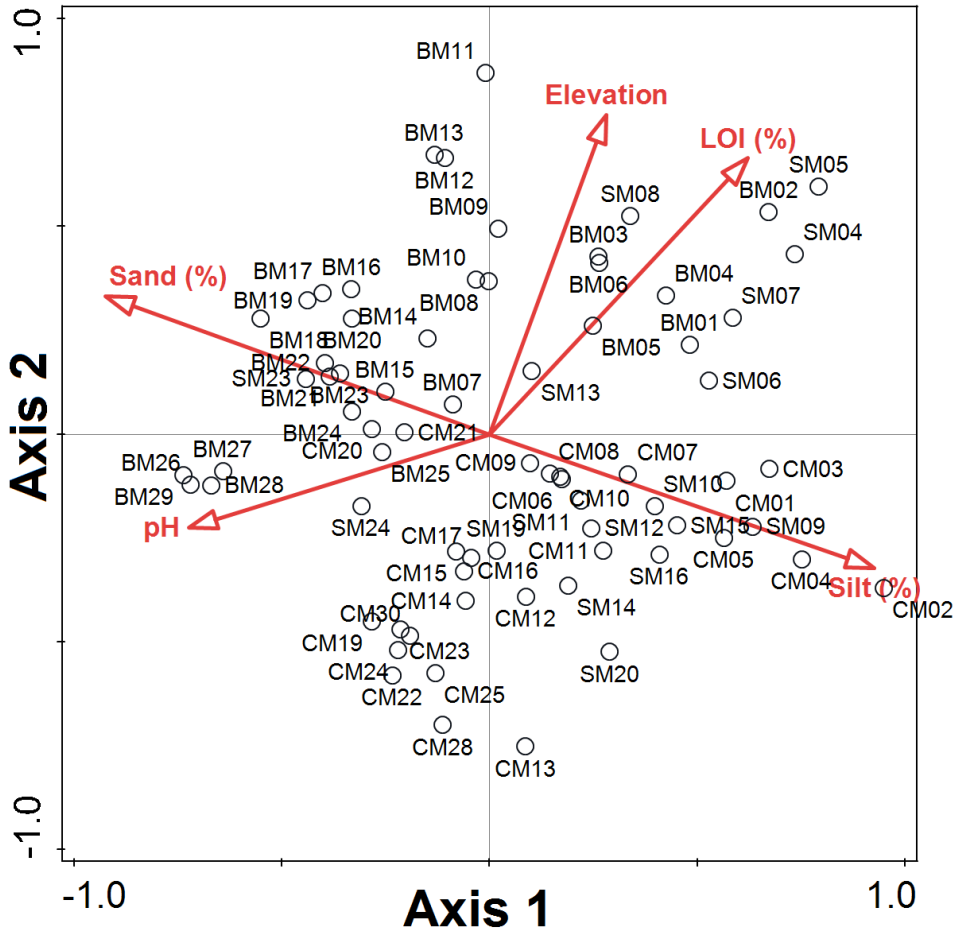
Axis 2
Axis 1
1.0
-1.0
-1.0
1.0
Elevation
LOI (%)
Sand (%)
pH
Silt (%)
BM11
BM13
BM12
BM09
BM10
BM17
BM16
BM19
BM14
BM08
BM18
BM20
BM22
BM15
SM23
BM21
BM23
BM07
BM24
CM21
CM20
BM27
BM26
BM28
BM29
BM25
CM09
CM08
CM07
CM06
CM10
SM24
CM17
SM19
SM11
SM12
SM15
SM09
CM11
CM05
CM15
CM16
SM16
CM04
CM14
CM12
SM14
CM02
CM30
CM19
CM23
CM24
SM20
CM22
CM25
CM28
CM13
SM08
BM03
BM06
BM04
SM07
BM01
BM05
SM06
SM13
SM05
BM02
SM04
CM03
SM10
CM01

(a)

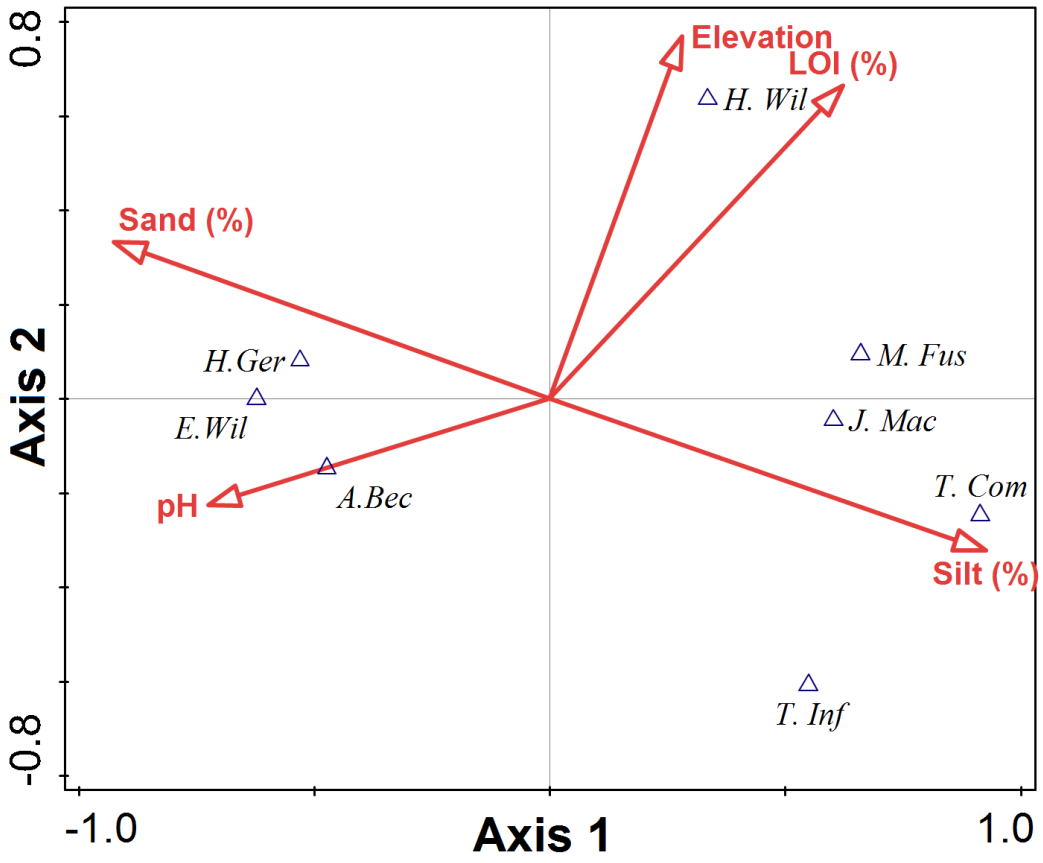

(b)

Figure 4.20: Canonical Correspondence Analysis biplots of (a) sample-environment and (b) foraminiferal species-environment from the Solway training set. Samples with fewer than 40 individuals and species that contribute less than 5% of the dead assemblage were excluded

4.6 Individual Contributions of Environmental Variables on Foraminiferal Assemblages

The five environmental variables investigated account for 64%, 43%, 52% and 40% of the variation in foraminiferal assemblages at Skinburness Marsh, Cardurnock Marsh, Bowness Marsh and in the Solway training set respectively (Figure 4.21). The partial CCAs for Skinburness Marsh showed that the total 64% explained variation is composed of the elevation (18%), LOI (15%), silt fraction (15%), sand fraction (14%), pH (16%) and intercorrelation amongst the variables (23%). The 43% variation of foraminiferal assemblages explained in Cardurnock Marsh is composed of the elevation (9%), LOI (5%), silt fraction (3%), sand fraction (3%), pH (6%) and a strong intercorrelation amongst the environmental variables (74%). The total

foraminiferal assemblage variation in Bowness Marsh explained is 52%, where 13% of the total variation is contributed by the elevation, 8% by the LOI, 6% by the silt fraction, 6% by the sand fraction, 16% by the pH and 50% of the total variation explained by intercorrelation amongst the variables. For the Solway training set, 40% of the total variation in species assemblages is accounted for by the five environmental variables. Only 1% of the total variation is attributed to the elevation, 4% to the LOI, 2% to the silt fraction, 2% to the sand fraction, 8% to the pH and 82% attributed to intercorrelation amongst the five environmental variables.

For Skinburness Marsh and Cardurnock Marsh, the elevation contributed the most to the variation in foraminiferal species distribution, while the pH and elevation contributed the highest for Bowness Marsh. For the Solway training set, pH contributed the highest with 8% of the total variation explained, while the elevation explained only 1% of the variation in foraminiferal distribution. The strong intercorrelation amongst the variables (82%) for the Solway training set shows that although the elevation (the main variable affecting tidal submergence of the area) might be the main controlling factor in the foraminiferal assemblages' distribution in the marshes, the effects of other environmental variables should also be taken into account. The variation of foraminiferal distribution in a marsh due to intercorrelation amongst the variables is common, as these variables (LOI, pH, silt and sand fractions) are also dependent on the frequency of tidal flooding in the marsh (Horton & Edwards, 2006). Intercorrelation amongst variables has also been observed in the other foraminifera contemporary marsh studies (Horton *et al.*, 1999; Horton *et al.*, 2003; Edwards, 2001; Horton & Edwards, 2003; Horton & Edwards, 2005; Horton & Edwards, 2006; Best, 2016).

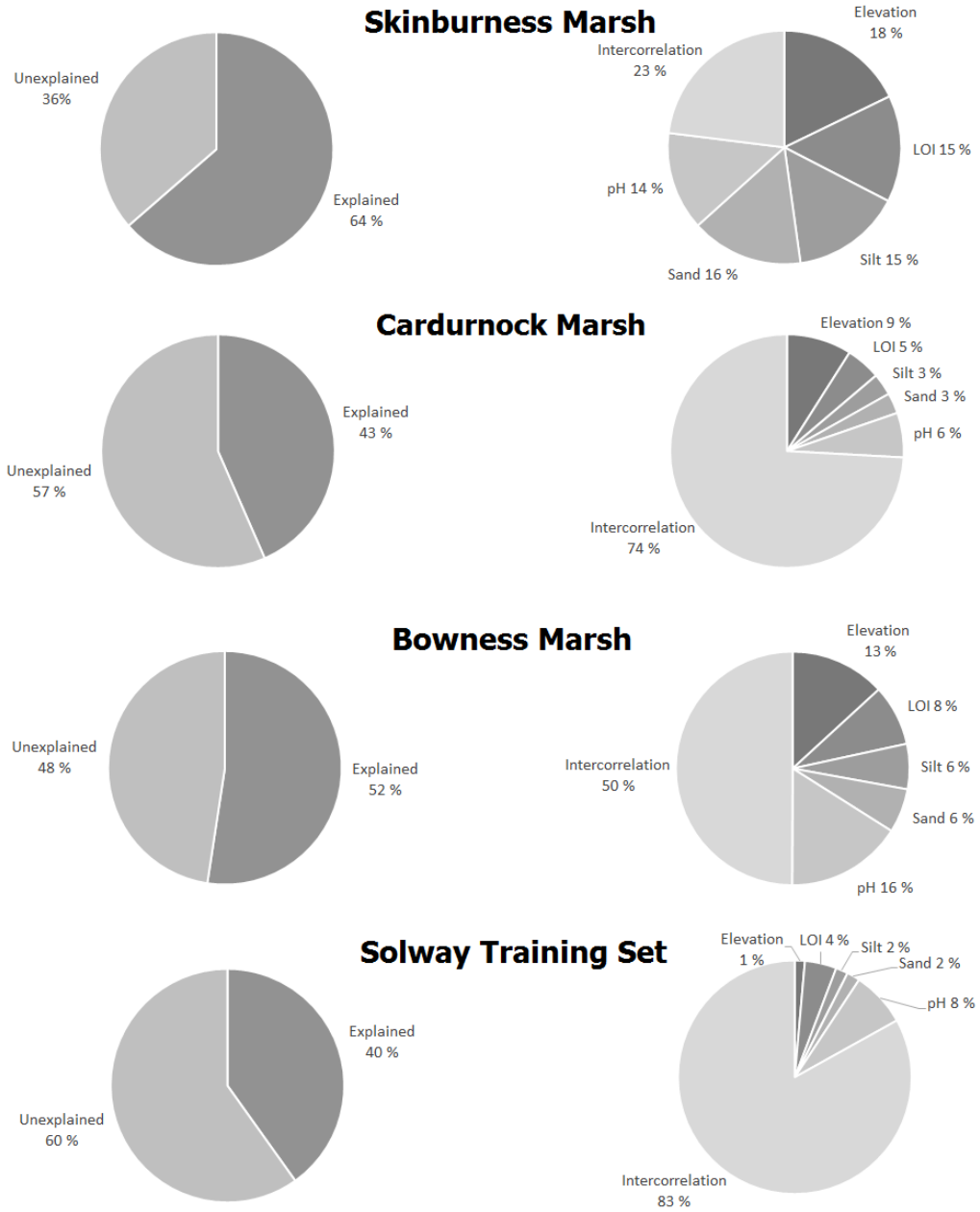

Figure 4.21: Pie charts showing the total variation of the foraminiferal training set of Skinburness Marsh, Cardurnock Marsh, Bowness Marsh and the Solway training set respectively in explained and unexplained portion components representing the individual contributions of elevation, LOI, silt fraction, sand fraction, pH and intercorrelation amongst variables

4.7 Development of a Local Foraminifera-Based Transfer Function

The Solway training set was used to develop the local transfer function for this study, consisting of all 72 foraminiferal samples from the three contemporary marshes. The foraminiferal data for the 72 contemporary samples of the Solway training set were

plotted against SWLI, which ranged from 275 to 302 (Figure 4.22). Component selection for the local transfer function developed was based on the prediction statistics (RMSEP and r^2_{boot}) amongst the lowest five components. Based on these, component three was selected as it performed better than component one and two, with minimal improvement in the following components (Table 4.2).

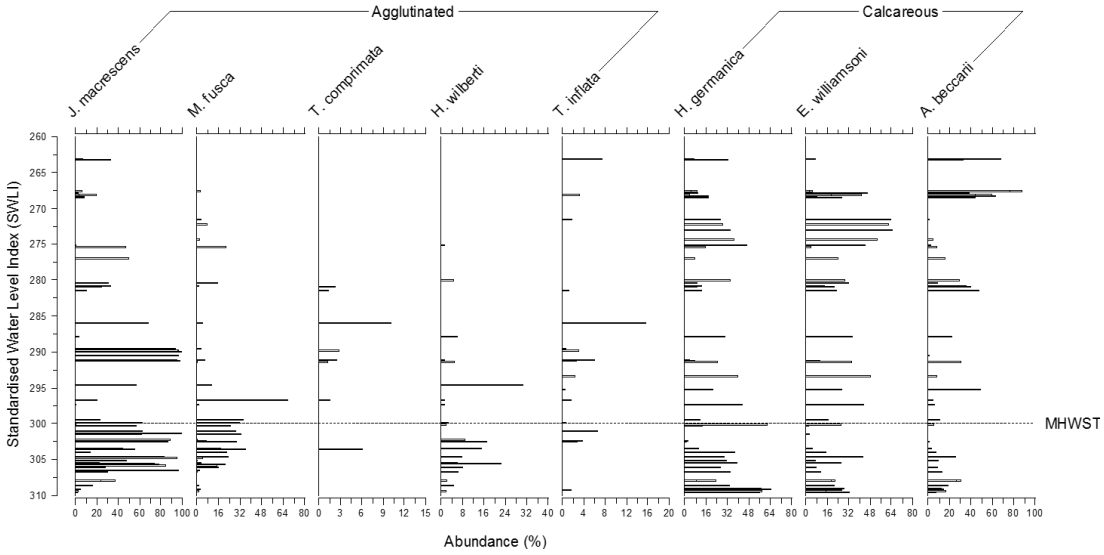

Figure 4.22: Contemporary foraminiferal samples from Skinburness Marsh, Cardurnock Marsh and Bowness Marsh ordered by elevation (expressed as standardised water level index)

Table 4.2: Summary of the performance of the local transfer function developed from the training set (the selected component three is in bold)

Name	Component	RMSEP	% Change	r^2_{boot}
L-1	1	12.09	-	0.30
L-1	2	11.16	7.73	0.42
L-1	**3**	**11.04**	**1.04**	**0.46**
L-1	4	11.03	0.08	0.46
L-1	5	11.18	-1.29	0.46

The local transfer function developed showed a linear relationship between the observed and predicted SWLI (Figure 4.23). The r^2_{boot} values (which showed the regression value for the observed SWLI and predicted SWLI of the transfer function) for the Solway training set component three is 0.46, with the RMSEP value of 11.04. The local training set produced a high scatter between the observed SWLI and

predicted SWLI, possibly due to the fact that the foraminiferal assemblages distribution in Skinburness Marsh, Cardurnock Marsh and Bowness Marsh were also strongly influenced by the other environmental variables (resulting in high intercorrelation values), as shown in Figure 4.23. In an idealised situation where the distribution of foraminifera in these three sites is controlled solely by elevation of the marsh, a linear one-to-one relationship would be observed (Horton & Edwards, 2006). The effect of these other variables on the foraminiferal assemblages' distribution reduced the precision of the transfer function for reconstructions of the fossil samples. If the effect of the other environmental variables becomes more dominant than elevation (as shown for Bowness Marsh and the Solway training set in Figure 4.21), no meaningful prediction can be made using the transfer functions developed (Horton & Edwards, 2006).

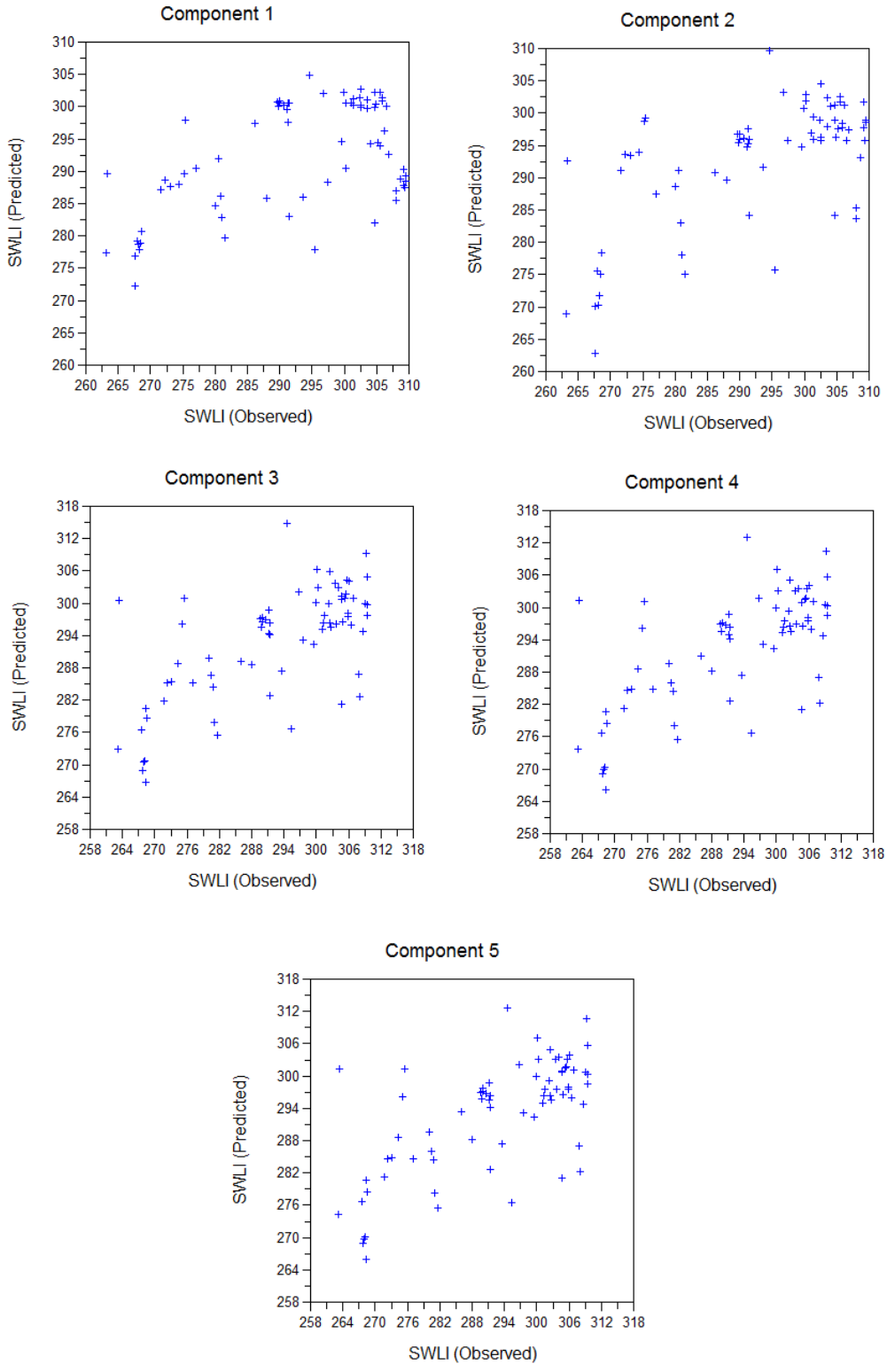

Figure 4.23: Scatter plots showing the relationship between observed SWLI (measured during fieldwork) and predicted SWLI (produced by the WA-PLS transfer function) derived from the local Solway training set

4.8 Transfer Function Application and Assessment of Reliability: Modern Analogue Technique

To predict the palaeo surface marsh elevation (PMSE) of fossil foraminiferal assemblages from the palaeo study sites, calibration was undertaken using the C2 program (Juggins, 2007). The SWLI estimated for each fossil sample were calculated using the WA-PLS predictions, and the error range was derived by bootstrapping (1000 cycles). The 'reliability' of the transfer function produced were first assessed using the modern analogue technique (MAT) to consider the similarity/dissimilarity between the modern assemblages used to develop the transfer function with the fossil assemblages.

Based on the result of MAT on the fossil samples with the local transfer function developed, the utilisation of the transfer function to estimate the PMSE of the fossil samples were deemed unfeasible due to the high number of samples with poor modern analogues (Table 4.3). This is due to the dissolution of the calcareous foraminiferal species observed in all of the cores obtained from the palaeo study sites.

Table 4.3: Modern analogue technique (MAT) results for each palaeo sites

Site	Modern Analogues		
	Good	Close	Poor
Allonby	23 (44%)	7 (14%)	22 (42%)
Cowgate Farm	14 (37%)	6 (16%)	18 (47%)
Pelutho	29 (60%)	4 (8%)	15 (32%)
Herd Hill	10 (46%)	3 (14%)	9 (40%)

Only dead foraminiferal assemblages were included in the analyses, as dead assemblages show less spatial and temporal variation compared to live assemblages. Post-depositional changes where certain foraminiferal species are retained or removed from the dead population occur during the process when the foraminiferal assemblage dies. Modern analogues or training sets were consistently derived from only the dead surface foraminiferal assemblages; therefore the effect between the presence and absence of these species will not affect the calibration of the fossil material, as the foraminifera assemblages found in the fossil sample during the time

of deposition would have undergone similar processes as the contemporary surface samples (Horton & Edwards, 2006).

However, if post-depositional changes occur during the process when the foraminiferal assemblages shift from a surface to a sub-surface environment, changes in the relative abundance of key foraminiferal taxa may result in errors during the reconstruction of relative sea level from fossil material. In sea-level research, the dissolution of calcareous foraminiferal species has been observed previously (e.g. Scott & Medioli, 1980; Jonasson & Patterson, 1992; Murray & Alve, 1999; Edwards & Horton, 2000) and is most common in a low pH environment where the sediment is rich in organic content, and there is an input of acidic runoff from nearby land areas. When post depositional dissolution of the calcareous foraminiferal species occur, the resulting fossil assemblage found in cores will be enriched with agglutinated foraminiferal species which would normally have a minor contribution in the lower marsh or tidal flats environments. This will eventually result in poor transfer function performance as there would be lack of modern analogues for the fossil samples (Horton & Edwards, 2006).

The use of MAT was able to identify samples that might have experienced the effects of post-depositional dissolution of calcareous foraminifera, as the samples will have resulted in having poor modern analogues. The presence of test linings in the clastic units at the palaeo study sites was used as evidence for the presence of calcareous foraminiferal species in the fossil samples, although it was not possible to identify the species of the calcareous remains. In this study, fossil samples having higher abundance of *M. fusca* and *H. wilberti* in particular also resulted in samples having poor modern analogues, as the dominance might be biased due to the calcareous foraminiferal dissolution which were therefore absent in the fossil samples.

4.9 Summary

The three contemporary marshes investigated, Skinburness Marsh, Cardurnock Marsh and Bowness Marsh were described in this chapter, including the foraminiferal assemblages and zonation along with the environmental parameters of the surface sediment observed in each saltmarsh. A local transfer function was developed based on the three marshes in this study. The prediction of the PMSE value of fossil samples

based on the local transfer function was not feasible, as the transfer function resulted in a high number of fossil samples with poor modern analogues. This is due to the lack of the calcareous species in the fossil samples. The indicative meaning of the fossil samples will therefore be determined qualitatively based on the contemporary foraminiferal assemblages from the three saltmarshes, combined with the lithostratigraphy and environmental parameters of the surface sediments.

The results from this study have highlighted the importance of the preservation of microfossils for the successful development and utilisation of a transfer function. Although the transfer function developed may result in a good statistical predictability, the high number of fossil samples with poor modern analogues (as a result of the dissolution of calcareous foraminifera) as observed in this study will eventually result in an unreliable reconstruction. The assessment of the different estuarine settings (i.e. microtidal, mesotidal or macrotidal) when developing a local transfer function should also be considered. For example, in a macrotidal estuarine setting, the calcareous foraminiferal species may be deposited higher on the acidic and organic saltmarsh environment, hence poorly preserved in the fossil assemblage. This was observed in other recent studies within similar estuarine settings (e.g. Elliot, 2015; Best, 2016). Further research on the different estuarine and coastal environment is therefore needed, to determine the factors affecting post-depositional preservation of the proxy utilised.

CHAPTER 5

ALLONBY

5.0 Introduction

The site at Allonby (NY 0949 4410) is located on the northwest Cumbrian coastline, approximately 1.5 km from the present coastline, 12 km from the southern bank of Moricambe Bay and 22 km from the southern shore of the Solway Firth (Figure 5.1). The site is bordered by a gently sloping hill towards the south and the Black Dub stream towards the north which flows into Allonby Bay at Dubmill. Low-lying farmland surrounds the site to the west and east and a drainage channel separates the two fields investigated at this site (Figure 5.2a). The study area is currently used as grazing for domestic livestock and is approximately 300 m long by 200 m wide.

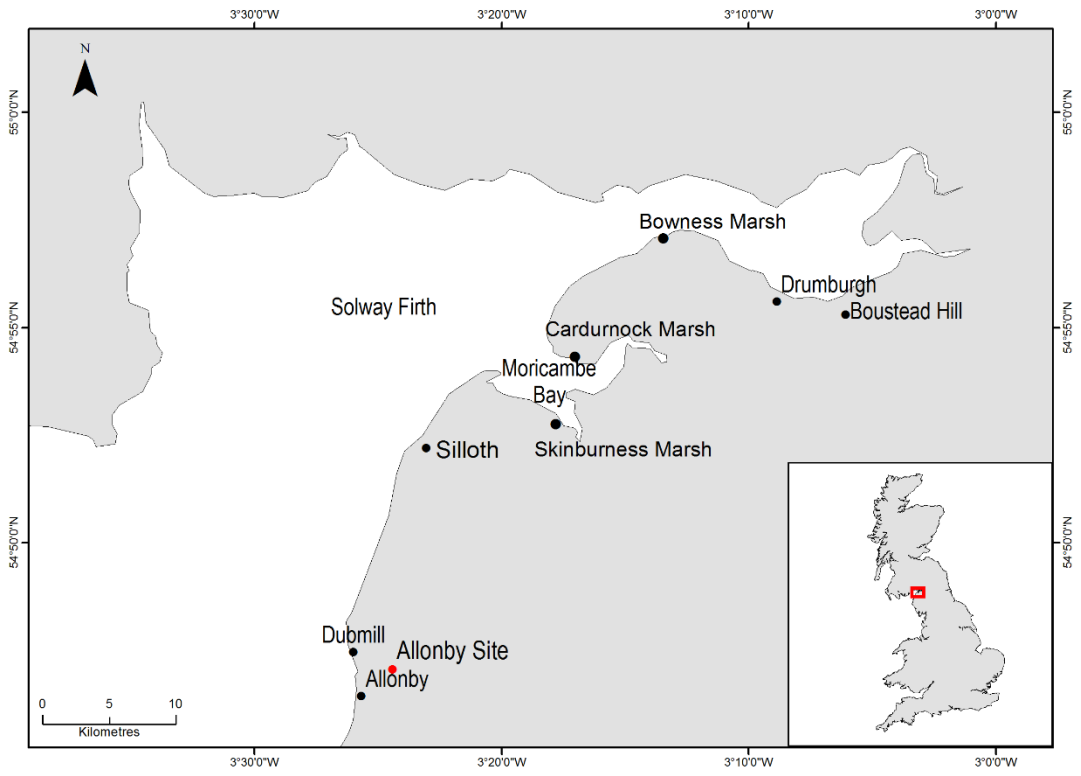

Figure 5.1: Location of the study site at Allonby marked in red

5.1 Borehole Location and Stratigraphy

Three transects of boreholes were cored across the site to establish a detailed stratigraphy (Figure 5.2). The first transect was cored from south to north at the site, and the other two transects were cored from west to east. The surface altitude of the boreholes ranged from 6.97 m OD and 7.69 m OD. Borehole A6 reached the maximum depth of 1.90 m (5.20 m OD) at the site, terminating on bedrock. Boreholes A1, A2, A3, A4, A5 A6 and A7 terminated on bedrock, boreholes A8, A9, A10, A11 and A12 terminated in a stiff blue/grey silt-clay with orange mottling unit, while boreholes A12 and A13 terminated in a sandy blue/grey silt-clay with gravel unit. The general lithostratigraphy of the area consisted of a basal clastic unit of organic blue/grey silt-clay with sand and gravels deposited on the bedrock overlain by a peat with *Phragmites* unit. A second clastic unit of organic blue/grey silt-clay occurred above this, and this in turn was overlain by another unit of peat with *Phragmites*.

Borehole A1 reached a depth of 1.24 m (5.85 m OD) and terminated on bedrock. A sandy blue/grey silt-clay with gravel unit overlaid the bedrock, with more organic detritus found towards the top of the unit. This was overlain by the silty peat with *Phragmites* unit and wood at a depth of 0.87 m (6.22 m OD), and surface peat unit at a depth of 0.20 m (6.89 m OD).

Borehole A2 reached the bedrock at a depth of 1.24 m (5.89 m OD). A unit of sandy blue/grey silt-clay with gravel was deposited on the bedrock, which transitioned into the silty peat with *Phragmites* unit at a depth of 0.74 m (6.39 m OD) and the surface peat unit at a depth of 0.24 m (6.89 m OD).

In borehole A3, the maximum depth reached was 1.23 m (5.94 m OD). The basal clastic unit overlying the bedrock consisted of a unit of organic and sandy brown silt-clay with gravel. It was overlain by a unit of organic blue/grey silt-clay with gravel at a depth of 0.79 m (6.38 m OD). This transitioned into the silty peat with *Phragmites* unit at a depth of 0.60 m (6.57 m OD) and the surface peat unit at a depth of 0.21 m (6.96 m OD).

Borehole A4 reached the bedrock at a depth of 1.24 m (5.83 m OD). The bedrock was overlain by a unit of organic blue/grey silt-clay with gravel and transitioned into

the peat with *Phragmites* and wood remains at a depth of 0.95 m (6.12 m OD). This unit was overlain by a second clastic unit consisting of organic blue/grey silt-clay at a depth of 0.66 m (6.41 m OD) and transitioned into the silty peat with *Phragmites* unit at a depth of 0.46 m (6.61 m OD). The surface peat unit occurred at a depth of 0.18 m (6.89 m OD).

For borehole A5, the maximum depth reached was 1.40 m (5.58 m OD). The bedrock was overlain by the sandy blue/grey silt-clay with gravel unit and transitioned into a more organic blue/grey silt-clay unit at a depth of 1.30 m (5.68 m OD). This unit transitioned into the silty peat with *Phragmites* unit at a depth of 0.47 m (6.51 m OD) and the surface peat unit at a depth of 0.24 m (6.74 m OD).

In borehole A6, the maximum depth reached was 1.90 m (5.23 m OD) and no basal clastic unit was observed. Instead, a peat with *Phragmites* unit was deposited on the bedrock, and was overlain by a clastic unit of organic blue/grey silt-clay unit at a depth of 0.75 m (6.38 m OD). This transitioned into the silty peat with *Phragmites* unit at a depth of 0.51 m (6.62 m OD) and the surface peat unit at a depth of 0.16 m (6.97 m OD).

Borehole A7 reached the maximum depth at 1.70 m (5.30 m OD), and terminated on bedrock. A unit which consisted of sandy organic blue/grey silt-clay with gravel overlaid the bedrock. This unit transitioned into organic brown silt-clay at a depth of 1.62 m (5.38 m OD), and was overlain by a silty peat with *Phragmites* unit at a depth of 1.57 m (5.43 m OD). This unit was overlain by a second clastic unit which consisted of organic blue/grey silt-clay at a depth of 0.99 m (6.01 m OD) and transitioned into the silty peat with *Phragmites* unit at a depth of 0.64 m (6.36 m OD). The surface peat unit occurred at a depth of 0.49 m (6.51 m OD).

Borehole A8 terminated on bedrock at 1.43 m (5.82 m OD). The bedrock was overlain by the organic blue/grey silt-clay with gravel unit, which transitioned into silty peat with *Phragmites* unit at a depth of 1.33 m (5.92 m OD). This unit was overlain by an organic blue/grey silt-clay unit at a depth of 1.18 m (6.07 m OD). This clastic unit transitioned into the silty peat with *Phragmites* unit at a depth of 0.65 m (6.60 m OD) and the surface peat unit at a depth of 0.17 m (7.08 m OD).

Borehole A9 reached an impenetrable depth at 1.64 m (5.42 m OD) in the stiff and sandy blue/grey silt-clay with orange mottling unit. The basal clastic unit was overlain by a more organic blue/grey silt-clay unit at a depth of 0.87 m (6.19 m OD) and transitioned into the peat with *Phragmites* unit at a depth of 0.53 m (6.53 m OD). This was overlain by a unit of organic brown silt-clay at a depth of 0.48 m (6.58 m OD) which then transitioned into the surface peat unit at a depth of 0.26 m (6.80 m OD).

For borehole A10, the maximum depth reached was 0.78 m (6.19 m OD) in the stiff and sandy blue/grey silt-clay with orange mottling unit. This was overlain by the silty peat with *Phragmites* unit at a depth of 0.67 m (6.30 m OD). This organic unit was overlain by an organic blue/grey silt-clay unit at a depth of 0.62 m (6.35 m OD) which transitioned into the surface peat unit at a depth of 0.26 m (6.71 m OD).

Boreholes A11 and A12 both terminated in the stiff and sandy blue/grey silt-clay with orange mottling unit at a depth of 0.33 m (7.00 m OD) and 0.38 m (7.24 m OD) respectively. This clastic unit was overlain by the surface peat unit at a depth of 0.20 m (7.13 m OD) for borehole A11 and at a depth of 0.16 m (7.46 m OD) for borehole A12.

Borehole A13 reached an impenetrable depth at 0.91 m (6.78 m OD) in the sandy blue/grey silt-clay with gravel unit. This basal clastic unit was overlain by an organic stiff brown clay-silt unit at a depth of 0.84 m (6.85 m OD). This unit transitioned into an organic blue/grey silt-clay with orange mottling unit at a depth of 0.68 m (7.01 m OD), and transitioned into the surface peat unit at a depth of 0.32 m (m OD).

Borehole A14 reached an impenetrable depth at 0.54 m (6.77 m OD) in the sandy blue/grey silt-clay with gravel unit, with orange mottling towards the top of the clastic unit. This clastic unit was overlain by the surface peat unit at a depth of 0.36 m (6.95 m OD).

A sample core was taken at Allonby from borehole A7 as it contained all main stratigraphic units recorded. Core A7 was used for all laboratory analyses and to establish a chronology for the site. The results of laboratory analyses undertaken on core A7 are discussed in detail in the following sections.

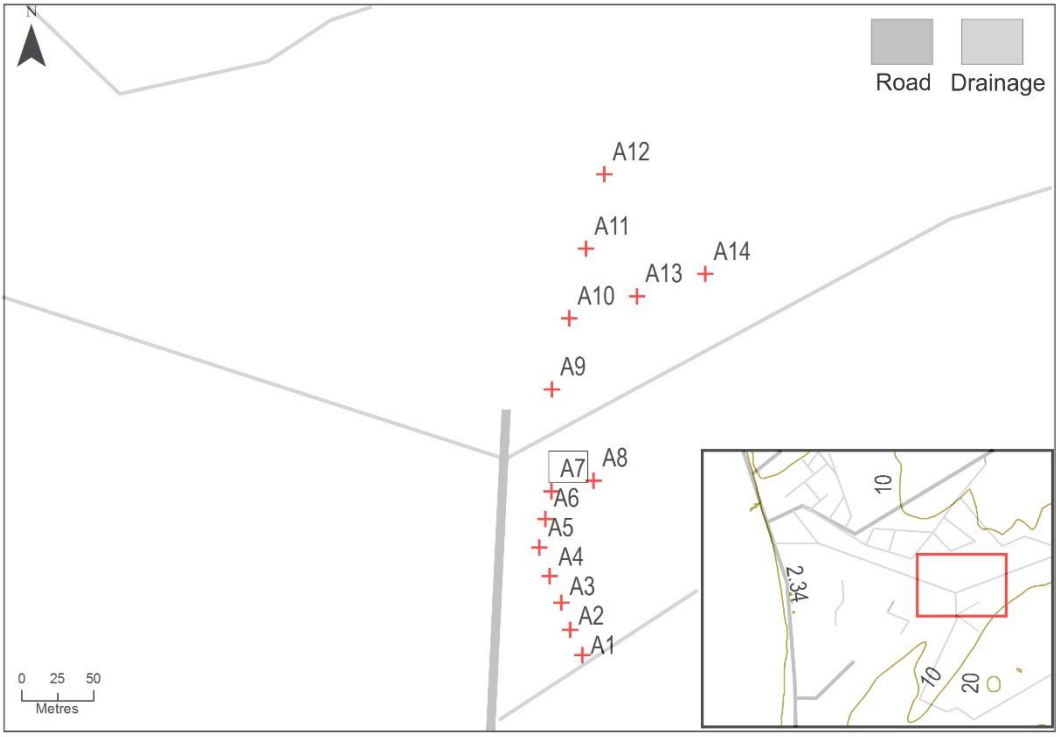
N
Road
Drainage
A12
A11
A14
A13
A10
A9
A8
A7
A6
A5
A4
A3
A2
A1
0 25 50
Metres
10
2.34
10
20

(a)

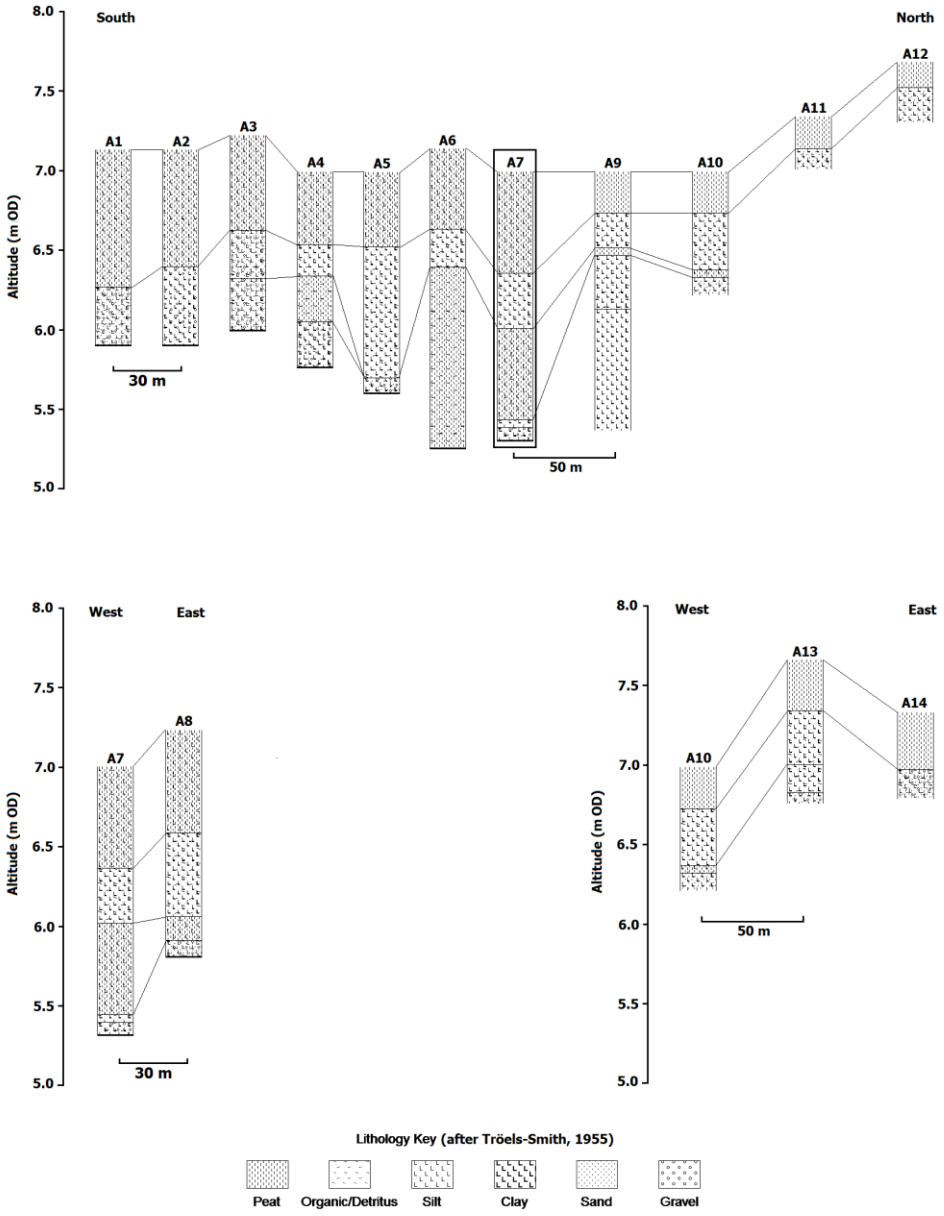
South
North
A1
A2
A3
A4
A5
A6
A7
A9
A10
A11
A12
30 m
50 m
Altitude (m OD)
8.0
7.5
7.0
6.5
6.0
5.5
5.0
West
East
A7
A8
30 m
A10
A13
A14
50 m
Lithology Key (after Tröels-Smith, 1955)
Peat
Organic/Detritus
Silt
Clay
Sand
Gravel

(b)

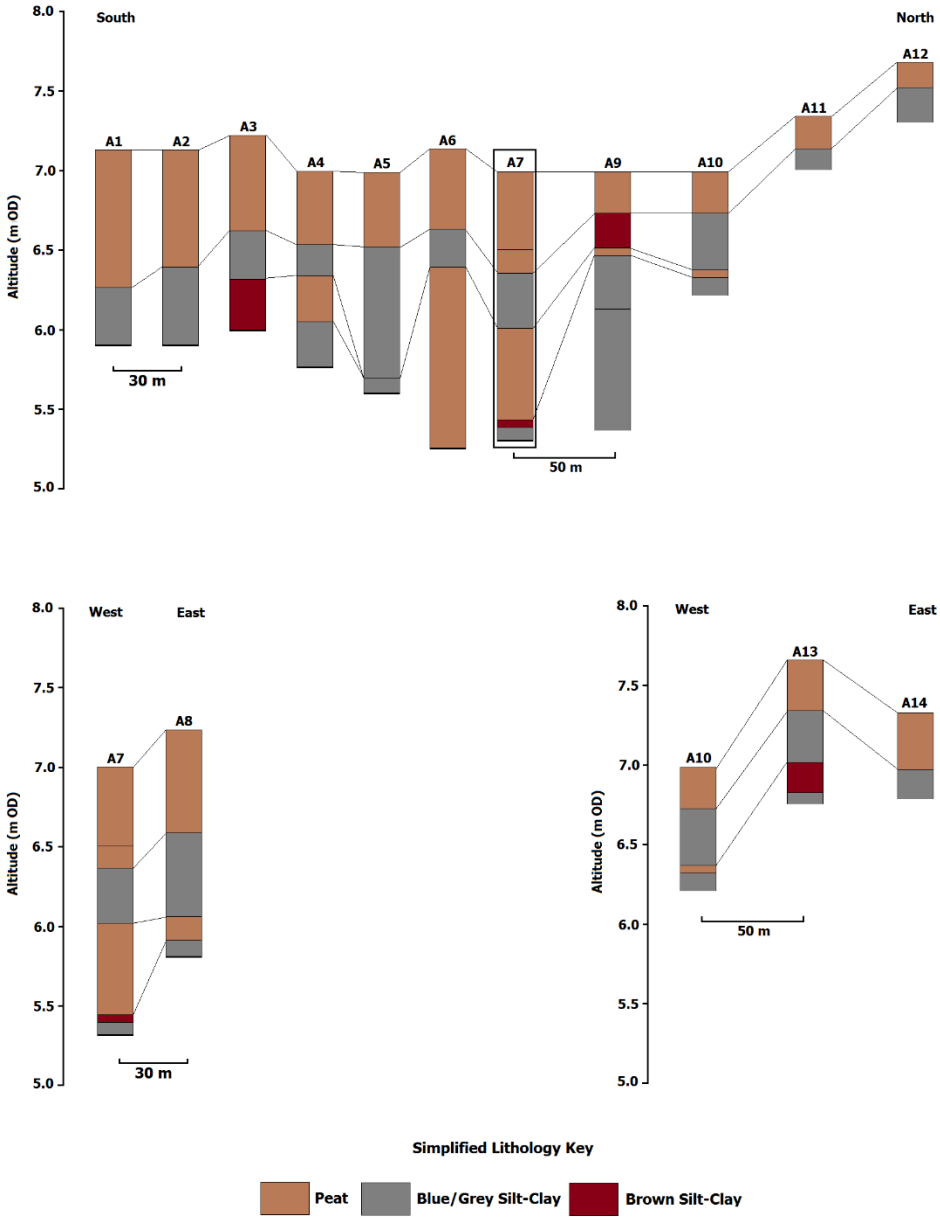

(c)

Figure 5.2: (a) Location of boreholes and sample core (A7) at Allonby with contour line marking the altitudes (m OD) of surrounding areas (Source: © Crown Copyright and Database Right (2018) Ordnance Survey, Digimap Licence) (b) The lithostratigraphy of the boreholes and sample core from Allonby (c) The simplified lithostratigraphy of the boreholes and sample core from Allonby. Sample core is marked by a black square

5.2 Sediment Composition

Core A7 terminated on the bedrock at 1.70 m (5.30 m OD). The surface elevation recorded for core A7 was 7.00 m OD. Towards the base of the core in the basal clastic unit, increased sand content was recorded. The sand content decreased in the clastic unit and basal organic unit, and was highest towards the surface of the core. The sand fraction found in core A7 consisted of mainly very fine sand and fine sand. The sediment description of core A7 is summarised in Table 5.1.

Table 5.1: Sediment description of core A7 including depth, altitude and the Tröels-Smith (1955) sediment classification

Depth (m)	Altitude (m OD)	Sediment Description	Tröels-Smith Sediment Classification (1955)
0 – 0.49	7.00 – 6.51	Very dark brown peat with roots and organic remains, some brown silt	Th4; Ag+, Nig. = 4, Strf. = 0, Sicc. = 1, Elas. = 1
0.49 – 0.64	6.51 – 6.36	Very dark brown peat with *Phragmites*, roots and organic remains, increased brown silt	Th3; Ag1, Nig. = 4, Strf. = 0, Sicc. = 1, Elas. = 1, Lim. = 0
0.64 – 0.99	6.36 – 6.01	Blue/grey silt-clay with *Phragmites*, roots and organic remains	Ag2; As2, Th+, Dl+, Nig. = 2, Strf. = 0, Sicc. = 2, Elas. = 0, Lim. = 2
0.99 – 1.57	6.01 – 5.43	Very dark brown peat with *Phragmites*, roots and organic remains and brown silt	Th3; Ag1; Dl+, Nig. = 4, Strf. = 0, Sicc. = 1, Elas. = 1, Lim. = 2
1.57 – 1.62	5.43 – 5.38	Brown silt-clay with *Phragmites*, roots and organic remains	Ag2; As1; Th1; Dl+, Nig. = 3, Strf. = 0, Sicc. = 2, Elas. = 0, Lim. = 2

1.62 – 1.70	5.38 – 5.30	Blue/grey silt-clay with roots and organic remains, sand and gravel	Ag2; As2; Dl+; Ga+; Gg+ (min), Nig. = 4, Strf. = 0, Sicc. = 3, Elas. = 0, Lim. = 2

5.3 Loss on Ignition

Loss on ignition analyses were undertaken on samples from core A7 to give an estimate of the organic carbon content and carbonate content of the sediment. Samples were taken every 8 cm throughout the core, from each stratigraphic unit recorded and analysed for organic carbon and carbonate content. Fluctuations can be noted in the percentage of organic carbon content of the samples from the Allonby core, with a maximum of 59% reached at a depth of 1.18 m (5.82 m OD) and a minimum of 4% at a depth of 1.66 m (5.34 m OD). Very low percentages of carbonate content were observed throughout the core, with a range of 1% to 6% recorded. A maximum of 6% of carbonate content was observed at 0.54 m (6.46 m OD) in the silty *Phragmites* peat unit. No correlation between the percentages of carbonate content with the change of stratigraphic horizons in the core was observed. The organic carbon and carbonate content of core A7 are shown in Figure 5.3.

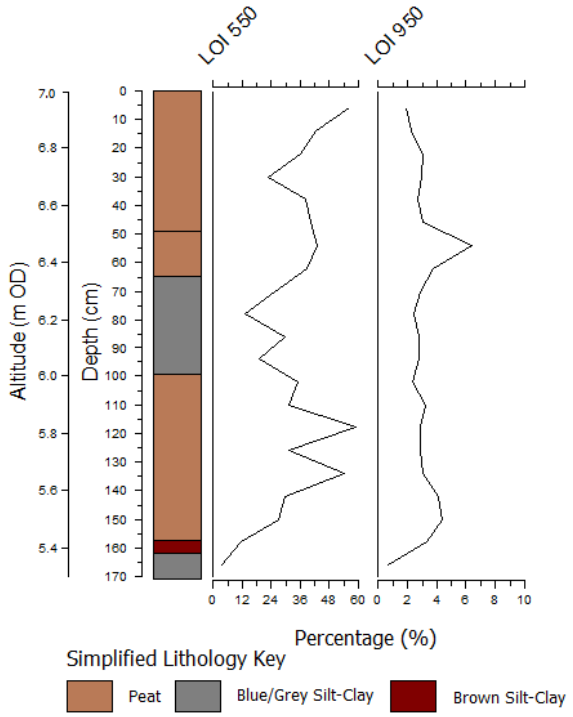

Figure 5.3: Plot of loss on ignition analyses for Allonby showing organic carbon and carbonate content of the sediment throughout core CGF1

5.4 Particle Size Analysis

Samples for particle size analysis were taken every 8 cm throughout the core from each stratigraphic unit and the data were categorised into clay, silt and sand fractions (Figure 5.4). Particle size analysis showed fairly homogeneous sediment dominated mostly by silt throughout the entire core with very limited variation in the clay content. The percentages of clay in core A7 ranged from 1% at a depth of 0.08 m (6.92 m OD) to 6% at a depth of 1.20 m (5.80 m OD). The silt content in the sediment ranged between 59% at a depth of 0.08 m (6.92 m OD) and 95% at a depth of 1.04 m (5.96 m OD). The sand content in core A7 showed a minimum of 0.02% at a depth of 1.04 m (5.96 m OD) and a maximum of 40% sand was recorded towards the top of the core at 0.08 m (6.92 m OD), which was composed mainly of very fine sand.

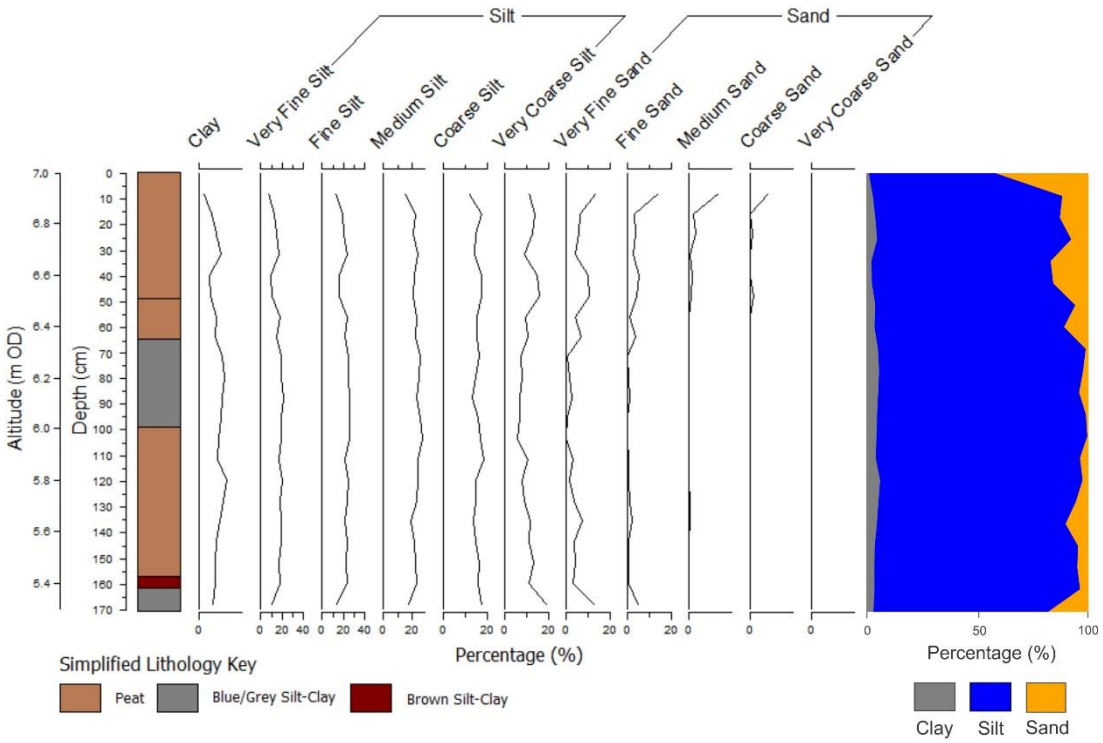

Figure 5.4: Diagram showing particle size analysis for core A7 from Allonby

5.5 Chronology

The chronology for the environmental changes recorded in core A7 was established through accelerator mass spectrometry (AMS) radiocarbon dating of four bulk sediment samples undertaken at DirectAMS Radiocarbon Dating Service in Washington, USA. The radiocarbon ages obtained were calibrated using OxCal v.4.3 (Ramsey, 2009) and the IntCal13 atmospheric curve (Reimer *et al.*, 2013). All dates were calibrated to cal BP (Table 5.2).

Table 5.2: Four radiocarbon dates obtained from Allonby core A7

Lab Code	Code-Depth (cm)	Altitude (m OD)	Material Dated	Fraction	Radiocarbon Age		Cal BP (2σ Ranges)
					BP	1σ Error	
D-AMS 022222	ALL-35	6.65-6.66	Peat	Bulk carbon	6377	34	7418-7255
D-AMS 025777	ALL-78	6.22-6.23	Organic clay	Bulk carbon	7359	32	8306-8041
D-AMS 025776	ALL-100	6.00-6.01	Peat	Bulk carbon	7209	41	8158-7954
D-AMS 022223	ALL-139	5.61-5.62	Peat	Bulk carbon	7203	49	8160-7946

An age-depth model for core A7 was developed using Bacon v2.3.4 (Blaauw & Christen, 2011). The red dotted line shows modelled median ages along core A7 and the grey stippled lines indicate the 95% confidence intervals of the modelled age-depth relationship. The transparent blue violin plots show the four calibrated AMS ^{14}C dates from Allonby. The upper left graph shows the iteration history of the model. The middle and right graphs show prior (green lines) and posterior (grey histograms) density functions for accumulation rate and memory of the model (Figure 5.5).

The mean 95% confidence of the age-depth model developed for core A7 covered 354 years, with a minimum of 167 years modelled at 35 cm and a maximum of 427 years modelled at 60 cm. 100% of the dates obtained from Allonby lie within the age-depth model's 95% range, although samples ALL-139 and ALL-78 appear to be younger and older respectively when compared to the model's prediction. It is therefore possible that contamination and/or sediment reworking might have occurred at these depths resulting in the incorporation of older carbon into sample ALL-139, while sample ALL-78 might have been contaminated by younger carbon from the upper sediment horizon.

The main stratigraphic boundaries of core A7 (0.64 m and 0.99 m; 6.36 m OD and 6.01 m OD) were included in the age-depth model (shown in the horizontal dotted lines across the model in Figure 5.5). The sedimentation rates were calculated based on the dated samples and the main stratigraphic boundaries (mean age obtained from the model's prediction) and shown on the right side of Figure 5.5.

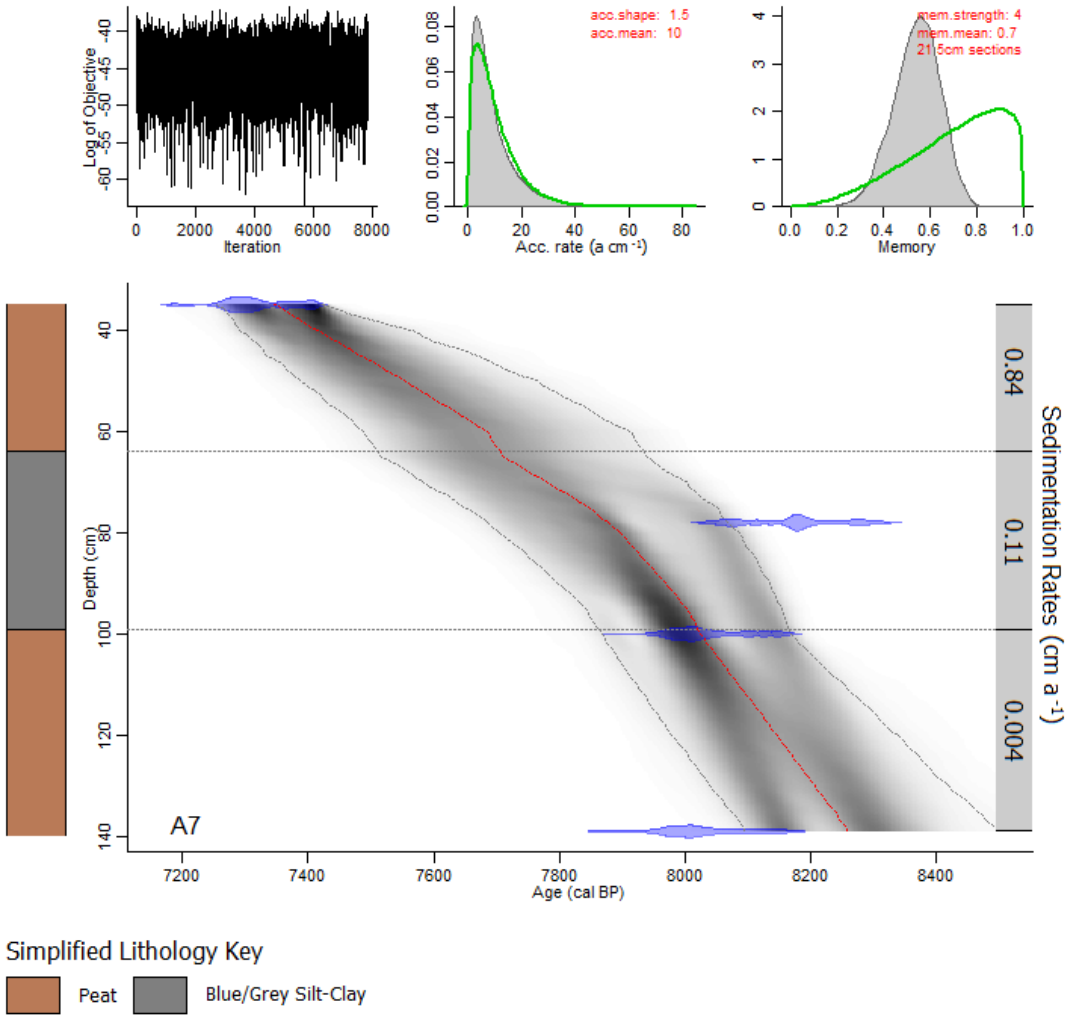

Figure 5.5: Age-depth model for core A7 based on Bacon v2.3.4 modelling routines (Blaauw & Christen, 2011) and calculated sedimentation rates from the AMS ^{14}C dates calibrated with IntCal13 (Reimer *et al.*, 2013). Dotted lines on the model indicates the main stratigraphic units in the A7 core

5.6 Foraminiferal Analysis

The preservation of foraminiferal tests in the samples from core A7 varied, with some samples containing very few foraminiferal tests. It was therefore not possible to obtain a minimum count of 40 individuals in some of the samples despite increasing the sample volume. Although the low foraminiferal counts may provide information on the palaeoenvironment of the site at the time of deposition (e.g. the dominance of *Jadammina macrescens* in low counts may indicate a high saltmarsh environment), samples with fewer than 40 individuals were consistently removed from any statistical analysis undertaken in this study, as the low count might contribute to an erroneous

and misleading species assemblage distribution for the sample. Samples were taken at 1 or 2 cm intervals throughout the whole core.

The samples analysed from Allonby revealed five main agglutinated saltmarsh species comprising of *J. macrescens*, *Miliamminia fusca*, *Tiphotrocha comprimata*, *Haplophragmoides wilberti* and *Trochammina inflata* (Figure 5.6). No calcareous species were found in core A7, although test linings were observed in the core. The agglutinated saltmarsh foraminiferal species were observed between the depths of 0.36 m (6.64 m OD) to 1.38 m (5.62 m OD) (Figure 5.6). No foraminifera were observed in the basal sandy organic blue/grey silt-clay with gravel unit (1.70 m to 1.62 m; 5.30 m OD to 5.38 m OD), the organic brown silt-clay unit (1.62 m to 1.57 m; 5.38 m OD to 5.43 m OD), deeper sections of the silty peat with *Phragmites* unit (1.57 m to 1.37 m; 5.43 m OD to 5.63 m OD) and in the surface peat unit from 0.35 m (6.65 m OD) towards the top of the core.

The foraminifera found in core A7 were dominated mainly by *J. macrescens* and *M. fusca*, with low frequencies of *T. comprimata*, *H. wilberti* and *T. inflata*. Variations between the dominance of *J. macrescens* and *M. fusca* were observed in the organic unit and minerogenic unit, with *J. macrescens* generally dominating the organic unit. The increased frequencies of *M. fusca* corresponded to the deposition of the organic blue/grey silt-clay unit. The presence of test linings was also observed where there was an increase of dominance in *M. fusca*. A small peak of *T. inflata* was observed at the depth of 1.16 m (5.84 m OD), although very low individuals counts was recorded for this depth.

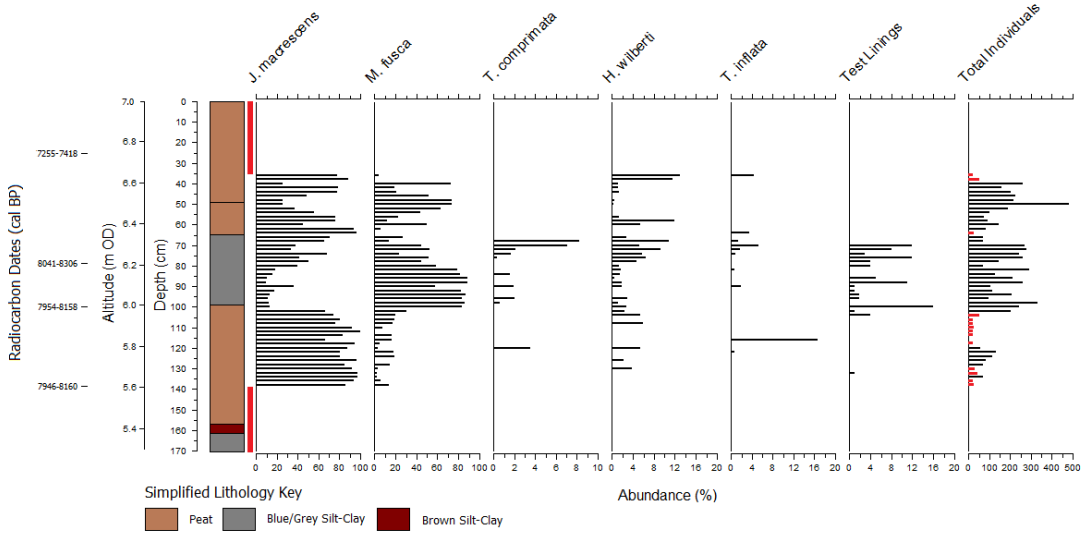

Figure 5.6: Foraminiferal diagram from Allonby core A7. Foraminiferal frequencies are expressed as a percentage of total foraminifera. All samples including samples with low individual counts (below 40 individuals; marked with red lines) were included in this diagram. Red blocks next to the stratigraphy diagram indicates the zone where foraminifera was absent in the core

The silty peat with *Phragmites* unit was dated at a depth of 1.39 m (5.61 m OD) and represented the first presence of foraminifera in the core. The measured age for the sample was 8160-7946 cal BP, although this date appear to be younger than expected based on the age-depth model developed (Section 5.5). The second date was obtained at the point of the transition from the silty peat with *Phragmites* unit to the overlying organic blue/grey silt-clay unit at a depth of 1.00 m (6.00 m OD), and resulted in an age of 8158-7954 cal BP. The third date at 8306-8041 cal BP obtained was at a depth of 0.78 m (6.22 m OD), where a change in biostratigraphy was observed. Sample ALL-35 which marks the absence of foraminifera from the core was dated at 7418-7255 cal BP.

The date obtained for sample ALL-78 is out of sequence and produced an age older than expected, and older than both samples ALL-100 and ALL-139. Contamination and/or sediment reworking might have occurred at this depth through the mixing of the intertidal sediments which occurred during periods of flood and ebb tides, resulting in the incorporation of older carbon into sample ALL-78. However, the three oldest dates ALL-139, ALL-100 and ALL-78 produced mean ages of 8030 cal BP, 8031 cal BP and 8170 cal BP respectively, which are in very close proximity to each other.

The date obtained from ALL-78 is deemed erroneous based on the microfossil evidence (discussed in Section 5.11), and should therefore be treated with caution.

5.7 Holocene Relative Sea-Level and Environmental Changes at Allonby

The interpretation of Holocene relative sea-level and environmental changes for Allonby is based on microfossil analyses, changes in lithostratigraphy and the sediment composition of core A7.

5.8 Microfossil Interpretation: Foraminifera

The bottom 0.31 m of the core is barren of any foraminifera (Figure 5.7). The first presence of foraminifera was recorded at 1.38 m (5.62 m OD) and dated at 8160-7946 cal BP, recording marine transgression at the site. The presence of agglutinated foraminifera dominated mainly by *J. macrescens* suggest that the area may have developed into a high saltmarsh environment, as evidenced by the contemporary samples collected from Skinburness Marsh and Bowness Marsh in this study (Chapter 4; Section 4.3.1 and Section 4.3.3).

At the transition from the silty peat with *Phragmites* unit to the overlying organic blue/grey silt-clay unit at 1.00 m (6.00 m OD) dated at 8158-7954 cal BP, the foraminiferal assemblage is dominated mainly by *M. fusca*. A reduced abundance of *J. macrescens* with the presence of test linings was also noted at this transition. An intertidal mudflat environment may have expanded at the site, replacing the saltmarsh environment. The foraminiferal assemblage dominated by *M. fusca* and the presence of test linings suggests an intertidal mudflat environment close to the fringing saltmarsh (Lloyd *et al.*, 1999). Occurrence of the agglutinated species *M. fusca* was also noted in the lower saltmarsh environment (between MHWST and MHWNT) at Cardurnock Marsh (Chapter 4; Section 4.3.2).

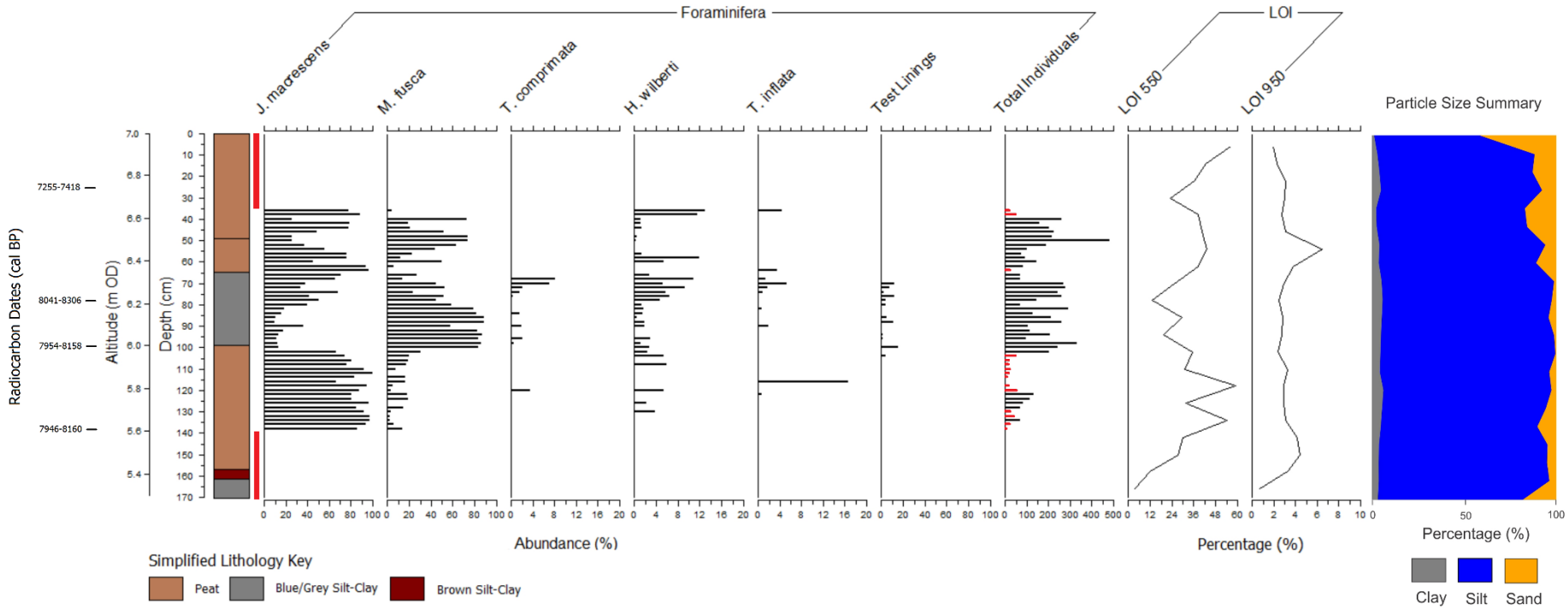

Figure 5.7: Summary diagram showing foraminifera, particle size analyses and loss on ignition undertaken on samples from core A7

The transition from organic blue/grey silt-clay unit to the overlying silty peat with *Phragmites* unit at a depth of 0.64 m (6.36 m OD) records a species domination mainly by *J. macrescens* and *M. fusca*, although the abundance of *M. fusca* is reduced and no test linings were observed. The microfossil evidence combined with the change in lithostratigraphy in this zone would suggest that there was a negative tendency in sea level, and a saltmarsh environment developed at the site. Peaks of *H. wilberti* were observed at the depths of 0.38 m (6.62 m OD) and 0.36 m (6.64 m OD). The presence of *J. macrescens* and *H. wilberti* are associated with an environment occurring at the level of extreme high water (Gehrels & Long, 2008). The site would have therefore still supported a saltmarsh environment.

From the depth of 0.35 m (6.65 m OD) towards the top of the core at 7.00 m OD, no foraminifera were observed in the surface peat unit. The regressive contact which records a negative marine tendency at the site was dated at 7418-7255 cal BP, and the site transitioned into a freshwater environment.

5.9 Sediment Deposition and Relative Sea-Level Interpretation

The site at Allonby is located on a low-lying land below 10 m OD and would have been inundated by increasing sea level during the period of marine transgression recorded. The deposition of the basal blue/grey silt-clay with gravel unit and the brown silt-clay unit may have resulted either from slope wash processes, fluvial processes or through inundation during period of marine transgression at the site. It is more likely that the minerogenic units were deposited at the site through slope wash or fluvial processes, as both units are barren of any foraminifera. The deposition of the basal blue/grey silt-clay with gravel unit may have resulted from glaciofluvial processes (Walker, 1966), while the brown silt-clay unit may have resulted from fluvial processes, depositing sediments in the flood plain near the site during storm events or extreme weather at high tide period.

The site at Allonby is surrounded by higher ground to the north, south and east of the site (Figure 5.2a). A British Geological Survey (BGS) borehole located at Newtonfield Farm (NY 1078 4338), 1.4 km southeast from the site, revealed sediment units composed of soft sandstone with sand and gravel 5.50 m beneath the top soil, overlain by yellow/brown sandy clay (5.20 m below the surface top soil). A BGS

borehole located at Brownrigg Hall Farm (NY 1000 4370), 0.5 km southeast from the site at Allonby also recorded a sediment unit 27.4 metres deep composed of glacial sand and gravel with clay bands occurring beneath the top soil.

The clastic unit was overlain by a silty peat with *Phragmites* unit. Between 1.57 m (5.43 m OD) to 1.39 m (5.61 m OD), this organic unit is barren of any foraminifera, and would appear to be of terrestrial origin. At a depth of 1.38 m (5.62 m OD) in the silty peat with *Phragmites* unit, the first occurrence of agglutinated foraminifera was observed, and this transgressive contact indicating positive sea-level tendency was dated at 8160-7946 cal BP. It is likely that a saltmarsh environment would have developed in the area, recording the initial marine transgression at the site. This date may indicate the first recording of the Main Postglacial Transgression at the site and also possibly the contribution of freshwater input into the ocean as a result of the drainage of the glacial Lake Agassiz-Ojibway in North America in addition to the Main Postglacial Transgression.

The silty peat with *Phragmites* unit was overlain by an organic blue/grey silt-clay unit and was dated at 8158-7954 cal BP. Sea level would have continued to increase and resulted in the expansion of the intertidal mudflat environment evidenced by the deposition of the organic blue/grey silt-clay unit at the site, and by the change in biostratigraphy. At Skelwith Pool, Morecambe Bay, an increase of sea level at a rate $\geq$ 0.4 cm a^{-1} resulted in an expansion of the intertidal environment over the coastal lowlands, but an increase of sea level with a rate $\leq$ 0.2 cm a^{-1} did not result in widespread inundation as the intertidal deposition and saltmarsh accretion kept pace with the rising sea level (Zong & Tooley, 1996). The rate of relative sea-level increase at the site during the deposition of the organic blue/grey silt-clay unit may therefore have been more rapid compared to the initial transgressive contact at 1.38 m (5.62 m OD). Sedimentation rates of 0.004 cm a^{-1}, 0.11 cm a^{-1} and 0.84 cm a^{-1} were recorded for the sediment accumulated between 1.39 m to 0.99 m (5.61 m OD to 6.01 m OD), 0.99 m to 0.62 m (6.01 m OD and 6.38 m OD) and 0.62 m to 0.35 m (6.38 m OD to 6.65 m OD) respectively.

A possible decrease in relative sea level was observed at a depth of 0.78 m (6.22 m OD) evidenced by the change in biostratigraphy, although the date obtained from sample ALL-78 at this depth produced the erroneous date of 8306-8041 cal BP. The

organic blue/grey silt-clay unit was overlain by another unit of peat with *Phragmites* unit, recording a negative tendency in sea level at 0.64 m (6.36 m OD). A saltmarsh may have developed at the site as evidenced by change in the lithostratigraphy and biostratigraphy.

Marine regression from the site was recorded at a depth of 0.35 m (6.65 m OD) as the saltmarsh environment transitioned into a more freshwater environment, evidenced by the absence of foraminifera in the sediment sequence from 0.35 m (6.65 m OD) towards the top of the core. This regressive contact was dated at 7418-7255 cal BP. No further changes in the biostratigraphy and lithostratigraphy were observed in the top 0.35 m of the core.

5.10 Relative Sea-Level Reconstruction for Allonby

A relative sea-level reconstruction for the site at Allonby was developed through a combination of lithostratigraphic and biostratigraphic analyses, determination of indicative meanings and calculation of sea-level index points.

5.11 Determination of Indicative Meaning

As the predicted palaeo surface marsh elevation (PMSE) values based on the transfer function utilised on core A7 were deemed unreliable due to the high number of fossil samples with poor modern analogues, the assigned reference water level based on the changes in lithostratigraphy and biostratigraphy (foraminiferal assemblages) was therefore used for the calculation of sea-level index points.

Based on the lithostratigraphy and biostragraphy of samples ALL-139 and ALL-100, the indicative meaning associated with a high saltmarsh environment was ascribed. The lithostratigraphy of samples ALL-139 and ALL-100 consisted of the silty peat with *Phragmites* unit and high organic carbon content (Figure 5.3). The biostratigraphy of sample ALL-139 showed a dominance of the agglutinated saltmarsh species *J. macrescens* (85%) which is mostly associated with a high saltmarsh environment, as evidenced by the contemporary foraminifera collected from Skinburness Marsh and Bowness Marsh (Chapter 4; Sections 4.3.1 and 4.3.3). The biostratigraphy of sample ALL-100 showed an increased presence of *M. fusca* (83%), immediately prior to the

transition into the overlying organic blue/grey silt-clay unit and is also interpreted as a high saltmarsh environment.

The reference water level for both samples ALL-139 and ALL-100 at the depths of 1.39 m (5.61 m OD) and 1.00 m (6.00 m OD) respectively are therefore determined to be the midpoint between HAT and MHWST at Skinburness Marsh as the characteristics of samples ALL-139 and ALL-100 are reflected most closely in the contemporary samples collected from Skinburness Marsh (dominance of *J. macrescens* and increase of *M. fusca* prior to the transition). This provides the indicative meaning of HAT of 6.3 m OD and MHWST of 4.9 m OD (the reference water level as the midpoint between HAT and MHWST), with the indicative range of ±1.4 m covering HAT and MHWST (Chapter 3; Section 3.9).

Sample ALL-78 was not ascribed to an indicative meaning due to the erroneous date of the sample. Sample ALL-78 which recorded a possible decrease in relative sea level (based on the change in foraminiferal assemblage), produced a date older than samples ALL-100 and ALL-139, both of which recorded marine transgressions at the site. A sea-level index point therefore is also not calculated for sample ALL-78.

Sample ALL-35 was also ascribed an indicative meaning associated with a high saltmarsh environment, based on the lithostratigraphy consisting of the surface peat unit and the biostratigraphy dominated by the agglutinated saltmarsh species *J. macrescens*. The reference water level for sample ALL-35 is therefore also determined to be the midpoint between HAT (6.3 m OD) and MHWST (4.9 m OD) measured at Skinburness Marsh, with the indicative range covering of ±1.4 m.

5.12 Post-Depositional Lowering of Sediments

All of the sea-level index points produced from Allonby are of intercalated samples, and would have been subjected to post-depositional lowering (PDL). The PDL of sediments in core A7 was estimated based on the geotechnical model developed by Brain *et al*. (2011, 2012), as discussed in Chapter 3 (Section 3.9.1). Minimal PDL of sediments is observed in core A7, which ranged between 0.001 to 0.200 m. Figure 5.8 shows the PDL of sediments at 0.02 m intervals throughout core A7.

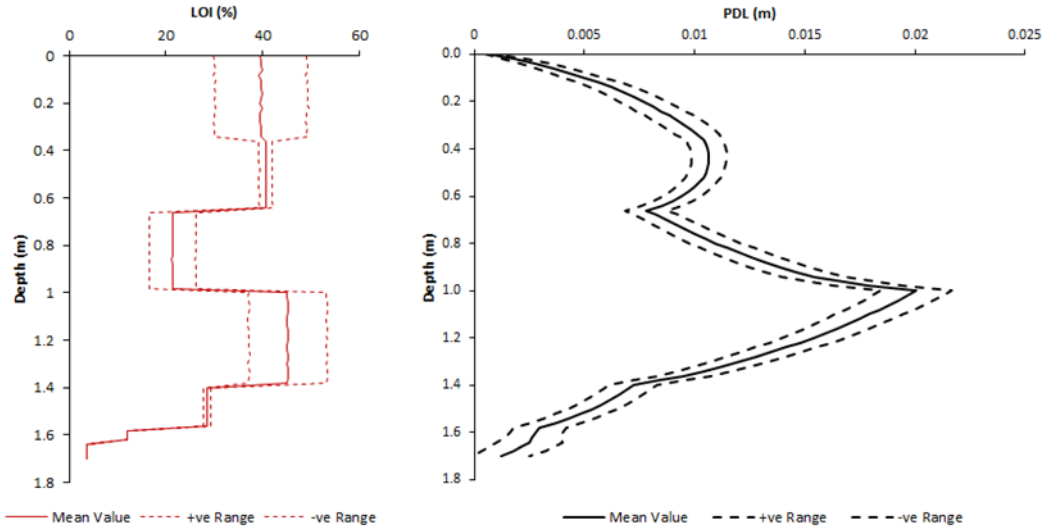

Figure 5.8: Geotechnical and physical properties showing the averaged downcore organic content, expressed as % loss on ignition and the model estimates of post-depositional lowering. Abbreviations: LOI = Loss on ignition; PDL = Post-depositional lowering

5.13 Sea-Level Index Points

The sample's age, reference water level and indicative range along with the associated errors and correction for each sample are required for the calculation of sea-level index points (Chapter 3; Section 3.9). Three sea-level index points were produced for Allonby site (Table 5.3). The complete SLIPs table following Shennan *et al.* (2018) is presented in the appendix of this thesis.

Table 5.3: Sea-level index points produced from A7

Lab Code	Latitude	Longitude	Radiocarbon Age		Cal BP (2σ Ranges)			Altitude (m OD)	Compaction Correction (m)	RSL (m)	Tendency
			BP	1σ Error	Min	Mean	Max				
D-AMS 022222	54.783	-3.408	6377	34	7255	7320	7418	6.65	+0.010	+1.06±1.46	Negative
D-AMS 025776	54.783	-3.408	7209	41	7954	8031	8158	6.00	+0.020	+0.42±1.46	Positive
D-AMS 022223	54.783	-3.408	7203	49	7946	8030	8160	5.61	+0.010	+0.02±1.46	Positive

Samples ALL-35, ALL-100 and ALL-139 produced sea-level index points of 1.06±1.46 m, 0.42±1.46 m and 0.02±1.46 m respectively. Figure 5.9 shows the sea-level index points from Allonby plotted against the relative sea-level predictions based on the BRADLEY2011, KUCHAR2012 and BRADLEY2017 models in Shennan *et al*. (2012), Kuchar *et al*. (2012) and Shennan *et al*. (2018) respectively for the southern Solway Firth at location NY 2481 5666.

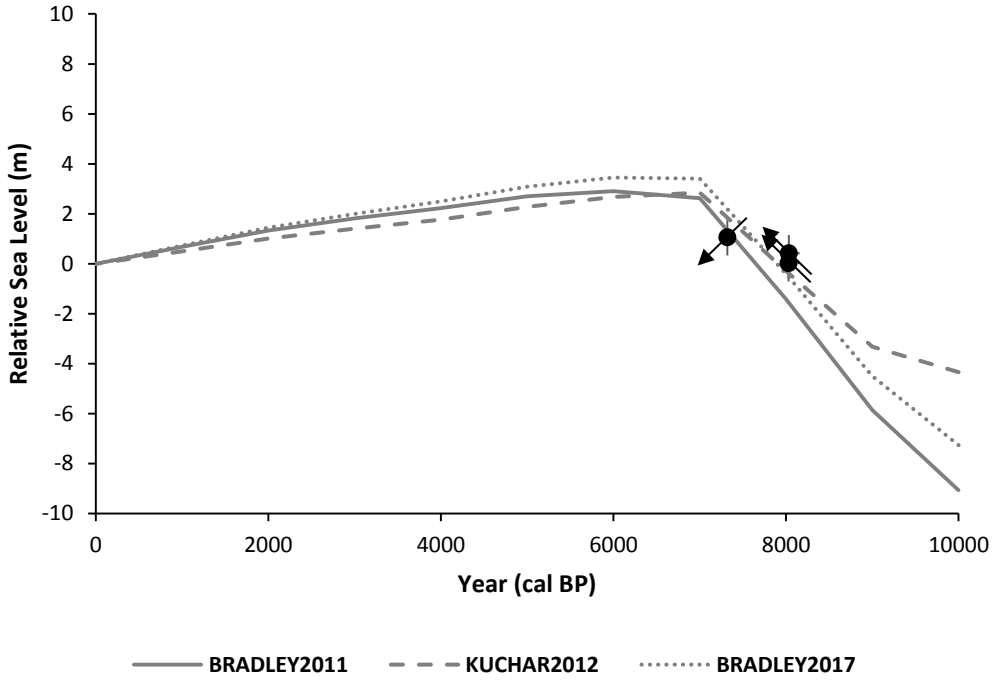

Figure 5.9: Graph showing two sea-level index points from Allonby. The black line is the modelled relative sea-level curves for southern Solway Firth based on Shennan *et al*. (2012; 2018) and Kuchar *et al*. (2012). All sea-level index points include associated individual vertical and age error bars

5.14 Summary

The site at Allonby has provided a record of Holocene sea-level changes as evidenced by the changes in lithostratigraphy and biostratigraphy of core A7. The three sea-level index points from Allonby broadly agree with the recorded dates of marine transgression and marine regression of other sites located on the southern shore of the Solway Firth apart from the later marine regression recorded at Drumburgh Moss. The initial increase in relative sea-level at Allonby as a result of the Main Postglacial Transgression or a combination of both Main Postglacial Transgression and drainage

of Lake Agassiz-Ojibway was dated at 8031 cal BP, while a marine regression at Allonby was dated at 7320 cal BP.

CHAPTER 6

COWGATE FARM

6.0 Introduction

The site at Cowgate Farm (NY 0967 4737) is located on the northwest Cumbrian coastline, approximately 1 km from the present coastline, 10 km from the southern bank of Moricambe Bay and approximately 20 km from the southern shore of the Solway Firth. The site is located 400 metres from Cowgate (NY 0922 4776) and is situated near a gently-sloping hill to the south, with flat and low-lying farmland to the north, east and west of the site. Drainage channels are located in the north and west of the site, and to the east of the site, a small road connecting the farming areas and town is present (Figure 6.2a). The site at Cowgate Farm is approximately 150 m long by 200 m wide and located within a field that is currently being used as a grazing area for domestic livestock. The closest contemporary saltmarsh investigated to the site is Skinburness Marsh (Figure 6.1).

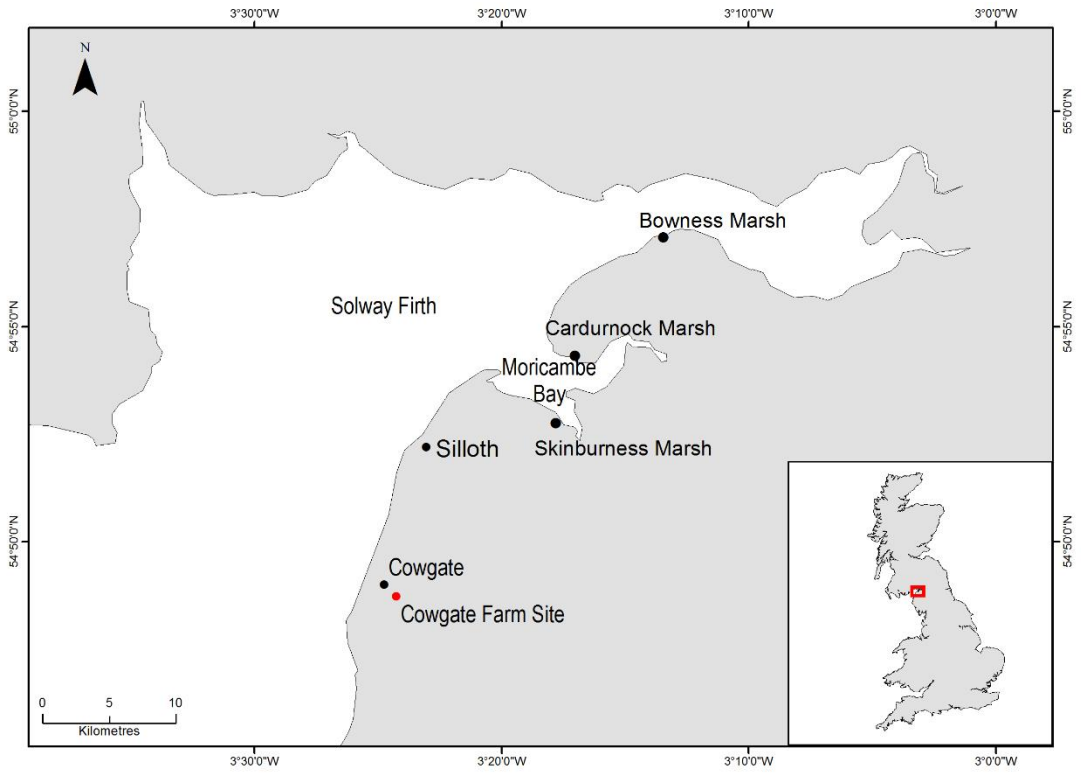

Figure 6.1: Location of the study site at Cowgate Farm marked in red

6.1 Borehole Location and Stratigraphy

A detailed stratigraphy of the site was established through four transects of boreholes, which were cored across the study site (Figure 6.2). The surface elevation of the boreholes and the sample cores at Cowgate Farm ranged from 7.6 m OD to 8.1 m OD. The maximum depth reached at Cowgate Farm was 2.18 m (5.8 m OD) in borehole CGF2. All boreholes terminated in impenetrable stiff pink/brown clay containing small gravel, except for borehole CGF11 which terminated in a grey and sandy fine gravel unit. The general stratigraphy recorded at Cowgate Farm was basal sand and silt overlain by peat with *Phragmites*.

Borehole CGF1 reached a depth of 1.52 m (6.48 m OD) and terminated in stiff pink/brown clay with small gravel. It was overlain by a sandy blue/grey silt-clay at 1.41 m (6.59 m OD). The sandy blue/grey silt-clay unit was overlain by a similar unit containing organic remains at 1.28 m (6.72 m OD). This organic clastic unit then transitioned into the peat with *Phragmites* unit at 1.25 m (6.75 m OD), and the surface peat unit at 0.25 m (7.75 m OD).

Borehole CGF2 reached an impenetrable depth at 2.18 m (5.72 m OD) in the pink/brown clay with small gravel unit. This unit was overlain by a blue/grey silt-clay unit at 1.50 m (6.40 m OD), which transitioned into a sandy blue/grey silt-clay unit at 1.32 m (6.58 m OD). The clastic unit transitioned into the surface peat with *Phragmites* unit at 1.28 m (6.62 m OD).

Borehole CGF3 terminated in the pink/brown clay with small gravel unit at 1.44 m (6.56 m OD). The basal clastic unit was overlain by a blue/grey silt-clay unit at 1.30 m (6.70 m OD), which was then overlain by an organic blue/grey silt-clay unit at 1.20 m (6.80 m OD). This transitioned into the surface peat with *Phragmites* unit at 1.18 m (6.82 m OD).

In borehole CGF4, the maximum depth reached was 2.01 m (6.09 m OD) which terminated in the pink/brown clay with small gravel unit. The basal clastic unit was overlain by the blue/grey silt-clay unit at 1.81 m (6.29 m OD), which was overlain by a more organic blue/grey silt-clay unit at 1.50 m (6.60 m OD). This clastic unit then transitioned into the surface peat with *Phragmites* unit at 1.37 m (6.73 m OD).

Borehole CGF5 reached an impenetrable depth at 1.68 m (6.32 m OD) in the pink/brown clay with small gravel unit. This was overlain by the blue/grey silt-clay unit at 1.50 (6.50 m OD) and a shallow peat with *Phragmites* unit at 1.31 m (6.69 m OD). This organic unit was overlain by sandy blue/grey silt-clay unit at 1.25 m (6.75 m OD). The second clastic unit then transitioned into the surface peat with *Phragmites* unit at 1.20 m (6.80 m OD).

Borehole CGF6 terminated in the pink/brown clay with small gravel unit at 1.71 m (6.29 m OD). This was overlain by the blue/grey silt-clay unit at 1.50 m (6.50 m OD) and a more organic blue/grey silt-clay unit at 1.27 m (6.73 m OD). The clastic unit then transitioned into the surface peat with *Phragmites* unit at 1.21 m (6.79 m OD).

For borehole CGF7, the maximum depth reached was 1.82 m (6.28 m OD) in the pink/brown clay with small gravel unit. This was overlain by an organic blue/grey silt-clay unit at 1.50 m (6.60 m OD) that transitioned into the surface peat with *Phragmites* unit at 1.38 m (6.72 m OD).

Borehole CGF8 terminated in the unit of pink/brown clay with small gravel at 1.95 m (5.75 m OD). This was overlain by a blue/grey silt-clay unit with a large pieces of wood and organic materials at 1.80 m (5.90 m OD). This was overlain by an organic blue/grey silt-clay unit at 1.36 m (6.34 m OD) and a peat with *Phragmites* unit at 1.21 m (6.49 m OD). This organic unit was overlain by another blue/grey silt-clay unit at 0.50 m (7.20 m OD), which then transitioned into the surface peat with *Phragmites* unit at 0.42 m (7.28 m OD).

Borehole CGF9 terminated in the pink/brown clay unit at 1.45 m (6.25 m OD) and was overlain by the organic blue/grey silt-clay unit at 1.36 m (6.34 m OD). This then transitioned into the surface peat with *Phragmites* unit at 1.26 m (6.44 m OD).

In borehole CGF10, the maximum depth reached was 1.45 m (6.55 m OD) which terminated in the pink/brown clay with small gravel unit. This was overlain by the organic blue/grey silt-clay unit at 1.36 m (6.64 m OD). The clastic unit then transitioned into the surface peat with *Phragmites* unit at 1.23 m (6.77 m OD).

Borehole CGF11 terminated at 0.50 m (7.50 m OD) in a unit consisting of grey and sandy fine gravel which was overlain by the surface peat with *Phragmites* unit. The presence of the grey gravel in the stratigraphy may be attributed to the construction of the drainage ditch and road found next to the site investigated, located east of CGF11.

A sample core was taken at Cowgate Farm from borehole CGF1 as it contained all the major stratigraphic units recorded at the site. Core CGF1 was used for all laboratory analysis and to establish a chronology for the site. The results of laboratory analyses undertaken on core CGF1 are discussed in detail in the following sections.

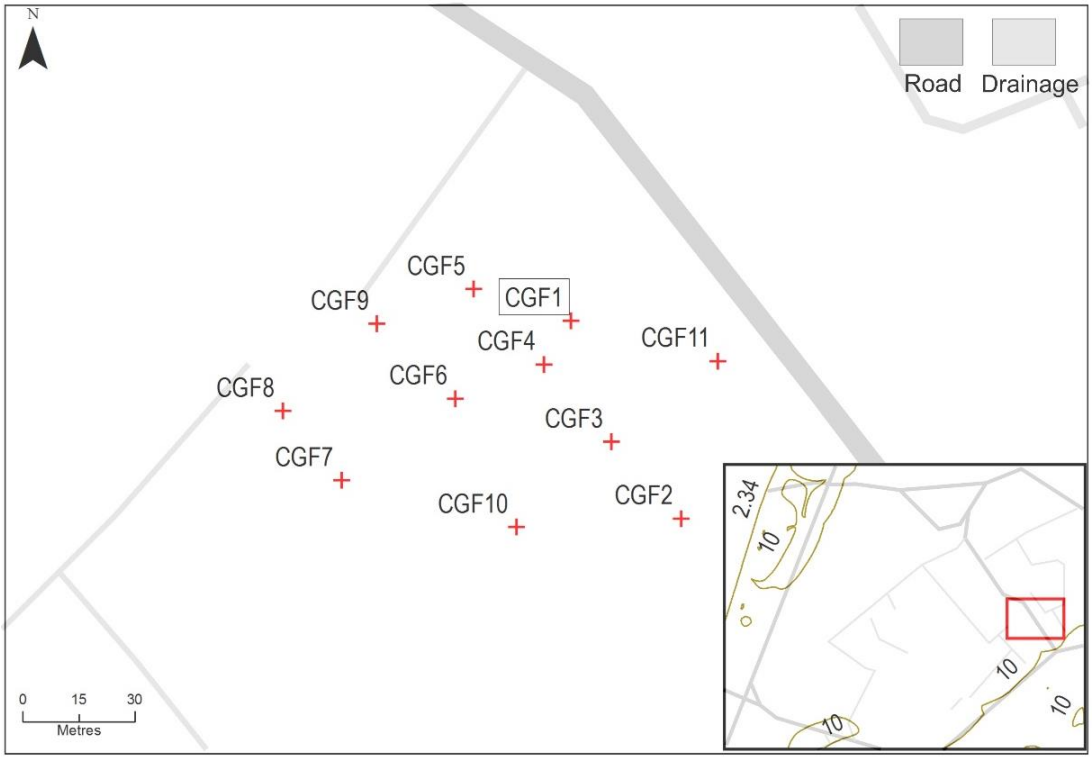

(a)

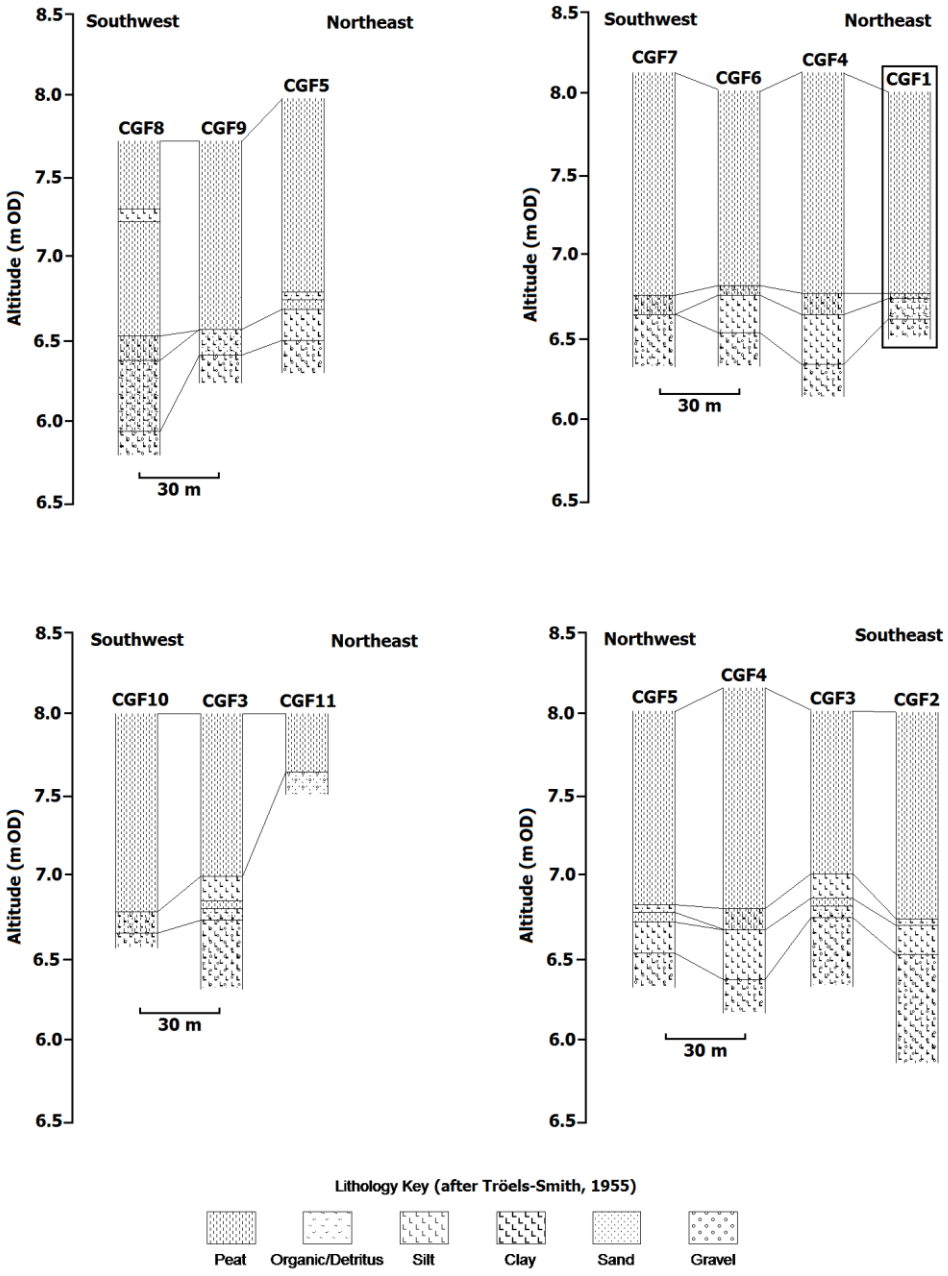
Southwest
Northeast
CGF8
CGF9
CGF5
CGF7
CGF6
CGF4
CGF1
CGF10
CGF3
CGF11
Northwest
Southeast
CGF2
Altitude (m OD)
8.5
8.0
7.5
7.0
6.5
6.0
30 m
Lithology Key (after Tröels-Smith, 1955)
Peat
Organic/Detritus
Silt
Clay
Sand
Gravel

(b)

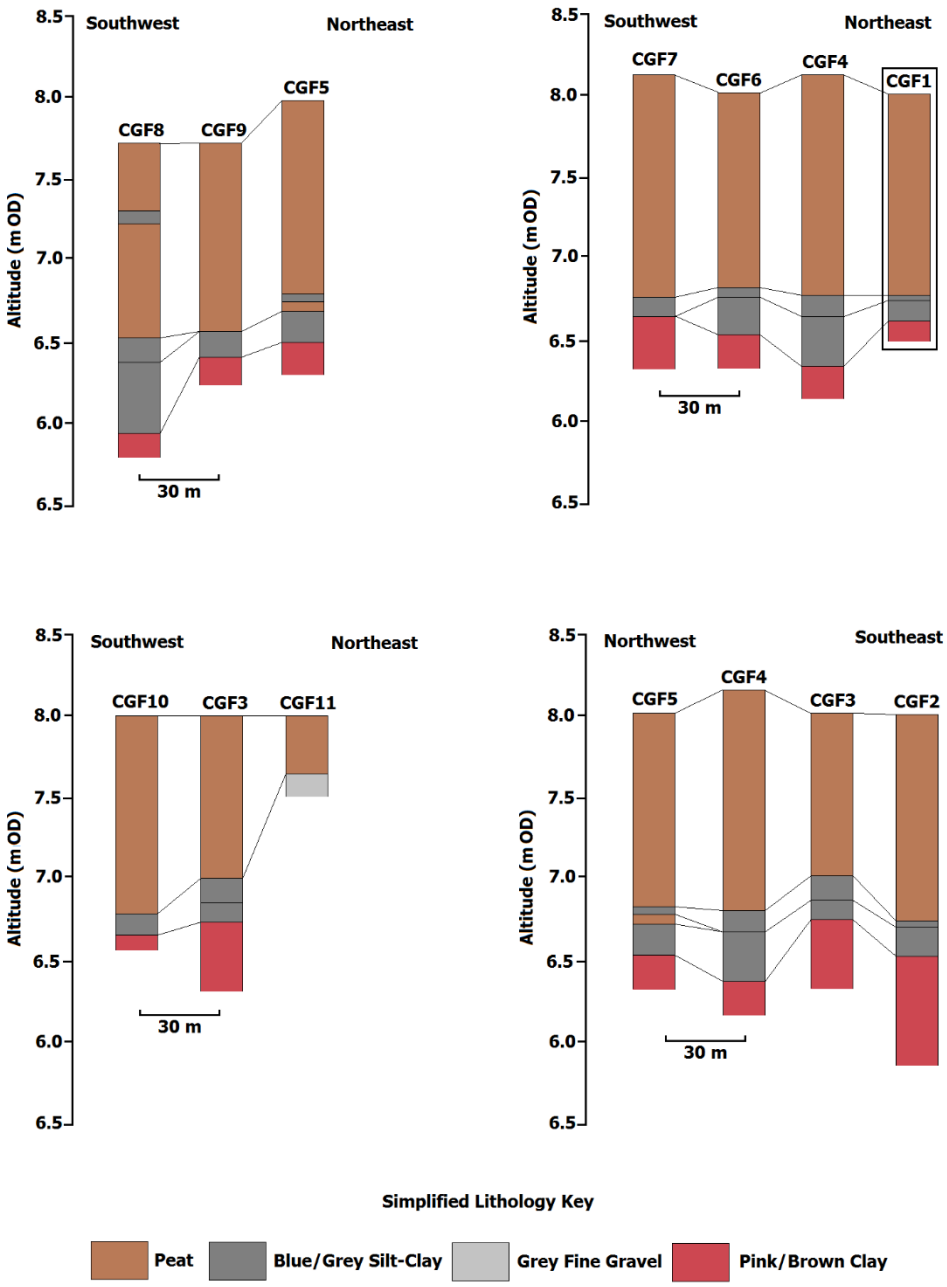

(c)

Figure 6.2: (a) Location of boreholes and sample core (CGF1) at Cowgate Farm with contour line marking the altitudes (m OD) of surrounding areas (Source: © Crown Copyright and Database Right (2018) Ordnance Survey, Digimap Licence) (b) The lithostratigraphy of the boreholes and sample core from Cowgate Farm (c) The simplified lithostratigraphy of the boreholes and sample core from Cowgate Farm. Sample core is marked in a black square

6.2 Sediment Composition

Core CGF1 terminated in the pink/brown clay unit at 1.52 m (6.48 m OD). The surface elevation recorded for core CGF1 was 8.00 m OD. The sand content of the sediment was highest towards the base of the core and decreased in the organic unit. At approximately 0.20 m depth from the surface of the core, the sand content increased again. Coarser sand was observed towards the base of the core in the blue/grey silt-clay unit and finer sand in the overlying units. The sediment description of core CGF1 is summarised in Table 6.1.

Table 6.1: Sediment description of core CGF1 including depth, altitude and the Tröels-Smith (1955) sediment classification

Depth (m)	Altitude (m OD)	Sediment Description	Tröels-Smith Sediment Classification (1955)
0 – 1.25	8.00 – 6.75	Very dark brown peat with *Phragmites*, roots and organic remains	Th4, Nig. = 4, Strf. = 0, Sicc. = 1, Elas. = 1
1.25 – 1.28	6.75 – 6.72	Blue/grey silt-clay with *Phragmites*, roots, organic remains and sand	Th2; Ag2; Ga+, Nig. = 2, Strf. = 0, Sicc. = 2, Elas. = 1, Lim. = 2
1.28 – 1.41	6.72 – 6.59	Sandy blue/grey silt-clay with wood fragments	Ag2; As1; Ga1; Dl+, Nig. = 2, Strf. = 0, Sicc. = 2, Elas. = 0, Lim. = 1
1.41 – 1.52	6.59 – 6.48	Blue/grey silt-clay transition into pink/brown clay with small gravel	Ag; As2; Gg+ (min), Nig. = 2, Strf. = 0, Sicc. = 3, Elas. = 0, Lim. = 2

6.3 Loss on Ignition

Loss on ignition analyses were undertaken on samples from core CGF1 to give an estimate of the organic carbon content and carbonate content of the sediment. In the peat with *Phragmites* unit and the surface peat unit, samples were taken at 17

cm intervals from 0.05-1.06 m (7.95-6.94 m OD) as there was only one major stratigraphic unit identified, and 11 cm intervals between 1.06-1.17 m (6.94-6.83 m OD) as the stratigraphy changed from the peat with *Phragmites* unit to the clastic unit. Samples were then taken at 2 cm intervals between 1.17-1.50 m (6.83-6.50 m OD) where changes in the stratigraphy were more frequent towards the base of the core. Fluctuations can be observed in the percentage of organic carbon content which ranged from 2% to 76%, with a limited change in the percentage of carbonate content throughout the core (a maximum of 8%). The organic carbon content and carbonate content of core CGF1 are shown in Figure 6.3.

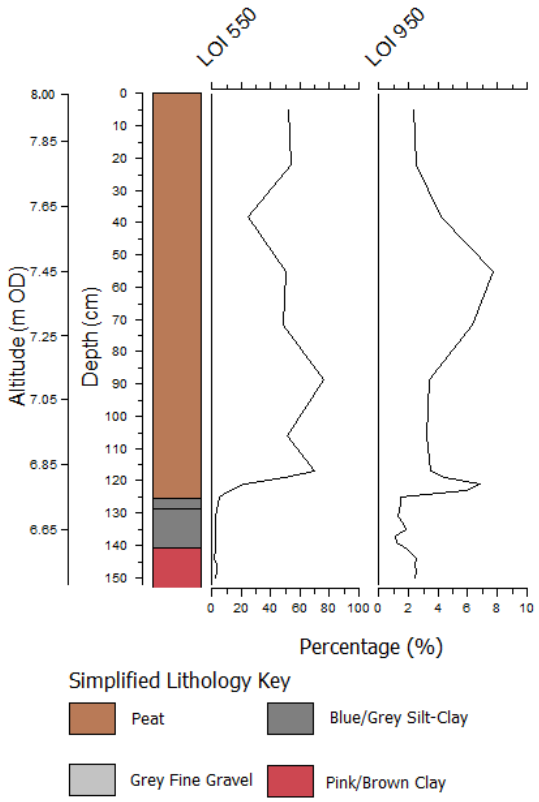

Figure 6.3: Plot of loss on ignition analyses for Cowgate Farm showing organic carbon and carbonate contents of the sediment throughout core CGF1

6.4 Particle Size Analysis

In the peat with *Phragmites* unit and the surface peat unit, samples were taken at 17 cm intervals for particle size analysis from 0.05-1.06 m (7.95-6.94 m OD) as there was only one major stratigraphic unit identified, and 11 cm intervals between 1.06-1.17 m (6.94-6.83 m OD) as the stratigraphy changed from the peat with *Phragmites*

unit to the clastic unit. Samples were then taken at 2 cm intervals between 1.17-1.50 m (6.83-6.50 m OD) where changes in the stratigraphy were more frequent towards the base of the core (Figure 6.4). There was minimal change in clay content throughout the core, with the percentage of clay content ranging between 1% at a depth of 1.29 m (6.71 m OD) and 7% at a depth of 1.25 m (6.75 m OD). The silt content remained high throughout the core, and comprised the majority of the sediment composition with a range between 35% at a depth of 1.29 m (6.71 m OD) and 94% at a depth of 0.38 m (7.62 m OD). The silt content decreased slightly closer to the surface at depths of 0.22 m (7.78 m OD) and 0.05 m (7.95 m OD).

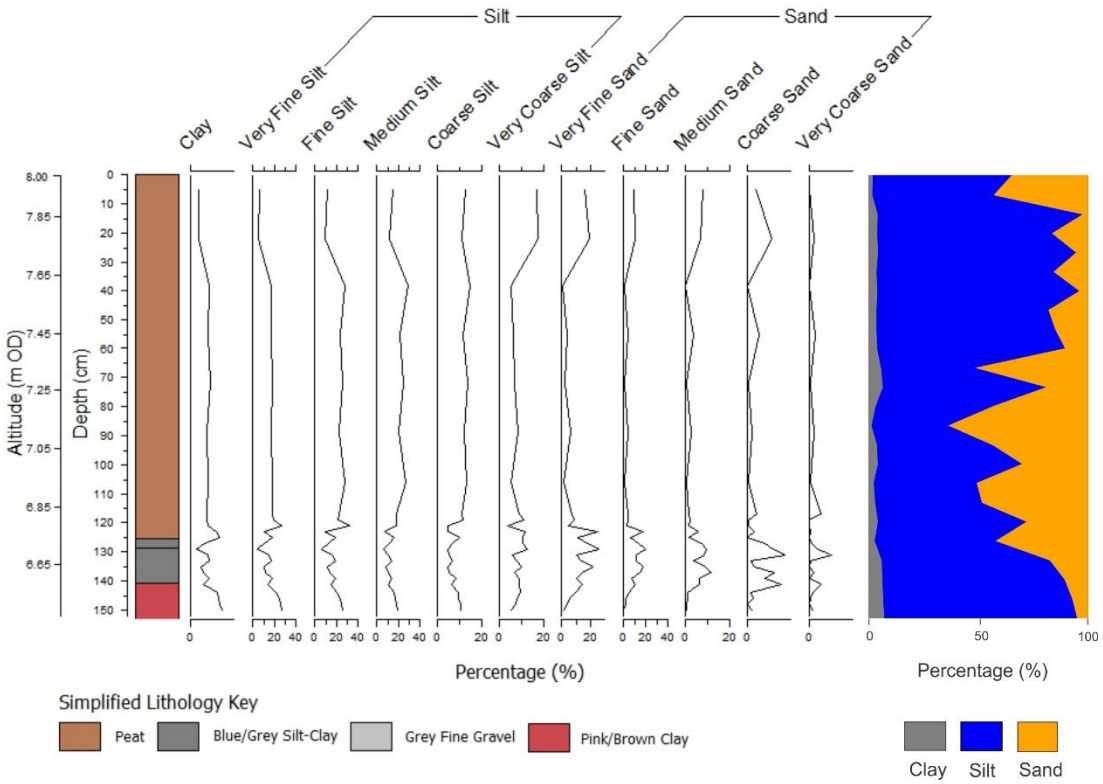

Figure 6.4: Diagram showing particle size analysis for core CGF1 from Cowgate Farm

6.5 Chronology

The chronology for the core CGF1 was established through accelerator mass spectrometry (AMS) radiocarbon dating of four bulk sediment samples undertaken at DirectAMS Radiocarbon Dating Service in Washington, USA. The radiocarbon ages obtained were then calibrated using OxCal v.4.3 (Ramsey, 2009) and the IntCal13 atmospheric curve (Reimer *et al.*, 2013). All dates were calibrated to cal BP (Table 6.2).

Table 6.2: Four radiocarbon dates obtained from Cowgate Farm core CGF1

Lab Code	Code-Depth (cm)	Altitude (m OD)	Material Dated	Fraction	Radiocarbon Age		Cal BP (2σ Ranges)
					BP	1σ Error	
D-AMS 016391	CGF-29	7.71-7.70	Peat	Bulk carbon	5655	50	6557-6310
D-AMS 016392	CGF-111	6.89-6.90	Peat	Bulk carbon	7521	55	8412-8200
D-AMS 016393	CGF-127	6.73-6.74	Organic clay	Bulk carbon	7345	36	8298-8028
D-AMS 016394	CGF-135/141	6.65-6.59	Wood	Bulk carbon	7583	41	8450-8334

An age-depth model for core CGF1 was developed using Bacon v2.3.4 (Blaauw & Christen, 2011). The red dotted line shows modelled median ages along core CGF1 and the grey stippled lines indicate the 95% confidence intervals of the modelled age-depth relationship. The transparent blue violin plots show the four calibrated AMS ^{14}C dates from Cowgate Farm. The upper left graph shows the iteration history of the model. The middle and right graphs show prior (green lines) and posterior (grey histograms) density functions for accumulation rate and memory of the model (Figure 6.5).

The mean 95% confidence range of the age-depth model is 481 years, a minimum of 209 years at 137 cm and a maximum of 690 years at 69 cm. Based on the age-depth model for core CGF1, 100% of the dates from core CGF1 lie within the age-depth model's 95% range although sample CGF-111 appears to be older than expected. It is therefore possible that contamination and/or sediment reworking might have occurred at this depth resulting in the incorporation of older carbon into the sample.

The main stratigraphic boundary of core CGF1 at 125 cm (6.75 m OD) was included in the age-depth model (shown in the horizontal dotted lines across the model in Figure 6.5). The sedimentation rates were calculated based on the dated samples and the main stratigraphic boundary (mean age obtained from the model's prediction) and shown on the right side of Figure 6.5. The blue/grey silt-clay from 138 cm (6.62 m OD) to 125 cm (6.75 m OD) showed a slightly higher accumulation rate when compared to the accumulation of the peat unit from 125 cm (6.75 m OD) to 29 cm (7.71 m OD).

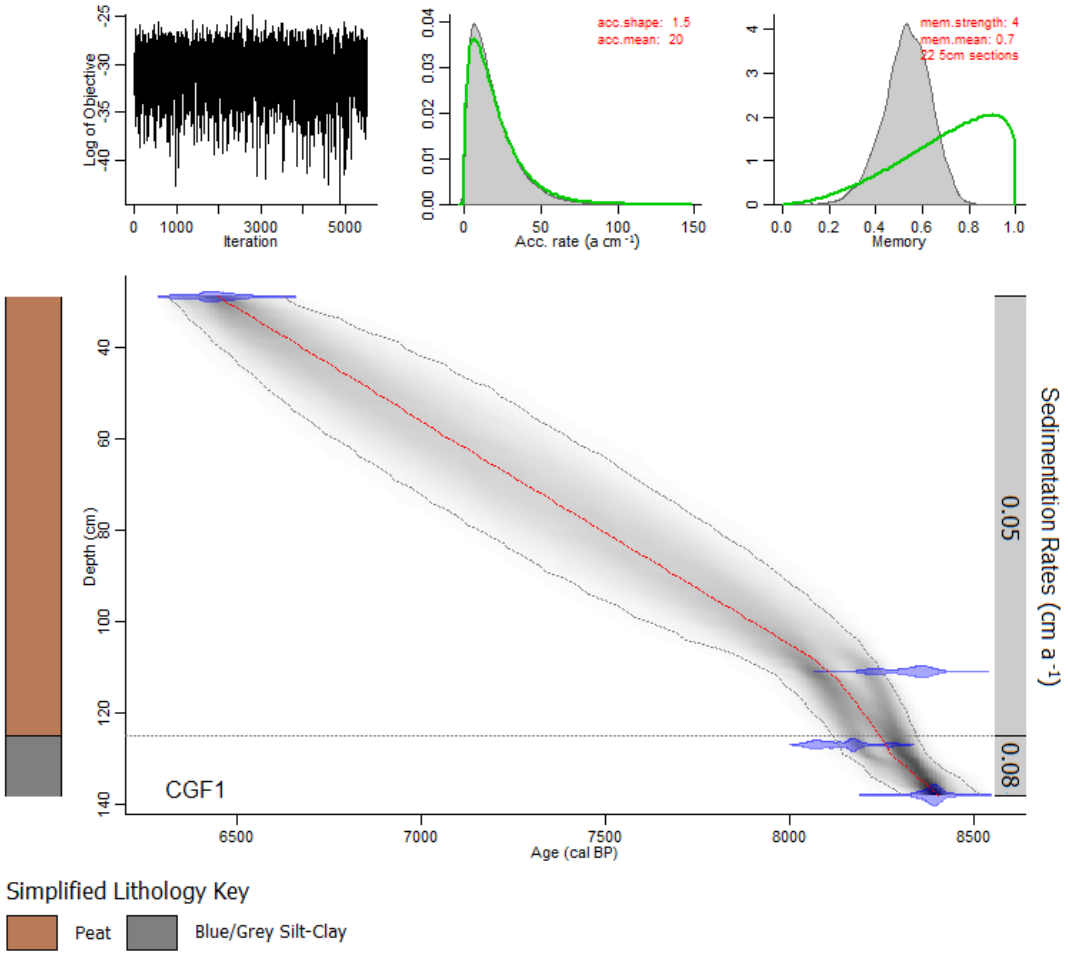

Figure 6.5: Age-depth model for the CGF1 core profile based on Bacon v2.3.4 modelling routines (Blaauw & Christen, 2011) and calculated sedimentation rates from the AMS ^{14}C dates calibrated with IntCal13 (Reimer *et al.*, 2013). Dotted line on the model indicates the main stratigraphic unit in the CGF1 core

6.6 Foraminiferal Analysis

The preservation of foraminiferal tests in the samples from core CGF1 varied. Some samples contained very few foraminiferal tests and it was not possible to obtain a minimum count of 40 individuals despite increasing the sample volume. Samples were taken at 1 or 2 cm intervals throughout the whole core.

A total of five agglutinated saltmarsh foraminiferal species were identified in core CGF1 and no calcareous foraminiferal species were found (Figure 6.6). The agglutinated foraminifera species of *Jadammina macrescens*, *Miliamminia fusca*, *Tiphotrocha comprimata*, *Haplophragmoides wilberti* and *Trochammina inflata* were

only observed in the peat with *Phragmites* unit from 1.11 m (6.89 m OD) to 0.31 m (7.69 m OD). No foraminifera were observed in the pink/brown clay with small gravel unit (1.52 m to 1.41 m; 6.48 m OD to 6.59 m OD), the sandy blue/grey silt-clay unit (1.40 m to 1.28 m; 6.60 m OD to 6.72 m OD), organic sandy blue/grey silt-clay unit (1.27 m to 1.25 m; 6.73 m OD to 6.75 m OD), the deeper section of the peat with *Phragmites* unit (1.24 m to 1.12 m; 6.76 m OD to 6.88 m OD respectively) and from 0.30 m (7.70 m OD) towards the top of the core in the surface peat unit.

The foraminifera in core CGF1 were dominated mainly by *J. macrescens* and *M. fusca*, with varying abundances of *H. wilberti* and *T. inflata* and low frequencies of *T. comprimata*. Five distinct peaks of *H. wilberti* are observed at depths 0.46 m (7.54 m OD), 0.50 m (7.50 m OD), 0.80 m (7.20 m OD), 0.84 m (7.16 m OD) and 1.11 m (6.89 m OD). Three out of these five depths however have very low individual counts (below 40 individuals), and therefore the interpretation of this dominance of *H. wilberti* should be treated with caution.

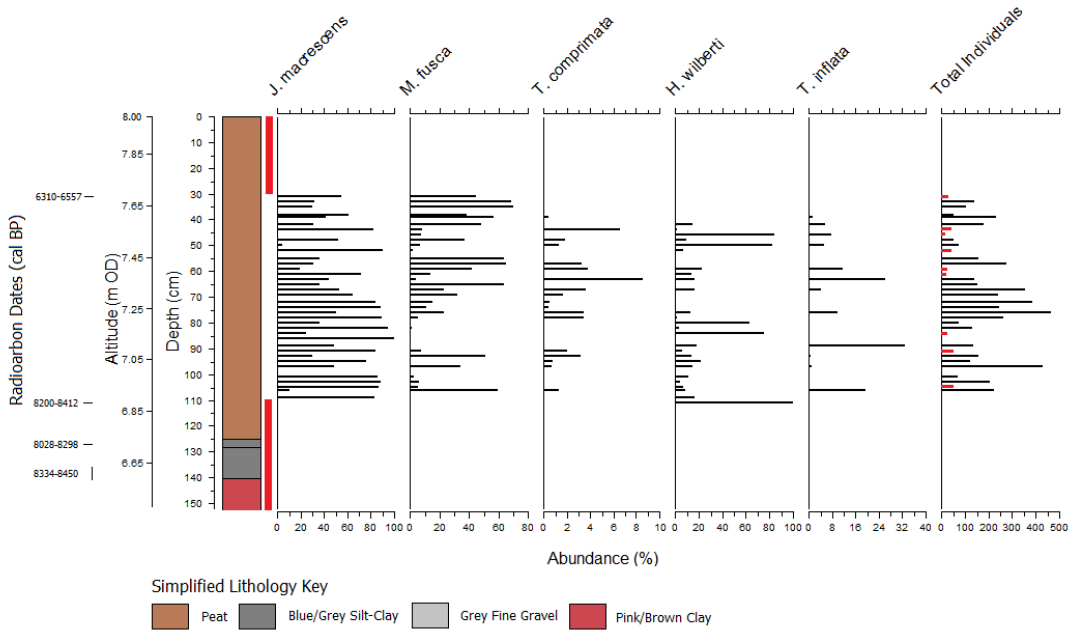

Figure 6.6: Foraminiferal diagram from Cowgate Farm core CGF1. Foraminiferal frequencies are expressed as a percentage of total foraminifera. All samples including samples with low individual counts (below 40 individuals; marked with red lines) were included in this diagram. Red blocks next to the stratigraphy diagram indicates the zone where foraminifera was absent in the core

6.7 Pollen Analysis and Zonation

300 pollen and spore grains were counted for each sample from core CGF1. Samples were taken at intervals of 2 cm, 3 cm or 4 cm throughout the core, with closer sampling intervals at depths where greater stratigraphic changes were observed (Figure 6.7).

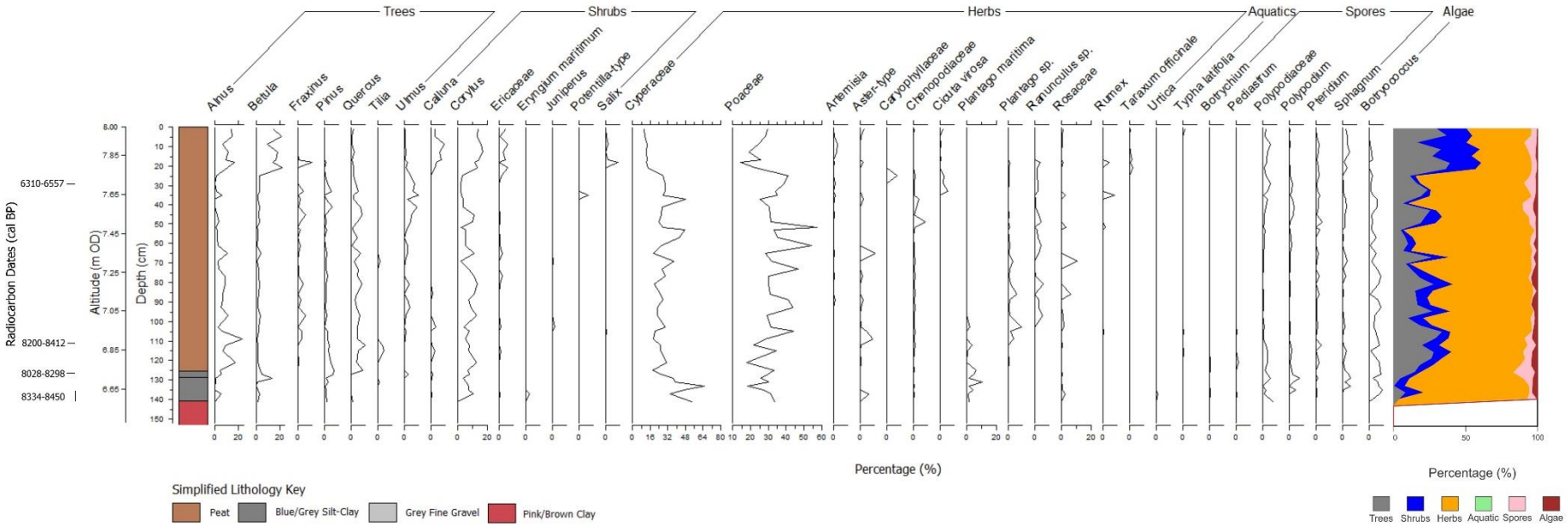

Figure 6.7: Pollen diagram from Cowgate Farm core CGF1. Pollen frequencies are expressed as a percentage of total land pollen

Four local pollen assemblage zones were identified (Figure 6.8). From the base of the core to 1.41 m (6.59 m OD) in the pink/brown clastic unit, no pollen was found. The pollen zonation for Cowgate Farm is summarised and tabulated in Table 6.3 below.

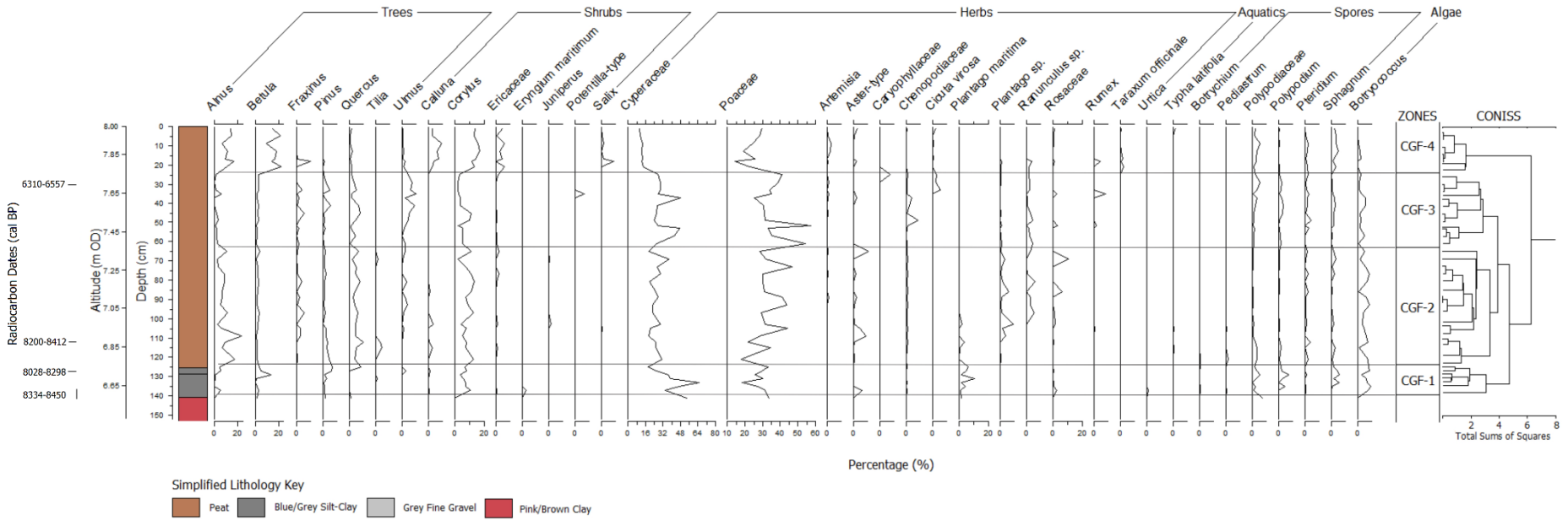

Figure 6.8: Pollen zonation for Cowgate Farm based on stratigraphically constrained cluster analysis

Table 6.3: Pollen zonation for Cowgate Farm based on stratigraphically constrained cluster analysis

Pollen Zone	Depth (cm)	Altitude (m OD)	Pollen Characteristics
CGF-1	126-141	6.74-6.59	A general low presence (maximum of approximately 5%) of arboreal pollen, in particular *Alnus* and *Betula*, was observed throughout the zone, with the exception at the depth of 1.29 m (6.71 m OD) where an abundance of *Betula* increased to 13% then decreased again. Low frequencies of *Pinus* (1-6%) were observed throughout the zone. Minimal occurrence of *Quercus* (1.4%) at a depth of 1.41 m (6.59 m OD) and *Ulmus* (2.7%) at a depth of 1.27 m (6.73 m OD) were also observed in the zone. No *Corylus* pollen was observed in the sample at a depth of 1.41 m (6.59 m OD), and the presence of *Corylus* started approximately at a depth of 1.37 m (6.73 m OD) and continued through the zone. The zone is dominated mainly by Cyperaceae and Poaceae, with maximum abundance of Cyperaceae reaching 65% at a depth of 1.33 m (6.67 m OD) and Poaceae reaching 33% at a depth of 1.41 m (6.59 m OD). *P. maritima* was also present throughout the zone, with the abundance ranging from 1.2% to 10.5%. The presence of spores were also observed in the zone, with Polypodiaceae, *Polypodium* and *Sphagnum* notable. The presence of *Botryococcus* algal spores was also noted in the zone.

CGF-2	63-126	7.37-6.74	Reduced presence of *Betula* pollen. Presence of *Alnus* and *Quercus* however increased, with a maximum abundance of 23% at a depth of 1.09 m (6.91 m OD) and 14% at a depth of 1.12 m (6.88 m OD). Low frequencies of *Pinus* pollen and minimal frequencies of *Fraxinus* and *Ulmus* pollen were also observed in this zone. The presence of *Corylus* pollen continued in this zone, with increased frequencies, from 2 to 13%. Very low frequencies of *Calluna* pollen was also observed in this zone. The zone is dominated mainly by Poaceae, followed by Cyperaceae. Poaceae reached a maximum of 47% at a depth of 0.73 m (7.27 m OD) and Cyperaceae reached a maximum of 38% at a depth of 0.69 m (7.31 m OD). Low frequencies of Chenopodiaceae, *P. maritima*, *Plantago sp*. and *Ranunculus sp*. were also noted. Low frequencies of spores were also recorded, notably Polypodiaceae, *Pteridium* and *Sphagnum*. The low presence of *Botryococcus* alga spores was also noted in the zone.
CGF-3	23-63	7.77-7.37	*Alnus* pollen abundance decreased. An increase in *Ulmus* pollen was observed with a maximum of 10% at a depth of 0.35 m (7.65 m OD). The presence of *Quercus* pollen was noted and low frequencies of *Pinus* and *Fraxinus* pollen were also recorded. The presence of *Corylus* pollen, with a range of 2-11% was recorded. No *Calluna* pollen was observed in this zone.

			This zone was dominated mainly by Poaceae followed by Cyperaceae, with a maximum of 48% at a depth of 0.37 m (7.63 m OD) for Poaceae, and 58% at a depth of 0.52 m (7.48 m OD) for Cyperaceae. Increased frequencies of Chenopodiaceae were also observed, with sporadic occurrence of Caryophyllaceae, *Ranunculus sp*. and *Rumex*. Low frequencies of spore species were recorded, notably Polypodiaceae and *Pteridium*. *Polypodium* spores were observed and low frequencies of *Botryococcus* algal spores were also noted.
CGF-4	0-23	8.00-7.7	A notable increase in arboreal pollen was observed, in particular *Alnus* and *Betula* pollen ranging from 7 to 17% and 10 to 23% respectively. The presence of *Quercus* pollen decreased in this zone, with minimal frequencies of *Fraxinus* and *Ulmus* at the beginning of the zone and disappearing towards the top of the zone. No *Pinus* pollen was observed in this zone. The presence of *Corylus* pollen increased. *Calluna* pollen increased, reaching a maximum of 14% at a depth of 0.90 m (7.10 m OD). The frequency of *Calluna* pollen decreased from 0.90 m to the top of the zone. The sporadic occurrence of Ericaceae pollen was also noted in this zone. A decrease in the dominance of Poaceae and Cyperaceae was observed in this zone. A notable decrease of Cyperaceae pollen compared to Poaceae was also observed. Low frequencies of Polypodiaceae and *Sphagnum* were observed. No *Polypodium* or *Botryococcus* spores were recorded.

6.8 Holocene Relative Sea-Level and Environmental Changes at Cowgate Farm

The interpretation of Holocene relative sea-level and environmental changes for Cowgate Farm are based on microfossil analyses, changes in lithostratigraphy and sediment composition, and the dated samples from core CGF1.

6.9 Microfossil Interpretation: Foraminifera

No foraminifera were observed in the pink/brown clay clastic unit, blue/grey silt-clay unit and the deepest 0.14 m section of the peat with *Phragmites* unit, which constitutes the deepest 0.41 m of the core (6.48 m OD to 6.89 m OD). The sequence in the deepest 0.27 m of the core corresponds to a zone where high sand content was observed (Figure 6.9). If the blue/grey silt-clay unit is of marine origin (as it is consistent with the blue/grey silt-clay unit observed at Allonby, Pelutho and Herd Hill where foraminifera were preserved), the absence of foraminifera in the core could be attributed to the increased sand content in the core (du Châtelet *et al.*, 2009). Sandy environments are unfavourable for foraminifera, as their tests cannot be preserved in the sand. A high energy environment in the area during these periods could also result in the absence or removal of foraminifera in the bottom 0.27 m of the core in the blue/grey silt-clay unit.

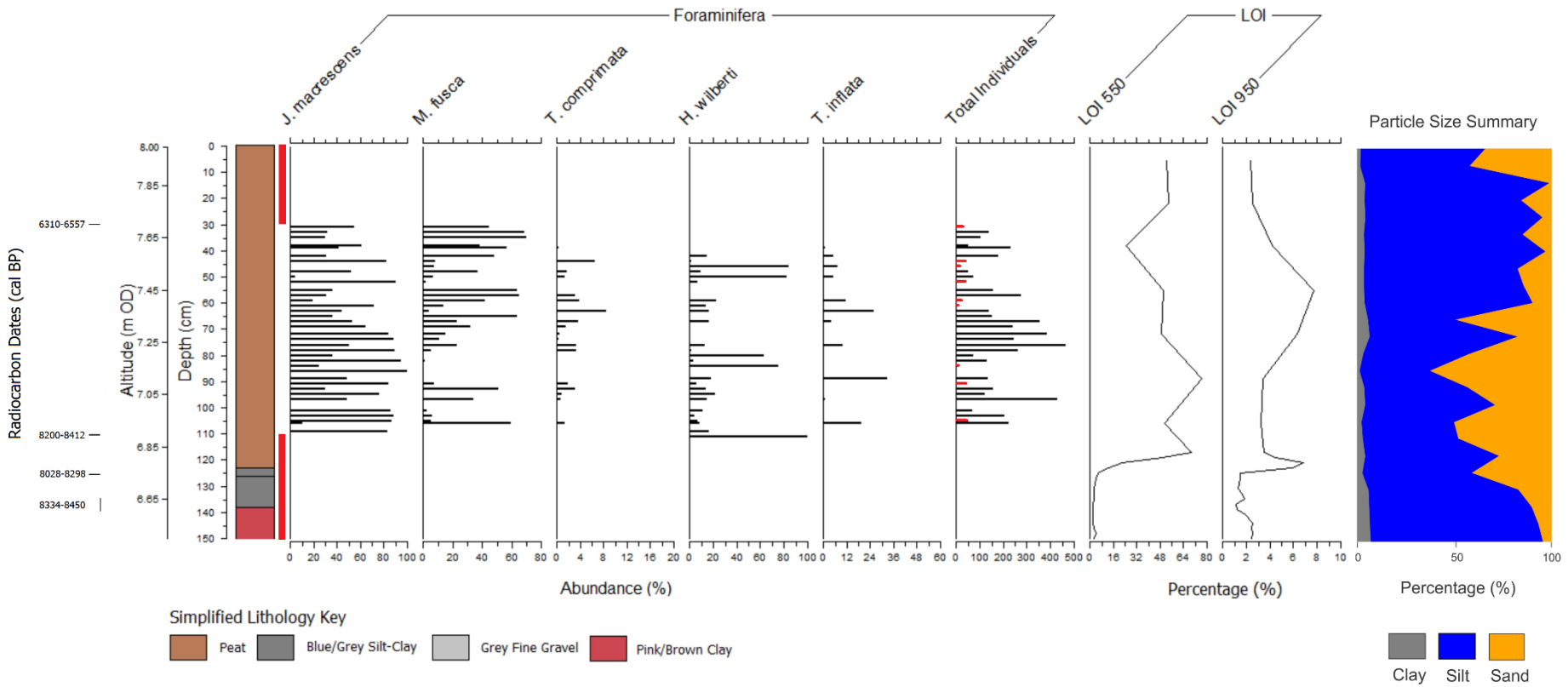

Figure 6.9: Summary diagram showing foraminifera, particle size and loss on ignition analyses undertaken on samples from core CGF1

A study on the correlation of foraminiferal assemblages with grain size was undertaken by du Châtelet *et al*. (2009). It demonstrated that when the sediment is coarse grained (size >195µm; classed as medium, coarse and very coarse sand in this study) both density and species richness of foraminifera are low (with less than three individuals per 50 cm^3 and less than two species per station). Sediments that are relatively fine grained (size <95µm; classed as fine clay, silt and very fine sand in this study) are associated with foraminiferal assemblages with high density and species richness.

Apart from the variation in grain sizes, the percentage of organic matter of the sediment has also been identified as a limiting factor influencing the distribution and abundance of foraminifera (du Châtelet *et al*., 2009). Foraminiferal density is low and species richness is high in sediments with lower organic matter content (content <2%). Conversely, when organic matter is higher in the sediments, foraminiferal density is high but with lower species richness. This was observed at this site where only five main agglutinated foraminifera were identified in the peat with *Phragmites* unit of the core (Figure 6.9).

No microfossils were preserved in the deepest section of the peat with *Phragmites* unit (1.25 m to 1.11 m; 6.75 m OD to 6.89 m OD). Freshwater peat (evidenced by the absence of foraminifera) would have developed upon the blue/grey silt-clay unit, from a depth of 1.25 m to 1.11 m (6.75 m OD to 6.89 m OD). A marine transgression into the site was then recorded by the presence of the agglutinated saltmarsh foraminifera *J. macrescens*, *M. fusca*, *T. comprimata*, *H. wilberti* and *T. inflata* at 1.11 m (6.89 m OD) to 0.29 m (7.71 m OD), dated at 8412-8200 cal BP. Relative sea level later decreased and the site transitioned into a freshwater environment, evidenced by the absence of foraminifera from the core. A negative marine tendency was recorded by sample CGF-29 (6495-6353 cal BP) at a depth of 0.29 m (7.71 m OD).

J. macrescens and *M. fusca* are generally associated with a high saltmarsh environment, as evidenced by the contemporary marsh data in this study (Chapter 4; Figure 4.8 and Figure 4.12). This may therefore suggest that the site remained as a saltmarsh environment throughout the period of marine transgression and regression recorded, as evidenced by the foraminiferal assemblages and the lithostratigraphy in core CGF1 where microfossils were present.

6.10 Microfossil Interpretation: Pollen

Several possible pollen source areas were identified at Cowgate Farm. Cowgate Farm is located near a slope (Figure 6.2a), and runoff from the slopes could result in deposition of pollen grains at the site. Pollen grains that are buoyant (e.g *Pinus* pollen) could have been deposited in the area when the site was flooded, and this is common in wave affected sediments (Tipping, 1995). Pollen grains could also be wind pollinated and transported into the site from nearby areas. The interpretation for each pollen zone is described below.

Zone CGF-1 (Figure 8 and Table 2)

A small peak of *Betula* was recorded at 1.29 m (6.71 m OD), but generally low arboreal pollen percentages were recorded for this zone. It is likely that birch, pine and alder trees were present at the time in the pollen catchment area of Cowgate Farm. The low frequencies of arboreal pollen in zone CGF-1 correspond to the deposition of the minerogenic clastic unit in the core (Figure 6.10). This may suggest that the arboreal pollen was transported from nearby areas as development of woodland at Cowgate Farm site may have been restricted due to inadequate soil cover (Selby, 1997). Based on the isochrone map (Birks, 1989), birch was well established in major parts of central and northern England before 10000 cal BP, and further expansion of birch in other parts of England was recorded by 9750 cal BP.

Alder was first observed at Cowgate Farm at a depth of 1.37 m (m OD) although at very low frequency. Zone CGF-1 (126-141 cm) was dated at 8334-8450 cal BP, obtained from sample CGF-135/141. Lloyd *et al*. (1999) recorded the development of an alder carr at the base of the sediment sequence in Boustead Hill, which was dated at 8304-7928 cal BP, and the first occurrence of *Alnus* pollen in Drumburgh Moss was dated at 8947-8403 cal BP. At Quick Moss, Northumberland, alder, birch, elm, pine and oak were first recorded at 8010 cal BP (Rowell & Turner, 1985). The first appearance of *Betula*, *Quercus*, *Ulmus* and *Corylus* pollen with high percentages of *Pinus*, were recorded at 8995-8483 cal BP in Skelwith Pool, Morecambe Bay (Zong & Tooley, 1996). A mixed woodland landscape indicated by *Betula*, *Quercus*, *Ulmus*, *Alnus* and *Corylus* was observed at Hallsenna Moor, Cumbria earlier and was dated

at 9406-8999 cal BP (Walker, 2004). Therefore the date of 8450-8334 cal BP obtained at Cowgate Farm broadly agrees with these pollen trends.

This zone was characterised by high frequencies of Poaceae and Cyperaceae, suggesting an open grassland area dominated mainly by grass and sedges. It is probable that trees were growing in the pollen catchment area close to the site whilst the grass and sedges were confined mostly to the low lying areas of the site itself (Wells, 1997). The presence of *P. maritima* was also recorded in zone CGF-1, suggesting that sea plantain was present in the pollen catchment area at the time of sediment deposition. This might suggest a saltmarsh environment had developed in the surrounding or nearby areas (Tooley, 1974; Lloyd *et al.*, 1999).

The presence of *Corylus* pollen was recorded in zone CGF-1 (126-141 cm), suggesting that hazel was present in the pollen catchment area of the site. Hazel is known to grow in the understorey of lowland oak, ash or birch woodland (birch pollen was also recorded in this zone), and is also found in grasslands and hedgerows. The first rapid expansion of *Corylus* was recorded at 9500 cal BP in northwest England, western Scotland and in parts of coastal Wales (Birks, 1989). Zone CGF-1, which recorded the first presence of hazel was dated at 8450-8334 cal BP and therefore agrees with the date of expansion of *Corylus* recorded by Birks (1989). Polypodiaceae, *Polypodium* and *Sphagnum* spores were also present in zone CGF-1. The presence of ferns and peat moss are common in acidic wetlands including bogs and swamps, and these may have developed at the site or in nearby areas as relative sea level increased and marine influence expanded into the site. *Polypodium* is a common understorey element of oak and elm woodland (Tipping, 1995).

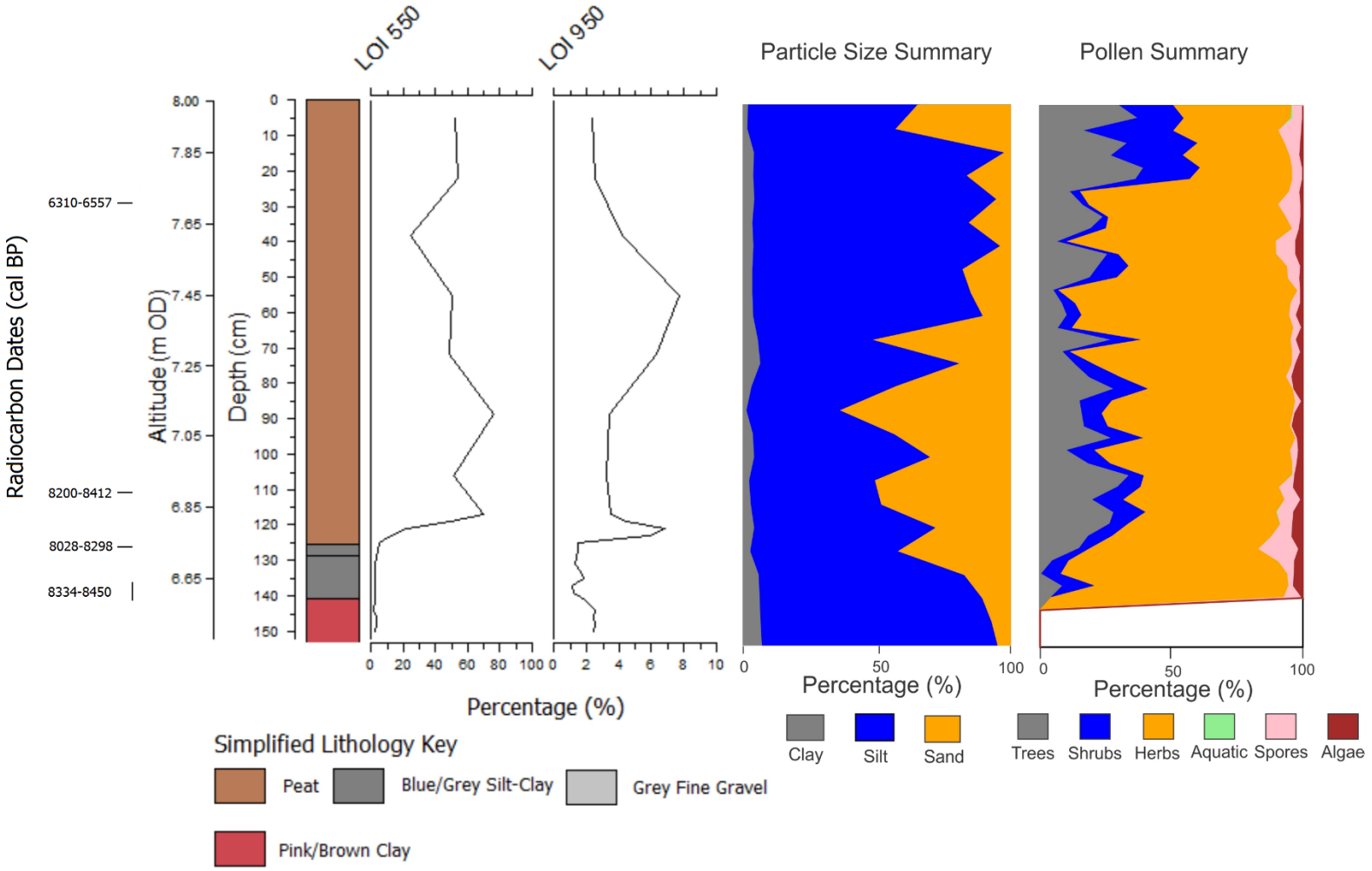

Figure 6.10: Summary diagram showing loss on ignition, particle size and pollen analyses undertaken on samples from core CGF1

Zone CGF-2 (Figure 9 and Table 2)

Increased frequencies of arboreal pollen, in particular *Alnus* and *Quercus* were observed in zone CGF-2 with low frequencies of *Betula*, *Fraxinus*, *Pinus* and *Ulmus*. This suggests a mixed woodland had developed within the pollen catchment area (Tipping, 1995), although this was still limited as evidenced by the relatively low frequencies of arboreal pollen. The woodland may have been established as the marine influence decreased from the site and soil cover at the site increased, evidenced by the sediment in the core transitioning from the minerogenic clastic unit into the peat with *Phragmites* unit. This transition was dated at 8412-8200 cal BP. Prior to 8000 cal BP, alder might have been widely spread throughout the British Isles, although it would have been in small amounts (Birks, 1989).

Alder expansion was recorded in Neasham Fen, Darlington soon after 7626-7968 cal BP, and at 8169-7694 cal BP in Red Moss, Lancashire. Alder was recorded in Valley Bog, Teesdale at 6750 cal BP, though not at high frequencies (Chambers, 1978). This might suggest the possibility of a delay in alder expansion in certain upland areas such as Teesdale (Chambers, 1978). A clear alder expansion was not observed at Cowgate Farm, although a general increase in *Alnus* pollen frequency was observed in zone CGF-2, beginning at 8412-8200 cal BP. Alder fruits are able to float and remain viable for a period of approximately a year, and therefore water currents are often suggested as the main dispersal mechanism for *Alnus* pollen (Birks, 1989). This could potentially explain the slight increase in alder recorded during the period of marine transgression in the area. Alder pollen is also known to be produced in abundance, and is well-dispersed compared to other trees (Bennett & Birks, 1990).

The first presence of *Quercus* was recorded at Cowgate Farm at a depth of 1.25 m (6.65 m OD) while the first presence of *Ulmus* was observed at a depth of 1.27 m (6.73 m OD) although both occurred in low frequencies. A date of 8298-8028 cal BP was obtained for pollen zone CGF-2 from sample CGF-127. Oak was present in southwest England by 9500 cal BP and spread at a rate of approximately 350-500 m a^{-1} through England, Wales and southern Scotland until 8000 cal BP (Birks, 1989). The isochrone map (Birks, 1989) suggests that oak would have been established at the study area after 8500 cal BP, and this was observed in zone CGF-2. Elm was present in southern England by 9500 cal BP, and later spread through northern

England and major parts of Scotland at approximately 8800 cal BP (Birks, 1989). Elm would have been present in the study area after 9000 cal BP based on the isochrones maps (Birks, 1989), although local expansion of elm may have been hindered by the presence of acidic soils at the site.

The presence of *Corylus* pollen was also recorded. Hazel is known to grow in the understorey of lowland oak, ash or birch woodland, and is found interspersed amongst a relatively open community of grass and sedges (Wells, 1997). The sporadic occurrence of *Calluna* pollen was also observed, and heather is known to grow in bogs and acidic pine and oak woodland.

Zone CGF-2 is characterised mainly by Poaceae and Cyperaceae, indicating an open community dominated by grass and sedges. The presence of *P. maritima* pollen was also recorded in zone CGF-2, which might suggest a saltmarsh environment was present in the pollen catchment area near the site, due to sea plantain's ability to grow in sandy soils in coastal areas. Undifferentiated *Plantago sp.* pollen was also recorded in this zone, indicating that plantains were present at the site. A low occurrence of Chenopodiaceae pollen was recorded, suggesting that goosefoot and other flowering plants, evidenced by the presence of Rosaceae pollen, were present. The occurrence of *Aster*-type and *Artermisia* pollen were recorded and can also indicate a saltmarsh environment (Lloyd *et al*., 1999). The low occurrence of spores of Polypodiaceae, *Polypodium*, *Pteridium* may represent ferns that formed the understorey components of the woodlands that developed at the site and the surrounding areas. The presence of peat moss was recorded, with *Sphagnum* pollen observed in the zone and *Pteridium* is known to grow on dry bog surfaces, or in the clearings of, or under, an open canopy woodland that would have developed in the area (Tipping, 1995).

Zone CGF-3 (Figure 8 and Table 2)

The overall increase in arboreal pollen might suggest an increased development of a mixed woodland in the pollen catchment area. Changes in the percentages of arboreal pollen are due mainly to variations in *Corlyus*, which may indicate secondary woodland near the site or the understorey component was being cleared (Dumayne-Peaty and Barber, 1998). The environment at Cowgate Farm was still characterised

by an open community dominated by grasses and sedges, as recorded by the high percentages of Poaceae and Cyperaceae in the zone. Other herb pollen is also present in this zone, although in very low proportions, and would have formed elements of the grass and sedge environment. The presence of spores including Polypodiaceae, *Polypodium*, *Pteridium* although in very low frequencies, suggest that these species might have formed the understorey components of the mixed woodland that have developed in the area. Chambers (1978) suggests that the ratio between trees-herbs-shrubs at a particular site should be treated with caution as the grasses and sedges may be over represented. This might explain the high frequencies of grasses and sedges with lower arboreal pollen frequencies observed at Cowgate Farm, as the arboreal pollen might be transported into the pollen catchment area rather than growing locally.

The local presence of pine trees was widely recorded in south England at 9000 cal BP and by 8800 cal BP, pine had spread to the southern Lake District in Cumbria and much of central England (Birks, 1989). Pine trees were absent or are very rare in southwest England, the Cumberland lowland, the southern Scotland lowland as well as the lowland areas in northeast England throughout the Holocene (Birks, 1989). At Cowgate Farm the frequencies of *Pinus* pollen were low throughout the sediment sequence. Pollen data from northwest England (Walker, 1966) and from southern Scotland (Birks, 1977) indicated that the English pine populations did not reach Galloway, while the Scottish pine populations did not expand extensively southward to Galloway (Birks, 1989).

At Priestside Flow, located at the northern Solway Firth however, high frequencies of *Pinus* pollen were observed in the sediment sequences dated at 8791-8992 cal BP and 8174-7932 cal BP (Lloyd *et al.*, 1999). It was hypothesised that the pine found particularly in Galloway Hills in southwest Scotland originated from northeast Ireland, as pine established at Priestside Flow and Galloway Hills at the same time, around 7500-7000 cal BP, through distant seed dispersal, although the possibility that it originated from northern England should not be completely dismissed (Birks, 1989).

Zone CGF-4 (Figure 8 and Table 2)

Increased percentages of arboreal pollen throughout this zone, characterised mainly by *Alnus* and *Betula*, were observed. This suggests further development of the mixed woodland in the area (Tipping, 1995; Dumayne-Peaty and Barber, 1998), as relative sea level decreased and soil cover in the pollen catchment area developed. By 7500 cal BP, alder was well established in parts of northwest England and southwest Scotland, and became abundant by 7000 cal BP throughout England, Wales and southern Scotland, in high altitude areas and parts of the northern Pennines (Birks, 1989). The establishment of an alder carr woodland was also recorded at Walton Moss, Cumbria between 7540 and 7400 cal BP (Hughes *et al.*, 2000). Zone CGF-4 (0-23 cm) was dated at 6557-6310 cal BP (obtained from sample CGF-29; 29 cm, 7.71 m OD), which recorded the highest occurrence of alder at a depth of 0.18 m (7.82 m OD). The overall increase in arboreal pollen in zone CGF-4 occurred at a later date compared to the other sites in northwest England and southwest Scotland, and may be due to the influence of marine conditions at Cowgate Farm prior to the transition to zone CGF-4.

Although no clear elm decline was recorded at Cowgate Farm, *Ulmus* pollen was virtually absent or occurred in very low frequencies at the site soon after 6557-6310 cal BP. The earliest record of a widespread decline in elm in the British Isles was recorded at 5130 cal BP in Ennerdale Water, 5100 cal BP in Blea Tarn and 5540-4860 cal BP in Blelham Tarn in the Lake District, Cumbria (Pennington, 1964) and was attributed to anthropogenic effect, climatic downturn and pathogenic attack. The decrease in elm continued throughout the Bronze Age from 4000-2800 cal BP (Chiverell, 2006). Tipping (1995) recorded two episodes of elm decline in Kirkpatrick-Fleming, southern Scotland. The first decline was abrupt and without evidence of human disturbance, dated at 4830 cal BP. The second elm decline was recorded 4580 cal BP and was associated with agricultural practices.

A notable increase in *Corylus*, *Calluna* and Ericaceae pollen was also observed in zone CGF-4. Hazel would have formed the understorey component of the lowland mixed woodland, as recorded by the arboreal pollen species present. Heather is known to grow on heaths, moors and grasslands with poor nutrients, and also in open woodland on acidic soils, ranging from dry exposed habitats to wet peat bogs. At Cowgate Farm

the increase in heather corresponds to the transition from the peat with *Phragmites* to the overlying peat unit. A shift of dominance from *Eriophorum vaginatum* to *Calluna* was observed at Walton Moss, indicating a change to a prolonged period of deep mire water tables and dry oligotrophic conditions in the area (Hughes *et al*., 2000; Hughes & Barber, 2004).

An increase in Poaceae and a decrease in Cyperaceae was observed. The change in ratios between sedges and grasses may indicate a change of environment from reed swamp to a more freshwater limnic sediment and turfa (Zong and Tooley, 1999), and possible evidence of changing groundwater table in the area (Zong and Tooley, 1999). This hypothesis is also supported by the absence of foraminifera at the start of the zone CGF-4. Lloyd *et al*. (1999) recorded a similar pollen pattern at Priestside Flow, where the negative tendency of sea level was evidenced by the transition from the clastic unit to the surface *turfa* and a shift to the dominance of Poaceae in the area. A similar increase of *Calluna* and Cyperaceae pollen in Quick Moss, Northumberland at approximately 4900 cal BP is attributed to the probable expansion of blanket peat in the area as a result of marine regression (Rowell & Turner, 1985). At Cowgate Farm, the marine regression in the area was recorded at the start of Zone CGF-4 dated at 6557-6310 cal BP. Low frequencies of spores including Polypodiaceae were observed. Ferns would have formed the understorey components of the mixed woodland, although in lower abundance.

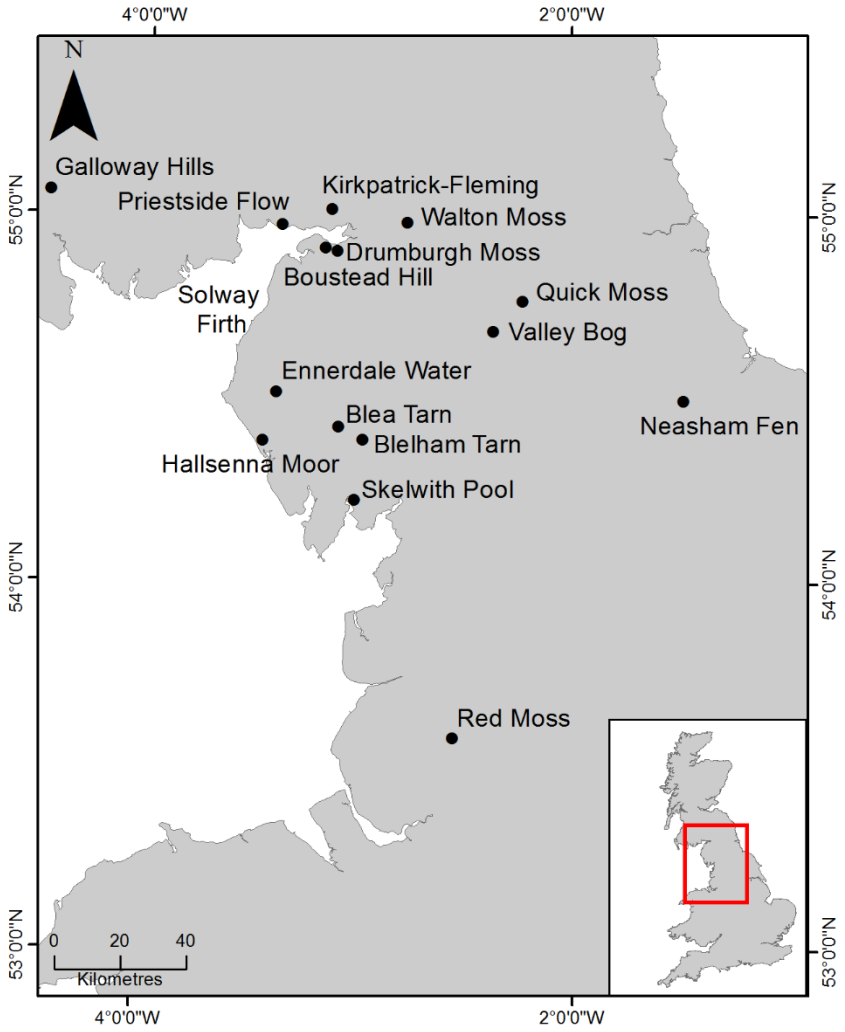

Figure 6.11: Location map of pollen sites in England mentioned in the text

6.11 Sediment Deposition and Relative Sea-Level Interpretation

The site at Cowgate Farm is located on low-lying land below 10 m OD, and would have been inundated during the period of marine transgression which is likely to represent the onset of the Main Postglacial Transgression or a combination of both the Main Postglacial Transgression and the RSL increase as a result of the drainage of Lake Agassiz-Ojibway in North America. The pink/brown clastic unit is barren of any foraminifera or pollen, and was most likely deposited through glaciofluvial processes (Walker, 1966).

The deposition of the basal sandy blue/grey silt-clay unit and the more organic blue/grey silt unit may have resulted either from slope wash processes, fluvial

processes or through inundation during the period of marine transgression at the site. This unit was dated through samples CGF-138/141 and CGF-127, resulting in ages of 8450-8334 cal BP and 8298-8028 cal BP respectively. If the absence of foraminifera is not due to dissolution or the increased sand content in the units, it is most probable that the deposition of both blue/grey silt-clay units are the result of sediment slope washing into the site, or through fluvial processes, although no major river system is located near the site at the present time. The presence of pollen taxa *P. maritima* (Section 6.7), which are known to grow in a saltmarsh environment, sea shores and meadows, was noted in the blue/grey silt-clay unit, although the occurrence is sporadic and of low frequency, and therefore the pollen might have been transported to the site from nearby pollen catchment areas. It is also possible that the sediment is lacustrine, which may explain the presence of *Phragmites* in the overlying unit.

If the absence of foraminifera in the blue/grey silt-clay unit is attributed to poor preservation (due to the high sand content in the sediment), and is therefore deemed of marine origin, the deposition of the unit at Cowgate Farm may have been through marine inundation at the site during an earlier event of relative sea level rise. The increased sand content in the core from the base to a depth of approximately 1.25 m (6.75 m OD), could have resulted from deposition through aeolian processes as the sand fraction consisted of very fine sand and fine sand.

The clastic units were overlain by the peat with *Phragmites* unit, indicating that a freshwater peat environment had developed at the site, and this transition was recorded at a depth of 1.25 m (6.75 m OD). A saltmarsh environment would have then developed at the site starting at a depth of 1.11 m (m OD) evidenced by the first presence of foraminifera in the core (Section 6.6), with the previous freshwater peat environment unable to keep pace with the rising sea level. This marine transgression was dated at 8412-8200 cal BP. This date may indicate the first recording of the Main Postglacial Transgression at the site, although the date seems to be older than those recorded at other sites investigated in this study. It is therefore possible that the marine transgression at Cowgate Farm also recorded the increased relative sea level as a result of the final drainage of glacial Lake Agassiz-Ojibway located in north-central North America, due to the collapse of the Laurentide Ice Sheet.

The transition from the peat with *Phragmites* unit representing a saltmarsh environment (evidenced by the presence of microfossil), to the overlying surface peat unit of freshwater origin at a depth of 0.29 m (7.71 m OD), corresponds to the absence of foraminifera in the core. This regressive contact in the core indicating a negative sea-level tendency was dated at 6557-6310 cal BP. No further changes in the biostratigraphy and lithostratigraphy were observed in the core from 0.29 m (7.71 m OD) to the top.

6.12 Relative Sea-Level Reconstruction for Cowgate Farm

Relative sea-level was reconstructed for Cowgate Farm through a combination of lithostratigraphic and biostratigraphic analyses, determination of indicative meanings and calculation of sea-level index points.

6.13 Determination of Indicative Meaning

As the predicted palaeo marsh surface elevation (PMSE) based on the transfer function utilised on core CGF1 was deemed unreliable, the assigned reference water level based on the changes in lithostratigraphy and biostratigraphy (foraminiferal assemblages) was therefore used for calculation of sea-level index points.

Based upon the lithostratigraphy and biostratigraphy of two of the dated samples CGF-29 and CGF-111 at depths of 1.11 m and 0.29 m respectively (6.89 m OD and 7.71 m OD), the indicative meanings associated with a saltmarsh environment were ascribed. The lithostratigraphy of both samples consisted of the peat with *Phragmites* unit, which is consistent with a saltmarsh environment. The ascribed indicative meaning of a saltmarsh environment is further supported by the occurrence of saltmarsh species e.g. *P. maritima*, *Aster*-type and *Artemisia* in core CGF1 where the presence of foraminifera was observed. The particle size recorded from samples collected in the high saltmarsh environment at all three contemporary saltmarshes investigated (Chapter 4; Section 4.4.1, 4.4.2 and 4.4.3) showed a high silt content (a minimum of 18% and a maximum of 73%) and sand content below 50%, consistent with the zone ascribed to a saltmarsh environment from core CGF1. High organic carbon content (a maximum of 76%) was observed in the samples where foraminifera

were observed in core CGF1, similar to the saltmarsh samples collected from higher elevation at Skinburness Marsh (Chapter 4; Section 4.4.1).

Both samples CGF-29 and CGF-111 were also dominated by the agglutinated saltmarsh species, in particular *J. macrescens* and *M. fusca*, both of which are generally associated with the high saltmarsh environment occurring between mean high water spring tide (MHWST) and highest astronomical tide (HAT), as evidenced by the contemporary foraminiferal distribution from the Skinburness Marsh and Bowness Marsh (Chapter 4; Sections 4.3.1 and 4.3.3).

The indicative meaning for samples CGF-29 and CGF-111 are therefore estimated to have occurred between the MHWST and HAT, based on the contemporary measurements at Skinburness Marsh (4.9 m OD and 6.3 m OD respectively), as both samples exhibited characteristics most similar to the contemporary samples collected from Skinburness Marsh. This resulted in a reference water level of 5.6 m OD with an indicative range of ±1.4 m for both samples.

The samples CGF-127 and CGF-135/141 were not assigned to any indicative meaning due to the lack of microfossil evidence indicating a marine environment. Sea-level index points therefore were also not calculated for samples CGF-127 and CGF-135/141.

6.14 Post-Depositional Lowering of Sediments

The issue of post-depositional lowering (PDL) of the sediments for the sea-level index points from Cowgate Farm was addressed using geotechnical model corrections (Chapter 3; Section 3.10.1). Minimal post-depositional lowering of sediments was observed in the core from Cowgate Farm, with samples CGF-29 and CGF-111 showing a compaction value of 0.010 m and 0.006 m respectively (Figure 6.12).

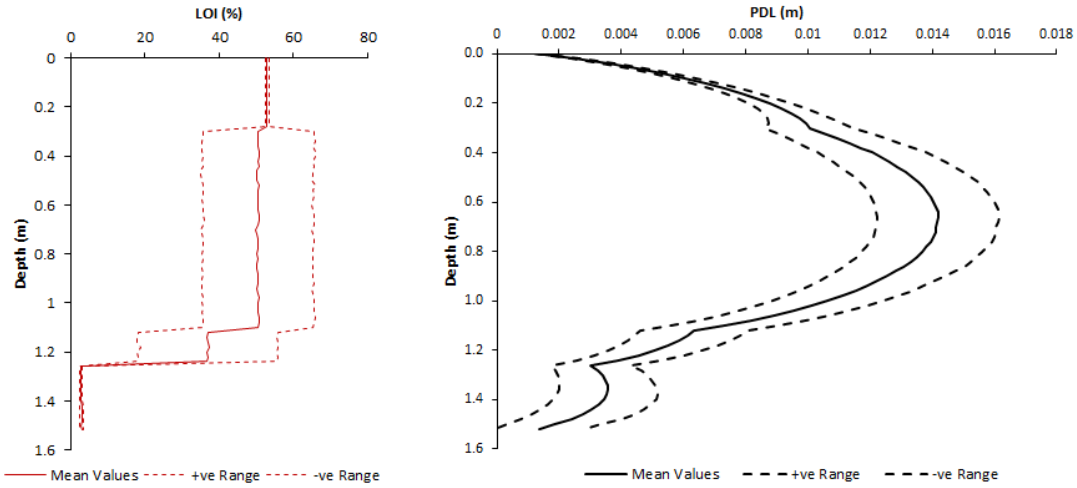

Figure 6.12: Geotechnical and physical properties showing the averaged downcore organic content, expressed as % loss on ignition and the model estimates of post-depositional lowering for core CGF1. Abbreviations: LOI = Loss on ignition; PDL = Post-depositional lowering

6.15 Sea-Level Index Points

When calculating a sea-level index point, the age, reference water level and indicative range along with the associated errors for each sample are required (Chapter 3; Section 3.9). Two sea-level index points were produced for the Cowgate Farm site (Table 6.4).

Table 6.4: Sea-level index points produced from CGF1

Lab Code	Latitude	Longitude	Radiocarbon Age		Cal BP (2σ Ranges)			Altitude (m OD)	Compaction Correction (m)	RSL (m)	Tendency
			BP	1σ Error	Min	Mean	Max				
D-AMS 016391	54.812	-3.405	5655	50	6310	6437	6557	7.71	+0.010	+2.12±1.46	Negative
D-AMS 016392	54.812	-3.405	7521	55	8200	8324	8412	6.89	+0.006	+1.30±1.46	Positive

The sea-level index points for sample CGF-29 at 7.71 m OD and sample CGF-111 at 6.89 m OD produced sea-level index points of 2.12±1.46 m and 1.30±1.46 m respectively. Figure 6.13 shows the sea-level index points from Cowgate Farm against the modelled relative sea-level curve for southern Solway Firth at the location of NY 2481 5666 based on the BRADLEY2011, KUCHAR2012 and BRADLEY2017 models (Shennan *et al.*, 2012; 2018; Kuchar *et al.*, 2012).

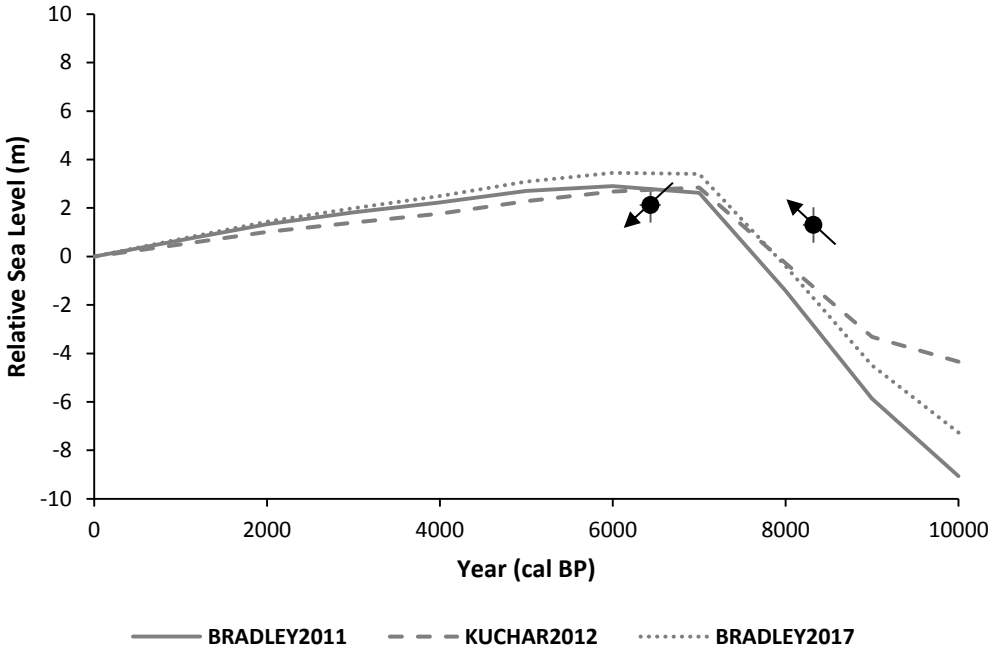

Figure 6.13: Graph showing two sea-level index points from Cowgate Farm. The black line is the modelled relative sea-level curves for southern Solway Firth based on Shennan *et al*. (2012; 2018) and Kuchar *et al*. (2012). All sea-level index points include associated individual vertical and age error bars

6.16 Summary

The site at Cowgate Farm has provided a record of Holocene sea-level changes as evidenced by the changes in lithostratigraphy and biostratigraphy of core CGF1. The two sea-level index points obtained from Cowgate Farm broadly agree with the general sea-level trend for the southern Solway Firth region, with the Holocene marine transgression recorded at 8324 cal BP, and the marine regression from the area dated at 6437 cal BP. The increased marine influence at the site, possibly as a result of the Main Postglacial Transgression, although it is possible that the transgression associated with the glacial Lake Agassiz-Ojibway flood is also

represented was recorded by the presence of agglutinated foraminifera and the presence of saltmarsh and coastal pollen taxa in the sediment. At the base of the sediment sequence dated at 8391 cal BP, the site was represented by an open grassland dominated mainly by grasses and sedges. As marine influence decreased and the site transitioned into a freshwater environment, a mixed woodland represented mainly by alder and birch would have developed.

CHAPTER 7

PELUTHO

7.0 Introduction

The study site at Pelutho (NY 1202 4920) is located on the northwest Cumbrian coastline, approximately 2 km from the present coastline, 7 km from the southern bank of Moricambe Bay and 17 km from the southern shore of the Solway Firth (Figure 7.1). The site is bordered by a gently sloping hill towards the south, with low-lying farmland surrounding the north, east and west of the site. A drainage channel is located west of the site, and a road lies to the east of the site (Figure 7.2a). The study site is approximately 200 m long by 60 m wide.

Figure 7.1: Location of the study site at Pelutho marked in red

7.1 Borehole Location and Stratigraphy

To establish a detailed stratigraphy of the site, three transects of boreholes were cored (Figure 7.2). The first transect was cored from south to north, while the other two transects were cored from west to east. The surface elevation of the boreholes in Pelutho ranged between 8.4 m OD and 9.5 m OD. Borehole P8 reached the maximum depth at the site, terminating on bedrock at a depth of 3.51 m (5.07 m OD). All boreholes terminated on bedrock, except for borehole P3 which terminated in a stiff pink/brown clay unit. The general stratigraphy of the study area is a basal clastic blue/grey clay unit that has developed on top of the underlying bedrock, and is overlain by a peat unit.

Borehole P1 reached a depth of 1.98 m (6.42 m OD) and terminated on bedrock. A unit of organic blue/grey silt-clay overlaid the bedrock, and was covered by a silty peat unit at a depth of 1.57 m (6.83 m OD) and the surface peat unit at a depth of 0.17 m (8.23 m OD).

Borehole P2 terminated on bedrock at a depth of 3.33 m (5.07 m OD). A silty peat unit overlaid the bedrock, and was covered by a unit of blue/grey silt-clay at a depth of 2.89 m (5.51 m OD). A second silty peat unit overlaid the blue/grey silt-clay unit at a depth of 2.85 m (5.55 m OD) and this was overlain by an organic blue/grey silt-clay unit at a depth of 2.13 m (6.27 m OD) and sandy blue/grey silt-clay unit at a depth of 1.65 m (6.75 m OD). This then transitioned into a silty peat unit at a depth of 1.52 m (6.88 m OD) and the surface peat unit at 0.35 m (8.05 m OD).

Borehole P3 reached an impenetrable depth of 2.87 m (5.53 m OD) in a stiff pink/brown clay unit. A sandy blue/grey silt-clay with gravel unit overlaid the pink/brown clay unit at a depth of 2.75 m (5.65 m OD), transitioning into an organic blue/grey silt-clay unit at a depth of 2.56 m (5.84 m OD). The organic blue/grey silt-clay unit was overlain by a silty peat unit at a depth of 2.43 m (5.97 m OD) and another unit of organic blue/grey silt-clay unit at 2.07 m (6.33 m OD). This then transitioned into a silty peat unit at a depth of 1.44 m (6.69 m OD) and the surface peat unit at 0.40 m (8.00 m OD).

Borehole P4 terminated on bedrock at a depth of 1.16 m (7.44 m OD). A unit of sandy blue/grey silt-clay with black mottling overlaid the bedrock, which transitioned into a more organic blue/grey silt-clay unit at a depth of the 0.63 m (7.97 m OD). This was then overlain by the surface peat unit at a depth of 0.42 m (8.18 m OD).

Borehole P5 reached a depth of 1.31 m (7.29 m OD) and terminated on bedrock. The bedrock was overlain by a sandy blue/grey with black mottling and transitioned into the surface peat unit at a depth of 0.29 m (8.31 m OD).

Borehole P6 terminated on bedrock at a depth of 1.86 m (6.74 m OD). A sandy blue/grey silt-clay unit overlaid the bedrock, and transitioned into a more organic blue/grey silt-clay unit at a depth of 1.41 m (7.19 m OD) and the surface peat unit at a depth of 0.26 m (8.34 m OD).

Borehole P7 reached a depth of 2.60 m (5.90 m OD) and terminated on bedrock. The bedrock was overlain by a sandy blue/grey silt unit which transitioned into a more organic sandy blue/grey silt-unit at a depth of 1.62 m (6.88 m OD). This then transitioned into the surface peat unit at a depth of 0.25 m (8.25 m OD).

Borehole P8 terminated on bedrock at a depth of 3.51 m (4.99 m OD). A unit of sandy blue/grey silt-clay overlaid the bedrock, and transitioned into an organic sandy blue/grey silt-clay unit at a depth of 1.34 m (7.16 m OD) and the surface peat unit at a depth of 0.24 m (8.26 m OD).

Borehole P9 reached a maximum depth of 1.78 m (6.82 m OD) and terminated on the bedrock. A sandy blue/grey silt-clay unit overlaid the bedrock, which transitioned into the more organic sandy blue/grey silt-clay unit at 1.52 m (7.08 m OD) and the surface peat unit at 0.35 m (8.25 m OD).

Borehole P10 terminated on bedrock at the maximum depth of 2.32 m (6.18 m OD). The bedrock was overlain by a sandy blue/grey silt-clay unit which transitioned into a more organic and sandy blue/grey silt-clay unit at 2.00 m (6.50 m OD). This was then overlain by the surface peat unit at 0.23 m (8.27 m OD).

Borehole P11 reached an impenetrable depth at 0.40 m (9.10 m OD) due to the presence of a small ridge at the site, hence the higher elevation of borehole P11.

Borehole P12 reached a maximum depth of 3.15 m (5.25 m OD) and terminated on bedrock. A unit of sandy blue/grey silt-clay with gravel overlaid the bedrock, which transitioned into a more organic blue/grey silt-clay unit at 2.98 m (5.42 m OD). The clastic unit was overlain by a peat unit at 2.75 m (5.65 m OD) which transitioned into a silty peat unit at 2.50 m (5.90 m OD). This was overlain by another organic blue/grey silt-clay unit at 2.26 m (6.14 m OD) which transitioned into the silty peat unit at 1.55 m (6.85 m OD) and the surface peat unit at 0.45 m (7.95 m OD).

A sample core was taken from borehole P12 as it contained all main stratigraphic units recorded. Core P12 was used for all laboratory analyses and to establish a chronology for the site. The results of laboratory analyses undertaken on core P12 are discussed in detail in the following sections.

(a)

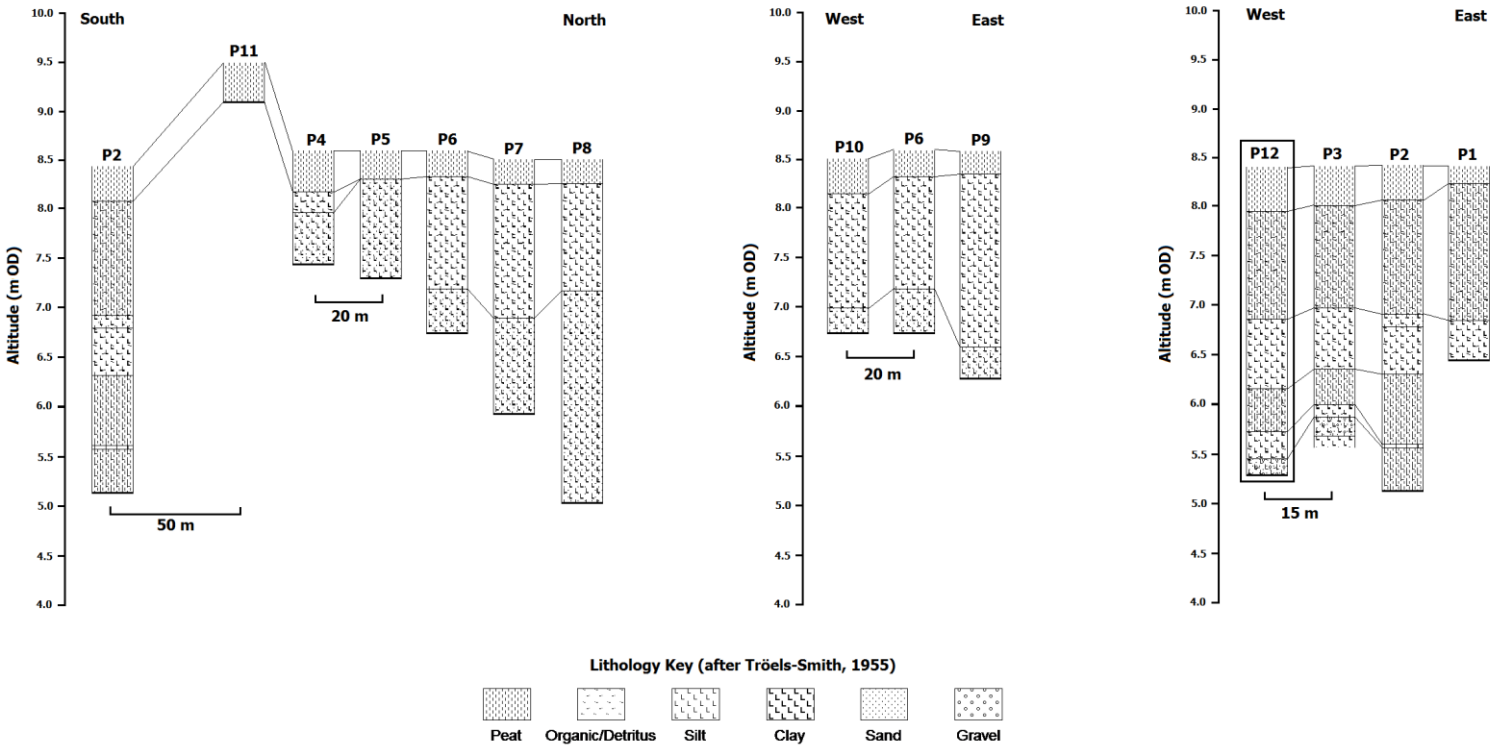
South
North
West
East
West
East
Altitude (m OD)
10.0
9.5
9.0
8.5
8.0
7.5
7.0
6.5
6.0
5.5
5.0
4.5
4.0
P2
P11
P4
P5
P6
P7
P8
P10
P6
P9
P12
P3
P2
P1
50 m
20 m
20 m
15 m
Lithology Key (after Tröels-Smith, 1955)
Peat
Organic/Detritus
Silt
Clay
Sand
Gravel

(b)

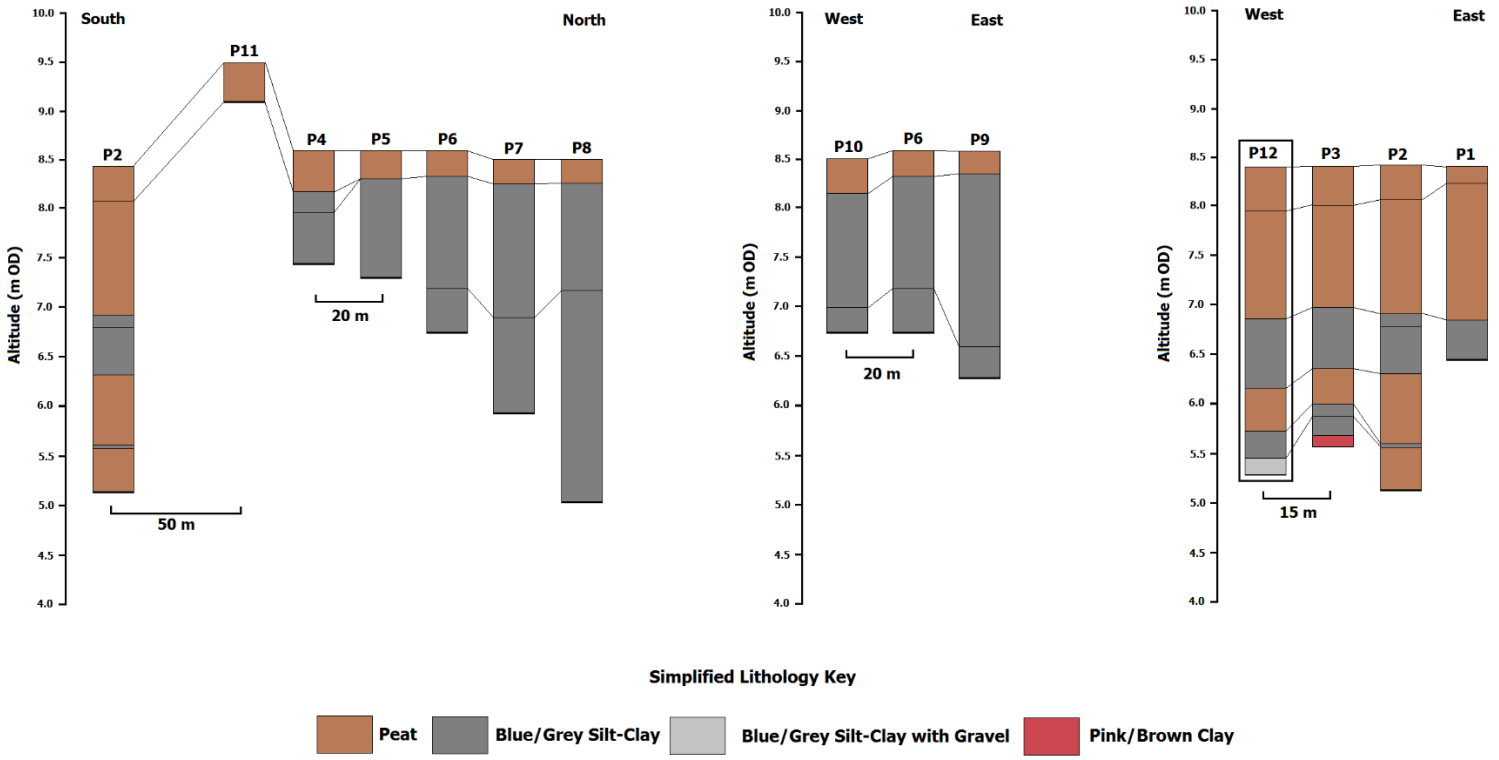

(c)

Figure 7.2: (a) Location of boreholes and sample core (P12) at Pelutho with contour lines marking the altitudes (m OD) of surrounding areas (b) The lithostratigraphy of the boreholes and sample core from Pelutho (c) The simplified lithostratigraphy of the boreholes and sample core from Pelutho. Sample core is marked by a black square

7.2 Sediment Composition

Core P12 terminated on bedrock at 3.15 m (5.25 m OD). The surface elevation recorded for core P12 was 8.40 m OD. The sand content in the sediment was highest at the base of the core, in the blue/grey silt-clay unit and within the surface peat unit. The sand fraction found in core P12 was composed of very fine sand and fine sand. The sediment description of core P12 is summarised in Table 7.1.

Table 7.1: Sediment description of core P12 including depth, altitude and the Tröels-Smith (1955) sediment classification

Depth (m)	Altitude (m OD)	Sediment Description	Tröels-Smith Sediment Classification (1955)
0 – 0.45	8.40 – 7.95	Very dark brown peat with roots and organic remains	Th4, Nig. = 4, Strf. = 0, Sicc. = 1, Elas. = 1
0.45 – 1.55	7.95 – 6.85	Very dark brown peat with roots and organic remains, incorporation of brown silt	Th4; Ag+, Nig. = 4, Strf. = 0, Sicc. = 1, Elas. = 1, Lim. = 0
1.55 – 2.26	6.85 – 6.14	Blue/grey silt-clay with roots, organic remains	Ag2; As2; Th+; Ga+, Nig. = 2, Strf. = 0, Sicc. = 2, Elas. = 0, Lim. = 2
2.26 – 2.70	6.14 – 5.70	Very dark brown peat with roots and organic remains, incorporation of brown silt	Th4; Ag+, Nig. = 4, Strf. = 0, Sicc. = 1, Elas. = 1, Lim. = 2
2.70 – 2.98	5.70 – 5.42	Blue/grey silt-clay with roots and organic remains	Ag2; As2; Th+, Nig. = 2, Strf. = 0, Sicc. = 2, Elas. = 0, Lim. = 2
2.98 – 3.15	5.42 – 5.25	Blue/grey silt-clay with roots and organic remains, sand and gravel	Ag2; As2; Dl+; Ga+; Gg+ (min), Nig. = 2, Strf. = 0, Sicc. = 3, Elas. = 0, Lim. = 1

To aid in the description of the sediment in the following sections, the different sediment units are numbered as follows: basal sandy blue/grey silt-clay and gravel unit (1), lower organic blue/grey silt-clay unit (2), lower silty peat unit (3), upper organic blue/grey silt-clay unit (4) and surface silty peat unit (5).

7.3 Loss on Ignition

Loss on ignition analyses were undertaken on samples from core P12 to give an estimate of the organic carbon content and carbonate content of the sediment. Samples were taken every 8 cm throughout the core, from each stratigraphic unit. The organic carbon content and carbonate content of core P12 are shown in Figure 7.3. Fluctuations can be noted in the percentage of organic carbon content of the samples from the core, which showed an increase correspondence to the deposition of the organic peat unit in the core. A minimum and a maximum of 2% and 94% respectively of organic carbon content were recorded in core P12. Limited changes in the percentage of carbonate content throughout core P12, ranging between 1% and 5% with no correlation between the percentages of carbonate content and the change of lithostratigraphy were observed.

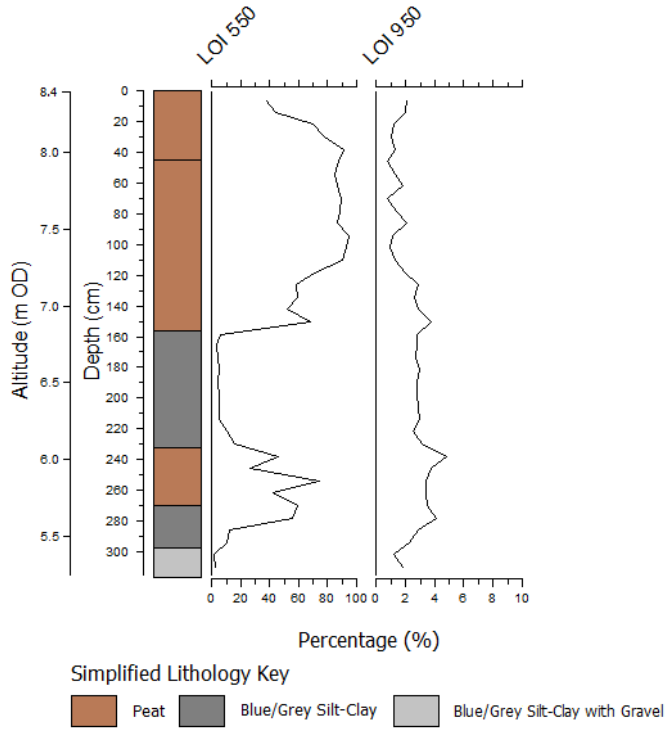

Figure 7.3: Plot of loss on ignition analyses for Pelutho showing organic carbon and carbonate contents of the sediment throughout core P12

7.4 Particle Size Analysis

Samples for particle size analysis were taken every 8 cm throughout the core (Figure 7.4). The particle size analysis showed very limited variation in the clay content throughout the core, ranging between 0.3% at a depth of 0.88 m (7.52 m OD) and 4% at a depth of 1.92 m (6.48 m OD). The percentages of sand showed sporadic increase throughout the core, with notable increase in the basal sandy blue/grey silt-clay with gravel unit (1), prior to the transition to the lower silty peat unit (3), the deeper part of the upper organic blue/grey silt-clay unit (4) and approximately the midpoint of the surface silty peat unit (5). The percentages of silt content recorded a minimum of 45% at a depth of 0.88 m (7.52 m OD) in the surface silty peat unit (5), and a maximum of 95% at a depth of 1.68 m (6.72 m OD) in the silty peat unit (5).

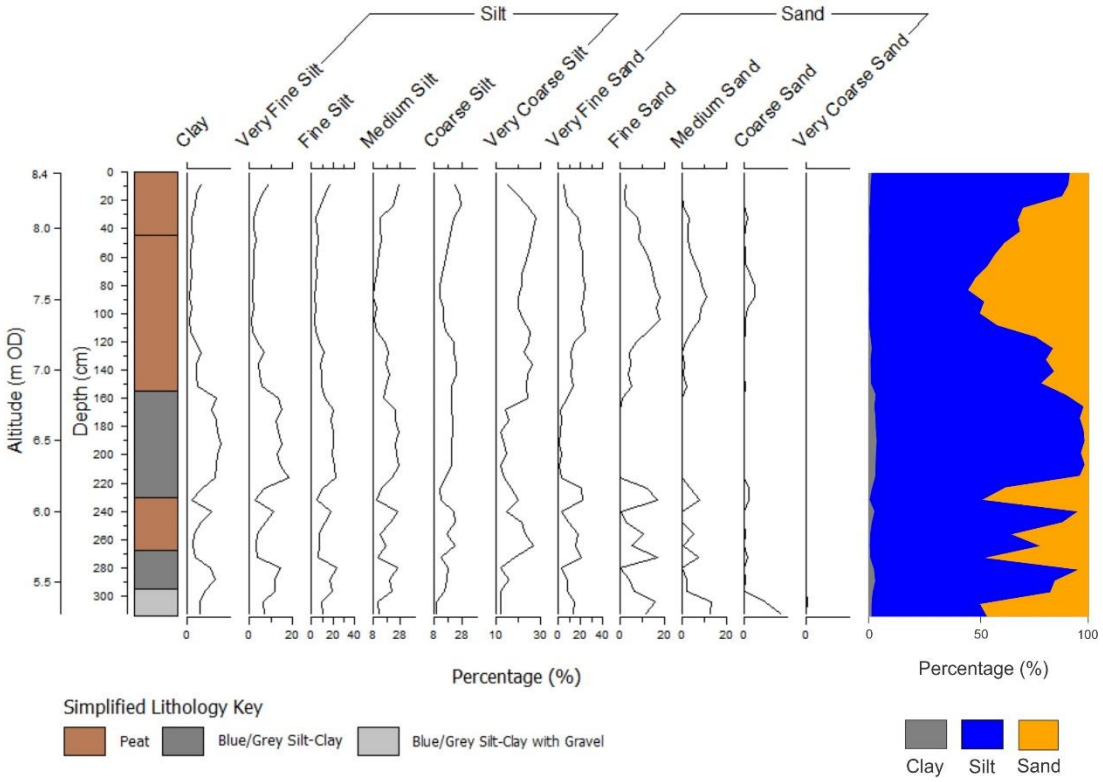

Figure 7.4: Diagram showing particle size analysis for core P12 from Pelutho

7.5 Chronology

The chronology for the core P12 was established through accelerator mass spectrometry (AMS) radiocarbon dating of three bulk sediment samples undertaken at DirectAMS Radiocarbon Dating Service in Washington, USA. The radiocarbon ages obtained were calibrated using OxCal v.4.3 (Ramsey, 2009) and the IntCal13 atmospheric curve (Reimer *et al.*, 2013). All dates were calibrated to cal BP (Table 7.2).

Table 7.2: Three radiocarbon dates obtained from Pelutho core P12

Lab Code	Code-Depth (cm)	Altitude (m OD)	Material Dated	Fraction	Radiocarbon Age		Cal BP (2σ Ranges)
					BP	1σ Error	
D-AMS 022226	PEL-151	6.89-6.90	Peat	Bulk carbon	6231	35	7254-7016
D-AMS 025778	PEL-240	6.00-6.01	Peat	Bulk carbon	6456	45	7435-7275
D-AMS 022227	PEL-289	5.51-5.52	Organic clay	Bulk carbon	7285	36	8174-8018

An age-depth model for core P12 was developed using Bacon v2.3.4 (Blaauw & Christen, 2011). The red dotted line shows modelled median ages along core P12 and the grey stippled lines indicate the 95% confidence intervals of the modelled age-depth relationship. The transparent blue violin plots show the four calibrated AMS ^{14}C dates from Pelutho. The upper left graph shows the iteration history of the model. The middle and right graphs show prior (green lines) and posterior (grey histograms) density functions for the accumulation rate and memory of the model (Figure 7.5). The mean 95% confidence of the age-depth model covers 392 years, a minimum of 204 years at 289 cm and a maximum of 450 years at 154 cm. Based on the age-depth model for core P12, 100% of the dates from Pelutho lie within the age-depth model's 95% range.

The main stratigraphic boundaries of core P12 (1.55 m, 2.26 m and 2.70 m; 6.85 m OD, 6.14 m OD and 5.70 m OD) were included in the age-depth model (shown in the horizontal dotted lines across the model in Figure 7.5). The sedimentation rates were calculated based on the dated samples and the main stratigraphic boundaries (mean age obtained from the model's prediction) and shown on the right side of Figure 7.5. Sedimentation rate increased slightly corresponding to the deposition of the upper organic blue/grey silt-clay unit (4) in the core.

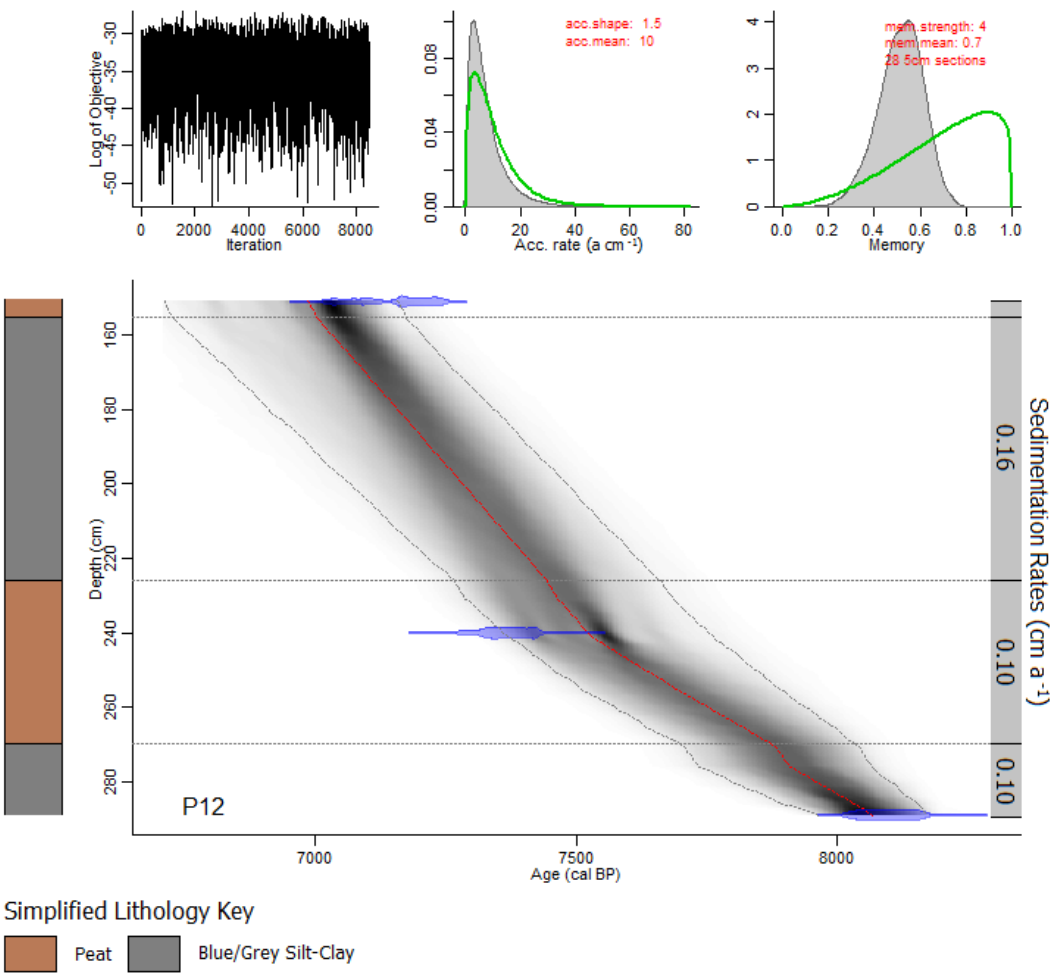

Figure 7.5: Age-depth model for the P12 core profile based on Bacon v2.3.4 modelling routines (Blaauw & Christen, 2011) and calculated sedimentation rates from the AMS ^{14}C dates calibrated with IntCal13 (Reimer *et al.*, 2013). Dotted lines on the model indicates the main stratigraphic units in the P12 core

7.6 Foraminiferal Analysis

There was variation in the preservation of foraminiferal tests in the samples from core P12, with some samples containing very few foraminiferal tests. It was therefore not possible to obtain a minimum count of 40 individuals in some of the samples despite increasing the sample volume. Samples were taken at 1 or 2 cm intervals throughout the whole core.

Five main agglutinated saltmarsh species comprised of *Jadammina macrescens*, *Miliamminia fusca*, *Tiphotrocha comprimata*, *Haplophragmoides wilberti* and *Trochammina inflata* were observed in the samples analysed (Figure 7.6). No

calcareous species were found, although low frequencies of test linings were observed in the core. No foraminifera were observed in the basal sandy blue/grey silt-clay with gravel unit (1) at the depths between 3.15 m (5.25 m OD) to 2.98 m (5.42 m OD). No foraminifera was observed in the deepest 0.30 m of the lower silty peat unit (3), and in the surface silty peat unit (5) from a depth of 1.51 m (6.89 m OD) towards the top of the core.

The presence of a single agglutinated saltmarsh species *J. macrescens* in low frequencies was observed at the depths of 2.82 m (5.58 m OD), 2.84 m (5.56 m OD), 2.86 m (5.54 m OD) and 2.88 m (5.52 m OD) in the lower organic blue/grey silt-clay unit (2). The foraminiferal assemblage was dominated mainly by *J. macrescens* and *M. fusca*, with low frequencies of *T. inflata*. A single peak of *T. comprimata* observed at a depth of 2.24 m (6.16 m OD) and sporadic occurrence of *H. wilberti* was also observed in the core. Peaks in the occurrence of *H. wilberti* were observed in the core at 2.40 m (6.00 m OD) and at 1.52 m (6.88 m OD).

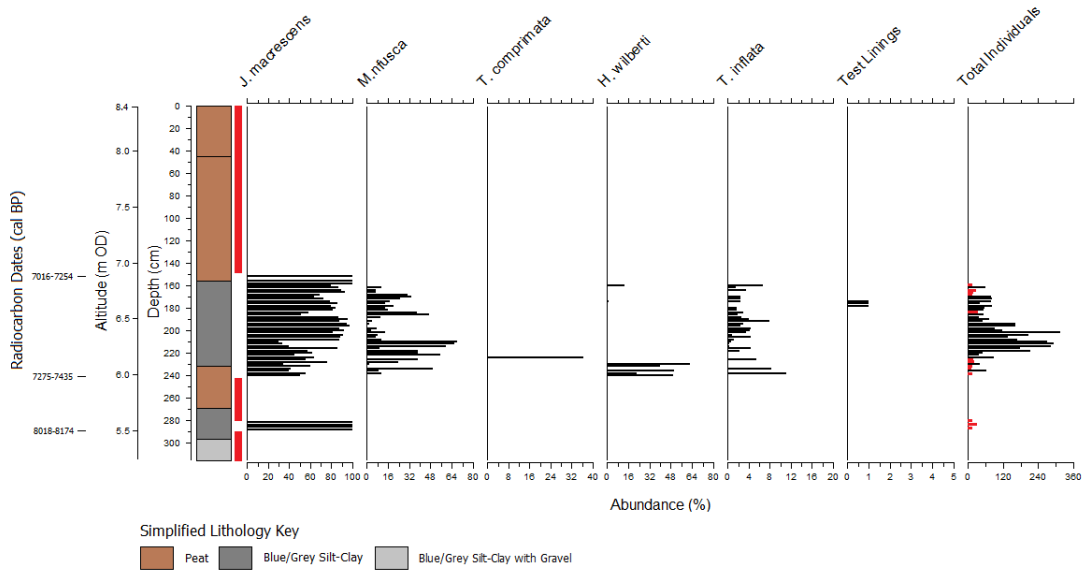

Figure 7.6: Foraminiferal diagram from Pelutho core P12. Foraminiferal frequencies are expressed as a percentage of total foraminifera. All samples including samples with low individual counts (below 40 individuals; marked with red lines) were included in this diagram. Red blocks next to the stratigraphy diagram indicates the zone where foraminifera was absent in the core

7.7 Holocene Relative Sea-Level and Environmental Changes at Pelutho

The interpretation of Holocene relative sea-level and environmental changes for Pelutho are based on microfossil analyses, changes in lithostratigraphy and the sediment composition of core P12.

7.8 Microfossil Interpretation: Foraminifera

No foraminifera were observed in the basal sandy blue/grey silt-clay with gravel unit (1). It is most probable that the clastic unit was deposited at the site through slope wash or fluvial processes (discussed in Section 7.9).

The first presence of foraminifera in the core recording a transgressive contact at the site was noted in the lower organic blue/grey silt-clay unit (2) (Figure 7.7) at a depth of 2.88 m (5.52 m OD) and was dominated by a single agglutinated saltmarsh species *J. macrescens*, which is mainly associated with a high saltmarsh environment, although the occurrence of *J. macrescens* in a lower saltmarsh and intertidal mudflat environment was also observed in the contemporary foraminifera samples from Cardurnock Marsh (Chapter 4; Section 4.3.2). The organic blue/grey silt-clay unit (2) is consistent with an intertidal mudflat environment, and therefore would have most likely been present at the site in a low saltmarsh environment or intertidal mudflat environment. However, no calcareous species or test linings were noted in the zone.

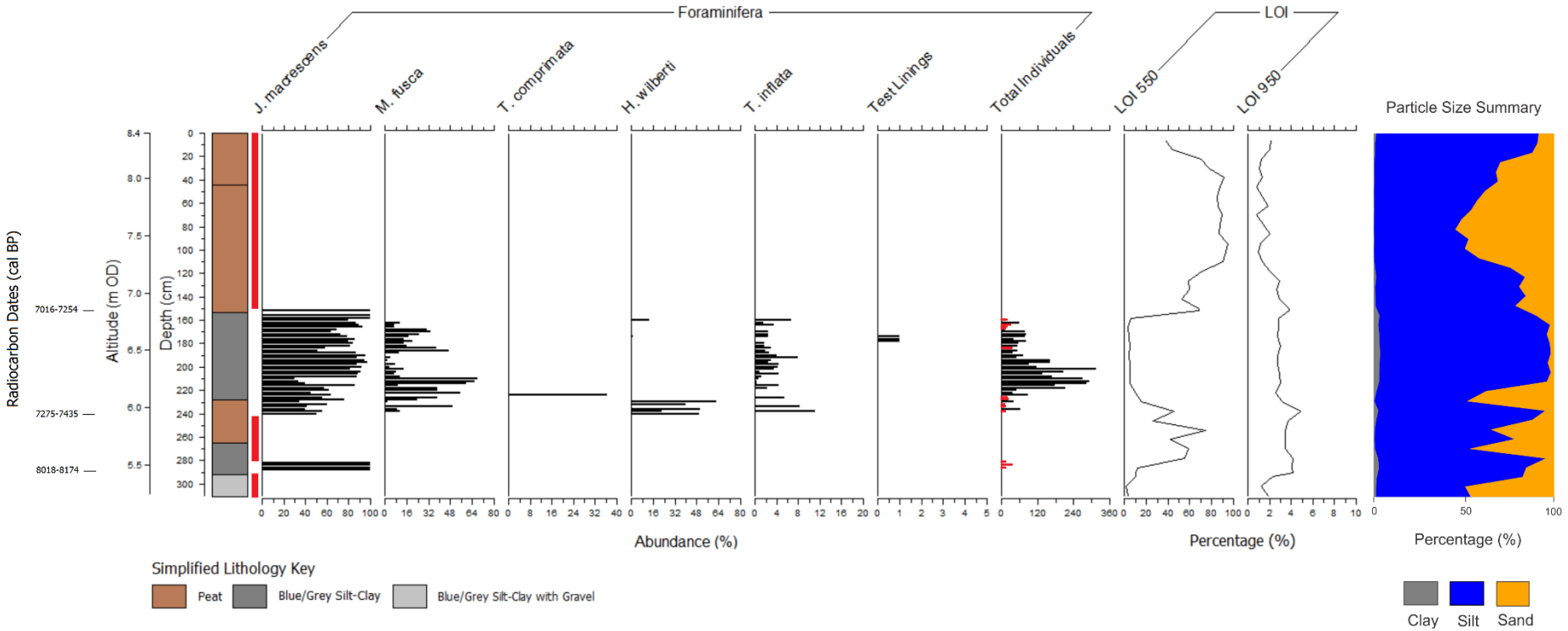

Figure 7.7: Summary diagram showing foraminifera, loss on ignition and particle size analyses undertaken on samples from core P12

A negative sea-level tendency was recorded at 2.70 m (5.70 m OD), evidenced by the absence of foraminifera in the deepest 0.30 m of the lower silty peat unit (3) overlying the organic blue/grey silt-clay unit (2). As relative sea level decreased from the site, a freshwater environment developed. The second presence of foraminifera dominated by *J. macrescens* was observed at a depth of 2.40 m (6.00 m OD), indicating that the previous freshwater environment had developed into a high saltmarsh environment, recording another transgressive contact at Pelutho. This is consistent with the dominance of *J. macrescens* in the sediment and distinct peaks of *H. wilberti*, which are associated with an environment occurring at the level of extreme high water (Horton & Edwards, 2006; Gehrels & Long, 2008).

The transition from the lower silty peat unit (3) to the overlying organic blue/grey silt-clay unit (4) recorded another positive sea-level tendency in the core at 2.26 m (6.14 m OD). This zone is dominated by *J. macrescens* and *M. fusca*, with low frequencies of *T. inflata*. The previous saltmarsh environment would have been replaced by an intertidal mudflat environment, as relative sea level continued to increase. No calcareous species and test linings were noted in this zone.

The occurrence of a single species of *J. macrescens* was observed from 1.58 m (6.82 m OD) to 1.52 m (6.88 m OD) in the surface silty peat unit (5), although the individual counts were also low. The microfossil evidence along with the transition from the organic blue/grey silt-clay unit (4) to the overlying silty peat unit (5) recorded a negative sea-level tendency in the core. As relative sea-level at the site decreased, the site developed into a high saltmarsh environment. The absence of foraminifera at 1.51 m (6.89 m OD) towards the top of the core suggests that the saltmarsh environment transitioned into a freshwater environment, recording the regressive contact in the core at Pelutho.

7.9 Sediment Deposition and Relative Sea-Level Interpretation

The origin of the basal clastic unit could be from marine inundation, slope wash or fluvial processes. As the basal sandy blue/grey silt-clay with gravel unit (1) is barren of any microfossils indicating marine influence, the sediment is most likely deposited at the site through glaciofluvial processes (Walker, 1966) similar to the unit recorded

at Allonby (Chapter 5; Section 5.9), or through slope wash into the area as the site is bordered by higher grounds towards the south (Figure 7.2a).

The basal sandy blue/grey silt-clay with gravel unit (1) is overlain by a more organic blue/grey silt-clay unit (2), where the first presence of foraminifera were observed in the core. The presence of the agglutinated foraminifera in this unit indicates that the deposition of the organic blue/grey silt-clay (2) recorded a transgressive contact at the site, and is consistent with an intertidal mudflat environment. The transgressive contact was dated at 8174-8018 cal BP, and is possibly related to the Main Postglacial Transgression or a combination of the Main Postglacial Transgression and the final drainage of glacial Lake Agassiz-Ojibway located in north-central North America (Törnqvist & Hijma, 2012).

The organic blue/grey silt-clay unit (2) was overlain by a silty peat unit (3), recording a negative tendency in sea level at the site. No foraminifera were observed in the deepest 0.30 m of the silty peat unit (3), indicating a freshwater environment had developed at the site. Foraminifera were again observed in the silty peat unit (3) at a depth of 2.40 m (6.00 m OD), recording another transgressive contact. The increased relative sea level was dated at 7435-7275 cal BP, with the previous freshwater environment developing into a saltmarsh environment.

The lower silty peat unit (3) was overlain by another unit of organic blue/grey silt-clay (4), recording a positive sea-level tendency in the core. Relative sea level at the site would have continued to increase resulting in another expansion of intertidal mudflat environment into the site.

The upper organic blue/grey silt-clay unit (4) was overlain by the surface silty peat unit (5), which recorded a decrease in relative sea level at the site and possible development of a saltmarsh. The change in lithostratigraphy and the change in foraminiferal assemblages are evidence of this. At a depth of 1.51 m (6.89 m OD), the absence of foraminifera was observed, suggesting that relative sea-level decreased leading to a freshwater environment. The regressive contact was dated at 7254-7016 cal BP. No further changes in biostratigraphy (foraminifera) were observed from 1.51 (6.89 m OD) towards the top of the core.

7.10 Relative Sea-Level Reconstruction for Pelutho

Relative sea-level reconstruction for the site at Pelutho was developed was developed through a combination of lithostratigraphic and biostratigraphic analyses, determination of indicative meanings and calculation of sea-level index points.

7.11 Determination of Indicative Meaning

As the predicted palaeo marsh surface elevation (PMSE) based on the transfer function utilised on core P12 were deemed unreliable, the assigned reference water level based on the changes in lithostratigraphy and biostratigraphy (foraminiferal assemblages) were therefore used for the calculation of sea-level index points.

The lithostratigraphy of sample PEL-289 consisting of organic blue/grey silt-clay unit (2) is consistent with a lower saltmarsh or an intertidal mudflat environment, however only a low presence of the agglutinated species *J. macrescens* with no calcareous species or test linings was observed. An indicative meaning relating to a lower saltmarsh environment was therefore assigned to sample PEL-289, as dominance of agglutinated species *J. macrescens* in the intertidal mudflat environment between mean high water spring tide (MHWST) and mean high water neap tide (MHWNT) was observed at Cardurnock Marsh (Chapter 4, Section 4.3.2).

For both samples PEL-240 and PEL-151, an indicative meaning associated with a high saltmarsh environment was assigned, consistent with the lithostratigraphy consisting of the silty peat unit (3 and 5) and the dominance of *J. macrescens* and peaks of *H. wilberti* which suggests an environment occurring at the level of extreme high water. The dominance of *J. macrescens* and peaks of *H. wilberti* are consistent with the high saltmarsh environment recorded at Skinburness Marsh and Bowness Marsh, where the dominance of mainly *J. macrescens* was observed between MHWST and highest astronomical tide (HAT). The foraminiferal assemblages of samples PEL-240 and PEL-151 are more consistent with the contemporary samples from Bowness Marsh (Chapter 4, Section 4.3.3) as the occurrence of *H. wilberti* was also noted between MHWST and HAT at the contemporary saltmarsh site.

As the indicative meaning for samples PEL-289, PEL-240 and PEL-151 have been ascribed based on samples from two different contemporary marshes (Cardunock Marsh and Bowness Marsh), the complete Solway training set with elevation values converted to standardised water level index (SWLI) (Figure 4.22) was used to determine the indicative range of the samples, as this eliminates the tidal variations between the two contemporary sites. The SWLI values for the respective contemporary sample most representative of the samples PEL-289, PEL-240 and PEL-151 were then converted back to elevation (m OD), to allow the calculation of the reference water level and indicative range.

The contemporary sample most representative of sample PEL-289 lies between the SWLI of 285 and 295 in the Solway training set, which falls below MHWST (Figure 4.22). This covers an altitude of 4.69 m OD (contemporary sample CM05) and 5.23 m OD (contemporary sample CM01). Based on these values, the reference water level for sample PEL-289 is the midpoint between 4.69 m OD and 5.23 m OD, resulting in an indicative range of ±0.5 m.

The contemporary samples most representative of samples PEL-240 and PEL-151 lies above MHWST with the SWLI ranging between 300 (contemporary sample BM20) and 310 (contemporary sample BM15) based on the Solway training set. This covers an altitude of 5.34 m OD and 5.83 m OD, with the reference water level for both samples PEL-240 and PEL-151 to be the midpoint of these altitudes, and an indicative range of ±0.5 m.

7.12 Post-Depositional Lowering of Sediments

All of the sea-level index points produced from Pelutho are of intercalated samples, and would have been subjected to post-depositional lowering (PDL). The PDL of sediments in core P12 were estimated based on the geotechnical model developed by Brain *et al*. (2011, 2012). Minimal PDL of sediments is observed in core P12. Samples PEL-151, PEL-240 and PEL-289 experienced a compaction of 0.010 m, 0.050 m and 0.020 m respectively. Figure 7.8 shows the PDL of sediments at a 0.02 m interval throughout core P12.

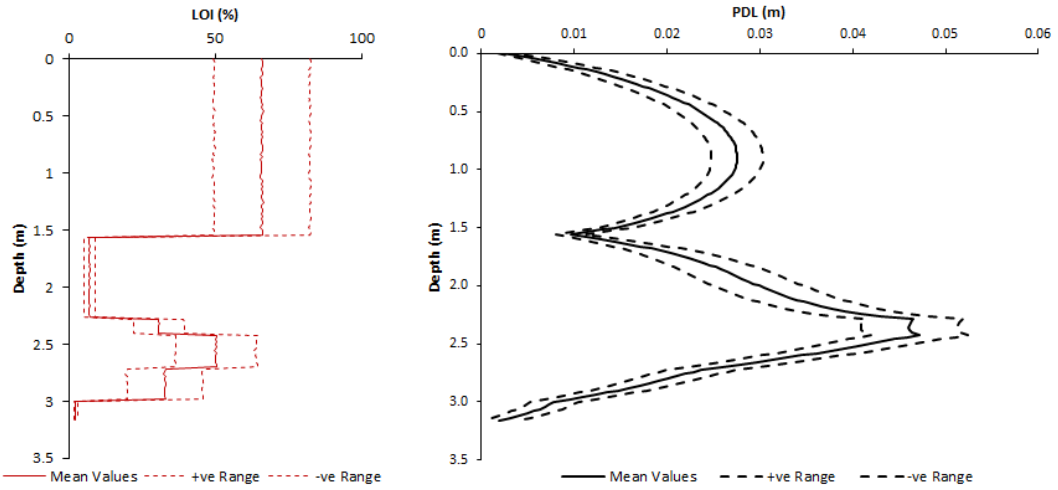

Figure 7.8: Geotechnical and physical properties showing the averaged downcore organic content, expressed as % loss on ignition and the model estimates of post-depositional lowering for core P12. Abbreviations: LOI = Loss on ignition; PDL = Post-depositional lowering

7.13 Sea-Level Index Points

The sample's age, reference water level and indicative range along with the associated errors for each sample are required for the calculation of sea-level index points (Chapter 3; Section 3.9). Three sea-level index points were produced for Pelutho (Table 7.3).

Table 7.3: Sea-level index points produced from P12

Lab Code	Latitude	Longitude	Radiocarbon Age		Cal BP (2σ Ranges)			Altitude (m OD)	Compaction Correction (m)	RSL (m)	Tendency
			BP	1σ Error	Min	Mean	Max				
D-AMS 022226	54.829	-3.371	6231	35	7016	7146	7254	6.89	+0.010	+1.35±0.56	Negative
D-AMS 025778	54.829	-3.371	6456	45	7275	7367	7435	6.00	+0.050	+0.50±0.57	Positive
D-AMS 022227	54.829	-3.371	7285	36	8018	8097	8174	5.51	+0.020	+0.58±0.57	Positive

Samples PEL-151, PEL-240 and PEL-289 produced sea-level index points of 1.35±0.56 m, 0.50±0.57 m and 0.58±0.57 m respectively. Errors and corrections associated with each sea-level index point were calculated based on the methods described in Chapter 3 (Section 3.9). Figure 7.9 shows the sea-level index points from Pelutho plotted against the modelled relative sea-level curve for southern Solway Firth at the location of NY 2481 5666 based on the BRADLEY2011, KUCHAR2012 and BRADLEY2017 models (Shennan *et al*., 2012; 2018; Kuchar *et al*., 2012).

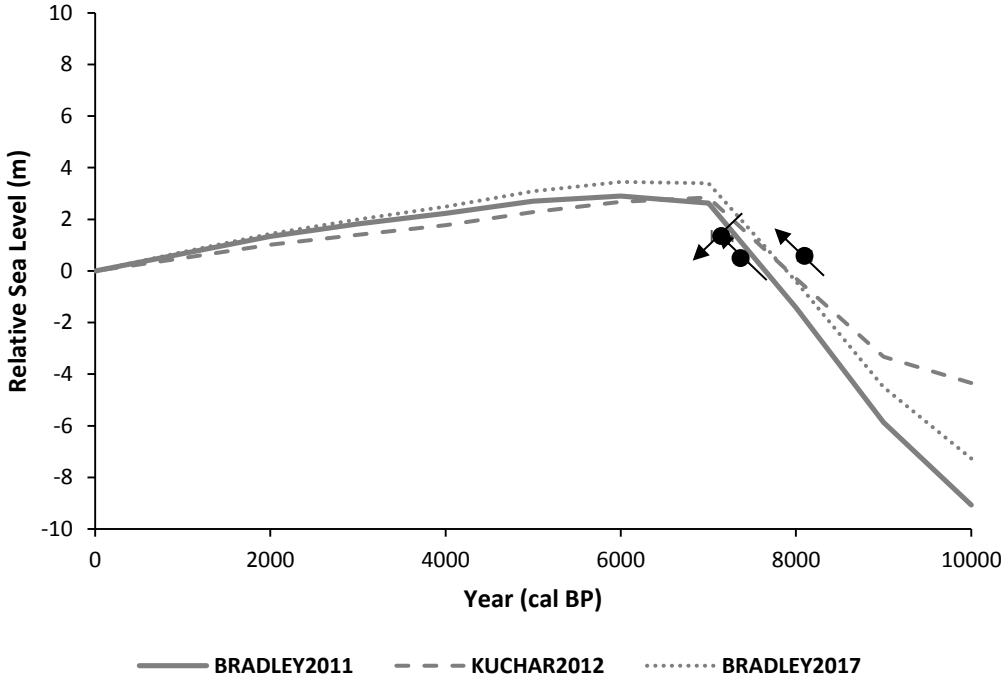

Figure 7.9: Graph showing three sea-level index points from Pelutho. The black line is the modelled relative sea-level curves for southern Solway Firth based on Shennan *et al*. (2012; 2018) and Kuchar *et al*. (2012). All sea-level index points include associated individual vertical and age error bars

7.14 Summary

The site at Pelutho has provided a record of Holocene sea-level changes. The three sea-level index points from Pelutho are consistent with the recorded dates of marine transgression and marine regression from other sites located on the southern shore of the Solway Firth. The transgressive contacts at Pelutho are possibly related to both the final drainage of glacial Lake Agassiz-Ojibway and the Main Postglacial Transgression in the Solway Firth, with the first and second dated at 8097 cal BP and

7367 cal BP respectively. The regressive contact indicating negative sea-level tendency at Pelutho was dated at 7146 cal BP.

CHAPTER 8

HERD HILL

8.0 Introduction

The study site at Herd Hill (NY 1794 6010) is located on the northwest Cumbrian coastline, approximately 200 metres from the present coastline on the southern shore of the Solway Firth, and approximately 3 km away from the northern bank of Moricambe Bay (Figure 8.1). The site is bordered by a gently sloping hill to the north and west of the site, and farmland to the east and south of the site (Figure 8.2a). Bowness Common, a raised peat bog, is situated southeast of Herd Hill and has been studied previously (Walker, 1966; Huddart *et al.*, 1977). The study area is approximately 100 m by 80 m.

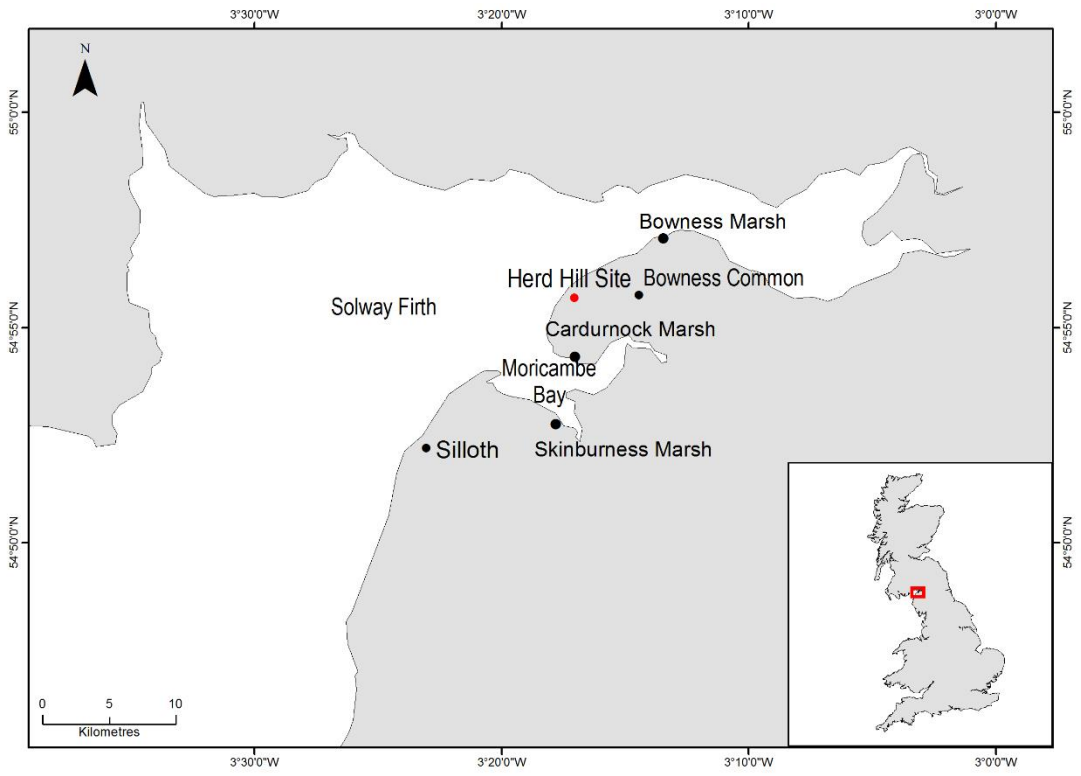

Figure 8.1: Location of the study site at Herd Hill marked in red

8.1 Borehole Location and Stratigraphy

Two transects of boreholes were cored across the site to establish a detailed stratigraphy (Figure 8.2). The first transect was cored from north to south, and the second transect was cored from west to east. The surface altitude of the boreholes ranged from 9.4 m OD to 9.6 m OD. Borehole HH1 reached the maximum depth of 2.58 m (6.92 m OD) at the site, terminating in a silty grey sand unit while boreholes HH2, HH3, HH4 and HH5 terminated on bedrock. The general lithostratigraphy at Herd Hill is a red sand and gravel unit over the bedrock, overlain by a silty brown sand and gravel unit which transitioned into a blue/grey silt-clay unit and the surface peat unit.

Borehole HH1 reached an impenetrable depth at 2.58 m (6.82 m OD) in the silty grey sand unit. The silty grey sand was overlain by a more organic grey sand at a depth of 0.92 m (8.48 m OD), and this was overlain by a unit of peat with stiff sandy brown silt-clay at 0.66 m (8.74 m OD). This then transitioned into the surface peat unit at a depth of 0.25 m (9.15 m OD).

Borehole HH2 terminated on bedrock at a depth of 1.21 m (8.19 m OD). A unit of red sand and gravel overlaid the bedrock and transitioned into the organic blue/grey silt-clay unit at 1.06 m (8.34 m OD). The blue/grey silt-clay unit was overlain by an organic brown silt-clay unit at a depth 0.58 m (8.82 m OD) and the surface peat unit at 0.50 m (8.90 m OD).

Borehole HH3 terminated on bedrock at a depth of 1.38 m (8.12 m OD). The bedrock was overlain by a unit of red sand and gravel, which transitioned into the organic blue/grey silt-clay unit at a depth of 1.18 m (8.32 m OD). The blue/grey silt-clay unit was overlain by peat incorporated with brown silt-clay at 0.51 m (8.99 m OD) which transitioned into the surface peat unit at 0.35 m (9.15 m OD).

Borehole HH4 reached a maximum depth of 1.68 (7.82 m OD), and terminated on bedrock. The bedrock was overlain by degraded bedrock material composed of red sand and gravel, and transitioned into a unit composed of brown silty sand and gravel at 1.47 m (8.03 m OD). This was overlain by the sandy blue/grey silt-clay unit at 1.23 m (8.27 m OD). The sandy blue/grey silt-clay unit was overlain by a more organic

blue/grey silt-clay unit at a depth of 0.89 m (8.61 m OD) and a unit composed of peat incorporated with brown silt-clay at 0.69 m (8.81 m OD). This transitioned into the surface peat unit at 0.23 m (9.27 m OD).

Borehole HH5 terminated on bedrock at 1.70 m (7.70 m OD). The bedrock was overlain by the red sand and gravel unit, which transitioned into the sandy grey silt-clay with gravel unit at a depth of 1.49 m (7.91 m OD), with brown silty sand and gravel at the bottom of the unit. This was overlain by an organic blue/grey silt-clay unit at 1.25 m (8.15 m OD) and peat incorporated with brown silt-clay at 0.51 m (8.89 m OD). This unit then transitioned into the surface peat unit at 0.16 m (9.24 m OD).

Borehole HH6 reached a maximum depth of 1.76 m (7.84 m OD), terminating on bedrock. The bedrock was overlain by the red sand and gravel unit, and transitioned into the overlying sandy grey silt-clay with gravel unit at a depth of 1.49 m (8.11 m OD) with brown silty sand and gravel at the bottom of the unit. This was overlain by an organic blue/grey silt-clay unit at 1.28 m (8.32 m OD) and peat incorporated with brown silt-clay at 0.51 m (9.09 m OD). The unit then transitioned into the surface peat unit at 0.17 m (9.43 m OD).

A sample core was taken at Herd Hill from borehole HH4 as it contained all main stratigraphic units recorded (Figure 8.2). Core HH4 was used for all laboratory analyses and to establish a chronology for the site. The results of laboratory analyses undertaken on core HH4 are discussed in detail in the following sections.

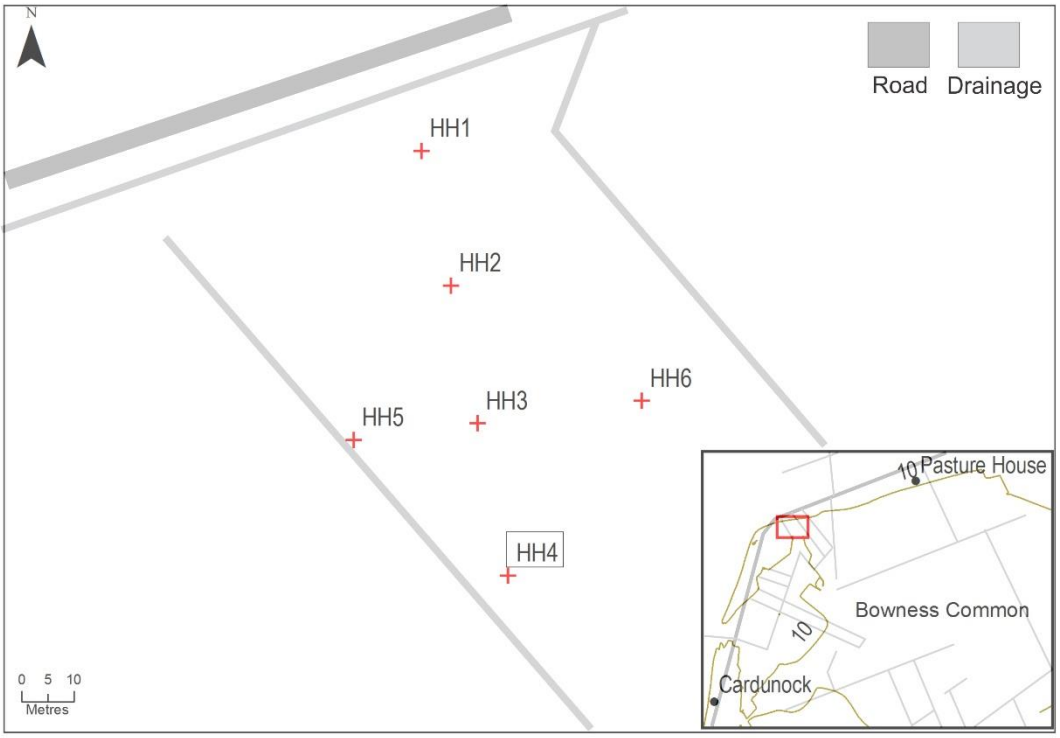
N
Road
Drainage
HH1
HH2
HH3
HH4
HH5
HH6
0 5 10
Metres
Pasture House
Bowness Common
Cardunock
10
10

(a)

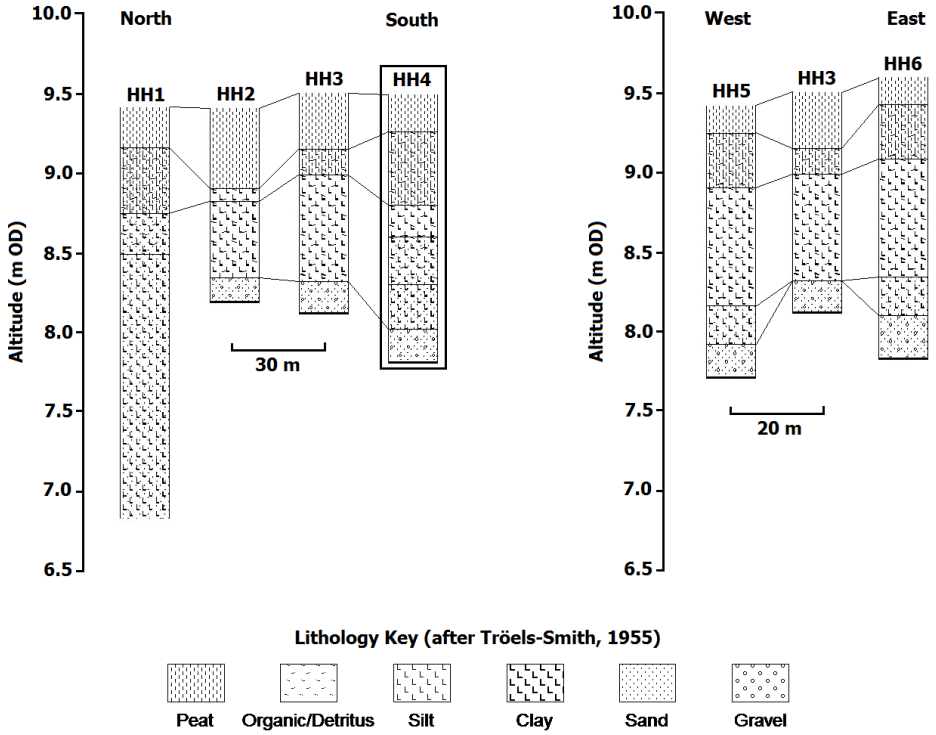
North
South
West
East
HH1
HH2
HH3
HH4
HH5
HH6
Altitude (m OD)
10.0
9.5
9.0
8.5
8.0
7.5
7.0
6.5
30 m
20 m
Lithology Key (after Tröels-Smith, 1955)
Peat
Organic/Detritus
Silt
Clay
Sand
Gravel

(b)

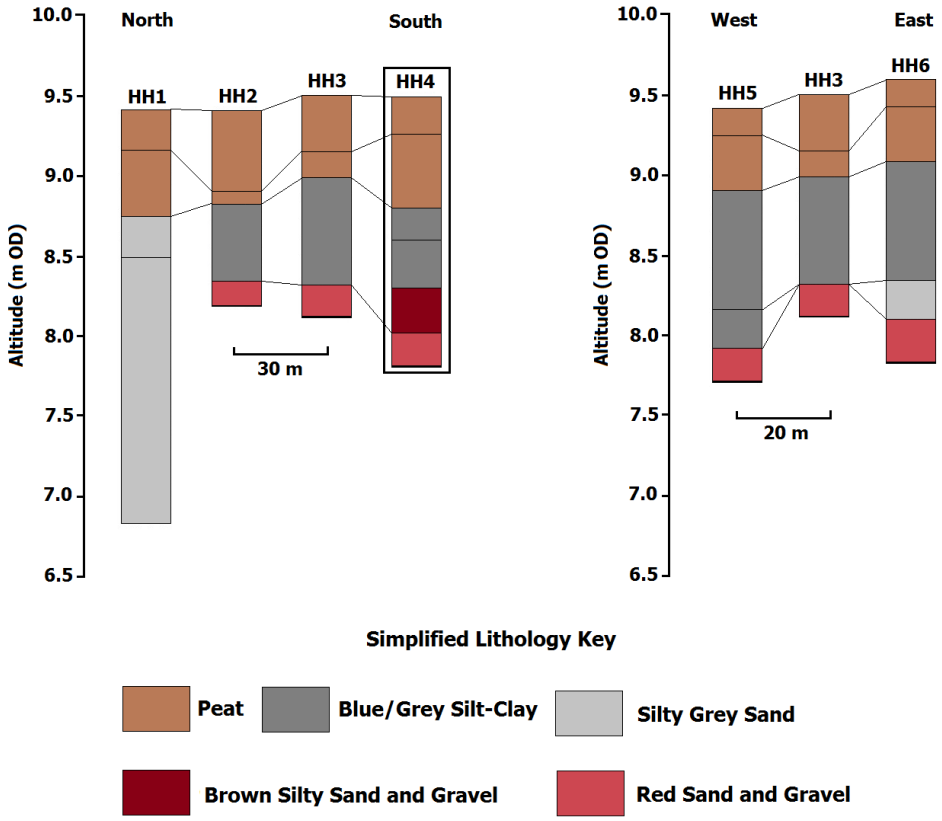

(c)

Figure 8.2: (a) Location of boreholes and sample core (HH4) obtained at Herd Hill with contour line marking the altitudes (m OD) of surrounding areas (Source: © Crown Copyright and Database Right (2018) Ordnance Survey, Digimap Licence) (b) The lithostratigraphy of the boreholes and sample core from Herd Hill (c) The simplified lithostratigraphy of the boreholes and sample core from Herd Hill. Sample core is marked in a black square

8.2 Sediment Composition

Core HH4 terminated on the bedrock at 1.68 m (7.82 m OD). The surface elevation recorded for core HH4 was 9.50 m OD. Towards the base of the core in the red sand and gravel unit, the overlying brown silty sand and gravel unit and sandy blue/grey silt-clay unit, increased sand content was recorded. The sand content decreased in the organic blue/grey silt-clay unit, and increased again towards the surface of the core in the peat unit. The sand fraction found in core HH4 consists mainly of very fine

sand and fine sand. The sediment description of core HH4 is summarised in Table 8.1.

Table 8.1: Sediment description of core HH4 including depth, altitude and the Tröels-Smith (1955) sediment classification

Depth (m)	Altitude (m OD)	Sediment Description	Tröels-Smith Sediment Classification (1955)
0 – 23	9.50 – 9.27	Very dark brown peat with roots and organic remains	Th4; Ga+, Nig. = 4, Strf. = 0, Sicc. = 1, Elas. = 1
23 – 69	9.27 – 8.81	Very dark brown peat with roots and organic remains, some brown silt	Th4; Ag+; Ga+, Nig. = 4, Strf. = 0, Sicc. = 1, Elas. = 1, Lim. = 0
69 – 89	8.81 – 8.61	Blue/grey silt-clay with roots, organic remains	Ag2; As2; Th+, Nig. = 2, Strf. = 0, Sicc. = 2, Elas. = 0, Lim. = 2
89 – 123	8.61 – 8.27	Blue/grey silt-clay with roots, organic remains and sand	Ag2; As2; Dl+; Ga+, Nig. = 2, Strf. = 0, Sicc. = 3, Elas. = 0, Lim. = 1
123 – 147	8.27 – 8.03	Brown silty sand and gravel	Ga3; Gg1 (min); Ag+, Nig. = 3, Strf. = 0, Sicc. = 3, Elas. = 0, Lim. = 1
147 – 168	8.03 – 7.82	Red sand and gravel	Ga2; Gg2 (min), Nig. = 3, Strf. = 0, Sicc. = 3, Elas. = 0, Lim. = 1

8.3 Loss on Ignition

Loss on ignition analyses were undertaken on samples from core HH4 to give an estimate of the organic carbon content and carbonate content of the sediment. Samples were taken at every 8 cm throughout the core, from each stratigraphic unit found in the core. The organic carbon content and carbonate content of core HH4 are shown in Figure 8.3. Fluctuations was noted in the percentage of organic carbon

content of the samples analysed from core HH4, with a clear distinction in the percentages of organic carbon between the clastic unit (comprising of the red sand and gravel unit, the brown silty sand and gravel unit, the blue/grey silt-clay unit) and the overlying silty peat unit and surface peat unit. Low percentages of organic carbon content were observed coinciding with the deposition of the clastic unit, while percentages of organic carbon content increased significantly in the overlying peat unit ranging between 2% to 97%. There was limited change in the percentage of carbonate content throughout core HH4, with a range of 0% to 2% observed.

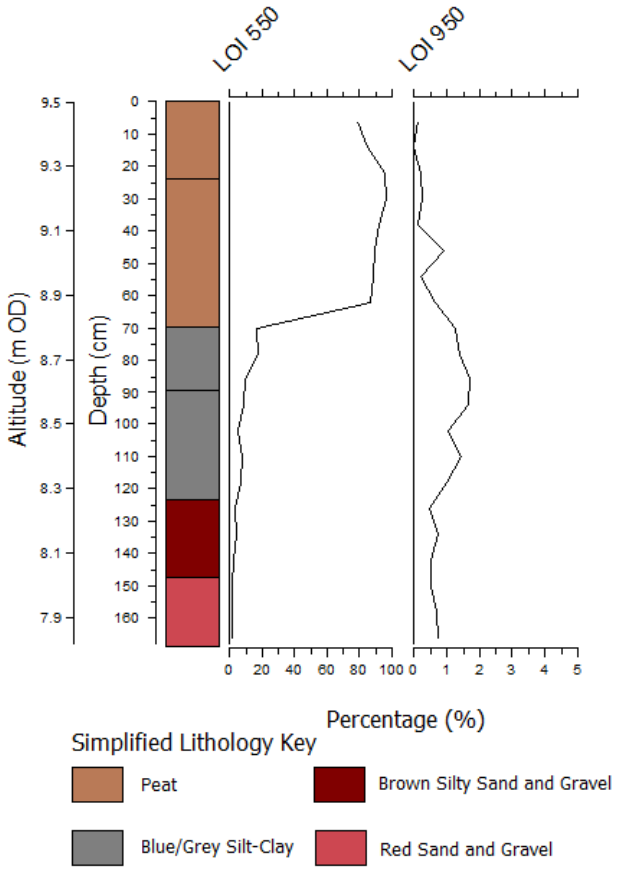

Figure 8.3: Plot of loss on ignition analyses for Herd Hill showing organic carbon and carbonate content of the sediment in core HH4

8.4 Particle Size Analysis

Samples for particle size analysis were taken every 8 cm throughout the core from each stratigraphic unit. Particle size analysis in core HH4 showed sediment dominated mostly by silt with increased sand content observed towards the bottom and the top of core HH4. Where increased sand content was observed, it was dominated mainly

by very fine and fine sand, which ranged between 0.3% and 61%. Limited variation in clay content throughout the core was observed, with a maximum of 7% observed at a depth of 1.52 m (7.98 m OD) and a minimum of 1% observed at a depth of 0.24 m (9.26 m OD). The percentage of silt content reached a maximum of 95% at 1.04 m (8.46 m OD), while the minimum silt content of 37% was noted at 1.44 m (8.06 m OD) in the brown silty sand and gravel unit.

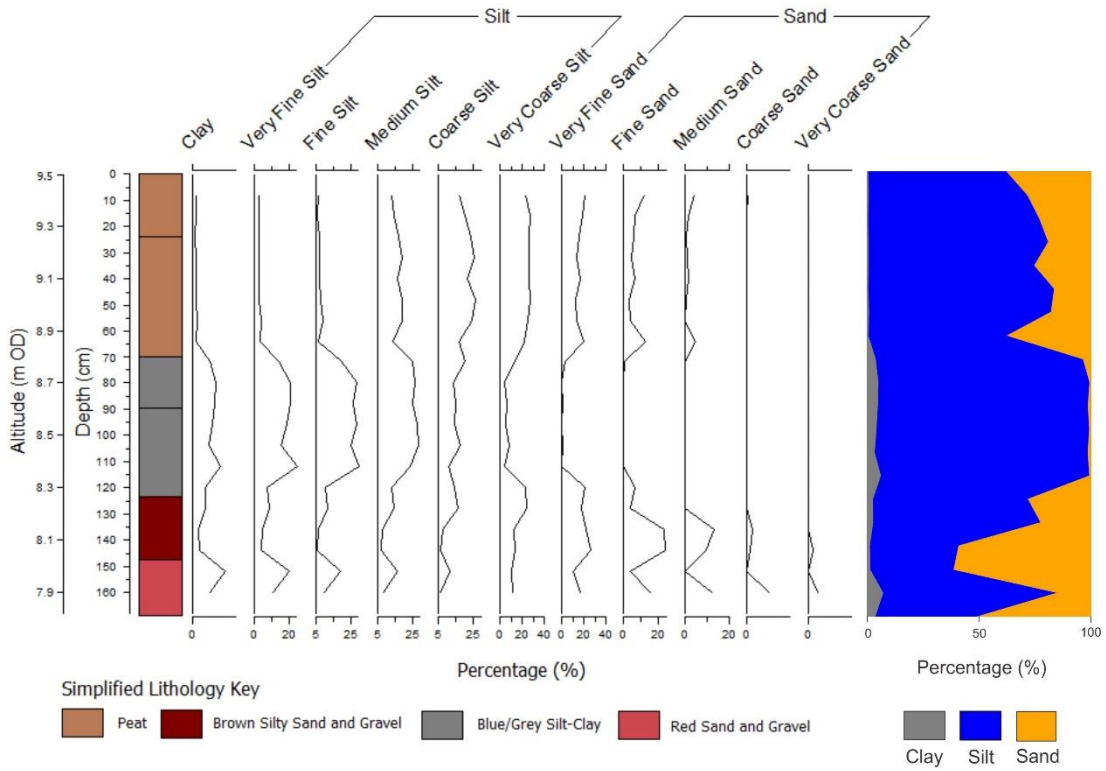

Figure 8.4: Diagram showing particle size analysis for core HH4 from Herd Hill

8.5 Chronology

The chronology for the core from Herd Hill was established through accelerator mass spectrometry (AMS) radiocarbon dating of three bulk sediment samples at DirectAMS Radiocarbon Dating Service in Washington, USA. Radiocarbon ages obtained were calibrated using OxCal v.4.3 (Ramsey, 2009) and the IntCal13 atmospheric curve (Reimer *et al.*, 2013). All dates were calibrated to cal BP (Table 8.2).

Table 8.2: Three radiocarbon dates obtained from Herd Hill core HH4

Lab Code	Code-Depth (cm)	Altitude (m OD)	Material Dated	Fraction	Radiocarbon Age		Cal BP (2σ Ranges)
					BP	1σ Error	
D-AMS 022224	HH-69	8.81-8.80	Peat	Bulk carbon	5236	46	6179-5914
D-AMS 022225	HH-115	8.35-8.34	Organic clay	Bulk carbon	6497	36	7475-7322
D-AMS 025779	HH-146	8.04-8.03	Silty sand	Bulk carbon	5059	26	5900-5741

An age-depth model for core HH4 was developed using Bacon v2.3.4 (Blaauw & Christen, 2011). The red dotted line shows modelled median ages along core HH4 and the grey stippled lines indicate the 95% confidence intervals of the modelled age-depth relationship. The transparent blue violin plots show the two calibrated AMS ^{14}C dates from Herd Hill (samples HH-69 and HH-115). Sample HH-146 was not included in the model due to the errorneous date obtained producing a date younger than both samples HH-69 and HH-115. The upper left graph shows the iteration history of the model. The middle and right graphs show prior (green lines) and posterior (grey histograms) density functions for accumulation rate and memory of the model (Figure 8.5).

The mean 95% confidence of the age-depth model spans 594 years, a minimum of 330 years at 69 cm and a maximum of 707 years at 94 cm. Based on the age-depth model for core HH4, 100% of the dates from Herd Hill lie within the age-depth model's 95% range. The main stratigraphic boundary of core HH4 was included in the age-depth model (shown in the horizontal dotted line across the model in Figure 8.5 at a depth of 89 cm).

The main stratigraphic boundary of core HH4 at 89 cm (8.61 m OD) was included in the age-depth model (shown in the horizontal dotted lines across the model in Figure 8.5). The sedimentation rate was calculated based on the dated samples and the main stratigraphic boundary, with the mean age obtained from the model’s prediction and shown on the right side of Figure 8.5.

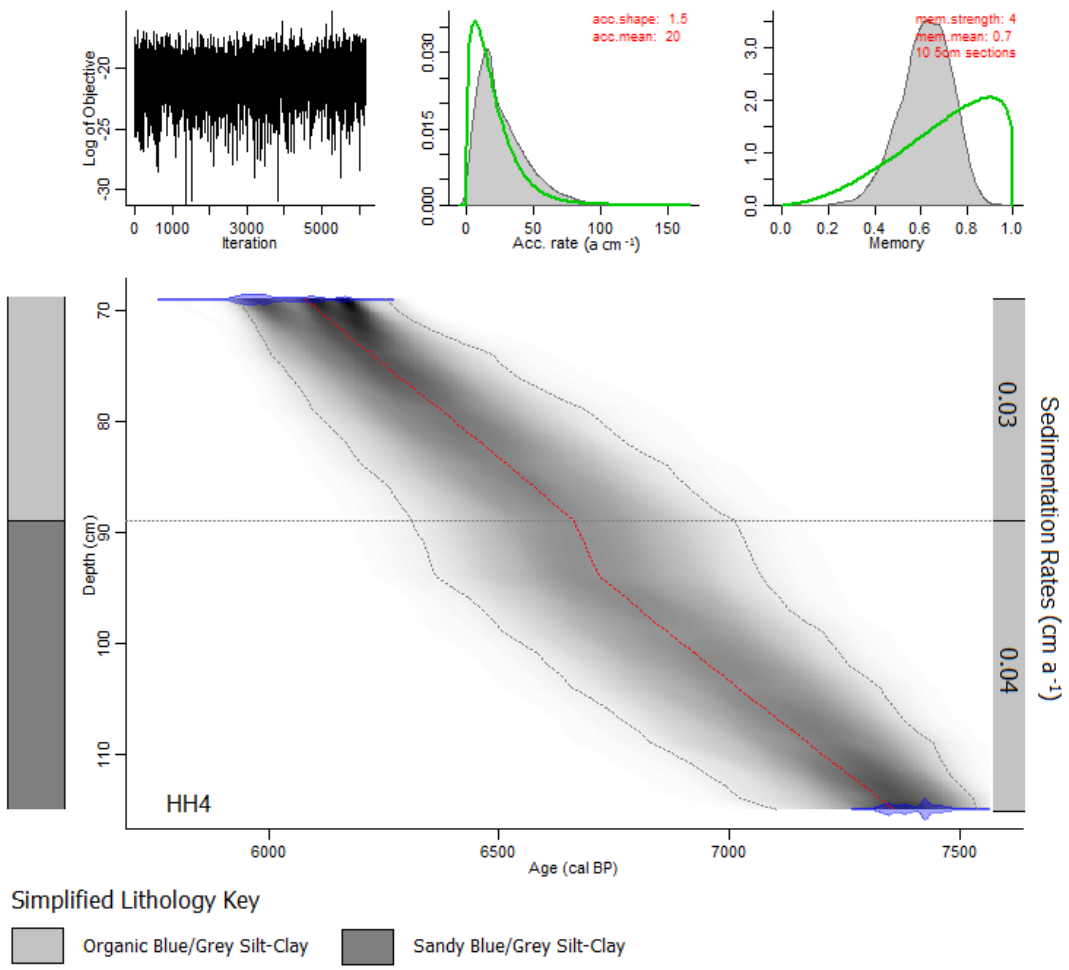

Figure 8.5: Age-depth model for the HH4 core profile based on Bacon v2.3.4 modelling routines (Blaauw & Christen, 2011) and calculated sedimentation rates from the AMS ^{14}C dates calibrated with IntCal13 (Reimer *et al.*, 2013). Dotted line on the model indicates the main stratigraphic unit in the HH4 core

8.6 Foraminiferal Analysis

The preservation of foraminiferal tests in the samples from core HH4 varied, with some samples containing very few foraminiferal tests. It was therefore not possible to obtain a minimum count of 40 individuals in some of the samples despite increasing the sample volume. Samples were taken at 1 or 2 cm intervals throughout core HH4.

The samples analysed revealed five agglutinated saltmarsh species comprised of *Jadammina macrescens*, *Miliamminia fusca*, *Tiphotrocha comprimata*, *Haplophragmoides wilberti* and *Trochammina inflata*. The agglutinated foraminiferal species were observed throughout the blue/grey silt-clay from the depths of 1.14 m

(8.36 m OD) to 0.70 m (8.80 m OD). No calcareous species were observed in the core, although presence of test linings were noted (Figure 8.6).

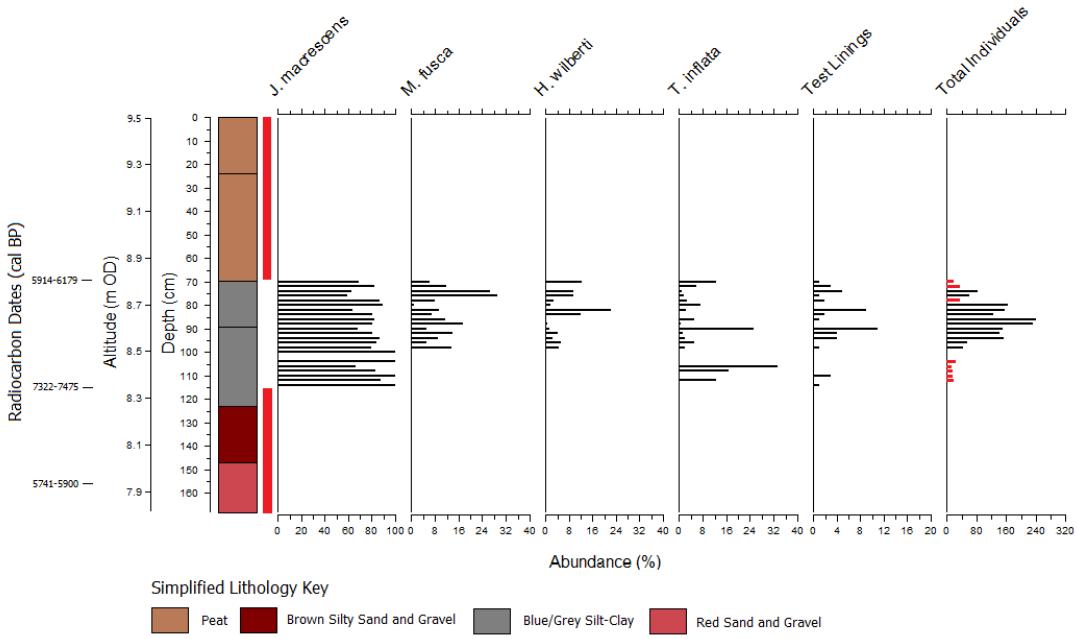

Figure 8.6: Foraminiferal diagram from Herd Hill core HH4. Foraminiferal frequencies are expressed as a percentage of total foraminifera. All samples including samples with low individual counts (below 40 individuals) were included in this diagram. Red blocks next to the stratigraphy diagram indicates the zone where foraminifera was absent in the core

8.7 Pollen Analysis and Zonation

300 pollen and spore grains were counted for each sample from core HH4. Samples were taken at 4 cm intervals throughout the core (Figure 8.7).

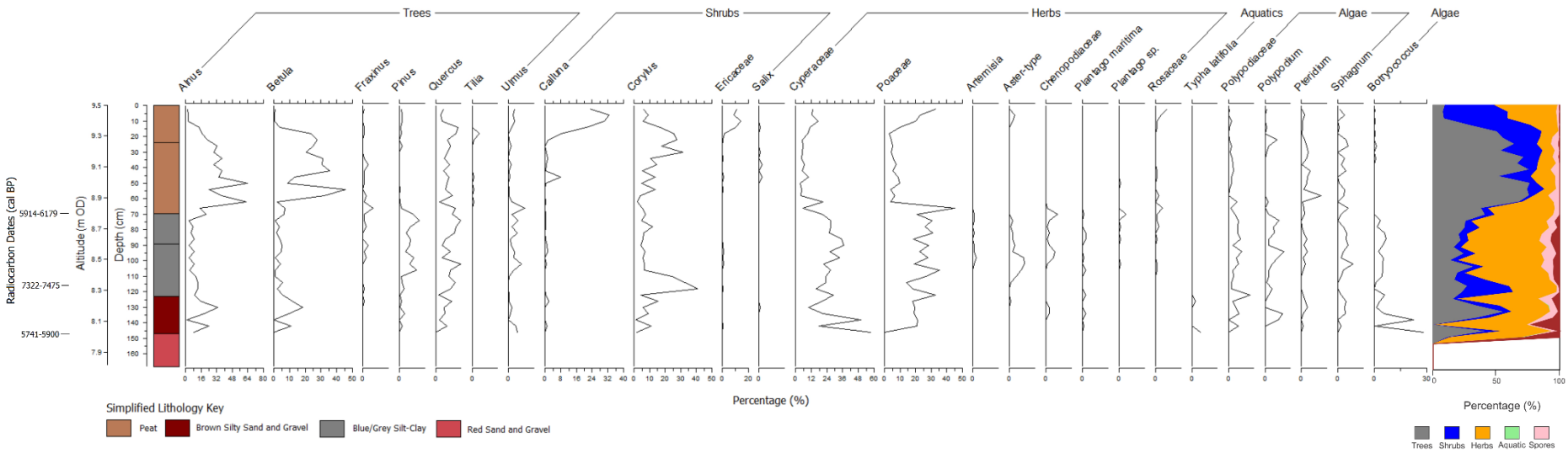

Figure 8.7: Pollen diagram from Herd Hill core HH4. Pollen frequencies are expressed as a percentage of total land pollen

Four local pollen assemblage zones were identified (Figure 8.8). From the base of the core at 1.68 m (7.82 m OD) to 1.47 m (8.03 m OD) in the red sand and gravel unit, no pollen was found. The pollen zonation for Herd Hill is summarised and tabulated in Table 8.3 below.

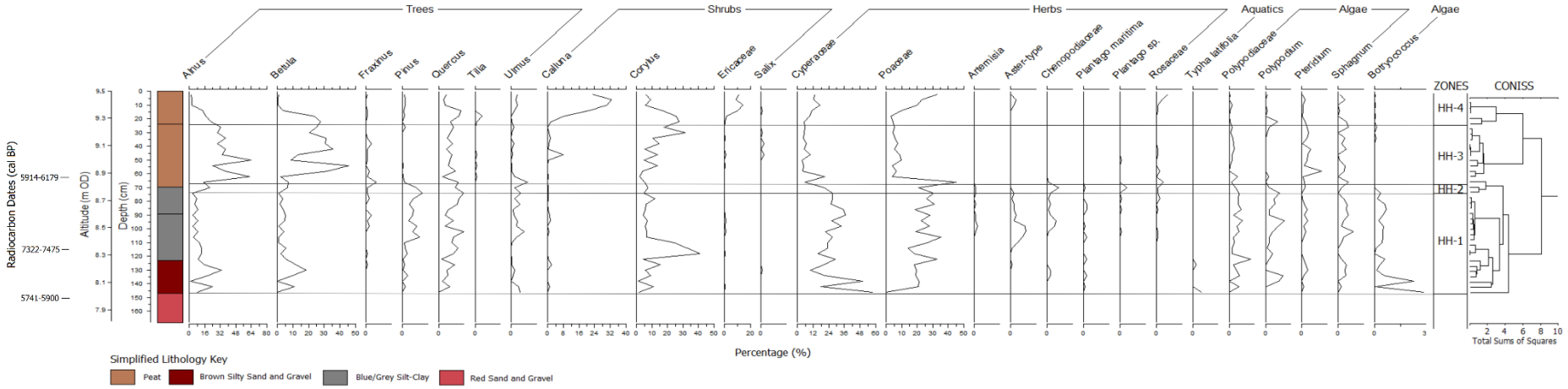

Figure 8.8: Pollen zonation for Herd Hill based on stratigraphically constrained cluster analysis

Table 8.3: Pollen zonation for Herd Hill based on stratigraphically constrained cluster analysis

Pollen Zone	Depth (cm)	Altitude (m OD)	Pollen Characteristics
HH-1	72-146	8.78-8.04	A general low presence of arboreal pollen was observed, apart from *Alnus* and *Betula* which occurred at higher frequencies in comparison to *Pinus*, *Quercus* and *Ulmus*. A minimum of 1% of *Alnus* was observed at 1.38 m (8.12 m OD), while a maximum 34% of *Alnus* occurrence was observed at 1.30 m (8.20 m OD). Occurrence of *Betula* ranged from 1% at a depth of 0.74 m (8.76 m OD) and 18% at 1.30 m (8.20 m OD). Maximum occurrence of both *Pinus* at 8% and *Quercus* at 10% were noted at a depth of 0.74 m (8.76 m OD). Occurrence of *Ulmus* remained below 5% throughout the zone. Occurrence of *Corylus* ranged between 1% at 1.38 m (8.12 m OD) and 41% at 1.18 m (8.32 m OD). Three peaks of *Corylus* were observed at the depths of 1.10 m (8.40 m OD), 1.14 m (8.36 m OD) and 1.18 m (8.32 m OD). The zone is dominated mainly by Cyperaceae and Poaceae. Maximum abundance of Cyperaceae reaching 57% was noted at a depth of 1.46 m (8.04 m OD), while minimum occurrence of Cyperaceae with 16% was noted at 1.18 m (8.32 m OD). Abundance of Poaceae ranged between 14% at 1.14 m (8.36 m OD) and 35% at 1.06 m (8.44 m OD). The presence of spores was also observed, with Polypodiaceae, *Polypodium, Pteridium* and *Sphagnum* notable. The presence of *Botryococcus* algal spores

			was noted, with the highest abundance occurring at the base of the pollen zone at 1.46 m (8.04 m OD).
HH-2	66-72	8.84-8.78	At a depth of 0.70 m (8.80 m OD), dominance of Poaceae and Cyperaceae were almost equal with 21% and 20% respectively. At a depth of 0.70 m (8.80 m OD), a shift to a dominance of Poaceae with abundance of 45% was observed, with only 6% of Cyperaceae noted. 21% and 15% of *Alnus* abundance were noted at 0.70 m (8.80 m OD) and 0.66 m (8.84 m OD) respectively.
HH-3	22-66	9.28-8.84	A notable increase in arboreal pollen, in particular *Alnus* and *Betula* was noted. Presence of *Alnus* pollen ranged between 24% at 0.54 m (8.96 m OD) and 64% at 0.50 m (9.00 m OD). A maximum 46% occurrence of *Betula* was observed at a depth of 0.54 m (8.96 m OD), while the minimum *Betula* occurrence was noted at 0.62 m (8.88 m OD) at 2%. General increase in *Corylus* abundance was observed, with a maximum of 31% at 0.30 m (9.20 m OD) and a minimum of 2% at 0.62 m (8.88 m OD). A clear decrease in abundance of Cyperaceae and Poaceae was noted. A minimum of 4% at 0.50 m (9.00 m OD) and a maximum of 21% at 0.62 m (8.88 m OD) were observed for Cyperaceae. Abundance of Poaceae ranged between 4% at 0.54 m (8.96 m OD) and 10% at 0.50 m (9.00 m OD). The presence of spores was also observed in the zone, with Polypodiaceae, *Pteridium* and *Sphagnum* notable.
HH-4	0-22	9.50-9.28	A notable decrease in arboreal pollen was recorded. Highest occurrence of *Alnus* and *Betula* at a depth of 0.18 m (9.32 m OD), with 17% and 24% respectively.

	At a depth of 0.10 m (9.40 m OD) towards the top of the core, arboreal pollen occurred below 5%. Notable increase in *Calluna* and Ericaceae pollen were observed. A maximum of 33% abundance of *Calluna* pollen was noted at 0.06 m (9.44 m OD), while a maximum of 14% Ericaceae was observed at 0.10 m (9.40 m OD). Abundance of *Corylus* recorded a maximum of 28% at a depth of 0.22 m (9.28 m OD) and a minimum of 6% at 0.10 m (9.40 m OD) and 0.02 (9.48 m OD). For Cyperaceae and Poaceae, a maximum of 17% and 33% were observed at 0.10 m (9.40 m OD) and 0.02 m (9.48 m OD) respectively.

8.8 Holocene Relative Sea-Level and Environmental Changes at Herd Hill

The interpretation of Holocene relative sea-level and environmental changes for Herd Hill are based on microfossil analyses, changes in lithostratigraphy and sediment composition of core HH4.

8.9 Microfossil Interpretation: Foraminifera

No foraminifera was observed in the basal red sand and gravel unit, the brown silty sand and gravel unit, and the deepest 0.08 m of the blue/grey silt-clay unit, which constituting the deepest 0.53 m of core HH4 (8.35 m OD to 7.82 m OD). The absence of foraminifera in the brown silty sand and gravel unit and the deepest 0.08 m of the blue/grey silt-clay unit may be attributed to the increased sand content in the core (Figure 8.9). The effect of increased sand content on absence of foraminifera is also discussed in Chapter 6 (Section 6.9).

The foraminiferal assemblage at Herd Hill is dominated mainly by the agglutinated species *J. macrescens*, which are often associated with a high saltmarsh environment.

However, the presence of *J. macrescens* was observed in a lower saltmarsh and intertidal mudflat environment at the contemporary Cardurnock Marsh (Chapter 4; Section 4.3.2). A notable presence of *M. fusca* was observed in the blue/grey silt-clay unit, which is associated with a low saltmarsh/intertidal mudflat environment (Lloyd *et al.*, 1999) and as observed in the contemporary foraminiferal samples in this study (Chapter 4; Section 4.3.2). Taken as a whole, the foraminiferal assemblage combined with the deposition of the blue/grey silt-clay unit suggests an intertidal mudflat environment close to the fringing saltmarsh. Test linings were also present in the zone where the agglutinated foraminifera were observed, further supporting the evidence for a lower saltmarsh/intertidal mudflat environment.

No foraminifera were observed from 0.68 m (8.82 m OD) towards the top of the core, corresponding to the transition from the blue/grey silt-clay unit to the peat unit. This would suggest that a freshwater environment had developed at the site from the former intertidal mudflat environment.

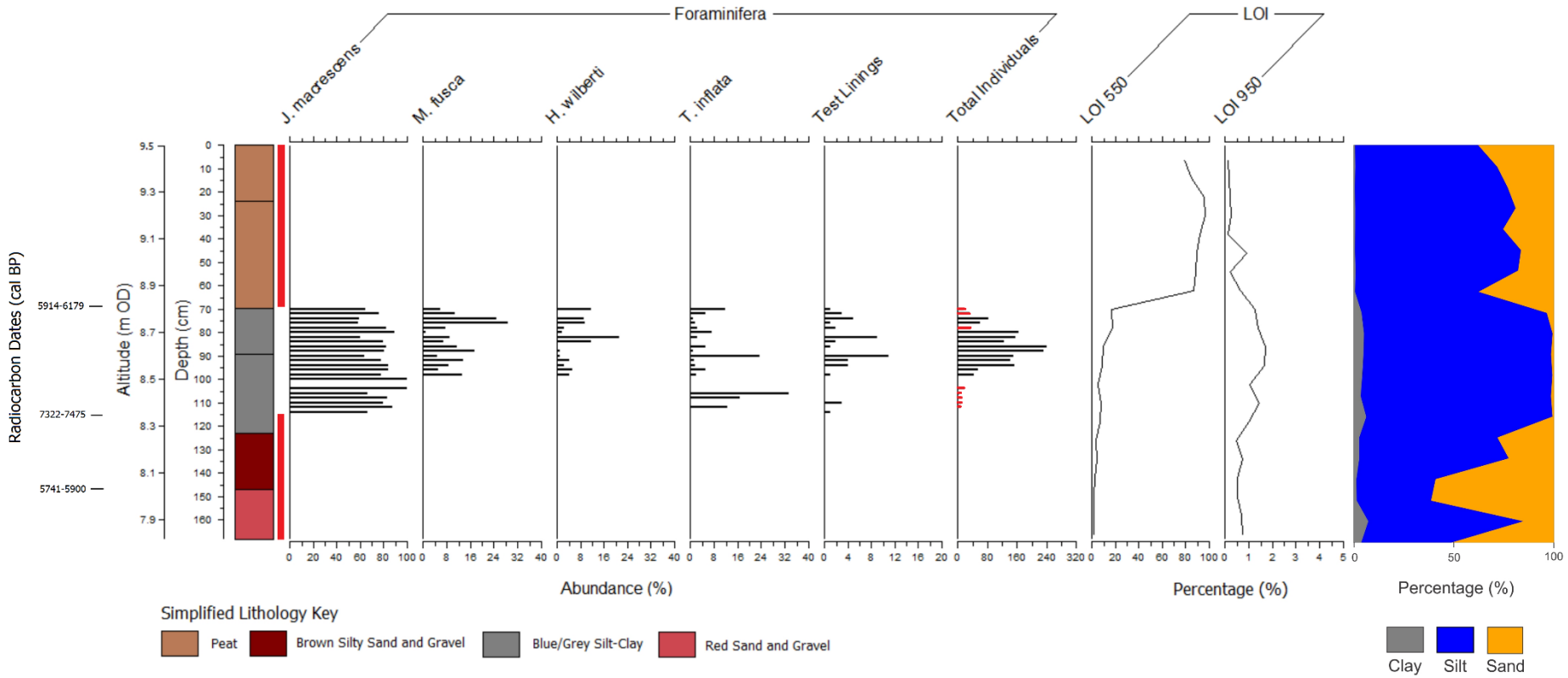

Figure 8.9: Summary diagram showing foraminifera, particle size analyses and loss on ignition undertaken on samples from core HH4

8.10 Microfossil Interpretation: Pollen

Several possible pollen source areas are identified at Herd Hill. Pollen grains that are buoyant (e.g *Pinus* pollen) may have been deposited when the site was flooded, and this is common in wave affected sediments (Walker, 1966; Tipping, 1995). Pollen grains could also be wind pollinated and transported into the site from nearby pollen catchment areas. The interpretation for each pollen zone is described below.

Zone HH-1 (Figure 8 and Table 2)

Two slight peaks of *Alnus* were observed at the depths of 1.42 m (8.08 m OD) and 1.30 m (8.20 m OD), while a single peak of *Betula* was observed at a depth of 1.30 m (8.20 m OD). Apart from these slight increased frequencies of *Alnus* and *Betula*, low frequencies of arboreal pollen were observed in zone HH-1 suggesting a low presence of alder, birch, pine, oak and elm trees were present in the pollen catchment area. The development of a mixed woodland at Herd Hill may have been restricted due to inadequate soil cover, as the low frequencies of arboreal pollen in zone HH-1 correspond to the deposition of the silty brown sand and gravel unit in the core (Figure 8.10).

Alder was first observed at Herd Hill at a depth of 1.46 m (8.04 m OD), although at very low frequencies. The first occurrence of alder in core HH4 was dated at 5900-5741 cal BP. The occurrence of *Alnus* pollen at Cowgate Farm in zone CGF-1 was dated at 8450-8334 cal BP, which was obtained from sample CGF-136/141 (Chapter 6; Section 6.10). The date obtained from Cowgate Farm broadly agrees with the development of an alder carr at the base of the sediment sequence at Boustead Hill dated at 8304-7928 cal BP, and the occurrence of alder at Drumburgh Moss which was dated at 8947-8403 cal BP (Lloyd *et al.*, 1999). Therefore, it is probable that the date for the first occurrence of alder at Herd Hill would correspond with those recorded at Cowgate Farm, Boustead Hill and Drumburgh Moss. A second date of 7475-7322 cal BP was obtained for zone HH-1 from a depth of 1.15 m (8.35 m OD).

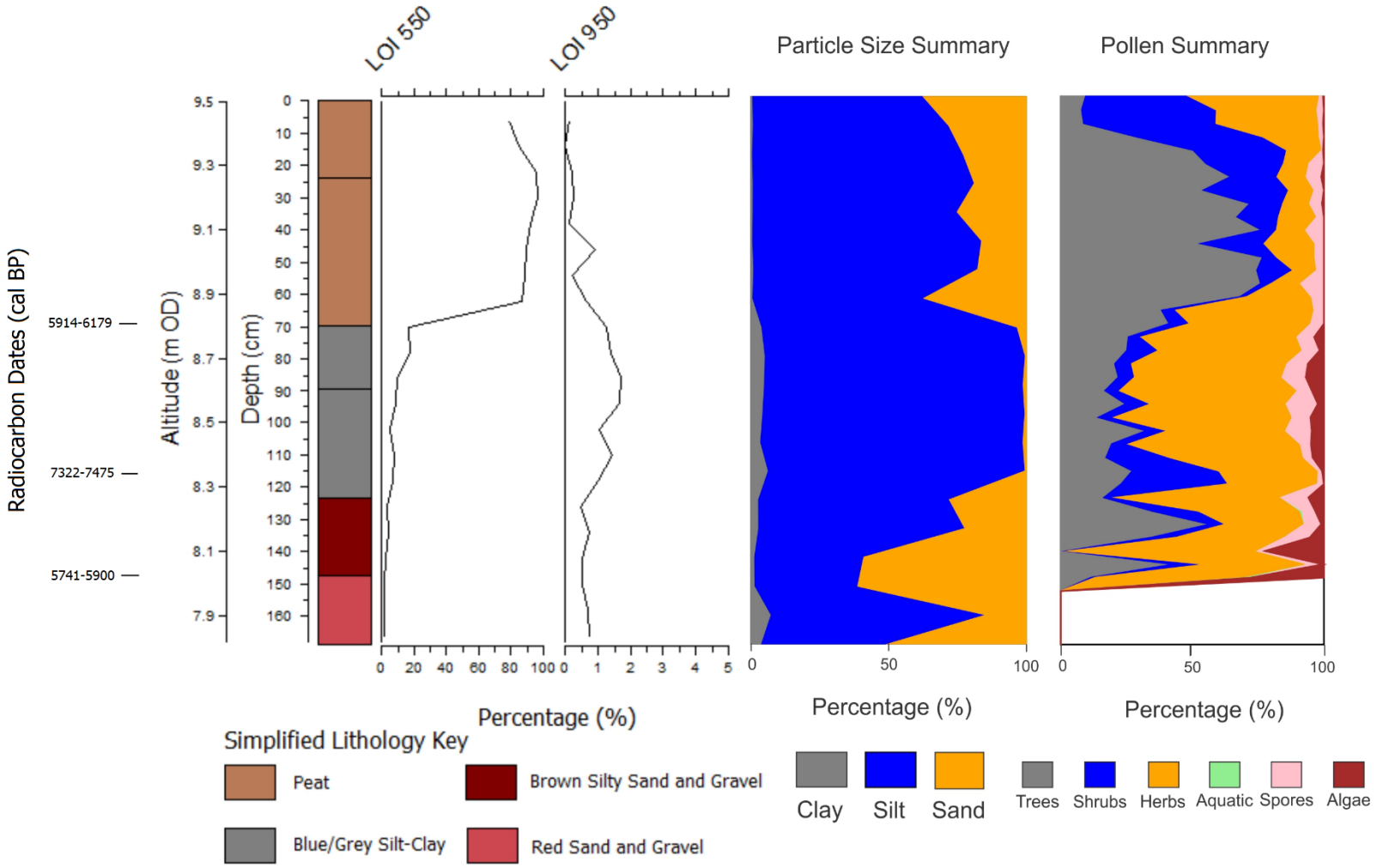

Figure 8.10: Summary diagram showing pollen, particle size analyses and loss on ignition undertaken on samples from core HH4

Zone HH-1 is characterised by high frequencies of Poaceae and Cyperaceae, suggesting that the site supported an open environment dominated mainly by grass and sedges. It is probable that trees were growing in the pollen catchment area close to the site whilst the grass and sedges were growing locally at the site. A notable presence of *Corylus* was observed throughout zone HH-1, indicating that heather was also present. *Aster*-type and Chenopodiaceae pollen were also observed in zone HH-1, and these are associated with a saltmarsh environment (Zong & Tooley, 1996; Lloyd *et al*., 1999) that might have developed close to the site.

Polypodiaceae, *Polypodium*, *Pteridium* and *Sphagnum* spores were also present in zone HH-1. The presence of ferns and peat moss are common in acidic wetlands including bogs, fens and swamps, which may have developed at the site or in nearby areas as relative sea level increased resulting in the increase of the groundwater table at the site, or as marine influence expanded into the site.

Zone HH-2 (Figure 9 and Table 2)

Generally low frequencies of arboreal pollen were observed with alder, birch, ash, pine, oak and elm noted. The frequencies of *Alnus* pollen were the highest amongst the arboreal pollen present, which may be attributed to the ability of alder fruits to float and remain viable for a period of approximately a year, with water currents often attributed as the main dispersal mechanism for *Alnus* pollen (Walker 1966; Birks, 1989).

Zone HH-2 is dominated mainly by Cyperaceae and Poaceae. At a depth of 0.70 m (8.80 m OD), the occurrence of Cyperaceae and Poaceae is almost equal, but a clear shift to the dominance by Poaceae was observed at a depth of 0.66 m (8.84 m OD). The change in ratios between sedges and grasses may indicate a change of environment from reed swamp to freshwater limnic sediment and turfa (Zong and Tooley, 1999), and a possible evidence of changing groundwater table in the area (Zong and Tooley, 1999). This shift to the dominance of Poaceae corresponds with the transition from the blue/grey silt-clay unit to the overlying peat unit, a more freshwater environment and was dated at 6179-5914 cal BP (sample HH-69). Low frequencies of *Corylus* and spores pollen were also observed in this zone indicating that heather and ferns were present at the site.

Zone HH-3 (Figure 9 and Table 2)

Increased percentages of arboreal pollen throughout this zone, characterised mainly by *Alnus* and *Betula*, with lower frequencies of *Quercus* pollen were observed. This suggests further development of the mixed woodland in the area (Walker 1966; Tipping, 1995; Dumayne-Peaty and Barber, 1998), as relative sea level decreased and soil cover in the pollen catchment area developed evidenced by the transition to the peat unit in the core. The date for the start of this zone is approximately 6179-5914 cal BP, which was obtained from sample HH-69 at a depth of 0.69 m (8.81 m OD). Two distinct peaks of alder were noted at the depths of 0.62 m (8.88 m OD) and 0.50 (9.00 m OD). Elm and pine were almost non-existent in zone HH-3 broadly agreeing with the dates of elm decline recorded at 5130 cal BP in Ennerdale Water, 5100 cal BP in Blea Tarn and 5540-4860 cal BP in Blelham Tarn in the Lake District, Cumbria (Pennington, 1964).

The percentages of Cyperaceae and Poaceae pollen decreased significantly in zone HH-3, with frequencies of both sedges and grasses below 20% throughout the zone. The notable occurrence of *Corylus* was still observed in zone HH-3, which may correspond to the increase in development of mixed woodland, as hazel is often associated as a component of the understorey of lowland oak, ash or birch woodland. Low frequencies of fern pollen (*Pteridium* and Polypodiaceae) and *Sphagnum* were also observed, indicating that ferns and moss were growing at the site.

Zone HH-4 (Figure 9 and Table 2)

An overall decrease in arboreal pollen was observed, with frequencies of arboreal pollen composed mainly of alder, birch and oak below 30% throughout the zone. The presence of elm was also noted, although in low frequencies. Although the start of zone HH-4 was not dated, the overall decrease in arboreal pollen might be attributed to increased anthropogenic activities of the area throughout the Bronze Age which started at approximately 4300 BP.

A notable increase in *Calluna* and Ericaceae pollen, alongside the presence of *Corylus* was also observed in zone HH-4. Hazel may have formed the understorey component of the mixed woodland as recorded by the arboreal pollen species present. Heather

is known to grow on heaths, moors and grasslands with poor nutrients, and also in open woodland on acidic soils, ranging from dry exposed habitats to wet peat bogs. The significant decrease in values for fern spores (in particular *Pteridium*) and the increase of *Calluna* pollen might suggest a transition from a fen environment to a peat bog at this time (Walker, 1966). The increase of *Calluna* and Ericaceae may correspond to a shift to a more freshwater peat environment at both sites.

A similar vegetation change was observed at Crag Lough, Northumberland, where a clearance of *Quercus* and *Corylus* woodland began at approximately at 4550 BP. A significant decline of *Alnus* and the spread of *Calluna vulgaris* was then observed at approximately 2350 BP (Coombes *et al*., 2009). The start of zone HH-4 might therefore correspond to a similar time period, although this would suggest that only 70 cm of peat accumulated over the period of approximately 3700 years (6018 cal BP to 2350 BP).

8.11 Sediment Deposition and Relative Sea-Level Interpretation

The red sand and gravel unit is most likely composed of degraded bedrock, as the site is underlain by New Red Sandstone of Permo-Triassic age (Lloyd *et al*., 1999; McMillan *et al*., 2011). The brown silty sand and gravel unit is barren of any foraminifera. If the brown silty sand and gravel unit is of marine origin which inundated the site during increased relative sea level, the high sand content in the unit might have prevented the preservation of foraminifera. However, the origin of the brown silty sand and gravel unit is deemed unknown at present.

The silty brown sand and gravel unit was overlain by a unit of blue/grey silt-clay where the presence of foraminifera was observed, indicating a marine origin. The deposition of the blue/grey silt-clay unit which recorded the transgressive contact in core HH4 was dated at 7475-7332 cal BP, and is most probably related to the Main Postglacial Transgression at the site. The increase of relative sea level would have resulted in an expansion of the intertidal mudflat environment at the site.

The blue/grey silt-clay unit transitioned to the overlying peat unit, indicating that the previous intertidal mudflat environment may have developed into a more freshwater environment as relative sea level decreased from the site, resulting in the absence of

foraminifera. This was evidenced by the absence of foraminifera at a depth of 0.69 m (8.81 m OD) towards the top of the core combined with the change in lithostratigraphy. The regressive contact indicating negative sea-level tendency at Herd Hill was dated at 6179-5914 cal BP. No further changes in biostratigraphy (foraminifera) were observed from 0.69 (8.81 m OD) towards the top of the core. The change in lithostratigraphy to the surface peat occurred at 0.23 m (9.27 m OD).

8.12 Relative Sea-Level Reconstruction for Herd Hill

Relative sea-level reconstruction for the site at Herd Hill was developed through a combination of lithostratigraphic and biostratigraphic analyses, determination of indicative meanings and calculation of sea-level index points. Foraminifera-based transfer functions were also developed.

8.13 Determination of Indicative Meaning

The assigned reference water level based on the changes in lithostratigraphy and biostratigraphy (foraminiferal assemblages) was used for the calculation of sea-level index points as the predicted palaeo marsh surface elevation (PMSE) based on the transfer function utilised on core HH4 was deemed unreliable.

The lithostratigraphy of sample HH-115 consisting of blue/grey silt-clay unit is consistent with a lower saltmarsh or an intertidal mudflat environment, with the dominance of *J. macrescens* and presence of test linings observed. This is consistent with the contemporary samples from Cardurnock Marsh (Chapter 4; Section 4.3.2).

For sample HH-69, an indicative meaning associated with a high saltmarsh environment was assigned, consistent with the lithostratigraphy of the peat unit, the dominance of *J. macrescens* and increased abundance of *H. wilberti* which suggest an environment occurring at the level of extreme high water, as observed in the contemporary samples collected from Bowness Marsh (Chapter 4; Section 4.3.3).

As the indicative meaning for samples HH-115 and HH-69 have been ascribed based on samples from two different contemporary marshes (Cardunock Marsh and Bowness Marsh), the complete Solway training set with elevation values converted to

standardised water level index (SWLI) (Figure 4.22) was used to determine the indicative range of the samples, as this eliminates the tidal variations between the two contemporary sites. The SWLI values for the respective contemporary sample most representative of the samples HH-115 and HH-69 were then converted back to elevation (m OD), to allow the calculation of the reference water level and indicative range.

The contemporary sample most representative of sample HH-115 lies between the SWLI of 285 and 295 in the Solway training set, which falls below MHWST (Figure 4.22). The presence of saltmarsh pollen species (e.g. *Aster*-type) in the blue/grey silt-clay unit from which sample HH-115 was dated, further supports the ascribed indicative meaning for the sample. This covers an altitude of 4.69 m OD (contemporary sample CM05) and 5.23 m OD (contemporary sample CM01). Based on these values, the reference water level for sample HH-115 is the midpoint between 4.69 m OD and 5.23 m OD, resulting in an indicative range of ±0.5 m.

The contemporary samples most representative of sample HH-69 lie above MHWST with the SWLI ranging between 300 (contemporary sample BM20) and 310 (contemporary sample BM15) based on the Solway training set. This covers an altitude of 5.34 m OD and 5.83 m OD, with the reference water level for both samples to be the midpoint of these altitude resulting in a value of 5.6 m OD, and an indicative range of ±0.5 m.

Sample HH-146 was not assigned to any indicative meaning due to the lack of microfossil evidence indicating a marine environment and the likelihood of an error for the date. A sea-level index point is therefore not calculated for sample HH-146.

8.14 Post -Depositional Lowering of Sediments

The post-depositional lowering (PDL) of sediments in core HH4 was estimated based on the geotechnical model developed by Brain *et al*. (2011, 2012), as discussed in Chapter 3 (Section 3.9.1). Minimal PDL of sediments is observed in the core from Herd Hill, which ranged between 0.001 to 0.013 m. Figure 8.11 shows the PDL of sediments at a 0.02 m interval throughout core HH4.

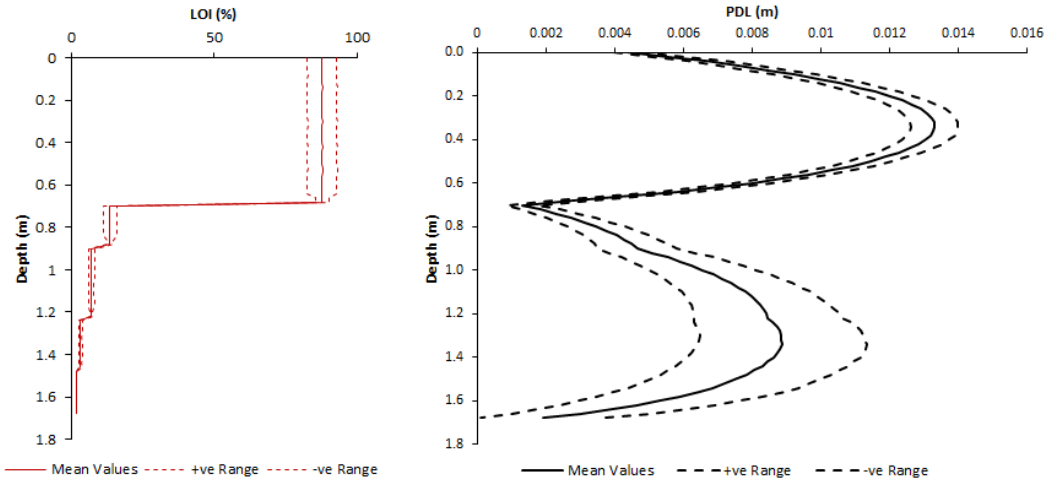

Figure 8.11: Geotechnical and physical properties showing the averaged downcore organic content, expressed as % loss on ignition and the model estimates of post-depositional lowering for core HH4. Abbreviations: LOI = Loss on ignition; PDL = Post-depositional lowering

8.15 Sea-Level Index Points

The sample's age, reference water level and indicative range along with the associated errors for each sample are required for the calculation of sea-level index points (Chapter 3; Section 3.9). Two sea-level index points were produced for Herd Hill (Table 8.4).

Table 8.4: Sea-level index points produced from HH4

Lab Code	Latitude	Longitude	Radiocarbon Age		Cal BP (2σ Ranges)			Altitude (m OD)	Compaction Correction (m)	RSL (m)	Tendency
			BP	1σ Error	Min	Mean	Max				
D-AMS 022224	54.928	-3.285	5236	46	5914	6018	6179	8.81	+0.001	+3.26±0.56	Negative
D-AMS 022225	54.928	-3.285	6497	36	7322	7401	7475	8.35	+0.008	+3.41±0.56	Positive

Samples HH-69 and HH-115 produced sea-level index points of 3.26±0.56 m and 3.41±0.56 m respectively. Errors and corrections associated with each sea-level index point were calculated based on the methods described in Chapter 3 (Section 3.9). Figure 8.12 shows the sea-level index points from Herd Hill plotted against the modelled relative sea-level curve for southern Solway Firth at the location of NY 2481 5666 based on the BRADLEY2011, KUCHAR2012 and BRADLEY2017 models (Shennan *et al*., 2012; 2018; Kuchar *et al*., 2012).

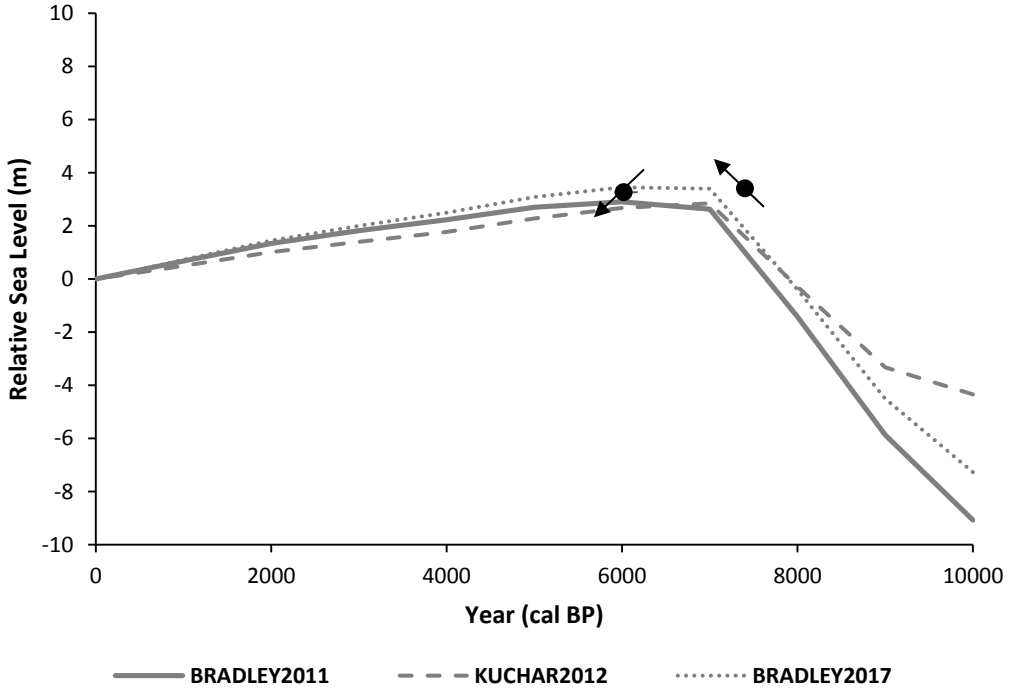

Figure 8.12: Graph showing two sea-level index points from Herd Hill. The black line is the modelled relative sea-level curves for southern Solway Firth based on Shennan *et al*. (2012; 2018) and Kuchar *et al*. (2012). All sea-level index points include associated individual vertical and age error bars

8.16 Summary

The site at Herd Hill has provided a record of Holocene sea-level changes evidenced by the changes in lithostratigraphy and biostratigraphy of core HH4. The two sea-level index points from Herd Hill broadly agree with the recorded dates of marine transgression and marine regression from other sites located at the southern shore of the Solway Firth, although the altitudes of sample HH-69 and HH-115 are higher than the existing sea-level index points. The transgressive contact at Herd Hill which

is likely a result of the Main Postglacial Transgression was dated at 7401 cal BP, while the regressive contact indicating negative sea-level tendency at Herd Hill was dated at 6018 cal BP.

CHAPTER 9

PASTURE HOUSE

9.0 Introduction

The study site at Pasture House (NY 1861 6030) is located east of the site at Herd Hill (Figure 9.1). The site is bordered by a road in the north, farmland to the east and west of the site and Bowness Common to the south (Figure 9.2a). The study area is approximately 120 m by 100 m. The geomorphology suggests that the site is composed of relict sand dunes, with small ridges present at Pasture House.

Figure 9.1: Location of the study site at Herd Hill and Pasture House marked in red

9.1 Borehole Location and Stratigraphy

Three transects of boreholes were cored at Pasture House to establish the stratigraphy of the site. Two transects were cored from north to south and the third transect was cored from east to west. The altitude of boreholes at Pasture House

ranged from 7.8 m OD to 9.7 m OD, with borehole PH4 reaching the maximum depth of 5.04 m (4.26 m OD).

Borehole PH1 was cored at the top of a ridge, terminating in a very sandy light brown peat unit at a depth of 0.77 m (8.83 m OD). The very sandy brown peat unit was overlain by a similar very sandy peat unit that was lighter in colour at 0.27 m (9.33 m OD).

Borehole PH2 terminated in a brown sand unit at 1.46 m (7.44 m OD). The brown sand unit occurred between the depths of 1.46 m (7.44 m OD) and 0.49 m (8.41 m OD). A unit of black peat occurred at 0.52-0.53 m (8.38-8.37 m OD), and a brown peat with charcoal unit was noted at 0.50-0.51 m (8.40-8.39 m OD). A unit of dark brown peat overlaid the brown sand unit at 0.49 m (8.41 m OD). Another unit of brown sand with organics occurred at 0.44 m (8.46 m OD). This transitioned into an organic brown silt-clay at 0.42 m (8.48 m OD) and the surface sandy peat unit at 0.34 m (8.56 m OD).

Borehole PH3 reached a maximum depth of 1.85 m (7.85 m OD) in a dense blue/grey silt-clay unit. This was overlain by a unit of sandy grey/brown silt-clay at 1.66 m (8.04 m OD) and brown organic silt-clay at 1.03 m (8.67 m OD). A unit comprised of organic brown sand occurred at 0.85 m (8.85 m OD), and was overlain by a black peat with occasional charcoal unit at 0.69 m (9.01 m OD). The surface unit at borehole PH3 comprised of a peat with occasional wood which occurred at 0.65 m (9.05 m OD), with increased sand content towards the bottom of the unit.

Borehole PH4 terminated in a stiff, brown silt-clay unit at 5.04 m (4.26 m OD). This was overlain by a sandy brown silt-clay at 4.05 m (5.25 m OD), and sandy blue/grey silt-clay at 3.05 m (6.25 m OD). A similar unit of blue/grey silt-clay with occasional wood overlaid the previous unit at 1.96 m (7.34 m OD). The blue/grey silt-clay unit was overlain by a dark brown peat unit at 1.09 m (8.21 m OD), and this in turn was overlain by an organic brown silt-clay at 0.94 m (8.36 m OD). The organic brown silt-clay unit transitioned into the sandy surface peat unit at 0.85 m (8.45 m OD).

Borehole PH5 reached an impenetrable depth at 3.57 m (5.03 m OD) in a stiff and sandy pink silt-clay unit. This was overlain by a sandy grey/brown silt-clay unit at

3.12 m (5.48 m OD) and a grey silt-clay unit at 3.00 m (5.60 m OD). The grey silt-clay unit was overlain by a sandy grey silt-clay unit at 1.87 m (6.73 m OD) and a brown sand unit at 0.55 m (8.05 m OD). A unit of dark brown peat occurred above this at 0.51 m (8.09 m OD), and a silty brown peat with sand occurred at 0.35 m (8.25 m OD). Borehole PH5 transitioned into the surface peat unit at 0.26 m (8.34 m OD).

Borehole PH6 terminated in a pink/brown silty sand unit at 2.80 m (5.60 m OD). This was overlain by a unit of grey silty sand at 1.30 m (7.10 m OD) and a unit of silty brown organic sand occurred above this at 0.90 m (7.50 m OD). The silty brown organic sand unit transitioned into a brown sand unit at 0.53 m (7.87 m OD) and the sandy surface peat unit at 0.31 m (8.09 m OD).

Borehole PH7 reached an impenetrable depth of 0.77 m (7.03 m OD) in an organic brown sand unit which transitioned into the surface peat unit at 0.29 m (7.51 m OD).

A sample core (PH4-a) was taken at Pasture House from borehole PH4, and was used for the particle size, loss on ignition and microfossil analyses of the site. A replicate core (PH4-b) was then taken approximately 1 metre away from borehole PH4. Both PH4-a and PH4-b cores terminated in the blue/grey silt-clay unit as the sediment was too stiff to core with the Russian corer.

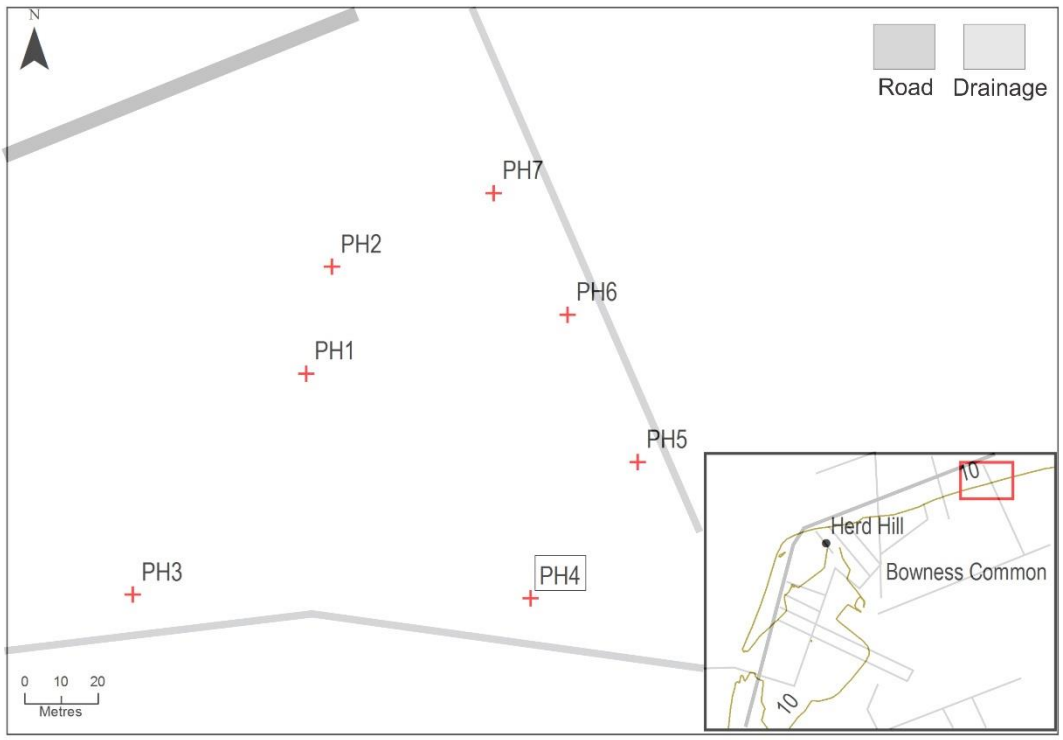
N
Road
Drainage
PH7
PH2
PH6
PH1
PH5
PH3
PH4
0 10 20
Metres
Herd Hill
Bowness Common
10
10

(a)

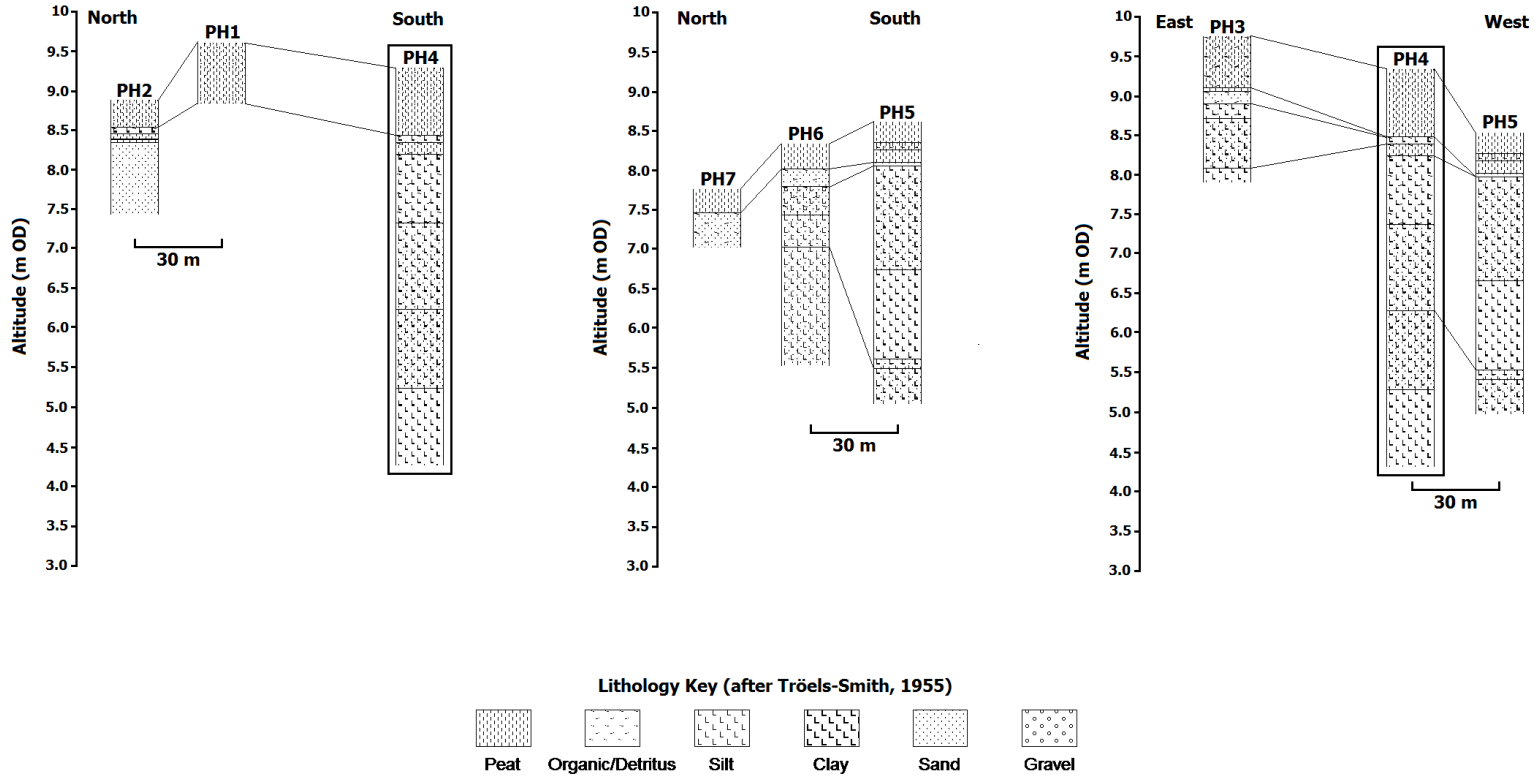
North
South
PH1
PH2
PH4
30 m
Altitude (m OD)
North
South
PH5
PH6
PH7
30 m
East
West
PH3
PH4
PH5
30 m
Lithology Key (after Tröels-Smith, 1955)
Peat
Organic/Detritus
Silt
Clay
Sand
Gravel

(b)

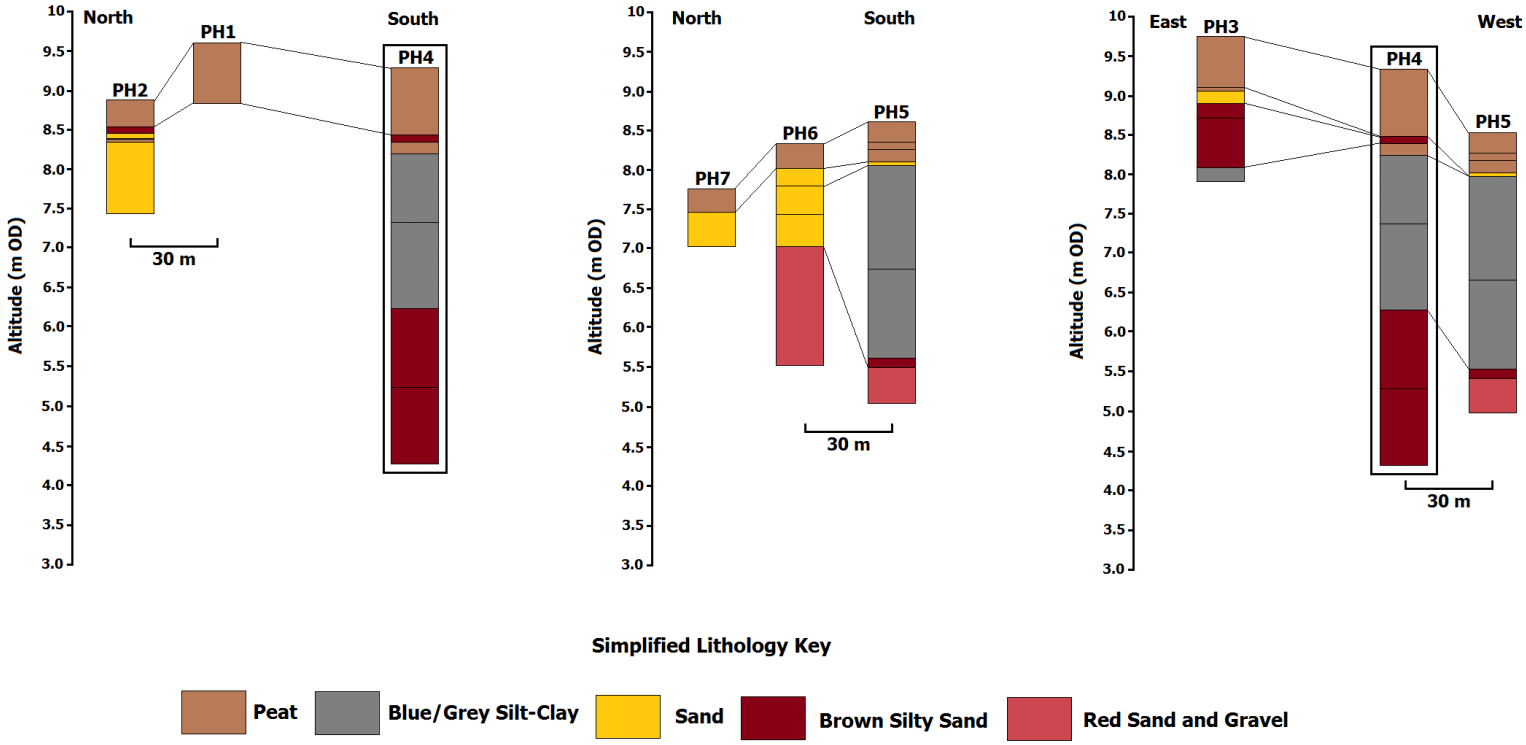

(c)

Figure 9.2: (a) Location of boreholes and sample core (PH4) obtained at Pasture House with contour line marking the altitudes (m OD) of surrounding areas (Source: © Crown Copyright and Database Right (2018) Ordnance Survey, Digimap Licence) (b) The lithostratigraphy of the boreholes and sample core from Pasture House (c) The simplified lithostratigraphy of the boreholes and sample core from Pasture House. Sample core is marked in a black square

9.2 Sediment Composition

Cores PH4-a and PH4-b terminated in the sandy blue/grey silt-clay unit at 1.94 m (m OD) and 2.10 m (7.20 m OD) respectively. The surface elevation recorded for both cores were 9.30 m OD. Towards the base of the core in the sandy blue/grey silt-clay unit and in the surface peat and sand units, sand content increased. The sand fraction found in the core consisted of very fine sand mainly, fine sand and medium sand. Core PH4-a was not continuous, with the first, second and third sections of the core covering 22-72 cm, 85-135 and 144-194 cm respectively, due to sampling difficulties. The sediment description of the cores PH4-a and PH4-b are summarised in Table 9.1 and Table 9.2 respectively.

Table 9.1: Sediment description of core PH4-a including depth, altitude and the Tröels-Smith (1955) sediment classification

Depth (m)	Altitude (m OD)	Sediment Description	Tröels-Smith Sediment Classification (1955)
22 – 43	9.08 – 8.87	Very dark brown peat with occasional wood	Th4; Dl+, Nig. = 4, Strf. = 0, Sicc. = 1, Elas. = 1
43 – 49	8.87 – 8.81	Very dark brown peat with occasional wood, sandy	Th4; Dl+; Ga+, Nig. = 4, Strf. = 0, Sicc. = 1, Elas. = 1, Lim. = 1
49 – 55	8.81 – 8.75	Light brown sand with some organic remains	Ga4; Dl+, Nig. = 2, Strf. = 0, Sicc. = 1, Elas. = 1, Lim. = 2
55 – 60	8.75 – 8.70	Very dark brown peat with occasional wood, sandy	Th4; Dl+; Ga+, Nig. = 4, Strf. = 0, Sicc. = 1, Elas. = 1, Lim. = 2
60 – 64	8.70 – 8.66	Light brown sand with some organic remains	Ga4; Dl+, Nig. = 2, Strf. = 0, Sicc. = 1, Elas. = 1, Lim. = 2
64 – 72	8.66 – 8.58	Very dark brown peat with occasional wood, sandy	Th4; Dl; Ga+, Nig. = 4, Strf. = 0, Sicc. = 1, Elas. = 1, Lim. = 2

85 – 99	8.58 – 8.31	Very dark brown peat with occasional wood and some silt, sandy	Th4; Dl+; Ag+; Ga+, Nig. = 4, Strf. = 0, Sicc. = 1, Elas. = 1, Lim. = 1
99 – 112	8.31 – 8.18	Dark brown silt-clay with organic remains, sandy	Ag2; As2; Dl+; Ga+, Nig. = 4, Strf. = 0, Sicc. = 3, Elas. = 0, Lim. = 2
112 – 135	8.18 – 7.95	Blue/grey silt-clay with organic remains	Ag2; As2; Dl+, Nig. = 2, Strf. = 0, Sicc. = 3, Elas. = 0, Lim. = 2
144 – 178	7.95 – 7.52	Blue/grey silt-clay with some organic remains	Ag2; As2; Dl+, Nig. = 2, Strf. = 0, Sicc. = 3, Elas. = 0, Lim. = 1
178 – 194	7.52 – 7.36	Blue/grey silt-clay with some organic remains and sand	Ag2; As2; Dl+; Ga+, Nig. = 2, Strf. = 0, Sicc. = 3, Elas. = 0, Lim. = 1

Table 9.2: Sediment description of core PH4-b including depth, altitude and the Tröels-Smith (1955) sediment classification

Depth (m)	**Altitude (m OD)**	**Sediment Description**	**Tröels-Smith Sediment Classification (1955)**
0 – 91	9.30 – 8.39	Very dark brown peat with occasional wood, sandy	Th4; Dl+; Ga+, Nig. = 4, Strf. = 0, Sicc. = 1, Elas. = 1
91 – 107	8.39 – 8.23	Dark brown silt-clay with organic remains	Ag2; As1; Th1; Dl+, Nig. = 3, Strf. = 0, Sicc. = 1, Elas. = 1, Lim. = 2
107 – 121	8.23 – 8.09	Very dark brown peat with occasional wood, some brown silt	Th4; Dl+; Ag+, Nig. = 4, Strf. = 0, Sicc. = 1, Elas. = 1, Lim. = 2
121 – 170	8.09 – 7.60	Blue/grey silt-clay with some organic remains	Ag2; As2; Dl+, Nig. = 2, Strf. = 0, Sicc. = 3, Elas. = 0, Lim. = 2

170 – 210	7.60 – 7.20	Blue/grey silt-clay with some organic remains and sand	Ag2; As2; Dl+; Ga+, Nig. = 2, Strf. = 0, Sicc. = 3, Elas. = 0, Lim. = 1

9.3 Loss on Ignition

Loss on ignition analyses were undertaken on samples from core PH4-a, to give an estimate of the organic carbon content and carbonate content of the sediment. Samples were taken at 2 cm, 4 cm and 16 cm from 0.22 m to 0.72 m (9.08 m OD to 8.58 m OD); at 4 cm, 6 cm and 16 cm from 0.85 m to 1.35 m (8.45 m OD to 7.95 m OD) and at every 16 cm from 1.44 m to 1.94 m (7.86 m OD to 7.36 m OD), from each stratigraphic unit found in the core. The organic carbon content and carbonate content of core PH4-a are shown in Figure 9.3.

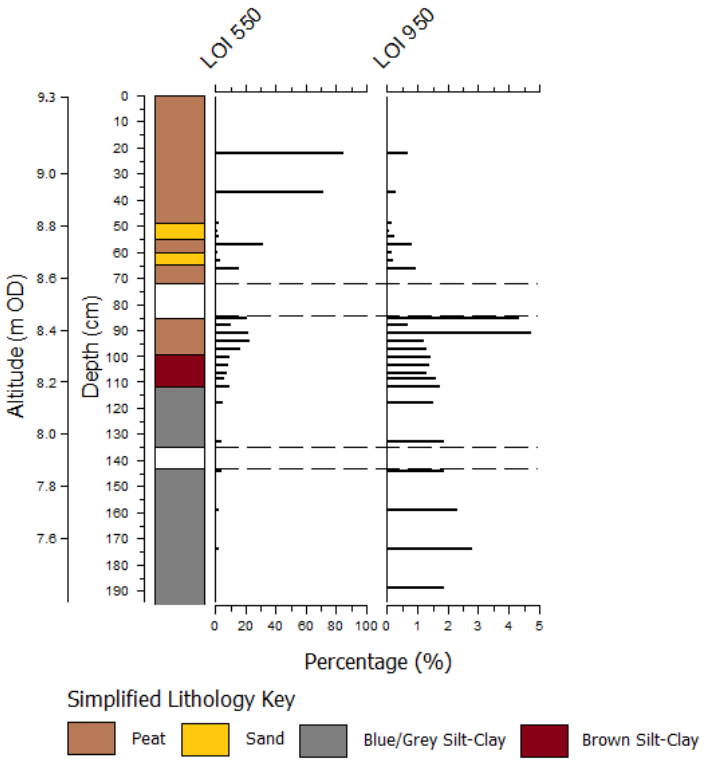

Figure 9.3: Plot of loss on ignition analyses for Pasture House showing organic carbon and carbonate content of the sediment in core PH4-a. Dashed lines represent a break in sedimentation

In the sandy blue/grey silt-clay unit and the more organic blue/grey silt-clay unit, low percentages of organic carbon were recorded, with a minimum of 0% at 1.89 m (7.41 m OD) and 4% at 1.33 m (7.97 m OD). From the depths of 1.00 m (8.30 m OD) to 1.18 m (8.12 m OD), organic carbon content ranged between 6% and 10%. The organic carbon in core PH4 increased slightly between the depths of 0.66 m (8.64 m OD) and 0.97 m (8.33 m OD), with a maximum of 23% recorded at a depth of 0.94 m (8.36 m OD) and a minimum of 16% recorded at 0.66 m (8.64 m OD). In the surface peat and sand units, a maximum of 85% organic carbon content was recorded at 0.22 m (9.08 m OD), and a minimum of 2% was recorded at 0.60 m (8.70 m OD).

Very low percentages of carbonate content were observed throughout the core, with a range of 0% to 5% observed. A maximum of 5% of carbonate content was observed at a depth of 0.91m (8.39 m OD).

9.4 Particle Size Analysis

Samples for particle size analysis were taken at 2 cm, 4 cm and 16 cm from 0.22 m to 0.72 m (9.08 m OD to 8.58 m OD); at 4 cm, 6 cm and 16 cm from 0.85 m to 1.35 m (8.45 m OD to 7.95 m OD) and at every 16 cm from 1.44 m to 1.94 m (7.86 m OD to 7.36 m OD), from each stratigraphic unit found in the core.

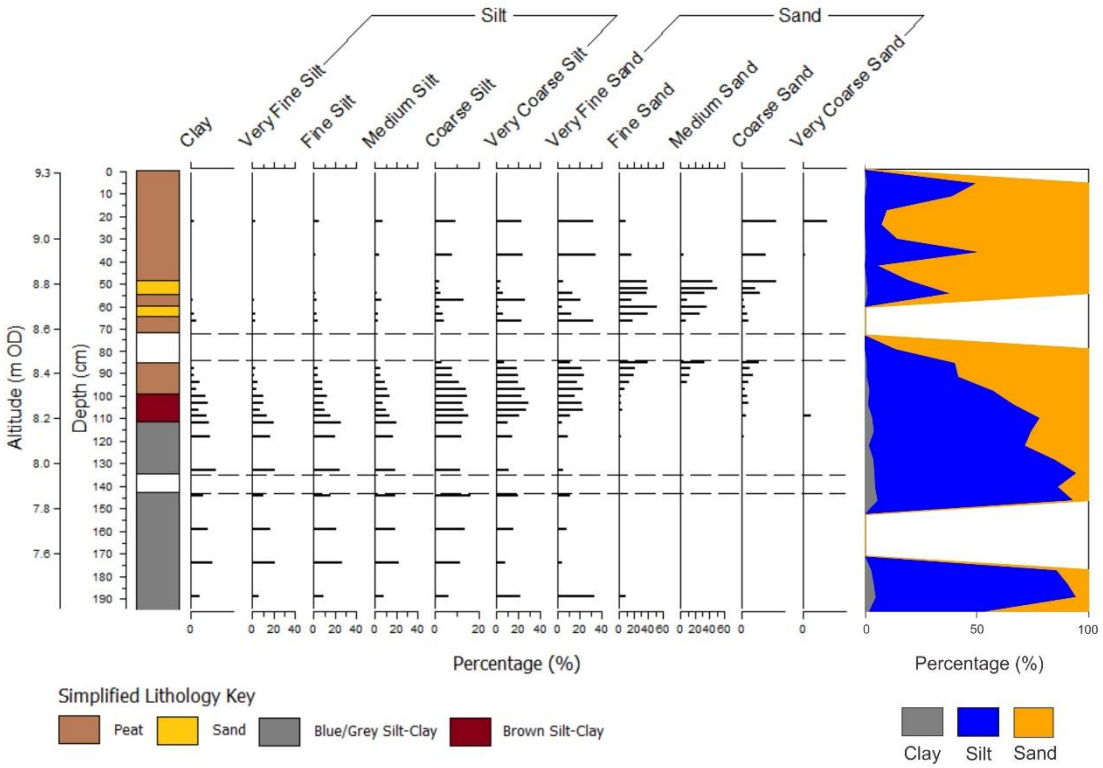

Figure 9.4: Diagram showing particle size analysis for core PH4-a from Pasture House. Dashed lines represent a break in sedimentation

Particle size analysis in core PH4-a showed sediment dominated mostly by silt with increased sand content observed towards the bottom of the core in the sandy blue/grey silt-clay unit and the surface peat and sand units.

The percentages of clay in the core showed minimal fluctuations, with a maximum of 6% observed at a depth of 1.33 m (7.97 m OD) and a minimum of 0% observed at a depth of 0.85 m (8.45 m OD). Core PH4-a was dominated mainly by silt, with the highest silt percentages observed in the blue/grey silt-clay unit. The percentage of silt content reached a maximum of 91% at 1.12 m (8.18 m OD), while the minimum silt content of 6% was noted at 0.60 m (8.70 m OD) in the surface peat and sand units. Increased sand content was observed in the basal sandy blue/grey silt-clay unit and the surface peat unit. A total of 44% sand was observed at 1.89 m (7.41 m OD) in the sandy blue/grey silt-clay unit, and decreased to 5% at 1.12 m (8.18 m OD) and 14% at 1.44 m (7.86 m OD). From 1.06 m (8.24 m OD) towards the top of the core at 0.22 m (9.08 m OD), increased sand content were noted, with 22% at 1.00 m (8.30 m OD) and 94% at 0.60 m (8.70 m OD), corresponding to the deposition of the surface peat and sand units.

9.5 Microfossil Analyses

Samples were taken at 2 cm, 4 cm or 8 cm intervals throughout cores PH4-a and PH4-b for diatom and foraminiferal analyses. Despite multiple samples from both cores, extremely poor preservation of foraminifera and diatoms was noted within the sediment. The identification of diatom species was ultimately deemed impossible in both cores. Foraminifera (*Jadammina macrescens* and *Trochammina inflata*) were present in sections of the blue/grey silt-clay unit of PH4-a and PH4-b cores (Figure 9.5), although the individual foraminiferal counts were low, despite increasing the samples' volume. Microfossil analyses was therefore not feasible on the cores from Pasture House and no chronology for the site was established.

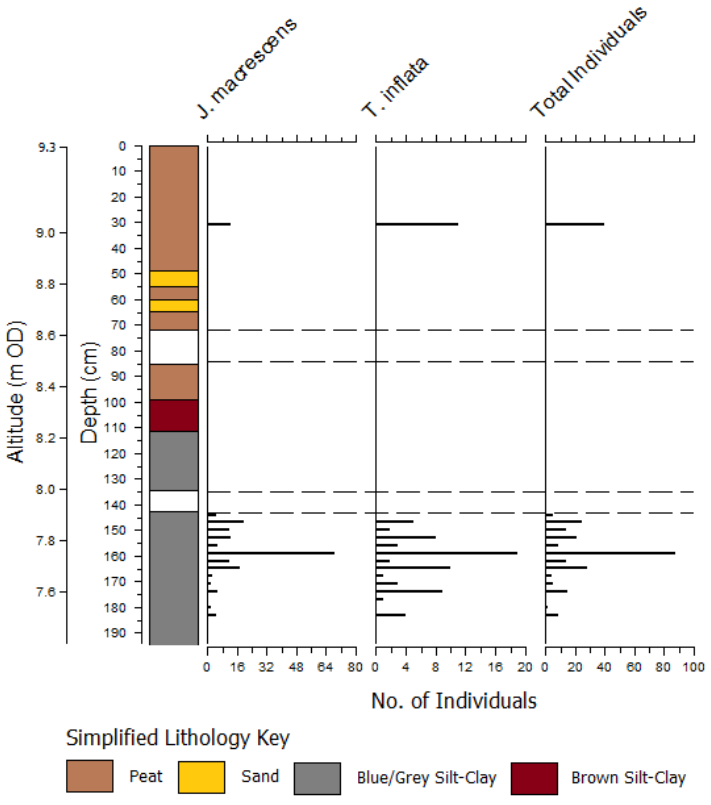

(a)

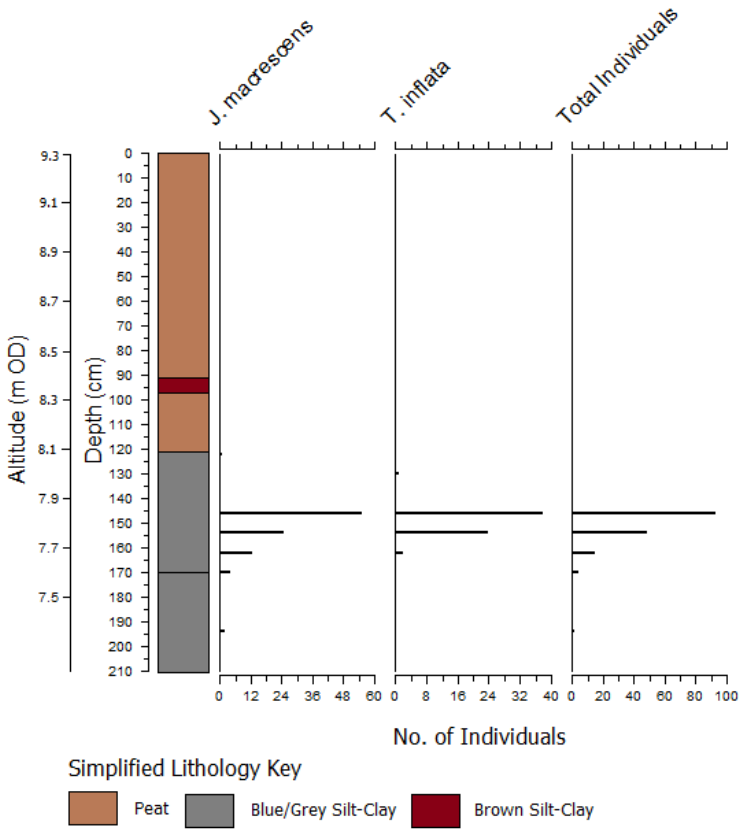

(b)

Figure 9.5: Foraminiferal diagram from Pasture House showing total individual counts (a) Core PH4-a, with dashed lines represent a break in sedimentation (b) Core PH4-b. All samples including samples with low individual counts (below 40 individuals) were included in this diagram

9.6 Summary

The geomorphology and lithostratigraphy at Pasture House suggest that the site is composed of relict sand bars and sand dunes, with units of sand interbedded within the surface peat unit. These relict sand bars have also been recorded in the inner estuary of the Solway Firth, behind the contemporary saltmarshes (Lloyd *et al.*, 1999).

CHAPTER 10

PALAEO-TIDAL CHANGES IN THE SOLWAY FIRTH

10.0 Introduction

This chapter illustrates the estimated changes in palaeo-tidal range in the Solway Firth for the study period between 10 ka BP to present day based on the model developed by Hill (personal communication; Chapter 3, Section 3.9.1). The tidal data were then used for the correction of the sea-level index points (SLIPs) produced in this study along with the existing SLIPs in the Solway Firth, which have not been included in the calculation of most of the SLIPs in the region prior to this study. Correcting for changes in palaeo-tidal range for SLIPs is important to prevent an underestimation or overestimation of the calculated relative sea level (RSL) for each SLIP, as changes in the tidal range of the sites will ultimately affect the reference water level ascribed to the respective SLIP.

10.1 Palaeo-Tidal Changes in the Solway Firth

Changes in the palaeo-tidal range in the Solway Firth from 10 ka BP to 1 ka BP relative to present day are shown in Figure 10.1. The SLIPs produced in this study along with the existing SLIPs from the southern and northern Solway Firth were corrected based on the palaeo-tidal data, and are presented in the following Section 10.2. The data of the presently available SLIPs from the southern and northern Solway Firth were obtained from Shennan *et al.* (2018), with the full details on each SLIPs as provided by the authors available in the online database.

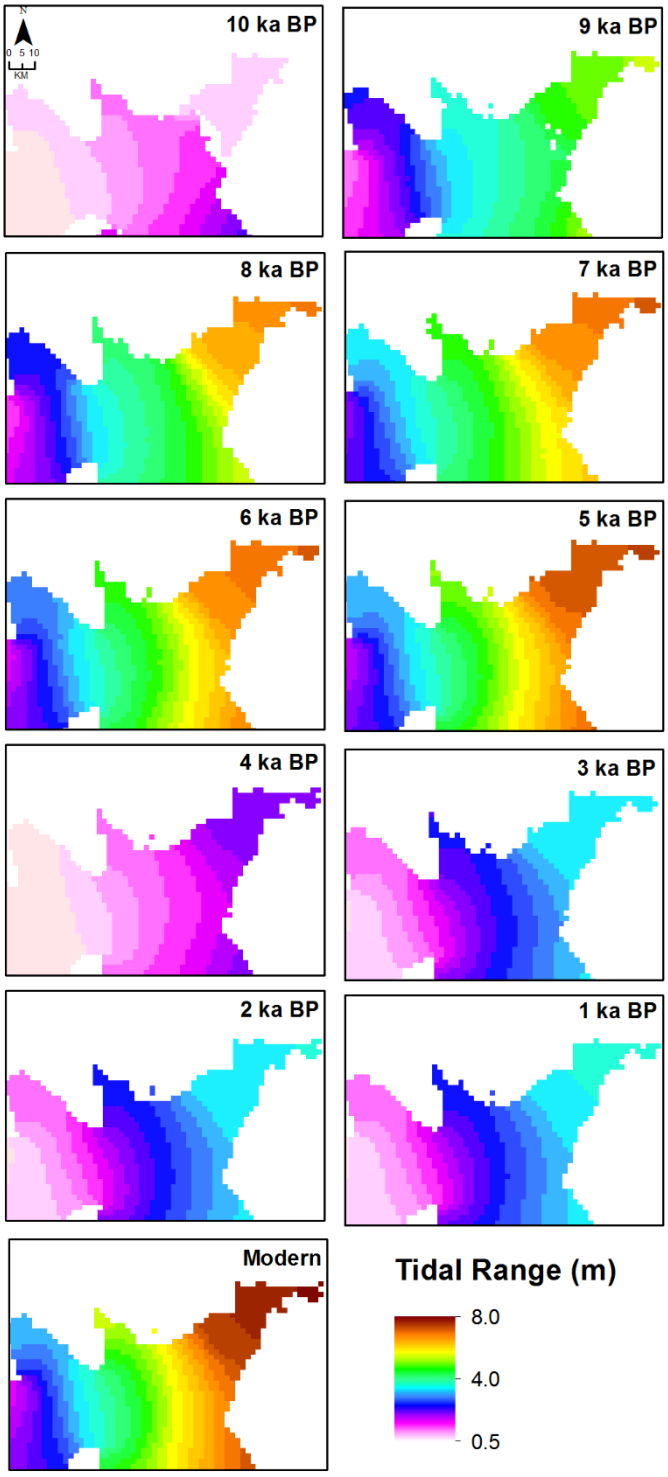

Figure 10.1: Maps showing the modern tidal range and changes in palaeo-tidal range in the Solway Firth from 10 ka BP to 1 ka BP, relative to the modern tidal range

10.2 Corrected SLIPs from the Solway Firth

SLIPs produced from this study showing the RSL at the sites investigated, along with the existing SLIPs from the northern and southern side of the Solway Firth are presented in Table 10.1, 10.2 and 10.3 respectively. Each SLIP was corrected for changes in palaeo-tidal range in accordance to their respective time period, with the updated RSL values also presented in the tables.

The palaeo-tidal model have a temporal resolution of 1000 years. The 98 SLIPs available for the region (including those from this study) were therefore categorised into ten different timeslices from 10 ka BP to 1 ka BP based on their mean ages (e.g. a SLIP with a mean age of 7320 is included in the 7 ka BP timeslice).

The palaeo-tidal model have a spatial resolution of approximately 1 km along the coastline. Therefore, all sites less than 1 km apart from each other would have the same tidal range (as they fall within the same triangle cell in the model). As most of the sites studied in the Solway Firth are clustered within the same sub-estuaries (e.g. in the Cree Estuary and Nith Estuary), different SLIPs from the same timeslice would have resulted in the same palaeo-tidal range prediction. However, a more complex linear function was also used in the model, which may result in different tidal ranges for sites less than a kilometre apart (Hill, personal communication 14th May 2019). When the raster files were produced for each timeslice, the changes in palaeo-tidal range along the coastline are presented at a 1 km resolution (Figure 10.1).

Table 10.1: SLIPs produced in this study corrected for changes in palaeo-tidal range

Lab Code	Lat.	Long.	Site Region	Radiocarbon Age		Cal BP (2σ Ranges)			Altitude (m OD)	RSL (m)	Palaeo-Tidal Range Correction (m)	Corrected RSL (m)
				BP	1σ Error	Min	Mean	Max				
D-AMS 022222	54.783	-3.408	Allonby	6377	34	7255	7320	7418	6.65	+1.06±1.46	-0.468	+1.53±1.46
D-AMS 025776	54.783	-3.408	Allonby	7209	41	7954	8031	8158	6.00	+0.42±1.46	-0.468	+0.89±1.46
D-AMS 022223	54.783	-3.408	Allonby	7203	49	7946	8030	8160	5.61	+0.02±1.46	-0.596	+0.62±1.46
D-AMS 016391	54.812	-3.405	Cowgate Farm	5655	50	6310	6437	6557	7.71	+2.12±1.46	-0.440	+2.56±1.46
D-AMS 016392	54.812	-3.405	Cowgate Farm	7521	55	8200	8324	8412	6.89	+1.30±1.46	-0.593	+1.89±1.46
D-AMS 022226	54.829	-3.371	Pelutho	6231	35	7016	7146	7254	6.89	+1.35±0.56	-0.469	+1.82±0.56
D-AMS 025778	54.829	-3.371	Pelutho	6456	45	7275	7367	7435	6.00	+0.50±0.57	-0.469	+0.97±0.57
D-AMS 022227	54.829	-3.371	Pelutho	7285	36	8018	8097	8174	5.51	+0.58±0.57	-0.590	+1.17±0.57
D-AMS 022224	54.928	-3.285	Herd Hill	5236	46	5914	6018	6179	8.81	+3.26±0.56	-0.450	+3.71±0.56
D-AMS 022225	54.928	-3.285	Herd Hill	6497	36	7322	7401	7475	8.35	+3.41±0.56	-0.469	+3.88±0.56

Table 10.2: Existing SLIPs from northern Solway Firth corrected for changes in palaeo-tidal range

Lab Code	Lat.	Long.	Site Region	Radiocarbon Age		Cal BP (2σ Ranges)			Altitude (m OD)	RSL (m)	Palaeo-Tidal Range Correction (m)	Corrected RSL (m)
				BP	1σ Error	Min	Mean	Max				
Q638	55.00	-3.48	Clarencefield	6645	120	7307	7527	7717	9.32	+4.12±0.43	-0.402	+4.52±0.43
Beta96322	54.93	-4.45	Cree Estuary	6470	80	7252	7378	7560	8.86	+4.86±0.21	-0.297	+5.16±0.21
Beta96321	54.93	-4.45	Cree Estuary	5770	90	6350	6571	6784	9.09	+5.49±0.21	-0.282	+5.77±0.21
SUERC44405	54.93	-4.40	Cree Estuary	7127	26	7877	7958	8005	6.55	+2.42±0.98	-0.297	+2.71±0.98
BIRM461	55.08	-3.54	Collin	3290	110	3254	3528	3828	9.00	+4.00±0.83	-2.563	+6.56±0.83
BIRM222	54.97	-3.30	River Annan	7540	150	8015	8342	8626	2.95	-2.07±1.01	-0.512	-1.56±1.01
UB3903	54.98	-3.09	Inner Solway Firth	7956	62	8631	8821	8998	2.27	-3.24±0.80	-0.465	-2.77±0.80
SUERC42711	54.93	-4.40	Cree Estuary	7452	25	8197	8266	8343	5.60	+1.87±0.98	-0.678	+2.54±0.98
Beta120961	54.89	-4.45	Cree Estuary	3380	70	3459	3627	3827	8.44	+4.44±0.21	-2.376	+6.82±0.21
UB3902	54.98	-3.09	Inner Solway Firth	7794	61	8421	8572	8753	2.41	-2.89±0.21	-0.465	-2.42±0.21
SUERC44406	54.93	-4.40	Cree Estuary	6963	36	7694	7794	7922	6.90	+2.80±0.21	-0.297	+3.10±0.21
I5069	54.88	-3.63	Southerness	1850	95	1562	1780	1989	5.30	+0.51±0.34	-2.357	+2.86±0.34
BIRM415	54.94	-4.42	Nith Estuary	6540	120	7247	7444	7656	6.43	+2.78±0.41	-0.403	+3.18±0.41
Beta96323	54.91	-4.46	Cree Estuary	8600	90	9444	9594	9887	2.43	-1.17±0.21	-1.208	+0.04±0.21
Beta105932	54.94	-4.42	Cree Estuary	6100	70	6790	6980	7166	8.66	+4.66±0.21	-0.282	+4.94±0.21
Beta96327	54.94	-4.42	Cree Estuary	8310	100	9032	9301	9489	-1.15	-5.15±0.21	-1.208	-3.94±0.21
SUERC42712	54.93	-4.40	Cree Estuary	7088	26	7854	7929	7968	6.42	+2.55±0.98	-0.297	+2.85±0.98
SUERC44369	54.93	-4.40	Cree Estuary	7980	27	8725	8873	8994	3.17	-0.66±0.98	-0.678	+0.01±0.98
SUERC44400	54.93	-4.40	Cree Estuary	7049	65	7729	7879	7996	6.49	+2.46±0.98	-0.297	+2.75±0.98
UB3897	54.98	-3.37	Inner Solway Firth	7302	68	7972	8110	8303	6.64	+1.35±0.21	-0.465	+1.82±0.21
SUERC44371	54.93	-4.40	Cree Estuary	7409	26	8179	8255	8318	5.60	+1.87±0.98	-0.678	+2.54±0.98
SRR26	54.93	-4.41	Cree Estuary	4746	50	5325	5492	5588	7.92	+4.07±0.41	-0.141	+4.21±0.41

Beta120963	55.01	-3.60	Nith Estuary	5560	60	6222	6355	6472	9.44	+4.35±0.21	-0.380	+4.73±0.21
UB3899	54.98	-3.37	Inner Solway Firth	6087	186	6506	6958	7413	8.73	+3.44±0.21	-0.400	+3.84±0.21
Beta100919	54.93	-4.40	Cree Estuary	6800	130	7439	7659	7925	7.16	+3.16±0.21	-0.297	+3.46±0.21
Beta84193	54.88	-3.63	Southerness	1760	70	1534	1678	1863	4.92	-0.17±0.21	-2.357	+2.19±0.21
SUERC44399	54.93	-4.40	Cree Estuary	7107	26	7865	7945	7996	6.42	+2.55±0.98	-0.297	+2.85±0.98
Beta96326	54.94	-4.42	Cree Estuary	8190	80	8996	9162	9406	-1.13	-4.73±0.21	-1.208	-3.52±0.21
SUERC44398	54.93	-4.40	Cree Estuary	7344	65	8018	8154	8320	5.54	+1.67±0.98	-0.678	+2.35±0.98
BIRM323	54.92	-3.58	Southerness	9390	130	10259	10636	11088	-1.05	-4.50±0.89	-5.170	+0.67±0.89
GU4658	55.02	-3.63	Nith Estuary	7680	50	8390	8473	8575	3.34	-1.26±0.22	-0.521	-0.74±0.22
Beta100914	54.93	-4.40	Cree Estuary	7820	80	8424	8621	8975	3.45	-0.35±0.41	-0.678	+0.33±0.41
Beta100917	54.93	-4.40	Cree Estuary	7510	310	7684	8344	9071	6.96	+2.96±0.21	-0.678	+3.64±0.21
GU4647	55.03	-3.64	Nith Estuary	7710	50	8413	8493	8585	3.78	-0.82±0.22	-0.521	-0.30±0.22
GU4652	55.04	-3.65	Nith Estuary	7090	90	7696	7908	8151	5.82	+0.73±0.21	-0.403	+1.13±0.21
GU4646	55.03	-3.64	Nith Estuary	7360	100	7998	8179	8374	6.82	+1.73±0.21	-0.521	+2.25±0.21
GU4645	55.03	-3.64	Nith Estuary	6950	80	7626	7786	7945	7.02	+1.73±0.21	-0.403	+2.13±0.21
GU4657	55.02	-3.63	Nith Estuary	7220	70	7935	8044	8179	6.24	+1.15±0.21	-0.521	+1.67±0.21
Beta100915	54.93	-4.40	Cree Estuary	7830	110	8426	8661	8980	5.81	+1.81±0.21	-0.678	+2.49±0.21
Beta83747	54.90	-4.45	Nith Estuary	3680	60	3846	4018	4221	8.97	+4.97±0.21	-3.718	+8.69±0.21
GU4656	55.02	-3.63	Nith Estuary	6790	90	7487	7642	7826	6.90	+2.30±0.21	-0.403	+2.70±0.21
GU375	54.97	-3.29	Inner Solway Firth	7812	131	8399	8645	8994	4.57	-0.65±0.43	-0.465	-0.18±0.43
Beta83746	54.90	-4.46	Nith Estuary	4050	90	4296	4559	4829	9.23	+5.23±0.21	-3.718	+8.95±0.21
GU64	54.97	-3.30	Newbie	7254	101	7873	8082	8319	5.79	+0.77±0.22	-0.515	+1.28±0.22
SUERC44397	54.93	-4.40	Cree Estuary	7392	39	8060	8238	8340	5.54	+1.67±0.98	-0.678	+2.35±0.98
SUERC44386	54.93	-4.40	Cree Estuary	7507	25	8214	8350	8388	5.47	+1.60±0.98	-0.678	+2.28±0.98
SUERC44387	54.93	-4.40	Cree Estuary	7831	65	8448	8626	8973	3.18	-0.65±0.98	-0.678	+0.02±0.98
Beta84189	54.90	-4.46	Cree Estuary	3050	60	3075	3252	3382	9.60	+5.60±0.21	-2.376	+7.98±0.21
Beta120962	54.89	-4.44	Cree Estuary	3470	80	3560	3743	3969	7.96	+3.96±0.21	-2.376	+6.34±0.21
SUERC42708	54.93	-4.40	Cree Estuary	7982	27	8725	8874	8995	3.16	-0.71±0.98	-0.678	-0.03±0.98
SUERC44385	54.93	-4.40	Cree Estuary	7977	26	8725	8871	8993	3.17	-0.66±0.98	-0.678	+0.01±0.98

Beta83750	54.91	-4.45	Nith Estuary	4050	50	4418	4538	4807	8.98	+4.98±0.21	-3.718	+8.70±0.21
Beta96325	54.93	-4.40	Cree Estuary	8580	80	9433	9561	9765	-0.51	-4.51±0.21	-1.208	-3.30±0.21
BIRM325	54.97	-3.31	Inner Solway Firth	7400	150	7938	8214	8511	5.60	+0.58±1.01	-0.465	+1.05±1.01
BIRM324	54.98	-3.38	Inner Solway Firth	6470	280	6734	7337	7922	8.73	+3.24±0.23	-0.387	+3.63±0.23
UB3895	54.98	-3.37	Inner Solway Firth	7033	57	7731	7868	7965	6.87	+2.07±0.21	-0.387	+2.46±0.21
SUERC42709	54.93	-4.40	Cree Estuary	7936	27	8640	8770	8977	3.17	-0.66±0.98	-0.678	+0.01±0.98
Beta83748	54.92	-4.41	Nith Estuary	3810	70	3989	4209	4415	8.59	+4.59±0.21	-3.718	+8.31±0.21
BIRM189	54.94	-4.42	Cree Estuary	6240	240	6566	7107	7576	6.38	+2.53±0.41	-0.297	+2.83±0.41
Beta96320	54.93	-4.45	Cree Estuary	5030	110	5489	5779	5998	9.16	+5.16±0.21	-0.141	+5.30±0.21
Beta96324	54.93	-4.40	Cree Estuary	8400	80	9142	9409	9538	0.88	-2.72±0.21	-1.208	-1.51±0.21
BIRM258	55.02	-3.52	Bankend	5410	160	5761	6184	6538	6.00	+0.90±0.22	-0.381	+1.28±0.22
Beta83749	54.93	-4.40	Nith Estuary	4010	80	4244	4495	4814	8.94	+4.94±0.21	-3.718	+8.66±0.21
Beta100918	54.93	-4.40	Cree Estuary	7210	120	7795	8039	8312	7.09	+3.49±0.21	-0.678	+4.17±0.21
Beta100916	54.93	-4.40	Cree Estuary	7240	90	7868	8068	8302	5.86	+2.26±0.21	-0.678	+2.94±0.21
GU4650	55.04	-3.65	Nith Estuary	7540	90	8178	8346	8537	4.59	-0.01±0.21	-0.521	+0.51±0.21
Beta83751	54.92	-4.41	Nith Estuary	4330	80	4647	4929	5283	8.21	+4.21±0.21	-3.718	+7.93±0.21
Beta92209	54.93	-4.40	Cree Estuary	9680	50	10432	10578	10710	-9.32	-9.77±0.21	-3.592	-6.18±0.21
GU4653	55.04	-3.65	Nith Estuary	7770	60	8414	8546	8693	3.38	-1.42±0.21	-0.521	-0.90±0.21
GU4649	55.04	-3.65	Nith Estuary	7210	100	7831	8038	8298	4.68	-0.41±0.21	-0.521	+0.11±0.21
GU4654	55.04	-3.64	Nith Estuary	7460	100	8039	8270	8420	6.10	+1.01±0.21	-0.521	+1.53±0.21
GU4655	55.02	-3.63	Nith Estuary	5910	70	6553	6736	6922	7.43	+2.34±0.21	-0.380	+2.72±0.21
SUERC44407	54.93	-4.40	Cree Estuary	6890	64	7607	7729	7916	6.90	+2.80±0.21	-0.297	+3.10±0.21
GU4648	55.03	-3.64	Nith Estuary	7170	80	7847	7994	8168	7.27	+4.15±2.67	-0.403	+4.55±2.67

Table 10.3: Existing SLIPs from southern Solway Firth corrected for changes in palaeo-tidal range

Lab Code	Lat.	Long.	Site Region	Radiocarbon Age		Cal BP (2σ Ranges)			Altitude (m OD)	RSL (m)	Palaeo-Tidal Range Correction (m)	Corrected RSL (m)
				BP	1σ Error	Min	Mean	Max				
HV4713	54.87	-3.19	Inner Solway Firth	5385	280	5491	6159	6794	6.17	+0.87±0.21	-0.400	+1.27±0.21
HV5228	54.87	-3.19	Inner Solway Firth	6870	95	7571	7718	7929	4.66	-0.14±0.21	-0.387	+0.25±0.21
HV4418	54.83	-3.37	Inner Solway Firth	4845	100	5321	5580	5877	8.70	+3.60±0.21	-0.227	+3.83±0.21
UB3892	54.91	-3.14	Inner Solway Firth	7353	53	8030	8167	8313	4.55	-0.76±0.21	-0.465	-0.29±0.21
B103261	54.91	-3.15	Inner Solway Firth	2430	60	2351	2505	2708	6.85	+1.05±0.21	-2.483	+3.53±0.21
B103262	54.91	-3.11	Inner Solway Firth	6510	60	7293	7425	7561	7.16	+1.36±0.21	-0.387	+1.75±0.21
UB4054	54.91	-3.11	Inner Solway Firth	6563	110	7264	7465	7623	6.68	+1.37±0.21	-0.387	+1.76±0.21
UB3893	54.91	-3.15	Inner Solway Firth	2587	56	2488	2711	2840	8.12	+2.32±0.21	-2.483	+4.80±0.21
HV6208	54.93	-3.21	Inner Solway Firth	6850	60	7583	7686	7822	4.73	-0.29±0.30	-0.387	+0.10±0.30
HV6207	54.93	-3.21	Inner Solway Firth	5875	220	6282	6714	7251	5.95	+0.43±0.30	-0.400	+0.83±0.30
UB3894	54.91	-3.14	Inner Solway Firth	7806	81	8414	8599	8973	4.44	-1.07±1.26	-0.465	-0.60±1.26
UB3891	54.91	-3.11	Inner Solway Firth	7315	79	7981	8124	8317	6.19	+0.68±1.26	-0.465	+1.15±1.26
HV4714	54.87	-3.19	Inner Solway Firth	4725	190	4880	5419	5890	4.80	+1.68±2.67	-0.227	+1.91±2.67

10.3 Summary

All the available SLIPs in the Solway Firth including those produced in this study have been corrected for changes in the tidal range over the Holocene. Tidal range in the Solway Firth increased between 8 ka BP to 5 ka BP, corresponding to the Main Postglacial Transgression in the area (and possibly combined with the freshwater input due to the drainage of glacial lakes Agassiz-Ojibway) and later decreased. The tidal range in the study region again showed an increase based on the modern day data. The changes in palaeo-tidal ranged between 0.227 m (HV47114) to 5.170 m (BIRM323), which were estimated for the time period of 5 ka BP and 10 ka BP respectively. The tidal range in the Solway Firth during the study period (10 ka BP to 1 ka BP) are consistently smaller than the present day tidal range, which have resulted in an underestimation of the altitude of RSL prior to the corrections (discussed in Chapter 11). The correction of palaeo-tidal range in the Solway Firth over the study period will now allow the identification of potentially different RSL changes between the northern shore and the southern shore of the Solway Firth due to the differential crustal rebound between the two localities.

CHAPTER 11

DISCUSSION

11.0 Introduction

This chapter discusses the results in this research in order to address the main objectives set out in this research:

1. To generate sea-level index points (SLIPs) from sites located along the currently understudied southern shore of the Solway Firth

2. To define the timing of sea-level and broader environmental changes recorded at each site using microfossil analyses and radiocarbon dating

3. To establish the contemporary distribution of foraminifera from three saltmarshes located in the study region

4. To examine, and correct for palaeo-tidal changes of the SLIPs produced in this study, and the ones that currently exist for the northern and southern Solway Firth

5. To compare the corrected SLIPs with relative sea-level (RSL) values produced from glacio-isostatic models

A critique of the methods used to reconstruct sea-level changes including an assessment of the contemporary foraminiferal and saltmarsh environments investigated are presented. This is followed by a discussion on the results obtained from the four palaeo sites investigated, illustrating the general trend of Holocene RSL in the region based on the new SLIPs produced. A comparison of SLIPs between the northern and southern Solway Firth (including those produced from this study) is then considered, examining if differential crustal rebound between the two localities exists, as evidenced by different records of relative sea level of the SLIPs.

11.1 Reliability of Palaeo Sea-Level Techniques

In order to reconstruct Holocene RSL and environmental changes along the Cumbrian coastline, the methodology included the selection of suitable study sites, microfossil analyses, development of a local transfer function, the determination of indicative meanings and calculation of SLIPs. The following sections will discuss these methods and techniques.

11.1.1 Preservation of Microfossils in the Palaeo Sites Cores

Several issues were identified with the preservation of microfossils. In the core obtained from Pasture House (PH4), and in the deeper section of the core from Cowgate Farm (CGF1), very poor preservation of the microfossils was noted, and this was attributed to the generally high sand content within the respective sediment units. From PH4 and CGF1, samples were prepared for diatom analysis. Very small and broken fragments of diatoms were observed but these were not identifiable. Samples were prepared for foraminiferal analysis on the core from Pasture House. However, foraminifera occurred at low frequencies (Chapter 9; Section 9.5). Good preservation of foraminifera was otherwise observed in cores from the four sites investigated.

The most crucial issue encountered with respect to the preservation of microfossils from all four sites (A7, CGF1, P12 and HH4) was the dissolution of the calcareous foraminiferal species in the fossil cores. No calcareous species were observed in all four cores in this study, although the presence of test linings was observed at Allonby, Pelutho and Herd Hill. The dissolution of the calcareous foraminifera in an acidic, low pH and organic saltmarsh deposit may result in a biased foraminiferal assemblage (e.g. Edwards & Horton, 2000; Gehrels *et al.*, 2001; Leorri *et al.*, 2010; Callard *et al.*, 2011; Best, 2016). If the calcareous species were deposited higher in the organic and acidic saltmarsh environment due to the macrotidal range of the Solway Firth, as was observed in the contemporary samples in this study, the calcareous species may have been dissolved and therefore not preserved in the sediment cores. However, the dissolution and poor preservation of the calcareous species were also noted in the minerogenic units of marine origin, with only test linings present (at Allonby and Herd Hill, and in very low frequencies at Pelutho). This led to a biased foraminiferal

assemblage within the core, with the saltmarsh foraminiferal species dominating the minerogenic units as well as the organic units of saltmarsh origin. The post depositional dissolution of the calcareous species may be due to input of acidic pore water at the sites, and this was also recorded at Boustead Hill in the southern Solway Firth (Lloyd *et al.*, 1999).

The dissolution of calcareous foraminiferal species in the cores has therefore led to some difficulty in the interpretation of RSL changes based solely on the foraminiferal assemblages. However, the changes in saltmarsh foraminifera assemblage and presence of test linings, combined with the lithostratigraphical changes and pollen analysis has enabled in the reconstruction of Holocene RSL at each site investigated.

11.1.2 Determination of Indicative Meaning for the SLIPs

The indicative meaning of SLIPs can be assigned based on either the environmental context of the microfossil proxy utilised (e.g. Zong & Tooley, 1996; Lloyd *et al.*, 1999; Lloyd *et al.*, 2013) or quantitatively through the development of transfer functions (e.g. Horton *et al.*, 1999; Edwards, 2001; Edwards, 2006; Horton & Edwards, 2006; Barlow *et al.*, 2013; 2014). The combined information on the lithostratigraphy, sediment composition and preserved microfossils within the sample allowed the determination of the indicative meaning for the calculation of SLIPs in this study. However, this could only be achieved when there was good preservation of microfossils within the fossil core. At Allonby and Pelutho, generally good preservation of microfossil was noted, with changes in foraminiferal assemblages corresponding to the different sediment units observed. However at Cowgate Farm and Herd Hill foraminifera were only present in one stratigraphic unit. The dissolution of the calcareous foraminiferal assemblages resulted in the biased dominance of the agglutinated foraminiferal assemblages, although the presence of test linings that occurred only within the minerogenic units increased the confidence in the determination of the indicative meaning of samples from the different lithostratigraphic units.

Despite the development of transfer function in this study, the high number of poor modern analogues in all of the fossil cores from Allonby, Cowgate Farm, Pelutho and Herd Hill was observed. This was attributed mainly to the dissolution of the calcareous

foraminiferal assemblages in the fossil samples and the low significance of elevation in explaining the variation in foraminiferal assemblage. Therefore, the predicted palaeo marsh surface elevation (PMSE) values based on the utilised transfer function on each core were ultimately deemed unreliable.

In this study, two methods of ascribing the indicative meaning of a SLIP were adopted. The first was based on the environmental context of the microfossil proxy utilised for the determination of the indicative meaning of the SLIPs, and the second was the development of a transfer function (Figure 4.23). However, the prediction of PMSE value for each SLIP was eventually unsuccessful, due to the dissolution of the calcareous foraminiferal assemblages within the fossil cores. The indicative meaning for all SLIPs in this study was therefore assigned with respect to the environmental preferences of the foraminiferal assemblages present in each sample. The determination of the indicative meanings for each sample in this study provided SLIPs that were in general agreement with the other available SLIPs (Huddart *et al*., 1977; Lloyd *et al*., 1999) and the modelled RSL curve for the southern Solway Firth in Bradley *et al*. (2011), Kuchar *et al.* (2012) and Shennan *et al*. (2018), thus providing confidence in the approach utilised.

11.1.3 Effect of Changes in Palaeo-Tidal Range

The two significant sources of vertical uncertainties in the calculation of SLIPs are the changes in the tidal range over time and the post-depositional compaction of sediments. These were addressed and quantified in the calculation of SLIPs in this study and have resulted in improved constraints of Holocene RSL changes for the study area. The changes of tidal range over the Holocene were also calculated for all the available SLIPs from the Solway Firth for the study period between 10 ka BP to 1 ka BP.

The changes of the tidal range for the SLIPs produced in this study throughout the Holocene occurs on a decimetre scale (Table 10.1). This had led to a minimal change in the calculation of SLIPs at respective palaeo sites (Allonby, Cowgate Farm, Pelutho and Herd Hill; Figure 11.1), as well as the resulting interpretation of Holocene sea-level changes at these sites. The tidal range changes over the Holocene however, may still potentially affect the coastal geomorphology and sedimentation of the area.

Although the effect of palaeo-tidal changes in the study area of this present study appear to be minimal, tidal range variations throughout the Holocene have proved to be significant (up to a metre scale) elsewhere (e.g. Horton *et al.*, 2013; Best, 2016) and along the northern shore of the Solway Firth (Chapter 10; Section 10.2). A more significant tidal range variation between present day and the past had led to an underestimation of RSL at the other sites in the Solway Firth, hence highlighting the importance of applying the corrections.

11.1.4 Effect of Compaction of Sediments in the Palaeo Cores

In general, minimal post-depositional lowering of sediments is observed in all of the cores utilised in this study. The minimal post-depositional lowering of the sediments may be attributed to the generally shallow depth of the cores from Allonby (172 cm), Cowgate Farm (152) and Herd Hill (168 cm), with the core from Pelutho recording the deepest sediment sequence of 315 cm. The effect of compaction which resulted in post-depositional lowering of the sediments is therefore concluded not to have resulted in a significant variation in the calculation of SLIPs, and therefore not have led to a misinterpretation of the reconstructed sea-level trends in this study. However, cores with deeper lithostratigraphic sequences and more pronounced transgressive changes are prone to larger effects of compaction and post-depositional lowering, leading to an increased distortion of the reconstructed sea-level trend (Brain *et al.*, 2015).

11.1.5 Chronology of the Dated Samples

The chronology for the changes in lithostratigraphy and biostratigraphy (foraminifera) were established through AMS radiocarbon dating of bulk sediments. A total of 14 dates were obtained (Sections 5.5; 6.5; 7.5 and 8.5) and out of the 14 dated samples, 10 were utilised in the calculation of SLIPs to constrain Holocene RSL changes at the respective sites. Three of the dates (ALL-78, CGF-127 and HH-146) produced ages that were out of sequence, while sample CGF-135/141 was excluded due to the lack of preserved microfossils indicating a marine origin.

Sample ALL-78 was obtained from a blue/grey silt-clay unit most likely deposited at the site at Allonby during an event of increased relative sea level, and the effect of

tidal washing and the resultant sediment reworking and resuspension within the intertidal mudflat environment might have led to the incorporation of older sediment (hence older carbon) into the sample which led to the contamination of the date. Samples CGF-127 and HH-146 both resulted in ages younger than expected (Table 6.2 and Table 8.2). Similar issues of reworked sediments and penetration of root fragments into the lower sediment column may have resulted in the incorporation of younger carbon into the samples.

All three samples that produced out of sequence ages were dated through bulk sediment. Alternative dating methods such as the dating of plant macrofossils which is commonly employed, or through the dating of individual foraminiferal tests (e.g. Martin *et al.*, 1996; Cearreta & Murray, 2000; Allison & Austin, 2003; Hearty *et al.*, 2004; Kaufman *et al.*, 2008; Wacker *et al.*, 2013) may also be explored, although the original issue of the lack of preserved microfossils, and absence of suitable plant macrofossils in the minerogenic units of the respective cores from Allonby, Cowgate Farm and Herd Hill may limit or prevent the success of the alternative dating approaches. Utilisation of geochemical techniques (e.g. identification of stable carbon isotope) on the fossil cores which have been employed to reconstruct saltmarsh accretion history (Dyer *et al.*, 2002; Tsompanoglou *et al.*, 2011), to identify storm records in lake sediments (Orme *et al.*, 2016) and to identify fluctuations in palaeo relative sea level, river discharge and catchment disturbance (Lamb *et al.*, 2007; Khan *et al.*, 2015) may also serve as an alternative to overcome some of the dating issues encountered and mentioned above.

11.1.6 Utilisation of Pollen Analysis as a Chronostratigraphic Marker

Generally good preservation of pollen grains was noted in the cores from Cowgate Farm and Herd Hill. The pollen analyses undertaken at Cowgate Farm and Herd Hill therefore have provided additional evidence of the broader environmental changes that have occurred in the region. For example, in core CGF1 from Cowgate Farm, the pollen assemblage, with the presence of saltmarsh species (e.g. *Aster*-type and *Artemisia*), supported the biostratigraphic changes evidenced by the presence of foraminifera in the core, that indicated a shift from a more freshwater environment into a saltmarsh environment. A change in the dominance between Cyperaceae and Poaceae in Cowgate Farm (zone CGF-4) and Herd Hill (zone HH-2) which potentially

indicated a change in environment from reed swamp to a more freshwater limnic sediment and turfa was also supported by the absence of foraminifera from the cores, which was interpreted as an indicator of marine regression from the site. The correspondence between the lithostratigraphic changes and the presence/absence of foraminifera along with the pollen analysis undertaken at Cowgate Farm and Herd Hill, has led to an increased confidence in the indicative meaning ascribed to the SLIPs obtained at the respective zones.

The pollen analyses undertaken has also provided chronostratigraphic markers when it was compared to other published pollen records. For example, although the start of zone HH-4 at Herd Hill which recorded a significant decrease of arboreal pollen was not dated, comparison was made with similar changes in pollen assemblages from other sites and related to the anthropogenic activities in the area (Chapter 8; Section 8.10).

11.1.7 Contemporary Saltmarsh Environment and Reliability of the Transfer Function Developed

A local training set was developed in this study, comprising of 72 contemporary foraminifera samples obtained from three different contemporary marshes (Chapter 4; Section 4.1). The contemporary foraminiferal samples collected in this study provided a continuous record of foraminifera covering the different tidal ranges present at each site.

For the local Solway training set, the five measured environmental parameters (elevation, pH, LOI, silt and sand) accounted for 40% of the total foraminiferal assemblage variation (Chapter 4; Section 4.5.4). From this 40%, elevation explained only 1% of the foraminiferal assemblage variation, while LOI, silt, sand and PH accounted for 4%, 2%, 2% and 8% respectively. The extremely low percentages of elevation in explaining the variation of foraminiferal assemblages may be due to the lower vertical range sampled at Skinburness Marsh, Cardurnock Marsh and Bowness Marsh (1.9, 5.0 and 4.0 metres respectively) which covered the highest astronomical tide (HAT) to mean high water neap tide (MHWNT). In comparison, the actual tidal range at each site covering HAT to mean low water spring tide (MLWST) covers a distance of 11.2, 14.2 and 11.6 metres respectively. This may result in a significantly

reduced statistical significance of elevation in explaining the total variation in foraminiferal assemblages (Mills *et al.*, 2013; Best, 2016).

Although the transect sampled at each contemporary marsh in this study covered the different saltmarsh zonation (upper, middle to lower and intertidal mudflat), the collection of more samples from the intertidal mudflat environment may have resulted in a higher statistical significance of elevation when explaining the variation of the foraminifera assemblages. For example, the tidal range sampled at Skinburness Marsh which covered the HAT to MHWNT (1.9 metres) was restricted mainly to the vegetated saltmarsh environment and accounted for 17% of the complete tidal range, while the tidal range covering MHWNT to MLWST (9.3 metres) in the intertidal mudflat environment accounted for 83% of the total tidal range but resulted in only one sample being collected. Due to the nature of the estuary which restricted the collection of more intertidal mudflat samples, only 17 samples in total were collected from the intertidal mudflat environment for the Solway training set as a whole, in comparison to 55 samples collected from the vegetated saltmarsh environment.

The transect sampled at Skinburness Marsh, Cardurnock Marsh and Bowness Marsh covered 17%, 35% and 35% of the total vertical tidal range at each site respectively. The inability to collect more samples from the intertidal mudflat environment allowing the whole tidal range to be considered, e.g. from HAT to mean tide level (MTL) or MLWST in a macrotidal estuarine settings was due to the locations being too far out into the estuary, resulting in potentially unsafe sample collection. Mills *et al.* (2013) suggested that when the sampled elevation range compared to the whole tidal range is low (<10%), the significance of the intercorrelations between the environmental variables in explaining the foraminiferal distribution at the site will be greater than that of the elevation, and this is a challenging issue that is often encountered in a macrotidal estuarine setting.

To overcome the issue of non-representation of the complete vertical tidal range in a macrotidal environment, Hill *et al.* (2007) sampled two sites within Severn Estuary and was successful in collecting samples from the complete vertical tidal range. However, despite sampling at three different saltmarshes located in the Solway Firth and Moricambe Bay and sampling a tidal range of >10%, sampling the entire tidal range was not possible. The issue on incomplete vertical tidal range sampling was

also observed in a study undertaken at the Humber Estuary, although this was mainly attributed to the land reclamation and presence of embankments within the estuary which resulted in a limited upper saltmarsh environment (Best, 2016).

The intercorrelation between the five environmental parameters accounted for 83% of the total foraminifera assemblage variation (Chapter 4; Section 4.5.4), illustrating the highly dynamic and interdependent relationship between the environmental parameters measured. The intercorrelation at Skinburness Marsh, Cardurnock Marsh and Bowness Marsh accounted for 23%, 74% and 50% respectively. The high intercorrelation between the environmental parameters is consistent with the findings of other studies undertaken in Cumbria (e.g. Zong & Horton, 1999), where the intercorrelation between the environmental parameters at Morecambe Bay accounted for 42% of the microfossil assemblage variation. As the intercorrelation between the environmental parameters for the Solway training set was 83%, high scattering between the samples was observed as a result in the local transfer function developed (Chapter 4; Section 4.7). This resulted in the poor performance of the local transfer function and the high number of poor modern analogues for the fossil samples.

The three contemporary saltmarshes investigated in this study were located in different parts of the estuary and located relatively near to the palaeo study sites, to provide the best representation of the fossil foraminiferal samples in the cores (Horton & Edwards, 2006). However, the environment of the area might have changed over time, and the present contemporary samples may no longer reflect the environment during deposition of the fossil assemblages, thus resulting in the poor modern analogues for the fossil samples. The inclusion of a single environmental parameter (elevation) within the transfer function excludes the effects of the other environmental variables, which contributed to the variation in foraminiferal assemblages (Zong & Horton, 1999). The exclusion of the other environmental parameters may also explain the high number of poor modern analogues for the fossil samples.

Apart from the low significance of elevation in explaining the foraminiferal assemblage variation thus resulting in poor modern analogues for the fossil samples, the high number of poor modern analogues was also attributed to the dissolution of the calcareous foraminiferal assemblage in the fossil cores, as discussed in Section 11.1.1

and Chapter 4 (Section 4.8). The absence of calcareous species in all of the fossil cores led to a biased assemblage dominated by the agglutinated foraminifera in all sediment sequences present in the fossil cores. This was not represented in the contemporary samples.

The dissolution of the calcareous species with only test linings present in fossil samples was also highlighted in Edwards & Horton (2000) and Edwards (2001). In an attempt to overcome the issue of the high number of fossil samples having poor modern analogues, all the calcareous species in the contemporary samples were grouped and classed as a single taxon, to be comparable to the test linings found in the fossil samples. This resulted in an agglutinated foraminifera-based transfer function that was capable of only distinguishing between the high saltmarsh environment and low saltmarsh/intertidal mudflat environment (Edwards & Horton, 2000).

Several issues however should be taken into consideration when developing the agglutinated foraminifera-based transfer function, in particular the fragile nature of the test linings itself which may be damaged or removed from the record during sediment accumulation or during sample preparation in the laboratory. When this occurs, the test linings are more likely to be under represented in the fossil samples, and therefore the total contribution of the test linings in comparison to the agglutinated species would be underestimated. The agglutinated foraminifera-based transfer function resulted in less samples having poor modern analogues, however, the transfer function developed was less precise with an increased scatter of the data, reflecting the fact that the assemblages dominated by a single calcareous component were less sensitive to changes in elevation. It was therefore concluded that the changes in the single calcareous species taxon could not be used to refine the sea-level reconstruction (Edwards & Horton, 2000).

In conclusion, the utilisation of a local training set developed from the contemporary samples collected in the Solway Firth was unsuccessful, and for this study was deemed to be an invalid method in producing a transfer function for the reconstruction of RSL changes at the palaeo study sites.

11.1.8 Summary

The methods and techniques used to reconstruct Holocene RSL changes along the Cumbrian coastline were deemed appropriate and successful. Ten new SLIPs have been produced from the sites at Allonby, Cowgate Farm, Pelutho and Herd Hill. The utilisation of transfer functions to predict the SWLI of the fossil foraminiferal assemblages based on their contemporary counterparts were however unsuccessful, and this was mainly due to the absence of calcareous foraminifera assemblages in the fossil cores as a result of dissolution of the tests. The use of a different microfossil proxy (e.g. diatoms) in addition to foraminifera, may be able to solve the issues encountered and should be considered in future studies of the area, although poor preservation of diatoms in particular within the sediments with increased sand content were also noted at some of the sites investigated in this study. The identification of suitable sites in the area which contain undisturbed and preserved sedimentary sequences, with good preservation of microfossil are therefore crucial for further reconstruction of palaeo sea-level changes along the Cumbrian coastline.

11.2 Holocene RSL Changes: Records from Allonby, Cowgate Farm, Pelutho and Herd Hill

The research undertaken in this study has revealed two episodes of Holocene RSL change, which are most likely associated with the Main Postglacial Transgression, although the transgression associated with the drainage of the glacial Lake Agassiz-Ojibway in North America may also have been represented at the sites. Holocene RSL changes were constrained at three coastal sites (Allonby, Cowgate Farm and Pelutho), and at one inner estuary site (Herd Hill). This allowed comparison of the sea-level records from the two different geomorphological settings, as well as a comparison of the RSL changes in the study area as a whole. The RSL changes observed at each site are summarised in the following sections, with the SLIPs produced from each site also presented.

11.2.1 Allonby

An episode of marine transgression was recorded at Allonby based on lithostratigraphical and biostratigraphical evidence. The transgressive contact at Allonby was evidenced by the presence of foraminifera in the silty peat with *Phragmites* unit at a depth of 1.38 m (5.62 m OD) resulting in a RSL of +0.62±1.46 m, and this marine transgression was dated at 8160-7946 cal BP. The regressive contact at Allonby indicating RSL fall at the site was dated at 7418-7255 cal BP, at a depth of 0.35 m (6.65 m OD) recording a RSL of +1.53±1.46 m. This was evidenced by the disappearance of foraminifera from core A7. The sea-level rise recorded at Allonby is most likely associated with the Main Postglacial Transgression or a combination of both Main Postglacial Transgression and the drainage of Lake Agassiz-Ojibway. The period of marine transgression at Allonby lasted for a duration of approximately 711 years.

11.2.2 Cowgate Farm

Microfossil evidence from core CGF1 suggests an episode of higher than present relative sea level occurred at the site in Cowgate Farm. A transgressive contact was evidenced by the presence of foraminifera in the peat with *Phragmites* unit at 1.11 m (6.89 m OD), and this was dated at 8200-8412 cal BP which recorded a RSL of +1.89±1.46 m. The regressive contact in core CGF1 was recorded at 0.29 m (7.71 m OD) evidenced by the absence of foraminifera in the core. This marine regression from the site at Cowgate Farm was recorded at 6557-6310 cal BP, which resulted in a RSL of +2.56±1.46 m. It is probable that the period of RSL rise at Cowgate Farm is correlated with the Main Postglacial Transgression, although the date of the transgressive contact would suggest an earlier transgression than at the other sites investigated. The period of RSL rise at Cowgate Farm lasted for approximately 1887 years. Given the longer duration of increased marine influence at Cowgate Farm, it is possible that the marine transgression recorded is a combination of both Main Postglacial Transgression and the transgression related to the drainage of the glacial Lake Agassiz-Ojibway.

11.2.3 Pelutho

Two episodes of marine transgression were recorded at the site in Pelutho based on lithostratigraphical and biostratigraphical evidence. The first period of higher than present RSL of +1.17±0.57 m was recorded at a depth of 2.89 m (5.51 m OD), corresponding to the first presence of foraminifera in the lower blue/grey silt-clay unit. The first transgressive contact at Pelutho was dated at 8174-8018 cal BP, and the date would suggest that the marine transgression into the site may have resulted from marine transgression associated with the Main Postglacial Transgression or a combination of both Main Postglacial Transgression and the drainage of Lake Agassiz-Ojibway, similar to those recorded at Allonby and Cowgate Farm. The second occurrence of foraminifera in core P12 in the organic unit at a depth of 2.40 m (6.00 m OD) recorded the second transgressive contact at Pelutho and a RSL of +0.97±0.57 m, and resulted in a date of 7435-7275 cal BP. The second episode of sea-level rise at Pelutho ceased at 7254-7016 cal BP, at a depth of 1.51 m (6.89 m OD) and a RSL of +1.82±0.56 m, which was evidenced by the disappearance of foraminifera from core P12. The duration of the first episode of marine transgression into the site is unknown. The second episode of marine transgression and regression at Pelutho was recorded over a shorter period of 221 years. The combined duration from the first transgressive contact until the final regressive contact at Pelutho was 951 years.

11.2.4 Herd Hill

Based on the lithostratigraphical and biostratigraphical evidence, an episode of higher than present RSL was recorded at Herd Hill, with the transgressive contact at 1.15 m (8.35 m OD) at a date of 7475-7322 cal BP, evidenced by the appearance of foraminifera in core HH4 resulting in a RSL of +3.88±0.56 m. The period of higher RSL at Herd Hill ceased at 6179-5914 cal BP, at a depth of 0.69 m (8.81 m OD) and recorded a RSL of +3.71±0.56 m. The episode of RSL rise at Herd Hill was recorded over the duration of approximately 1383 years and is most likely correlated with the Main Postglacial Transgression in the Solway Firth.

11.2.5 SLIPs

Ten new SLIPs for the northwest of Cumbria located on the southern shore of the Solway Firth were produced in this study (Figure 11.1).

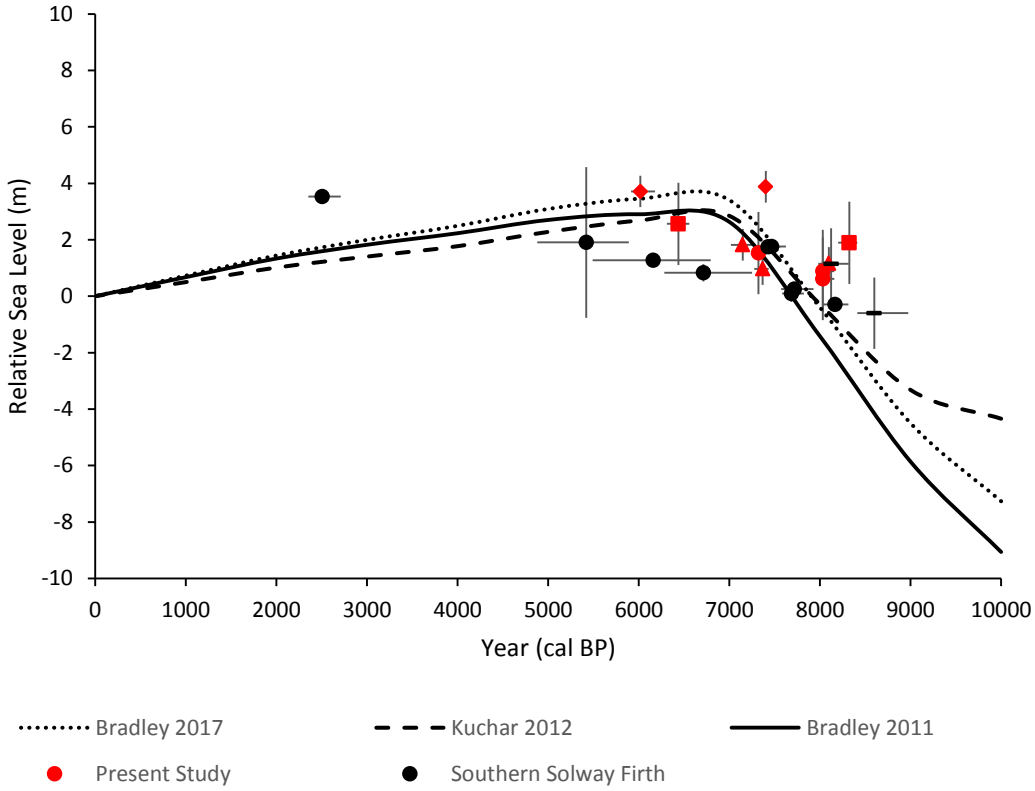

Figure 11.1: SLIPs produced in this study plotted against the available SLIPs from the southern Solway Firth. Circle symbol = Allonby; Square symbol = Cowgate Farm; Triangle symbol = Pelutho; Diamond symbol = Herd Hill; Black dashed symbol = Marine limiting dates

The SLIP obtained at Cowgate Farm (CGF-111; 8324 cal BP) has provided the earliest record of RSL rise for the southern Solway Firth, which was previously recorded at Drumburgh Moss (8125 cal BP) (Lloyd *et al.*, 1999). Apart from the regressive contact recorded at Drumburgh Moss dated at 2428 cal BP, the SLIP from Herd Hill (HH-69; 6018 cal BP) which constrained the Holocene RSL at the site has now provided the second youngest date for the region (Figure 11.1).

The SLIPs from this study show agreement with the dates of the recorded marine transgressions and marine regressions from the existing SLIPs for the southern Solway Firth (Tooley, 1974; 1978; Huddart *et al.*, 1977; Lloyd *et al.*, 1999) which

recorded the Main Postglacial Transgression in the region and with the modelled relative sea level (Bradley *et al.,* 2011; Kuchar *et al.,* 2012; Shennan *et al.,* 2018) as shown in Figure 11.1. All SLIPs plotted in Figure 11.1 have been corrected for changes in palaeo-tidal range.

11.2.6 Early to Middle Holocene RSL Changes

The ten new SLIPs obtained from Allonby, Cowgate Farm, Pelutho and Herd Hill have contributed towards the record of Holocene RSL changes along the Cumbria coastline. In particular, the new SLIPs have provided data from the region located between the southern shore of the Solway Firth and central Cumbria, with the SLIPs from Wedholme Flow the only ones available prior to this study.

The earliest record of RSL change in the region studied was recorded at Cowgate Farm, where a marine transgression was recorded at 8324 cal BP and attained a RSL of +1.89±1.46 m. At Allonby and Herd Hill, marine transgressions were recorded at 8030 cal BP and 6497 cal BP attaining RSL of +0.62±1.46 m and +3.88±0.56 m respectively. At Pelutho, two different episodes of relative sea-level rise were recorded, which began at 8097 cal BP and 7367 cal BP and resulting in RSL values of +1.17±0.57 m and +0.97±0.57 m respectively.

A similar onset of RSL rise recorded at Pelutho was recorded at Drumburgh Moss and dated at 8167 cal BP, at an altitude of 4.55 m OD (Lloyd *et al*., 1999) resulting in a RSL of -0.29±0.21 m (Table 10.3). This first marine transgression at Drumburgh Moss may have also recorded a combination of the drainage of Lake Agassiz-Ojibway in addition to the Main Postglacial Transgression in the Solway Firth. The foraminiferal assemblage zones at Drumburgh Moss showed a clear negative tendency from zone DBM-FZ2 to DBM-FZ3 (Figure 11.2, from Lloyd *et al*., 1999). A transition back to an intertidal flat assemblage in zone DBM-FZ4 representing the second positive marine tendency at Drumburgh Moss is as a result of the Main Postglacial Transgression, although this was not dated due to lack of suitable material (Lloyd *et al*., 1999).

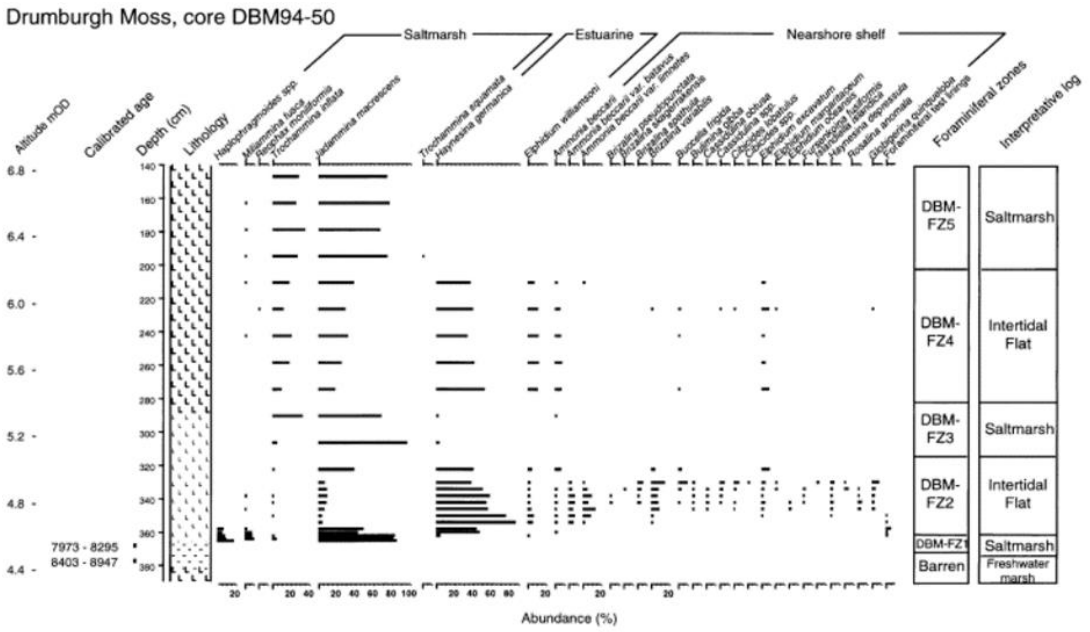

Figure 11.2: Foraminiferal diagram from Drumburgh Moss core DBM94-50 (Lloyd *et al.*, 1999)

It is therefore possible that the record from Pelutho and Drumburgh Moss have recorded two episodes of RSL changes during the early Holocene, based on the microfossil evidence of cores P12 and DBM94-50, and the lithostratigraphical evidence from core P12 (Chapter 6). It is also possible that Cowgate Farm may have recorded both events given the earlier marine transgression date (8324 cal BP) recorded and the longer duration of increased marine influence at the site.

However, based on the results obtained by Lawrence *et al.* (2016) which presented RSL data constraining the meltwater-driven sea-level rise related to the 8.2 ka event, the timing of the marine transgressions recorded at Pelutho and Drumburgh Moss occurred later than the dates obtained by the authors from their study site located in the Cree Estuary (NX 4592 6137), located on the northern Solway Firth. In the Cree Estuary, three abrupt sea-level rises (by 0.24-0.45 m, 0.67-0.73 m and 0.37-0.43 m) were recorded at 8760-8640 cal BP, 8595-8465 cal BP and 8323-8218 cal BP respectively (Lawrence *et al.*, 2016; also discussed in Chapter 2; Section 2.3.1).

Marine regressions at Allonby, Cowgate Farm, Pelutho and Herd Hill were recorded at 7320 cal BP, 6437 cal BP, 7146 cal BP and 6018 cal BP attaining RSL of +1.53±1.46 m, +2.56±1.46 m, +1.82±0.56 and +3.71±0.56 m respectively. The regressive contact recorded at Herd Hill most likely represents the end of the Main Postglacial

Transgression in the region. The much later regression at Drumburgh Moss (2505 cal BP; 6.85 m OD; RSL of +3.53±0.21 m) may have recorded a different episode of RSL changes that occurred in the second half of the Holocene, but was not recorded at the other sites (Allonby, Cowgate Farm, Pelutho, Herd Hill, Wedholme Flow, Bowness Common and Boustead Hill). It is also probable that earlier cessation of marine transgression at all of the sites apart from Drumburgh Moss was due to the difference in altitude and geomorphology of the sites.

11.2.7 Middle to Late Holocene RSL Changes

From 6018 cal BP onwards, no evidence of RSL changes were recorded at the four sites studied, in common with the records from Wedholme Flow, Bowness Common and Boustead Hill as falling sea level does not create the inland accommodation space for sea-level archives to be preserved well compared to an event of increased sea level. Only one SLIP from Drumburgh Moss constrained the RSL on the southern shore of the Solway Firth for the later part of the Holocene (Figure 11.1).

On the northern shore of the Solway Firth, only one SLIP constrained the second half of the Holocene, recording the last marine regression for the area. The regressive contact at Newbie Cottages (NY 1844 6449) was dated at 4847 cal BP (at 8.18 m OD), with marine regression at the other sites on the northern shore of the Solway Firth occurring earlier at approximately 7500-7000 cal BP (Lloyd *et al.*, 1999). The lack of evidence for a RSL rise in the mid-late Holocene along the northern Solway Firth would support the hypothesis suggesting that the isostatic land rebound had outpaced any RSL rise which occurred in that period. At sites located in the Cree Estuary further west in the Solway Firth, in addition to the Main Postglacial Transgression, a second episode of RSL rise was recorded at 5800 cal BP, with the regressive contact dated at 3100 cal BP (Wells, 1997; Smith *et al.*, 2002). The authors concluded that the marine transgression which occurred in the middle Holocene was however locally variable, with the cessation of the transgression occurring earlier further upstream, and later at sites located south of the river.

In southern Cumbria however, an episode of RSL rise which occurred in late Holocene was recorded at Morecambe Bay (Zong & Tooley, 1996), with the transgression dated at 3915 cal BP (6.19 m OD) and the regressive contact dated at 3631 cal BP (6.23 m

OD). A transgressive contact was also recorded at Skelwith Pool, Morecambe Bay and this was dated at 4403 cal BP (4.43 m OD; RSL of +0.20±0.20 m) (Zong & Tooley, 1996). As the sites investigated in this study are located closer to the centre of isostatic rebound in Scotland in particular, it is possible that the isostatic rebound of the land in the study area had outpaced the RSL rise that occurred later in the Holocene (which was more evident in Morecambe Bay as it is located farther away from the centre of isostatic rebound hence experiencing more land subsidence than sites located in north Cumbria).

11.2.8 Comparison between the Coastal Sites and the Inner Estuary Site

The marine transgression during the early Holocene is recorded to have occurred earlier at the open coastal sites; at 8324 cal BP at Cowgate Farm, at 8030 cal BP at Allonby and at 7367 cal BP at Pelutho compared to the inner estuary site at Herd Hill, recorded at 7401 cal BP, although Cowgate Farm possibly recorded an earlier marine transgression in addition to the Main Postglacial Trangsression. The marine transgression at Herd Hill is however consistent with the transgression recorded at sites located in the inner estuary at Wedholme Flow (7718 cal BP), Bowness Common (7686 cal BP) and Boustead Hill at 7465 cal BP (Huddart *et al.*, 1977; Lloyd *et al.*, 1999). Drumburgh Moss recorded an earlier transgression at 8167 cal BP, and as discussed previously in Section 11.2.6, may relate to a different and earlier transgression which was also recorded at Pelutho (8097 cal BP).

The marine regression at Allonby, Cowgate Farm, Pelutho and Herd Hill was recorded at 7320 cal BP, 6437 cal BP, 7146 cal BP and 6018 cal BP respectively, and probably represents the end of the Main Postglacial Transgression. Compared to the three open coastal sites, the decrease in RSL was recorded later in the inner estuary site at Herd Hill, and the date obtained (6018 cal BP) is more consistent with the regressive contacts at Wedholme Flow and Bowness Common which were recorded at 6159 cal BP and 6714 cal BP respectively (Huddart *et al.*, 1977).

RSL attained a higher altitude at Herd Hill (+3.88±0.56 m) during the marine transgression, in comparison to Allonby (+0.62±1.46 m), Cowgate Farm (+1.89±1.46 m) and Pelutho (+1.17±0.57 m). This is likely due to the relatively shallow depth, funnel shape and tide dominated nature of the Solway Firth estuary, with the spring

tidal range and the difference in ebb and flood duration increasing along the estuary as evidenced by the measurement of tidal range at the contemporary saltmarshes in this study (Chapter 4; Section 4.2). The increase of tidal range along the estuary was also supported by the tidal data obtained from the model by Hill (personal communication, 8th May 2018) where the tidal range at the coast nearest to the site at Allonby, Cowgate Farm, Pelutho and Herd Hill were measured at 7.84 m, 7.85 m, 7.86 m and 7.90 m respectively.

11.2.9 Comparison with Geophysical Model Predictions

The altitudes of the Main Postglacial Transgression shorelines identified at the four sites investigated in this study were compared to the RSL isobase map predicted by Smith *et al*. (2012). Smith *et al*. (2012) predicted that the RSL as a result of the Main Postglacial Transgression should occur at approximately 2 m OD to 4 m OD in the Solway Firth region. Based on the lithostratigraphical and biostratigraphical evidence, the RSL during the Main Postglacial Transgression at Allonby, Cowgate Farm, Pelutho and Herd Hill are predicted to have reached approximately 0.20 m OD, 0.96 m OD, 0.23 m OD and 4.97 m OD respectively. At Allonby and Pelutho, the Main Postglacial Transgression shoreline lies approximately 1.8 metres lower than those predicted in the model. The Main Postglacial Transgression shoreline at Cowgate Farm lies within 1 metre of the predicted shoreline in the model. At Herd Hill, the shoreline lies at 4.97 m OD, which is approximately 1 metre higher than that predicted in the model by Smith *et al*. (2012). The highest Main Postglacial Transgression shoreline observed at Herd Hill was attributed to the location of the site in the inner estuary, hence affected by the funnelling effect of the estuary (Section 11.2.8). The models in Smith *et al*. (2012) did not predict a significant difference between the west and east Solway Firth, with the principal gradient being towards the south. The altitudes of the Main Postglacial Transgression shorelines at the sites investigated in this study appear to have a southward gradient, although the influence of the Lake District ice mass in the model is unclear (Smith *et al*., 2012; Smith, personal communication 5th May 2018).

The Holocene RSL curve from the model predictions in Bradley *et al.* (2011), Kuchar *et al.* (2012) and Shennan *et al*. (2018) for the south Solway Firth region were also compared with the altitudes of SLIPs produced in this study. The background on each

model compared in this section is discussed in Chapter 2 (Section 2.4). The difference in altitude of relative sea level predicted by the models compared to those obtained from SLIPs produced in this study is shown in Figure 11.3.

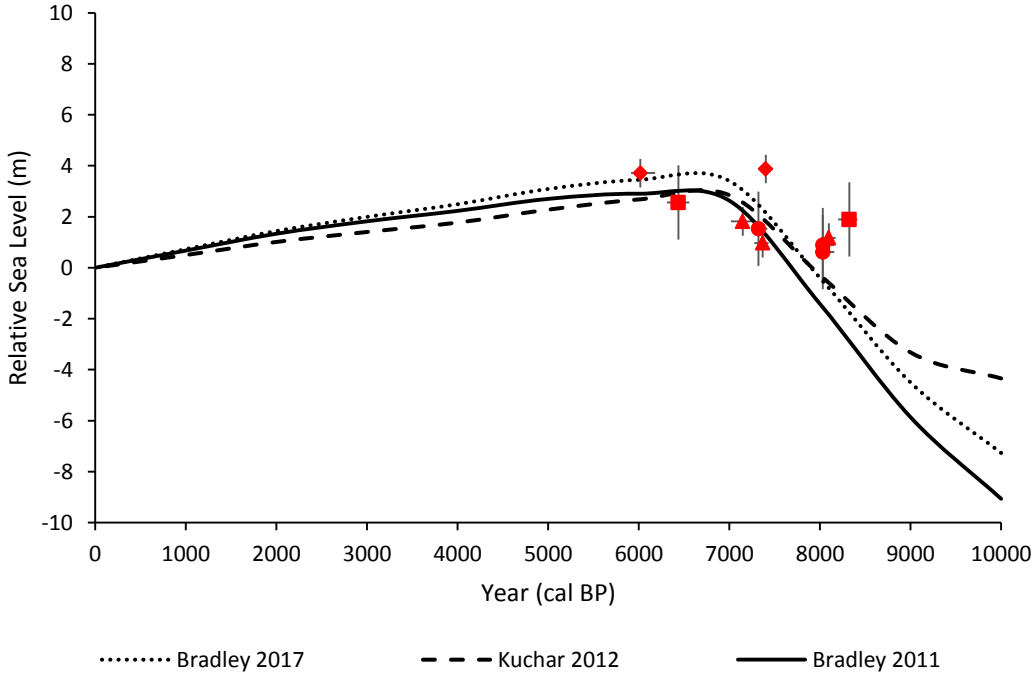

Figure 11.3: SLIPs produced in this study plotted against three geophysical model predictions. Circle symbol = Allonby; Square symbol = Cowgate Farm; Triangle symbol = Pelutho; Diamond symbol = Herd Hill

Data obtained in this study showed a reasonable agreement with the Holocene RSL trend based on the three models from approximately 8500 cal BP to 7500 cal BP, recording an RSL rise in the southern Solway Firth (Figure 11.1). The RSL model predictions based on Bradley *et al*. (2011), Kuchar *et al*. (2012) and Shennan *et al*. (2018) at approximately 8500 cal BP to 8000 cal BP however consistently suggested a lower RSL than evidenced by the data obtained in this study, and those in Lloyd *et al*. (1999), Huddart *et al*. (1977) and Tooley (1974; 1978), as shown in Figure 11.1. The RSL prediction based on the model by Kuchar *et al*. (2012) showed the least discrepancies when compared to the SLIPs in this study.

It is possible that the discrepancies between the SLIPs and the three model predictions between the period of 8500 cal BP to 8000 cal BP is due to the increase of RSL due to the input of freshwater as a result of the collapse of the glacial Lakes Agassiz-Ojibway, which recorded a RSL rise in the Cree Estuary (Lawrence *et al*.,

2016). The contribution of freshwater into the ocean which resulted in an eustatic sea-level rise may have not fully been considered in the geophysical models, leading to a mismatch between the SLIPs and the model's predictions.

Discrepancies between both Bradley *et al*. (2011) model and the data obtained in this study however decreased from 7500 cal BP onwards, illustrating a better fit between the two. Discrepancies between the calculated SLIPs which recorded marine regressions at the sites and the model was at a minimum of 0.19 metres (HH-69) and a maximum of 1.79 metres (ALL-35). The discrepancies from 7500 cal BP onwards also showed a general reduction for the Kuchar *et al*. (2012) and Shennan *et al*. (2018) models, ranging between 0.03 to 2.00 metres and 0.74 to 2.56 metres respectively.

The Bradley *et al*. (2011) model predicted a Holocene RSL maximum at 6000 cal BP, with relative sea level approximately 2.90 metres higher than present, while the Kuchar *et al*. (2012) and Shennan *et al*. (2018) models predicted a sea-level maximum at 7000 cal (2.84 metres) BP and 6000 cal BP (3.45 metres) respectively. The earliest marine regression in the region was recorded at 7320 cal BP at Allonby, followed by Pelutho at 7146 cal BP and Boustead Hill at 7090 cal BP. The field data therefore suggest an earlier cessation of marine transgression in the region compared to the Bradley *et al*. (2011) and Shennan *et al*. (2018) models (difference of approximately 1000 years), although the marine regression recorded in this study was better predicted by the Kuchar *et al*. (2012) model. The geographical and geomorphological variations between the different sites may also have resulted in the discrepancies in the timings recorded, as marine regressions were recorded at Cowgate Farm and Herd Hill at 6437 cal BP and 6018 cal BP respectively, resulting in a better fit with the trends predicted by the model of Bradley *et al*. (2011) and Shennan *et al*. (2018).

The SLIPs from the northern Solway Firth that have been corrected for changes in palaeo-tidal were also plotted against the Holocene RSL trend based on the three geophysical models, and were divided into those located in the northwest Solway Firth which were mostly obtained along the coastline of the Cree Estuary (Figure 11.4a) and those produced from other sites located on the northern Solway Firth coastline (Figure 11.4b).

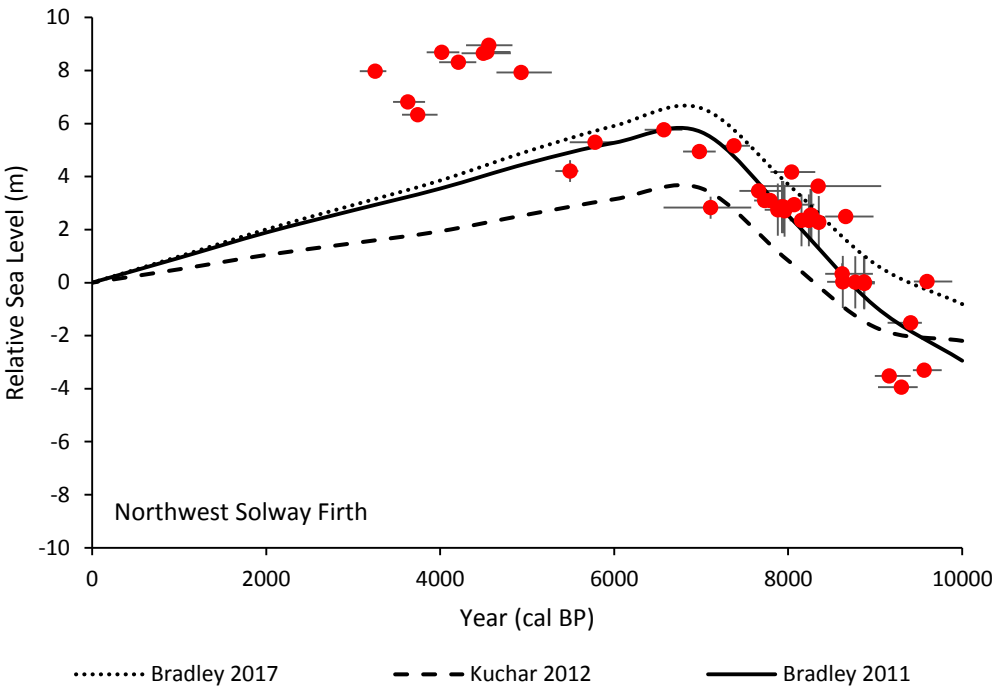

(a)

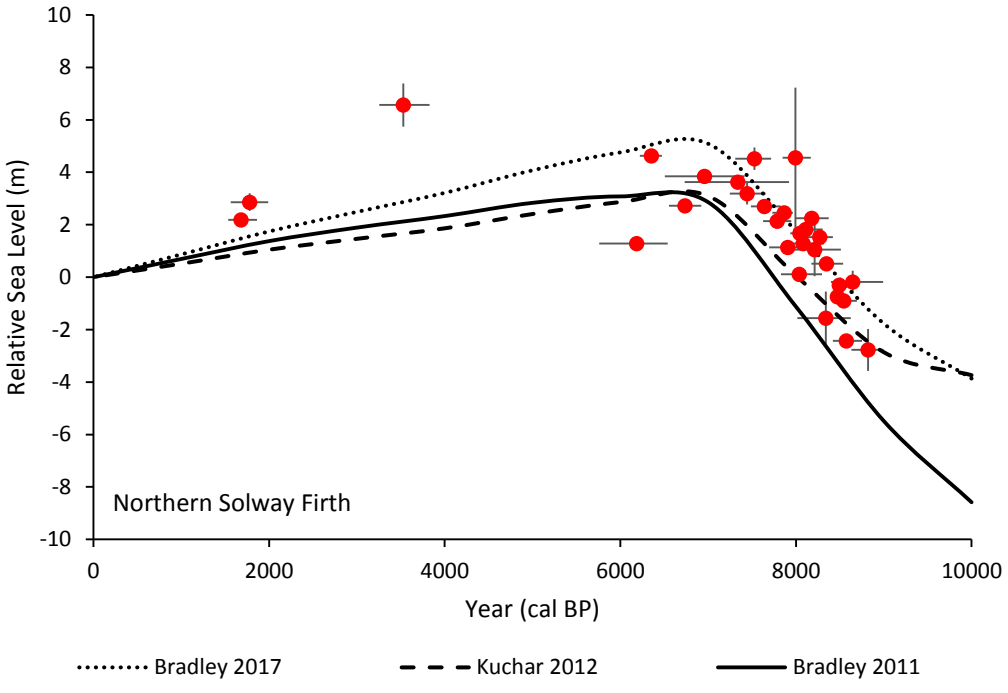

(b)

Figure 11.4: SLIPs corrected for changes in palaeo-tidal range from (a) Northwest Solway Firth and (b) Northern Solway Firth plotted against three geophysical model predictions

For the period between 10,000 BP to 5000 BP, the SLIPs from northwest and northern Solway Firth show generally good agreement with the RSL predicted by Bradley *et al.* (2011), Kuchar *et al.* (2012) and Shennan *et al.* (2018). However, from 5000 BP onwards, the RSL recorded by the SLIPs in both regions showed significantly higher values than those predicted by all three models. This was less evident prior to the correction for changes in palaeo-tidal range in both regions (Figure 11.5).

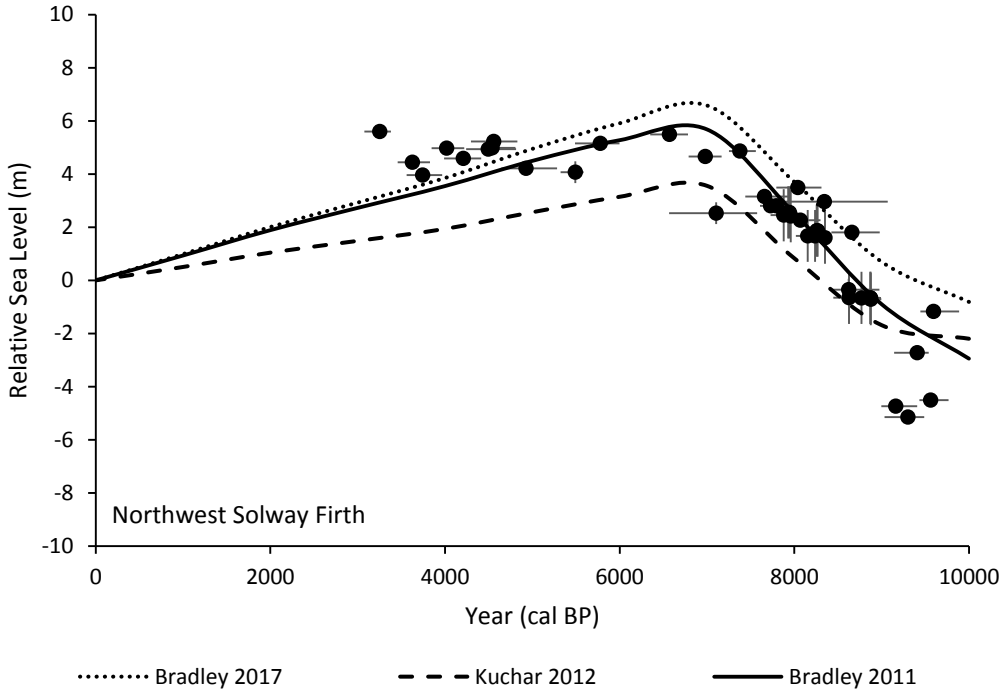

(a)

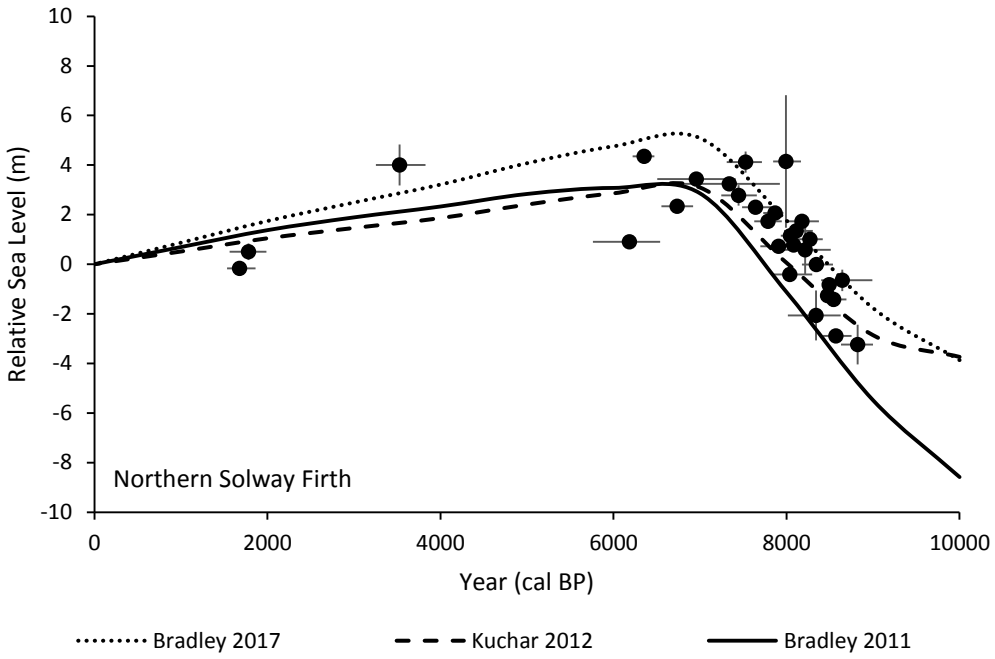

(b)

Figure 11.5: Uncorrected SLIPs from (a) Northwest Solway Firth and (b) Northern Solway Firth plotted against three geophysical model predictions

There appears to be a misfit between the three geophysical models and the RSL values between 5000 BP to 2000 BP in the northwest and northern Solway Firth (Figure 11.4). The data obtained from the SLIPs prior to the correction of changes in palaeo-tide were incorporated into the geophysical models to produce the RSL trends for the region (Bradley *et al.*, 2011; Kuchar *et al.*, 2012; Shennan *et al.*, 2018). Therefore the importance of quantifying the changes in palaeo-tidal range is demonstrated in order to refine the RSL predictions from the geophysical models. It is also worth noting that a limitation to this approach is that the palaeo-tidal model used in this study utilised the RSL predictions from the geophysical model developed by Bradley *et al.* (2011), with some of the data utilised in the model included uncorrected SLIPs from the Solway Firth.

11.2.10 Differential Crustal Rebound between Northern and Southern Solway Firth

To test the hypothesis that differential crustal rebound can be observed between the north and south Solway Firth coastline, a third order polynomial best line was drawn through the two different datasets: the SLIPs from the southern Solway Firth and those from the northern Solway Firth (Figure 11.6).

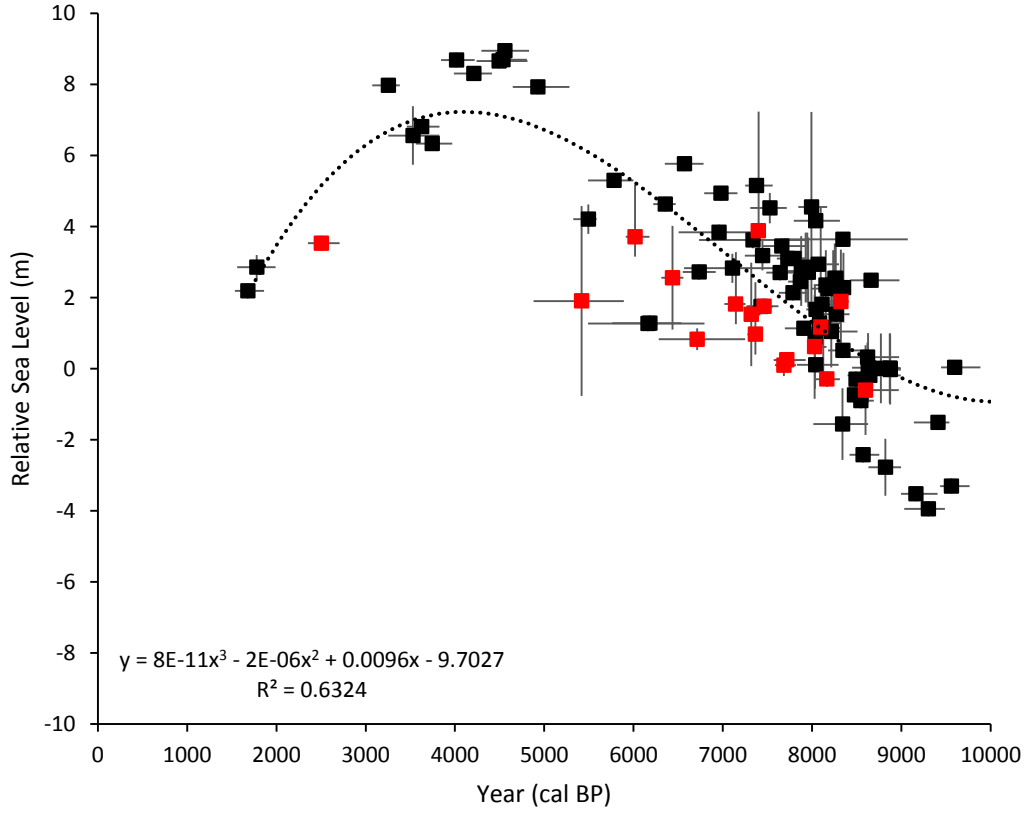

Figure 11.6: A 3rd order polynomial best fit line drawn against the full dataset of available SLIPs from the southern Solway Firth (red symbol) and northern Solway Firth (black symbol)

If differential crustal movement along the northern and southern coasts of the Solway Firth is absent or minimal, a random scatter between the two sets of data in each graph would be expected, i.e. the data points fall randomly above and below the best fit line, which may potentially indicate that there is minimal differential crustal movements between the two localities. The graph in Figure 11.6 showed a clear distinction between the SLIPs from the two localities, indicating that differential

crustal movement between the northern and southern Solway Firth exists. All SLIPs produced in the southern Solway Firth fell below the best fit line apart from two SLIPs (HH-69 and CGF-111), with the majority of the SLIPs from northern Solway Firth lying above the best fit line. The data points from northern Solway Firth that fell below the best fit line mainly before 8500 cal BP may have resulted from the inadequacy of the best fit line, in the time period where only SLIPs from one of the two localities are available (Lloyd *et al.*, 1999).

The difference in RSL values observed between the northern Solway Firth data and the southern Solway Firth data could potentially be a result of different factors. These include the re-advances of Scottish ice (e.g. during the Loch Lomond Stadial), that may have influenced isostatic recovery of the northern coastline to a greater extent than the southern shore as it is located farther away from the centre of the ice mass. The effect of the local Lake District ice mass on the crustal uplift could also cause RSL to be different on the northern and southern shores of the Solway Firth. It is also possible that the local geomorphology of the coastline, could result in different RSL records, particularly when considering open coastal sites and inner estuarine locations.

11.2.11 Palaeogeography in the Solway Firth

Simplified palaeogeographical maps for the Solway Firth for the period from 8 ka BP to 5 ka BP have been constructed using the corrected SLIPs for the region (Figure 11.7). Palaeogeographical maps were not drawn for the period of 10 ka BP, 9 ka BP and 4 ka BP to 1 ka BP due to the low number of SLIPs constraining the changes observed as this may lead to an erroneous or over-generalised prediction in the maps produced. For the time periods constrained by very few data, the influence of RSL in the Solway Firth as a system may not be accurately represented. The incorporation of surveyed geomorphological features that relates to the time period, could potentially assist in the palaeogeographical reconstructions and particularly in areas devoid of SLIPs.

The black shaded areas represent environments classed as terrestrial (no marine influence) and the white shaded areas represent environments classed as marine (i.e.

subtidal, intertidal/mudflat and saltmarsh). The red line represents the present day coastline.

Two assumptions were made when drawing each of the palaeogeographical maps: that the geomorphological features and the altitude of the coastline in the Solway Firth, had remained constant throughout the period between 8 ka BP to 5 ka BP. The expansion and contraction of the estuary are therefore based solely on the information derived from the SLIPs available for the Solway Firth.

To generate the palaeogeographical maps of the study region, a digital terrain model (DTM) obtained from ArcGIS online image service database (ESRI, 2011) was input into ArcMap v.10.5.1. The DTM provided the elevation information of the specific data points for the study area. The SLIPs for the time period selected at specific locations were then imported into the map, allowing the extent of marine inundation in the region to be plotted. All land that lies below the highest altitude reached by RSL in the Solway Firth (based on the SLIPs available for that particular time period) are assumed to have been inundated by the sea and therefore were classed as marine on the map. The elevation range in the DTM was then converted into a polygon (allowing extrapolation between the SLIPs) and reclassified using the classify tool in the software based on the highest altitude attained by the SLIPs. This enabled the map to be divided into either marine or terrestrial regions.

Table 11.1: SLIPs utilised in the palaeogeographical maps for each time period

Time (ka BP)	No. of SLIPs Available	Lab Code
8	37	GU4649, Beta100918, GU4657, Beta100916, GU64, UB3897, UB3891, SUERC44398, UB3892, GU4646, BIRM325, SUERC44397, SUERC44371, SUERC42711, GU4654, BIRM222, Beta100917, GU4650, SUERC44386, GU4658, GU4647, GU4653, UB3902, UB3894, Beta100914, SUERC44387, GU375, Beta100915, SUERC42709, UB3903, SUERC44385, SUERC44369, SUERC42708, D-AMS 022223, D-AMS025776, D-AMS016392, D-AMS022227
7	25	BIRM189, BIRM324, Beta96322, B103262, BIRM415, UB4054, Q638, GU4656, Beta100919, HV6208, HV5228, SUERC44407, GU4645, SUERC44406, UB3895, SUERC44400, GU4652, SUERC42712, SUERC44399, SUERC44405, GU4648, D-AMS 022222, D-AMS 025778, D-AMS 022226, D-AMS 022225
6	10	HV4713, BIRM258, Beta120963, Beta96321, HV6207, GU4655, UB3899, Beta105932, D-AMS 016391, D-AMS 022224
5	4	HV4714, SRR26, HV4418, Beta96320

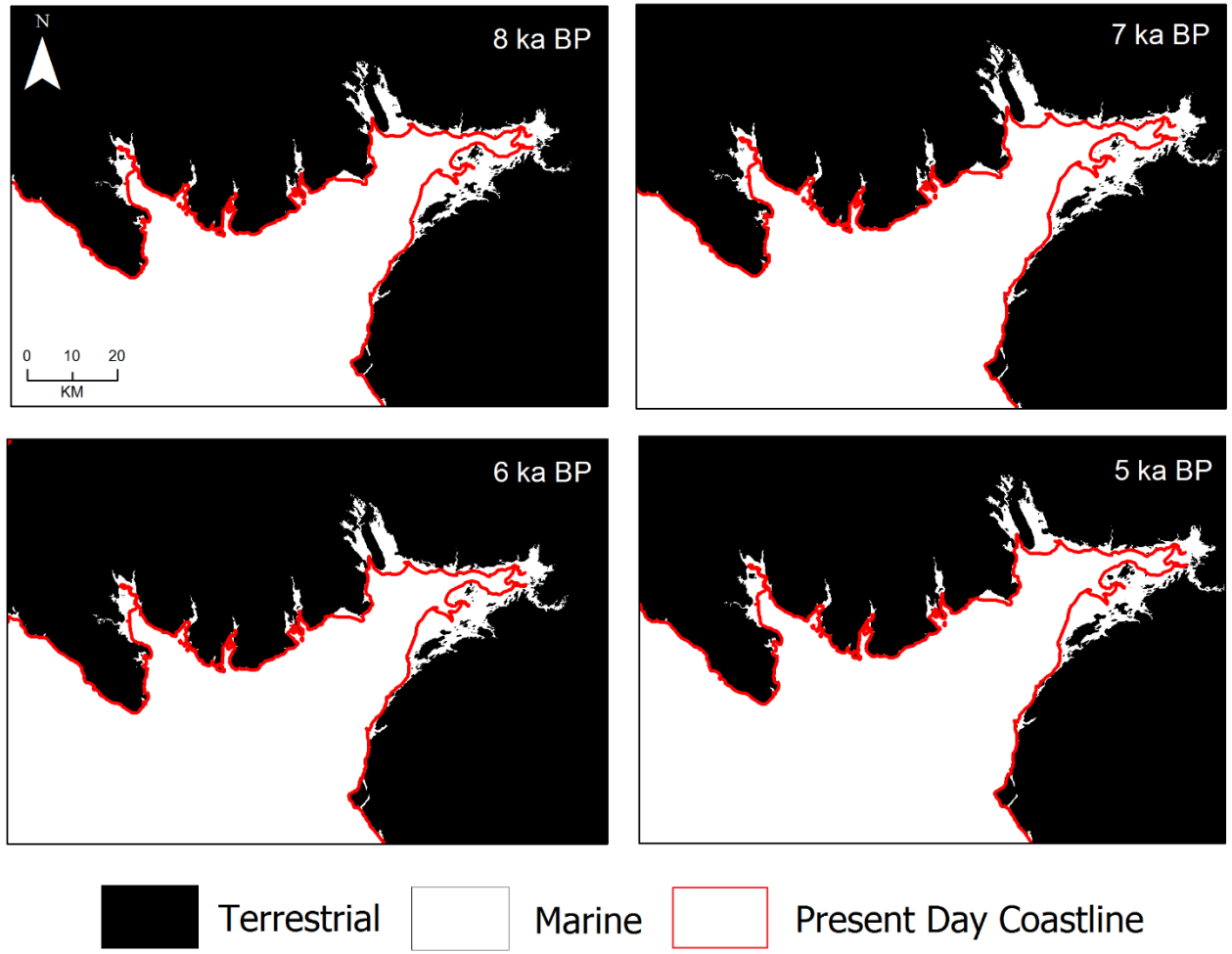

Figure 11.7: Palaeogeographical maps for the Solway Firth from 8 ka BP to 5 ka BP illustrating the reconstruction of HAT position over time, based upon SLIPs corrected for changes in palaeo-tidal range

The expansion of the estuarine environment is evidenced at 8 ka BP, 7 ka BP, 6 ka BP, while the contraction of the estuary is evidenced from 5 ka BP, in particular for the Solway Lowlands on the southern shore of the Solway Firth, corresponding to the Main Postglacial Transgression in the region. This was also shown in the palaeo-tidal maps for the Solway Firth, where palaeo-tidal range in the region increased during the same time period between 8 ka BP to 5 ka BP (Chapter 10; Figure 10.1), and further supported by the relative sea-level rise recorded by the SLIPs obtained in the Solway Firth (Figure 11.3 and Figure 11.4).

11.2.12 Summary

The reconstruction of Holocene relative sea level in the study area was produced through analyses of cores collected from three coastal sites (Allonby, Cowgate Farm and Pelutho) and one inner estuary site (Herd Hill). Two episodes of marine transgression in the early Holocene resulting in RSL changes along the northwest Cumbrian coastline were recorded and constrained in this study and ten new SLIPs were produced. The overall trend of the RSL changes recorded in this study is consistent with previous work, with the earliest record of transgression recorded at Cowgate Farm at 8324 cal BP (+1.89±1.46 m), and the latest regression recorded at Herd Hill at 6018 cal BP (+3.71±0.56 m). The ten new SLIPs now constrain the early Holocene RSL changes in the coastal region located between the southern shore of the Solway Firth and central Cumbria, where very few SLIPs existed prior to this study. The Main Postglacial Transgression shoreline predicted by Smith *et al*. (2012) is lower compared to the field data observed in this study, while the RSL predictions in Bradley *et al.* (2011), Kuchar *et al.* (2012) and Shennan *et al*. (2018) also showed discrepancies and had potentially underestimated the relative sea-level increase for the period between 8500 to 7500 cal BP and between 5000 to 2000 cal BP, suggesting more field data is needed to improve the models' predictions. The potential evidence of differential crustal rebound between the northern and southern shores of the Solway Firth was also illustrated based on the corrected SLIPs obtained from the two localities. The importance of correcting for changes in palaeo-tidal range was also highlighted, where tidal range in the Solway Firth increased significantly during the Main Postglacial Transgression (between 8 ka BP to 5 ka BP), which led to an underestimation of the RSL recorded through most of the SLIPs from the Solway Firth for that period.

CHAPTER 12

CONCLUSION

12.0 Introduction

This chapter will summarise the main conclusions of the reconstruction of Holocene relative sea-level changes along the northwest Cumbrian coastline. An assessment on the methods and techniques undertaken in this study will be reviewed and a summary on the wider implications of the research and recommendations for future work in the study area are presented.

12.1 Relative Sea-Level Changes along the Northwest Cumbria Coastline

Relative sea-level (RSL) changes were identified in the study area, with the earliest marine transgressions recorded at Allonby, Cowgate Farm and Pelutho. This is most likely correlated to the Main Postglacial Transgression, although it is possible that the transgression associated with the glacial Lake Agassiz-Ojibway flood is also represented. At Allonby, this marine transgression is thought to have started at 8030 cal BP, recording a RSL of +0.62±1.46 m, at Cowgate Farm at 8324 cal BP with RSL of +1.89±1.46 m, evidenced by the change in biostratigraphy of the core and at Pelutho at 8097 cal BP resulting in a RSL of +1.17±0.57 m, evidenced by the changes in the lithostratigraphy and supported with the occurrence of foraminifera. The second episode of RSL higher than present thought to be related to the Main Postglacial Transgression was potentially recorded at all four sites investigated in this study. At Allonby and Cowgate Farm, the increased RSL as a result of the Main Postglacial Transgression was believed to have continued and overlapped with the earlier episode of marine transgression, evidenced by the continuous presence of foraminifera within the sediment unit and the longer duration of increased marine influence recorded at the site. At Pelutho, the second marine transgression was dated at 7367 cal BP, resulting in a RSL of +0.97±0.57 m. At Herd Hill, the Main Postglacial Transgression was likely to have been recorded at 7401 cal BP with RSL of

+3.88±0.56 m. The higher attitude attained at Herd Hill compared to the other sites was attributed to the funnel shape effect of the estuary, with the site located in the inner estuary compared to the open coastal settings of Allonby, Cowgate Farm and Pelutho. The cessation of the Main Postglacial Transgression was recorded the earliest at 7320 cal BP (6.65 m OD; RSL of 1.53±1.46 m) at Allonby. The regressive contacts at Cowgate Farm, Pelutho and Herd Hill were recorded at 6437 cal BP (7.71 m OD; RSL of +2.56±1.46 m), 7146 cal BP (6.89 m OD; RSL of +1.82±0.56 m) and 6018 cal BP (8.81 m OD; RSL of +3.71±0.56 m) respectively. No subsequent increase in RSL was recorded at the sites investigated in this study, as it is probable that the glacio-isostatic rebound of the land in the study area had outpaced any increase in eustatic sea level that occurred in the late Holocene.

12.2 Methodological Conclusions

The multidisciplinary approach employed in this study has provided a greater insight into the history of Holocene relative sea level in the study area. For example, at Cowgate Farm, where lithostratigraphic changes were not apparent, the microfossil evidence provided a record of increased RSL at the site, illustrating a change from a freshwater environment into a saltmarsh environment. The foraminiferal analysis undertaken at all four sites provided a detailed record of marine transgressions and regressions, supporting the lithostratigraphical changes observed. The survey of contemporary foraminifera from the three saltmarshes located close to the palaeo sites clearly illustrated the variation in foraminiferal assemblages between the different intertidal environments.

The development and use of transfer functions in this study was ultimately deemed unreliable and therefore was unsuccessful in providing higher resolution estimates for the fossil samples. The local training set developed resulted in a large scatter between the predicted and observed sea water level index (SWLI), and this was attributed to the lack of contemporary samples from the intertidal mudflat environment (i.e. not covering the complete tidal elevation range). The training set developed in this study also resulted in a large number of fossil samples with no modern analogues, and this

issue was attributed mainly to the dissolution of calcareous foraminifera in all of the fossil cores.

The utilisation of pollen analysis has been recognised in this study, in particular as a chronostratigraphic marker when compared to published pollen records. The pollen records obtained from Cowgate Farm and Herd Hill also provided additional information about the vegetation and coastal changes at the sites in response to the fluctuations in RSL. The importance of correcting for changes in palaeo-tidal range and post-depositional lowering of sediments when utilising intercalated samples for the reconstructions of Holocene RSL were also demonstrated, although the effect of both palaeo-tidal changes and post-depositional compaction of the sediments appears to be minimal for the new sea-level index points (SLIPs) produced in this study.

12.3 Wider Implications of the Research

The results obtained from this study, and the discussion presented in this thesis, have wider implications for Holocene RSL research, especially for studies undertaken in a macrotidal estuarine settings. This study has produced new records of Holocene sea-level change from a previously understudied region located on the southern shore of the Solway Firth (Chapter 5, 6, 7, 8 and 9), through the development of 10 new SLIPs which will now improve the understanding, information and data available for the region (e.g. to refine the RSL prediction based on geophysical models in the future).

The challenges and problems encountered while undertaking sea-level research in a macrotidal estuarine settings were also highlighted in this study. The issue of sampling the complete tidal range to produce a good performing transfer function was discussed (Chapter 4 and Section 11.1.7), as well as the issue of fossil samples having poor modern analogues as a result of dissolution of calcareous species in fossil cores (Chapter 4; Section 4.8). When collecting samples from different locations along a macrotidal estuary, the variation in the tidal range along the coastline should be considered and quantified. The tidal survey undertaken in this study showed an increase of tidal range from the outer estuary into the inner estuary, which potentially

affected the foraminiferal assemblage and other environmental parameters at respective sites. Failing to quantify the tidal variations along the estuary will therefore likely lead to an erroneous indicative meaning assigned to the SLIPs, as well as problems when developing a local transfer function based on the samples collected.

The measurement of modern tidal variation along Moricambe Bay and the southern shore of the Solway Firth had illustrated that variation in tidal range (HAT difference of approximately 1 metre) exists along the estuary, even for sites located approximately 3 km apart (e.g. Skinburness Marsh and Cardurnock Marsh). However, as some of the palaeo sites are located more closely to each other (less than 1 km apart, e.g. sites located within the same sub-estuary), the tidal variation may not be accurately modelled as the spatial resolution of the palaeo-tidal model is 1 km. Increasing the palaeo-tidal model's resolution may be able to resolve the issue, leading to a more precise calculation of changes in RSL in the region.

The contemporary foraminiferal and environmental parameter data presented in this study (Chapter 4) are the first available from the southern Solway Firth, with the contemporary data from the Nith Estuary located on the northern Solway Firth the only set of data available prior to this study. Samples collected from the contemporary saltmarshes near to the palaeo study sites is important when ascribing the indicative meaning of the SLIPs produced, in order to provide the best representation for the fossil samples.

Changes in palaeo-tidal range for the SLIPs available for the Solway Firth were also quantified for the first time in this study. The results obtained based on the palaeo-tidal model developed by Hill (personal communication, 8th May 2018) and the calculations have shown that prior to the correction of changes in palaeo-tidal range, RSL in the Solway Firth was underestimated by up to ~5 metres (Chapter 10). The corrected SLIPs from the northern and southern shores of the Solway Firth will now provide more precise data for future research in the region.

Based on the newly produced and corrected SLIPs from the region, the differential crustal movement between the northern Solway Firth and the southern Solway Firth

which resulted in variation of relative sea-level values was illustrated in this study. Comparison between the corrected SLIPs and three geophysical model RSL predictions was made. Based on the results obtained, the discrepancies between the SLIPs and the model predictions highlighted the need for more field data in order to improve the model predictions, especially for the time period where very few SLIPs exist at present.

12.4 Recommendations for Future Work

To produce new constraints for Holocene RSL changes of the region in the future, extensive surveying and microfossil work would be required to identify sites that contain preserved sediment sequences and microfossils. The issue of the preservation of microfossils at the sites is crucial, as foraminifera (and diatoms) may be poorly preserved due to the nature of the sediment present at the sites. Therefore, the utilisation of geochemistry-based techniques and methods (discussed in Chapter 11; Section 11.1.5) may be considered in the future for the reconstruction of Holocene RSL history to overcome the issue of the poor microfossil preservation. The potential effects of the Lake District ice mass on the differential isostatic rebound of the land in Cumbria may also be further explored in the future, to better understand the complex relationship between land uplift and sea-level changes in the region. Another aspect of research that may potentially inform studies of Holocene RSL changes in the area concerns the formation of the sand dune system that is present along the southern coastline. A better understanding of the changing coastal geomorphology in the region as a result of increased RSL, may in turn lead to an improved interpretation regarding the variation in the cessation of marine influence observed at different sites investigated.

12.5 Summary

The overall aim of this study was to reconstruct the Holocene RSL changes for the northwest Cumbrian coastline and therefore the illustration of different RSL records between the northern and southern Solway Firth, and this was successfully undertaken through the development of ten new SLIPs constraining the period between 8324 cal BP to 6018 cal BP. Two possible episodes of RSL higher than present were evidenced from the four sites investigated, most likely related to the Main Postglacial Transgression, or a combination of the final drainage of the glacial Lake Agassiz-Ojibway and the Main Postglacial Transgression. Some of the challenges and issues encountered in reconstructing relative sea-level reconstruction were also highlighted, and recommendations for future work in the area were made. It is therefore hoped that this study has contributed to the knowledge of the history of Holocene RSL changes in northwest Cumbria in particular, and more generally of that along the southern coast of the Solway Firth.

APPENDIX

Unique Sample ID	Reference	Region Code	Sub-Region	Lat.	Long.	Dating Method	Radiocarbon Age (^{14}C a BP)	Radiocarbon Age Uncertainty (^{14}C a)
D-AMS 022222	Allonby (NY09494410)	3	S Solway Firth	54.78	-3.41	1	6377	34
D-AMS 025776	Allonby (NY09494410)	3	S Solway Firth	54.78	-3.41	1	7209	41
D-AMS 022223	Allonby (NY09494410)	3	S Solway Firth	54.78	-3.41	1	7203	49
D-AMS 016391	Cowgate Farm (NY09674737)	3	S Solway Firth	54.81	-3.41	1	5655	50
D-AMS 016392	Cowgate Farm (NY09674737)	3	S Solway Firth	54.81	-3.41	1	7521	55
D-AMS 022226	Pelutho (NY12024920)	3	S Solway Firth	54.83	-3.37	1	6231	35
D-AMS 025778	Pelutho (NY12024920)	3	S Solway Firth	54.83	-3.37	1	6456	45
D-AMS 022227	Pelutho (NY12024920)	3	S Solway Firth	54.83	-3.37	1	7285	36
D-AMS 022224	Herd Hill (NY17946010)	3	S Solway Firth	54.93	-3.29	1	5236	46
D-AMS 022225	Herd Hill (NY17946010)	3	S Solway Firth	54.93	-3.29	1	6497	36

APPENDIX

Unique Sample ID	Age (cal a BP)	Age 2σ Uncertainty + (cal a)	Age 2σ Uncertainty - (cal a)	Sample Depth/Overburden Thickness (m)	Depth to Consolidated Substrate (m)
D-AMS 022222	7320	98	65	0.35	1.35
D-AMS 025776	8031	127	77	1.00	0.70
D-AMS 022223	8030	130	84	1.39	0.31
D-AMS 016391	6437	88	124	0.29	1.23
D-AMS 016392	8324	156	114	1.11	0.41
D-AMS 022226	7146	108	130	1.51	1.64
D-AMS 025778	7367	68	92	2.40	0.75
D-AMS 022227	8097	77	79	2.89	0.26
D-AMS 022224	6018	161	104	0.69	0.99
D-AMS 022225	7401	74	79	1.15	0.53

APPENDIX

Unique Sample ID	Sample Elevation (m MSL)	Sample Elevation Uncertainty + (m)	Sample Elevation Uncertainty - (m)	Type	Primary Indicator Type	Secondary Indicator Type
D-AMS 022222	6.65	0.05	0.05	0	5	High Marsh Environment
D-AMS 025776	6.00	0.05	0.05	0	5	High Marsh Environment
D-AMS 022223	5.61	0.05	0.05	0	5	High Marsh Environment
D-AMS 016391	7.71	0.05	0.05	0	5	High Marsh Environment
D-AMS 016392	6.89	0.05	0.05	0	5	High Marsh Environment
D-AMS 022226	6.89	0.05	0.05	0	5	High Marsh Environment
D-AMS 025778	6.00	0.05	0.05	0	5	High Marsh Environment
D-AMS 022227	5.51	0.05	0.05	0	5	High Marsh Environment
D-AMS 022224	8.81	0.05	0.05	0	5	High Marsh Environment
D-AMS 022225	8.35	0.05	0.05	0	5	High Marsh Environment

APPENDIX

Unique sample ID	Supporting Evidence	Sample indicative meaning (m OD)	RSL (m)	RSL 2σ Uncertainty + (m)	RSL 2σ Uncertainty - (m)
D-AMS 022222	Litho- and/or biostratigraphy	(HAT-MHWST)/2	1.06	1.46	1.46
D-AMS 025776	Litho- and/or biostratigraphy	(HAT-MHWST)/2	0.42	1.46	1.46
D-AMS 022223	Litho- and/or biostratigraphy	(HAT-MHWST)/2	0.02	1.46	1.46
D-AMS 016391	Litho- and/or biostratigraphy	(HAT-MHWST)/2	2.12	1.46	1.46
D-AMS 016392	Litho- and/or biostratigraphy	(HAT-MHWST)/2	1.30	1.46	1.46
D-AMS 022226	Litho- and/or biostratigraphy	Uniquely Defined by Author	0.09	1.46	1.46
D-AMS 025778	Litho- and/or biostratigraphy	Uniquely Defined by Author	0.05	1.47	1.47
D-AMS 022227	Litho- and/or biostratigraphy	Uniquely Defined by Author	1.58	3.37	3.37
D-AMS 022224	Litho- and/or biostratigraphy	Uniquely Defined by Author	2.81	1.46	1.46
D-AMS 022225	Litho- and/or biostratigraphy	Uniquely Defined by Author	4.41	3.36	3.36

APPENDIX

Unique Sample ID	Corrected RSL (m)	Corrected RSL Error + (m)	Corrected RSL Error - (m)	Correction Type	Tidal Correction Values (m)	Reject	Why reject?	Notes
D-AMS 022222	1.78	1.46	1.46	1	-0.468	0	n/a	n/a
D-AMS 025776	1.14	1.46	1.46	1	-0.468	0	n/a	n/a
D-AMS 022223	0.87	1.46	1.46	1	-0.596	0	n/a	n/a
D-AMS 016391	2.56	1.46	1.46	1	-0.440	0	n/a	n/a
D-AMS 016392	1.89	1.46	1.46	1	-0.593	0	n/a	n/a
D-AMS 022226	2.02	1.46	1.46	1	-0.469	0	n/a	n/a
D-AMS 025778	1.17	1.47	1.47	1	-0.469	0	n/a	n/a
D-AMS 022227	0.77	3.37	3.37	1	-0.590	0	n/a	n/a
D-AMS 022224	3.61	1.46	1.46	1	-0.450	0	n/a	n/a
D-AMS 022225	3.48	3.36	3.36	1	-0.469	0	n/a	n/a

REFERENCES

Admiralty Tide Tables (2016). Admiralty Tide Tables, 2006, Volume 1, United Kingdom and Ireland including European Channel Ports, United Kingdom Hydrographic Office, London, pp. 465.

Alley, R. B., Clark, P. U., Huybrechts, P., & Joughin, I. (2005). Ice-sheet and sea-level changes. *Science*, *310*(5747), 456-460.

Allison, N., & Austin, W. E. (2003). The potential of ion microprobe analysis in detecting geochemical variations across individual foraminifera tests. *Geochemistry, Geophysics, Geosystems, 4*(2), pp. 9.

Auton, C., Walker, M., & Riding, J. (1998). A signal of marine transgression from the Cumbrian coast during the Late Weichselian. *Geoscience 98 Abstracts*.

Avnaim-Katav, S., Gehrels, W. R., Brown, L. N., Fard, E., & MacDonald, G. M. J. M. M. (2017). Distributions of salt-marsh foraminifera along the coast of SW California, USA: Implications for sea-level reconstructions. *131*, 25-43.

Ballantyne, C. K. (1986). Protalus rampart development and the limits of former glaciers in the vicinity of Baosbheinn, Wester Ross. *Scottish Journal of Geology, 22*(1), 13-25.

Ballantyne, C. K. (2010). Extent and deglacial chronology of the last British–Irish Ice Sheet: implications of exposure dating using cosmogenic isotopes. *Journal of Quaternary Science, 25*(4), 515-534.

Ballantyne, C. K., & Stone, J. O. (2009). Rock-slope failure at Baosbheinn, Wester Ross, NW Scotland: age and interpretation. *Scottish Journal of Geology, 45*(2), 177-181.

Ballantyne, C. K., Stone, J. O., & Fifield, L. K. (2009). Glaciation and deglaciation of the SW Lake District, England: implications of cosmogenic 36 Cl exposure dating. *Proceedings of the Geologists' Association, 120*(2), 139-144.

Balson PS. (2010). Drigg Spit: interpretative report. British Geological Survey Commissioned Report, CR/10/120.

Barber, D., Dyke, A., Hillaire-Marcel, C., Jennings, A., Andrews, J., Kerwin, M., Bilodeau, G., McNeely, R., Southon, J., Morehead, MD. (1999). Forcing of the cold event of 8,200 years ago by catastrophic drainage of Laurentide lakes. *Nature, 400*(6742), 344-348.

Barlow, N. L., Long, A. J., Saher, M. H., Gehrels, W. R., Garnett, M. H., & Scaife, R. G. (2014). Salt-marsh reconstructions of relative sea-level change in the North Atlantic during the last 2000 years. *Quaternary Science Reviews, 99*, 1-16.

Barlow, N. L., Shennan, I., Long, A. J., Gehrels, W. R., Saher, M. H., Woodroffe, S. A., & Hillier, C. (2013). Salt marshes as late Holocene tide gauges. *Global and Planetary Change, 106*, 90-110.

Barnes, B. (1975). Palaeoecological studies of the late Quaternary period in the Northwest Lancashire Lowlands. University of Lancaster.

Barnett, R. L., Garneau, M., & Bernatchez, P. (2016). Salt-marsh sea-level indicators and transfer function development for the Magdalen Islands in the Gulf of St. Lawrence, Canada. *Marine Micropaleontology, 122*, 13-26.

Bennett, K. (1999). Data-handling Methods for Quaternary microfossils. Past and present climate, environment and societal change, from http://chrono.qub.ac.uk/datah/depthage.html.

Bennett, K. D., & Birks, H. J. B. (1990). Postglacial history of alder (*Alnus glutinosa* (L.) Gaertn.) in the British Isles. *Journal of Quaternary Science, 5*(2), 123-133.

Best, L. A. (2016). Late Holocene Relative Sea-Level Change and the Implications for the Groundwater Resource, Humber Estuary, UK. University of York.

Birks, H. (1982). Mid-Flandrian Forest History Of Roudsea Wood National Nature Reserve, Cumbria. *New Phytologist, 90*(2), 339-354.

Birks, H. (1995). Quantitative palaeoenvironmental reconstructions. Statistical modelling of Quaternary science data*. Technical Guide, 5*, 161-254.

Birks, H. J. (1989). Holocene isochrone maps and patterns of tree-spreading in the British Isles. *Journal of Biogeography*, *16*(6), 503-540.

Birks, H. J. B. (1977) *The Flandrian forest history of Scotland: a preliminary synthesis. British Quaternary studies - recent advances.* F. W. Shotton (Ed.), Clarendon Press, Oxford, pp. 119-135.

Björck, S., Bennike, O., Possnert, G., Wohlfarth, B., & Digerfeldt, G. (1998). A high-resolution14C dated sediment sequence from southwest Sweden: age comparisons between different components of the sediment. *Journal of Quaternary Science: Published for the Quaternary Research Association, 13*(1), 85-89.

Blaauw, M. (2010). Methods and code for 'classical'age-modelling of radiocarbon sequences. *quaternary geochronology, 5*(5), 512-518.

Blaauw, M., & Christen, J. A. (2011). Flexible paleoclimate age-depth models using an autoregressive gamma process. *Bayesian analysis, 6*(3), 457-474.

Bowen, D., Phillips, F., McCabe, A., Knutz, P., & Sykes, G. (2002). New data for the last glacial maximum in Great Britain and Ireland. *Quaternary Science Reviews, 21*(1), 89-101.

Bradley, S. L., Milne, G. A., Shennan, I., & Edwards, R. (2011). An improved glacial isostatic adjustment model for the British Isles. *Journal of Quaternary Science, 26*(5), 541-552.

Bradwell, T., Stoker, M. S., Golledge, N. R., Wilson, C. K., Merritt, J. W., Long, D., Everest, J. D., Hestvik, O. B., Stevenson, A. G., Hubbard, A. L., Finlayson, A. G., & Mathers, H. E. (2008). The northern sector of the last British Ice Sheet: maximum extent and demise. *Earth-Science Reviews, 88*(3), 207-226.

Brain, M. J., Kemp, A. C., Hawkes, A. D., Engelhart, S. E., Vane, C. H., Cahill, N., Hill, T. D., Donelly, J. P., & Horton, B. P. (2017). Exploring mechanisms of compaction in salt-marsh sediments using Common Era relative sea-level reconstructions. *167*, 96-111.

Brain, M. J. (2016). Past, present and future perspectives of sediment compaction as a driver of relative sea level and coastal change. *Current Climate Change Reports, 2*(3), 75-85.

Brain, M. J., Kemp, A. C., Horton, B. P., Culver, S. J., Parnell, A. C., & Cahill, N. (2015). Quantifying the contribution of sediment compaction to late Holocene salt-marsh sea-level reconstructions, North Carolina, USA. *Quaternary Research, 83*(1), 41-51.

Brain, M. J., Long, A. J., Petley, D. N., Horton, B. P., & Allison, R. J. (2011). Compression behaviour of minerogenic low energy intertidal sediments. *Sedimentary Geology, 233*(1-4), 28-41.

Brain, M. J., Long, A. J., Woodroffe, S. A., Petley, D. N., Milledge, D. G., & Parnell, A. C. (2012). Modelling the effects of sediment compaction on salt marsh reconstructions of recent sea-level rise. *Earth and Planetary Science Letters, 345*, 180-193.

British Geological Survey (2018) 'Geology of Britain Viewer', available at: http://mapapps.bgs.ac.uk/geologyofbritain/home.html [Accessed:10/05/2018].

Brown, V. H., Evans, D. J., & Evans, I. S. (2011). The glacial geomorphology and surficial geology of the South-West English Lake District. *Journal of Maps*, *7*(1), 221-243.

Brown, V. H., Evans, D. J., Vieli, A., & Evans, I. S. (2013). The Younger Dryas in the English Lake District: reconciling geomorphological evidence with numerical model outputs. *Boreas, 42*(4), 1022-1042.

Callard, S. L., Gehrels, W. R., Morrison, B. V., & Grenfell, H. R. (2011). Suitability of salt-marsh foraminifera as proxy indicators of sea level in Tasmania. *Marine Micropaleontology, 79*(3-4), 121-131.

Carr, S., Holmes, R., van der, Van der Meer, J., & Rose, J. (2006). The Last Glacial Maximum in the North Sea Basin: micromorphological evidence of extensive glaciation. *Journal of Quaternary Science, 21*(2), 131-153.

Cearreta, A., & Murray, J. W. (2000). AMS 14C dating of Holocene estuarine deposits: consequences of high-energy and reworked foraminifera. *The Holocene, 10*(1), 155-159.

Chambers, C. (1978). A Radiocarbon-Dated Pollen Diagram From Valley Bog, On The Moor House National Nature Reserve. *New Phytologist, 80*(1), 273-280.

Charlesworth, J. K. (1927). I.—The Glacial Geology of the Southern Uplands of Scotland, West of Annandale and Upper Clydesdale. *Earth and Environmental Science Transactions of The Royal Society of Edinburgh, 55*(1), 1-23.

Chiverrell, R. (2006). Past and future perspectives upon landscape instability in Cumbria, northwest England. *Regional Environmental Change, 6*(1-2), 101-114.

Clark, C. D., Ely, J. C., Greenwood, S. L., Hughes, A. L., Meehan, R., Barr, I. D., Bateman, M. D., Bradwell, T., Doole, J., Evans, D. J. A., Jordan, C. J., Monteys, X., Pellicer, X. M., & Sheehy, M. (2018). BRITICE Glacial Map, version 2: a map and GIS database of glacial landforms of the last British–Irish Ice Sheet. *Boreas, 47*(1), 11-18.

Clark, C. D. (1999). Glaciodynamic context of subglacial bedform generation and preservation. *Annals of Glaciology, 28*, 23-32.

Clark, C. D., Hughes, A. L., Greenwood, S. L., Jordan, C., & Sejrup, H. P. (2012). Pattern and timing of retreat of the last British-Irish Ice Sheet. *Quaternary Science Reviews, 44*, 112-146.

Coombes, P., Chiverrell, R. C., & Barber, K. E. (2009). A high-resolution pollen and geochemical analysis of late Holocene human impact and vegetation history in southern Cumbria, England. *Journal of Quaternary Science, 24*(3), 224-236.

Davies, B. J. (2008). *British and Fennoscandian Ice-Sheet interactions during the quaternary.* Durham University.

Dawson, S., & Smith, D. (1997). Holocene relative sea-level changes on the margin of a glacio-isostatically uplifted area: an example from northern Caithness, Scotland. *The Holocene, 7*(1), 59-77.

Delaney, C. (2003). The last glacial stage (the Devensian) in northwest England. *North West Geography, 3*(1), 27-37.

Devoy, R. (1982). Analysis of the geological evidence for Holocene sea-level movements in southeast England. *Proceedings of the Geologists' Association, 93*(1), 65-90.

Dixon, E. E. L., Maden, J., Trotter, F. M., Hollingworth, S. E., & Tonks, L. H. (1926). *The geology of the Carlisle, Longtown and Silloth district* (Vol. 11): Printed under the authority of HM Stationery Off.

du Châtelet, É. A., Bout-Roumazeilles, V., Riboulleau, A., & Trentesaux, A. (2009). Sediment (grain size and clay mineralogy) and organic matter quality control on living benthic foraminifera. *Revue de micropaléontologie, 52*(1), 75-84.

Dumayne-Peaty, L., & Barber, K. (1998). Late Holocene vegetational history, human impact and pollen representativity variations in northern Cumbria, England. *Journal of Quaternary Science, 13*(2), 147-164.

Dyer, F., Thomson, J., Croudace, I., Cox, R., & Wadsworth, R. (2002). Records of change in salt marshes: a radiochronological study of three Westerschelde (SW Netherlands) marshes. *Environmental science & technology, 36*(5), 854-861.

Eastwood, T., Hollingworth, S. E., Rose, W. C. C., & Trotter, F. M. (1968). The geology of the country around Cockermouth and Caldbeck. In: Kidson, C., Tooley, M.J. (Eds.), *The Quaternary History of the Irish Sea*. Seel House Press, Liverpool, p. 119-154.

Edwards, R. J. (2006). Mid-to late-Holocene relative sea-level change in southwest Britain and the influence of sediment compaction. *The Holocene, 16*(4), 575-587.

Edwards, R., Gehrels, W. R., Brooks, A., Fyfe, R., Pullen, K., Kuchar, J., & Craven, K. (2017). Resolving discrepancies between field and modelled relative sea-level data: lessons from western Ireland. *Journal of Quaternary Science, 32*(7), 957-975.

Edwards, R., & Horton, B. (2000). Reconstructing relative sea-level change using UK salt-marsh foraminifera. *Marine Geology, 169*(1), 41-56.

Edwards, R., Van De Plassche, O., Gehrels, W., & Wright, A. (2004). Assessing sea-level data from Connecticut, USA, using a foraminiferal transfer function for tide level. *Marine Micropaleontology, 51*(3), 239-255.

Edwards, R. J. (2001). Mid-to late Holocene relative sea-level change in Poole Harbour, southern England. *Journal of Quaternary Science, 16*(3), 221-235.

Elliott, E. G. (2015) *Holocene sea-level change at the Steart Peninsula, Somerset: Development and application of a multi-proxy sea-level transfer function for the Severn Estuary region*. University of the West of England.

Engelhart, S. E., & Horton, B. P. (2012). Holocene sea level database for the Atlantic coast of the United States. *Quaternary Science Reviews, 54*, 12-25.

Engelhart, S. E., Horton, B. P., & Kemp, A. C. (2011). Holocene sea level changes along the United States' Atlantic Coast. *Oceanography*, *24*(2), 70-79.

ESRI, R. (2011). ArcGIS desktop: release 10. *Environmental Systems Research Institute, CA*.

Evans, D. J., Livingstone, S. J., Vieli, A., & Cofaigh, C. Ó. (2009). The palaeoglaciology of the central sector of the British and Irish Ice Sheet: reconciling glacial geomorphology and preliminary ice sheet modelling. *Quaternary Science Reviews, 28*(7), 739-757.

Everest, J. D., Bradwell, T., Fogwill, C. J., & Kubik, P. W. (2006). Cosmogenic ^{10}Be age constraints for the wester ross readvance moraine: insights into British ice-sheet behaviour. *Geografiska Annaler: Series A, Physical Geography, 88*(1), 9-17.

Ezer, T., Haigh, I. D., & Woodworth, P. L. (2015). Nonlinear sea-level trends and long-term variability on Western European Coasts. *Journal of Coastal Research, 32*(4), 744-755.

Faegri, N., & Iverson, J. (1989). *Handbook of pollen analysis*. Wiley, New York.

Finlayson, A., Fabel, D., Bradwell, T., & Sugden, D. (2014). Growth and decay of a marine terminating sector of the last British–Irish Ice Sheet: a geomorphological reconstruction. *Quaternary Science Reviews, 83*, 28-45.

Firth, C., Smith, D., & Cullingford, R. (1993). *Late Devensian and Holocene glacio-isostatic uplift patterns in Scotland.* In: *Quaternary Proceedings*, 3(1), pp. 14.

Firth, C. R., & Haggart, B. A. (1989). Loch Lomond stadial and Flandrian shorelines in the inner Moray Firth area, Scotland. *Journal of Quaternary Science, 4*(1), 37-50.

Fleming, K., Johnston, P., Zwartz, D., Yokoyama, Y., Lambeck, K., & Chappell, J. (1998). Refining the eustatic sea-level curve since the Last Glacial Maximum using far-and intermediate-field sites. *Earth and Planetary Science Letters*, *163*(1-4), 327-342.

Friedman, G. M., & Sanders, J. E. (1978). *Principles of sedimentology*. Wiley, New York.

GB Historical GIS / University of Portsmouth, History of Skinburness Marsh, in Allerdale and Cumberland | Map and description, *A Vision of Britain through Time*. Available at: http://www.visionofbritain.org.uk/place/2587 [Accessed 05/03/2018].

Gehrels, W. R., Belknap, D. F., & Kelley, J. T. (1996). Integrated high-precision analyses of Holocene relative sea-level changes: lessons from the coast of Maine. *Geological Society of America Bulletin, 108*(9), 1073-1088.

Gehrels, R., & Long, A. (2008). Sea level is not level: the case for a new approach to predicting UK sea-level rise. *Geography, 93*(1), 11.

Gehrels, W. R. (1994). Determining relative sea-level change from salt-marsh foraminifera and plant zones on the coast of Maine, USA. *Journal of Coastal Research*, *10*(4), 990-1009.

Gehrels, W. R. (1999). Middle and late Holocene sea-level changes in eastern Maine reconstructed from foraminiferal saltmarsh stratigraphy and AMS ^{14}C dates on basal peat. *Quaternary Research, 52*(3), 350-359.

Gehrels, W. R., Dawson, D. A., Shaw, J., & Marshall, W. A. (2011). Using Holocene relative sea-level data to inform future sea-level predictions: An example from southwest England. *Global and Planetary Change, 78*(3), 116-126.

Gehrels, W.R. (2007). Microfossil Reconstructions. In: Elias, S. (Ed.) *Encyclopedia of Quaternary Science*. Elsevier: Oxford, p. 3015-3024, pp. 3576.

Gehrels, W. R., Marshall, W. A., Gehrels, M. J., Larsen, G., Kirby, J. R., Eiríksson, J., Heinemeier, J., & Shimmield, T. (2006). Rapid sea-level rise in the North Atlantic Ocean since the first half of the nineteenth century. *The Holocene*, *16*(7), 949-965.

Gehrels, W. R., Kirby, J. R., Prokoph, A., Newnham, R. M., Achterberg, E. P., Evans, H., Black, S., & Scott, D. B. (2005). Onset of recent rapid sea-level rise in the western Atlantic Ocean. *Quaternary Science Reviews, 24*(18-19), 2083-2100.

Gehrels, W. R., Milne, G. A., Kirby, J. R., Patterson, R. T., & Belknap, D. F. (2004). Late Holocene sea-level changes and isostatic crustal movements in Atlantic Canada. *Quaternary International*, *120*(1), 79-89.

Gehrels, W. R., Roe, H. M., & Charman, D. J. (2001). Foraminifera, testate amoebae and diatoms as sea-level indicators in UK saltmarshes: a quantitative multiproxy approach. *Journal of Quaternary Science, 16*(3), 201-220.

Gehrels, W. R., & Woodworth, P. L. (2013). When did modern rates of sea-level rise start? *Global and Planetary Change, 100*, 263-277.

Grimm, E. (1991). *Tilia and Tiliagraph*. Illinois State Museum, Springfield, Illinois.

Grimm, E. (2004). *Tilia version 2.0.2*. Illinois State Museum, Springfield, Illinois.

Haggart, B. A. (1989). Variations in the pattern and rate of isostatic uplift indicated by a comparison of Holocene sea-level curves from Scotland. *Journal of Quaternary Science, 4*(1), 67-76.

Hall, G. F., Hill, D. F., Horton, B. P., Engelhart, S. E., & Peltier, W. R. (2013). A high-resolution study of tides in the Delaware Bay: Past conditions and future scenarios. *Geophysical Research Letters*, *40*(2), 338-342.

Hamilton, S., & Shennan, I. (2005). Late Holocene relative sea-level changes and the earthquake deformation cycle around upper Cook Inlet, Alaska. *Quaternary Science Reviews*, *24*(12-13), 1479-1498.

Hammer, Ø., Harper, D., & Ryan, P. (2001). Paleontological statistics software: package for education and data analysis. *Palaeontologia Electronica*, *4*(1), 9.

Hay, C. C., Lau, H. C., Gomez, N., Austermann, J., Powell, E., Mitrovica, J. X., Latychev, K., & Wiens, D.A. (2017). Sea level fingerprints in a region of complex Earth structure: the case of WAIS. *Journal of Climate*, *30*(6), 1881-1892.

Hearty, P. J., O'Leary, M. J., Kaufman, D. S., Page, M. C., & Bright, J. (2004). Amino acid geochronology of individual foraminifer (*Pulleniatina obliquiloculata*) tests, north Queensland margin, Australia: a new approach to correlating and dating Quaternary tropical marine sediment cores. *Paleoceanography, 19*(4), pp. 14.

Heiri, O., Lotter, A. F., & Lemcke, G. (2001). Loss on ignition as a method for estimating organic and carbonate content in sediments: reproducibility and comparability of results. *Journal of paleolimnology, 25*(1), 101-110.

Heyworth, A., & Kidson, C. (1982). Sea-level changes in southwest England and Wales. *Proceedings of the Geologists' Association, 93*(1), 91-111.

Hijma, M. P., & Cohen, K. M. (2010). Timing and magnitude of the sea-level jump preluding the 8200 yr event. *Geology, 38*(3), 275-278.

Hill, T. C., Woodland, W. A., Spencer, C. D., & Marriott, S. B. (2007). Holocene sea-level change in the Severn Estuary, southwest England: a diatom-based sea-level transfer function for macrotidal settings. *The Holocene, 17*(5), 639-648.

Hill, D., Griffiths, S., Peltier, W., Horton, B., & Törnqvist, T. (2011). High-resolution numerical modeling of tides in the western Atlantic, Gulf of Mexico, and Caribbean Sea during the Holocene. *Journal of Geophysical Research: Oceans, 116*(C10).

Hill, J., Collins, G. S., Avdis, A., Kramer, S. C., & Piggott, M. D. (2014). How does multiscale modelling and inclusion of realistic palaeobathymetry affect numerical simulation of the Storegga Slide tsunami? *Ocean Modelling, 83*, 11-25.

Hobbs, N. (1986). Mire morphology and the properties and behaviour of some British and foreign peats. *Quarterly Journal of Engineering Geology and Hydrogeology, 19*(1), 7-80.

Horton, B., Edwards, R., & Lloyd, J. (1999). UK intertidal foraminiferal distributions: implications for sea-level studies. *Marine Micropaleontology, 36*(4), 205-223.

Horton, B., Larcombe, P., Woodroffe, S., Whittaker, J., Wright, M., & Wynn, C. (2003). 2003: Contemporary foraminiferal distributions of the Great Barrier Reef coastline, Australia: implications for sea-level reconstructions, *Marine Geology, 3320*, 1-19.

Horton, B. P., & Edwards, R. J. (2003). Seasonal distributions of foraminifera and their implications for sea-level studies. SEPM (Society for Sedimentary Geology) Special Publication, *75*, 21-30.

Horton, B. P., & Edwards, R. J. (2005). The application of local and regional transfer functions to the reconstruction of Holocene sea levels, north Norfolk, England. *The Holocene, 15*(2), 216-228.

Horton, B. P., & Edwards, R. J. (2006). Quantifying Holocene sea level change using intertidal foraminifera: lessons from the British Isles. Cushman Foundation for Foraminiferal Research, Special Publication, 40, pp. 95.

Horton, B. P., Engelhart, S. E., Hill, D. F., Kemp, A. C., Nikitina, D., Miller, K. G., & Peltier, W. R. (2013). Influence of tidal-range change and sediment compaction on Holocene relative sea-level change in New Jersey, USA. *Journal of Quaternary Science, 28*(4), 403-411.

Horton, B. P., & Shennan, I. (2009). Compaction of Holocene strata and the implications for relative sea-level change on the east coast of England. *Geology, 37*(12), 1083-1086.

Hu, P. (2010). Developing a quality-controlled postglacial sea-level database for coastal Louisiana to assess conflicting hypotheses of Gulf Coast sea-level change. *Tulane University, New Orleans*.

Huddart, D. (1970). Aspects of glacial sedimentation in the Cumberland lowland. University of Reading.

Huddart, D. (1971a). A relative glacial chronology from the tills of the Cumberland lowland. *Proceedings of the Cumberland Geological Society, 3*, 21-32.

Huddart, D. (1971b). Textural distinction of Main Glaciation and Scottish Readvance tills in the Cumberland lowland. *Geological Magazine, 108*(4), 317-324.

Huddart, D. (1991). The glacial history and glacial deposits of the North and West Cumbrian lowlands. In: *Glacial deposits in Great Britain and Ireland.* Balkema, Rotterdam, 151-167.

Huddart, D., & Tooley, M. (1972). *Field Guide to the Cumberland Lowland*. Quaternary Research Association, Cambridge, 119-154.

Huddart, D., Tooley, M.J. & Carter, P.A. (1977). The coasts of north-west England. In: Kidson, C. & Tooley, M.J. (Eds.), *The Quaternary History of the Irish Sea*. Seel House Press, Liverpool, p. 119-154.

Huddart, D. (1994). *The late Quaternary glacigenic sequence: landforms and environments in coastal Cumbria*. In: Boardman, J. & Walden, J. (Eds). *The Quaternary of Cumbria: Field Guide*. Quaternary Research Association, Oxford, p. 59-77.

Huddart, D., & Glasser, N.F. (2002). *Quaternary of Northern England*. Geological Conservation Review Series, No. 25. Joint Nature Conservation Committee, Peterborough, pp. 745.

Hughes, P., & Barber, K. (2004). Contrasting pathways to ombrotrophy in three raised bogs from Ireland and Cumbria, England. *The Holocene, 14*(1), 65-77.

Hughes, P. D., Mauquoy, D., Barber, K., & Langdon, P. G. (2000). Mire-development pathways and palaeoclimatic records from a full Holocene peat archive at Walton Moss, Cumbria, England. *The Holocene, 10*(4), 465-479.

Imbrie, J., & Kipp, N. 1971. A new micropaleontologial method for quantitative paleoclimatology: Application to a Late Pleistocene Caribbean core. *The Late Cenozoic Glacial Ages. Yale Univ. Press, New Haven, 3*, 71-181.

Intergovernmental Panel on Climate Change (IPCC) (2007). Climate Change 2007: Synthesis Report. Contributions of Working Groups I, II and III to the Fourth Assessment Report of the Intergovernmental Panel on Climate Change. IPCC, 996.

Jelgersma, S., De Jong, J., Zagwijn, W. H., & Von Regteren Altena, J. F. (1970). The coastal dunes of the western Netherlands; geology, vegetational history and archeology. In: Kidson, C., Tooley, M.J. (Eds.), *The Quaternary History of the Irish Sea*. Seel House Press, Liverpool, p. 119-154.

Jennings, A., Andrews, J., Pearce, C., Wilson, L., & Ólfasdótttir, S. (2015). Detrital carbonate peaks on the Labrador shelf, a 13–7ka template for freshwater forcing from the Hudson Strait outlet of the Laurentide Ice Sheet into the subpolar gyre. *Quaternary Science Reviews, 107*, 62-80.

Jonasson, K. E., & Patterson, R. T. (1992). Preservation potential of salt marsh foraminifera from the Fraser River delta, British Columbia. *Micropaleontology*, *38*(3), 289-301.

Juggins, S. (2007). *C2: Software for Ecological and Palaeoecological Data Analysis and Visualisation* (User Guide Version 1.5). Newcastle upon Tyne, Newcastle University, pp. 77.

Kaufman, D. S., Polyak, L., Adler, R., Channell, J. E., & Xuan, C. (2008). Dating late Quaternary planktonic foraminifer Neogloboquadrina pachyderma from the Arctic Ocean using amino acid racemization. *Paleoceanography, 23*(3).

Kemp, A. C., Telford, R. J., & Shennan, I. (2015). Transfer functions. *Handbook of Sea-Level Research. Chichester: John Wiley and Sons*, 470-499.

Kemp, A. C., Horton, B. P., Culver, S. J., Corbett, D. R., van de Plassche, O., Gehrels, W. R., Douglas, B. C., & Parnell, A. C. (2009). Timing and magnitude of recent accelerated sea-level rise (North Carolina, United States). *Geology, 37*(11), 1035-1038.

Kemp, A. C., Telford, R. J., Horton, B. P., Anisfeld, S. C., & Sommerfield, C. K. (2013). Reconstructing Holocene sea level using salt-marsh foraminifera and transfer functions: lessons from New Jersey, USA. *Journal of Quaternary Science, 28*(6), 617-629.

Kendall, R. A., Mitrovica, J. X., Milne, G. A., Törnqvist, T. E., & Li, Y. (2008). The sea-level fingerprint of the 8.2 ka climate event. *Geology, 36*(5), 423-426.

Khan, N. S., Vane, C. H., Horton, B. P., Hillier, C., Riding, J. B., & Kendrick, C. P. (2015). The application of $\delta^{13}C$, TOC and C/N geochemistry to reconstruct Holocene relative sea levels and palaeoenvironments in the Thames Estuary, UK. *Journal of Quaternary Science, 30*(5), 417-433.

Kuchar, J., Milne, G., Hubbard, A., Patton, H., Bradley, S., Shennan, I., & Edwards, R. (2012). Evaluation of a numerical model of the British–Irish ice sheet using relative sea-level data: implications for the interpretation of trimline observations. *Journal of Quaternary Science, 27*(6), 597-605.

Lamb, A. L., & Ballantyne, C. K. (1998). Palaeonunataks and the altitude of the last ice sheet in the SW Lake District, England. *Proceedings of the Geologists' Association, 109*(4), 305-316.

Lamb, A. L., Vane, C. H., Wilson, G. P., Rees, J. G., & Moss-Hayes, V. L. (2007). Assessing $\delta^{13}C$ and C/N ratios from organic material in archived cores as Holocene sea level and palaeoenvironmental indicators in the Humber Estuary, UK. *Marine Geology, 244*(1-4), 109-128.

Lambeck, K. (1998). On the choice of timescale in glacial rebound modelling: mantle viscosity estimates and the radiocarbon timescale. *Geophysical Journal International*, *134*(2), 647-651.

Lawrence, T., Long, A. J., Gehrels, W. R., Jackson, L. P., & Smith, D. E. (2016). Relative sea-level data from southwest Scotland constrain meltwater-driven sea-level jumps prior to the 8.2 kyr BP event. *Quaternary science reviews, 151*, 292-308.

Leorri, E., Gehrels, W. R., Horton, B. P., Fatela, F., & Cearreta, A. (2010). Distribution of foraminifera in salt marshes along the Atlantic coast of SW Europe: Tools to reconstruct past sea-level variations. *Quaternary International, 221*(1-2), 104-115.

Li, Y.-X., Törnqvist, T. E., Nevitt, J. M., & Kohl, B. (2012). Synchronizing a sea-level jump, final Lake Agassiz drainage, and abrupt cooling 8200 years ago. *Earth and Planetary Science Letters, 315*, 41-50.

Livingstone, S. J., Cofaigh, C. Ó., & Evans, D. J. (2008). Glacial geomorphology of the central sector of the last British-Irish Ice Sheet. *Journal of Maps, 4*(1), 358-377.

Livingstone, S. J., Evans, D. J., & Cofaigh, C. Ó. (2010). Re-advance of Scottish ice into the Solway Lowlands (Cumbria, UK) during the Main Late Devensian deglaciation. *Quaternary Science Reviews, 29*(19), 2544-2570.

Livingstone, S. J., Evans, D. J., Cofaigh, C. Ó., Davies, B. J., Merritt, J. W., Huddart, D., Mitchell, W. A., Roberts, D. H., & Yorke, L. (2012). Glaciodynamics of the central sector of the last British–Irish Ice Sheet in Northern England. *Earth-Science Reviews, 111*(1), 25-55.

Livingstone, S. J., Ó Cofaigh, C., Evans, D. J., & Palmer, A. (2010). Sedimentary evidence for a major glacial oscillation and proglacial lake formation in the Solway Lowlands (Cumbria, UK) during Late Devensian deglaciation. *Boreas, 39*(3), 505-527.

Lloyd, J. M., Shennan, I., Kirby, J. R., & Rutherford, M. M. (1999). Holocene relative sea-level changes in the inner Solway Firth. *Quaternary International, 60*(1), 83-105.

Lloyd, J. M., Zong, Y., Fish, P., & Innes, J. B. (2013). Holocene and Lateglacial relative sea-level change in north-west England: implications for glacial isostatic adjustment models. *Journal of Quaternary Science, 28*(1), 59-70.

Long, A., Roberts, D., & Dawson, S. (2006). Early Holocene history of the west Greenland Ice Sheet and the GH-8.2 event. *Quaternary Science Reviews, 25*(9-10), 904-922.

Long, A., Scaife, R., & Edwards, R. (1999). Pine pollen in intertidal sediments from Poole Harbour, UK; implications for late-Holocene sediment accretion rates and sea-level rise. *Quaternary International, 55*(1), 3-16.

Long, A., & Tooley, M. (1995). Holocene sea-level and crustal movements in Hampshire and Southeast England, United Kingdom. *Journal of Coastal Research*, Special Issue No. 17, 299-310.

Long, A. J., Plater, A. J., Waller, M. P., & Innes, J. B. (1996). Holocene coastal sedimentation in the Eastern English Channel: new data from the Romney Marsh region, United Kingdom. *Marine Geology, 136*(1), 97-120.

Lowe, J. J., Rasmussen, S. O., Björck, S., Hoek, W. Z., Steffensen, J. P., Walker, M. J., Yu, Z. C. & Intimate Group (2008). Synchronisation of palaeoenvironmental events in the North Atlantic region during the Last Termination: a revised protocol recommended by the INTIMATE group. *Quaternary Science Reviews, 27*(1-2), 6-17.

Lowe, J.J. & Walker, M.J.C. (2015). *Reconstructing Quaternary Environments*. Third Edition, Routledge, Abingdon, pp. 538.

Martin, R. E., Wehmiller, J. F., Harris, M. S., & Liddell, W. D. (1996). Comparative taphonomy of bivalves and foraminifera from Holocene tidal flat sediments, Bahia la Choya, Sonora, Mexico (northern Gulf of California): taphonomic grades and temporal resolution. *Paleobiology, 22*(1), 80-90.

Massey, A. C., Gehrels, W. R., Charman, D. J., Milne, G. A., Peltier, W. R., Lambeck, K., & Selby, K. A. (2008). Relative sea-level change and postglacial isostatic adjustment along the coast of south Devon, United Kingdom. *Journal of Quaternary Science, 23*(5), 415-433.

Massey, A. C., Paul, M. A., Gehrels, W. R., & Charman, D. J. (2006). Autocompaction in Holocene coastal back-barrier sediments from south Devon, southwest England, UK. *Marine Geology, 226*(3-4), 225-241.

Massey, A. C., & Taylor, G. K. (2007). Coastal evolution in south-west England, United Kingdom: An enhanced reconstruction using geophysical surveys. *Marine Geology, 245*(1), 123-140.

McCarthy, M. R. (1995). Archaeological and environmental evidence for the Roman impact on vegetation near Carlisle, Cumbria. *The Holocene, 5*(4), 491-495.

McMillan, A., Merritt, J., Auton, C., & Golledge, N. (2011). *The Quaternary geology of the Solway*. British Geological Survey, pp. 77.

Merritt, J., & Auton, C. (2000). An outline of the lithostratigraphy and depositional history of Quaternary deposits in the Sellafield district, west Cumbria. Paper presented at the Proceedings of the Yorkshire Geological and Polytechnic Society.

Meteorological (Met) Office (2018). https://www.metoffice.gov.uk/ [Accessed:10/08/2018].

Mills, H., Kirby, J., Holgate, S., & Plater, A. (2013). The distribution of contemporary saltmarsh foraminifera in a macrotidal estuary: an assessment of their viability for sea-level studies. *Journal of Ecosystem and Ecography, 3*, 1-16.

Mitrovica, J. X., & Milne, G. A. (2003). On post-glacial sea level: I. General theory. *Geophysical Journal International, 154*(2), 253-267.

Moore, P. D., Webb, J. A., & Collison, M. E. (1991). *Pollen analysis*. Blackwell scientific publications, London, pp. 216.

Murray, J. (1971). *An Atlas of British Recent Foraminiferids*. American Elsevier, New York, pp. 244.

Murray, J. W. (2000). Revised taxonomy, an atlas of British Recent foraminiferids. *Journal of Micropalaeontology, 19*(1), 44-44.

Murray, J. W., & Alve, E. (1999). Natural dissolution of modern shallow water benthic foraminifera: taphonomic effects on the palaeoecological record. *Palaeogeography, Palaeoclimatology, Palaeoecology, 146*(1-4), 195-209.

Muto, T., & Steel, R. J. (1997). Principles of regression and transgression; the nature of the interplay between accommodation and sediment supply. *Journal of Sedimentary Research, 67*(6), 994-1000.

National Tidal and Sea Level Facility (NTSLF) (2018). This study uses data from the National Tidal and Sea Level Facilities (NTSLF), provided by the British Oceanographic Data Centre. https://www.ntslf.org/data [Accessed 05/10/2018].

Nilsson, M., Klarqvist, M., Bohlin, E., & Possnert, G. (2001). Variation in 14C age of macrofossils and different fractions of minute peat samples dated by AMS. *The Holocene, 11*(5), 579-586.

Oldfield, F. (1960a). Late Quaternary changes in climate, vegetation and sea-level in Lowland Lonsdale. *Transactions and Papers (Institute of British Geographers), 28*, 99-117.

Oldfield, F. (1960b). Studies In The Post-Glacial History Of British Vegetation: Lowland Lonsdale. *New Phytologist, 59*(2), 192-217.

Oldfield, F., & Statham, D. (1963). Pollen-Analytical Data From Urswicktarn And Ellerside Moss, North Lancashire. *New Phytologist, 62*(1), 53-66.

Orme, L. C., Reinhardt, L., Jones, R. T., Charman, D. J., Croudace, I., Dawson, A., Ellis, M., & Barkwith, A. (2016). Investigating the maximum resolution of µXRF core scanners: A 1800 year storminess reconstruction from the Outer Hebrides, Scotland, UK. *The Holocene, 26*(2), 235-247.

Peltier, W., Shennan, I., Drummond, R., & Horton, B. (2002). On the postglacial isostatic adjustment of the British Isles and the shallow viscoelastic structure of the Earth. *Geophysical Journal International, 148*(3), 443-475.

Peltier, W. R. (2005). On the hemispheric origins of meltwater pulse 1a. *Quaternary Science Reviews*, *24*(14-15), 1655-1671.

Peltier, W. (2002). On eustatic sea level history: Last Glacial Maximum to Holocene. *Quaternary Science Reviews*, *21*(1-3), 377-396.

Peltier, W. (1998). Postglacial variations in the level of the sea: Implications for climate dynamics and solid-earth geophysics. *Reviews of Geophysics, 36*(4), 603-689.

Pennington, W. (1964). Pollen analyses from the deposits of six upland tarns in the Lake District. *Phil. Trans. R. Soc. Lond. B, 248*(746), 205-244.

Piggott, M., Gorman, G., Pain, C., Allison, P., Candy, A., Martin, B., & Wells, M. R. (2008). A new computational framework for multi-scale ocean modelling based on adapting unstructured meshes. *International Journal for Numerical Methods in Fluids, 56*(8), 1003-1015.

Plater, A., Horton, B., Haworth, E., Appleby, P., Zong, Y., Wright, M. R., & Rutherford, M. M. (2000). Holocene tidal levels and sedimentation rates using a diatom-based palaeoenvironmental reconstruction: the Tees estuary, northeastern England. *The Holocene, 10*(4), 441-452.

Preuss, H. (1979). *Progress in computer evaluation of sea level data within the IGCP Project no. 61.* Paper presented at the Proceedings of the 1978 international symposium of coastal evolution in the Quaternary, Sao Paulo, Brazil.

Ramsey, C. B. (2009). Bayesian analysis of radiocarbon dates. *Radiocarbon, 51*(1), 337-360.

Reimer, P.J., Baillie, M.G.L., Bard, E., Bayliss, A., Beck, J.W., Bertrand, C.J.H., Blackwell, P.G., Buck, C.E., Burr, G.S., Cutler, K.B., Damon, P.E., Edwards, R.L., Fairbanks, R.G., Friedrich, M., Guilderson, T.P., Hogg, A.G., Hughen, K.A., Kromer, B., McCormac, G., Manning, S., Ramsey, C.B., Reimer, R.W., Remmele, S., Southon, J.R., Stuiver, M., Talamo, S., Taylor, F.W., van der Plicht, J., & Weyhenmeyer, C.E. (2004). IntCal04 terrestrial radiocarbon age calibration, 0-26 cal kyr BP. *Radiocarbon*, *46*(3), 1029-1058.

Reimer, P. J., Bard, E., Bayliss, A., Beck, J. W., Blackwell, P. G., Ramsey, C. B., Buck, C. E., Cheng, H., Edwards, R. L., Friedrich, M., Grootes, P. M., Guilderson, T. P., Haflidason, H., Hajdas, I., Hatté, C., Heaton, T. J., Hoffmann, D. L., Hogg, A. G., Hughen, K. A., Kaiser, K. F., Kromer, B., Manning,, S. W., Niu, M., Reimer, R. W., Richards, D. A., Scott, E. M., Southon, J. R., Staff, R. A., Turney, C. S. M., & van der Plicht, J. (2013). IntCal13 and Marine13 radiocarbon age calibration curves 0–50,000 years cal BP. *Radiocarbon, 55*(4), 1869-1887.

Robinson, M., & Ballantyne, C. K. (1979). Evidence for a glacial readvance pre-dating the Loch Lomond Advance in Wester Ross. *Scottish Journal of Geology, 15*(4), 271-277.

Rovere, A., Stocchi, P., & Vacchi, M. (2016). Eustatic and relative sea level changes. *Current Climate Change Reports*, *2*(4), 221-231.

Rowell, T., & Turner, J. (1985). Litho-, humic-and pollen stratigraphy at Quick Moss, Northumberland. *The Journal of Ecology*, *73*(1), 11-25.

Santisteban, J. I., Mediavilla, R., Lopez-Pamo, E., Dabrio, C. J., Zapata, M. B. R., García, M. J. G., Castaño, S., & Martínez-Alfaro, P. (2004). Loss on ignition: a qualitative or quantitative method for organic matter and carbonate mineral content in sediments? *Journal of Paleolimnology, 32*(3), 287-299.

Schlager, W. (1993). Accommodation and supply—a dual control on stratigraphic sequences. *Sedimentary Geology, 86*(1-2), 111-136.

Scott, D. B. (1976). Brackish-water foraminifera from southern California and description of Polysaccammina ipohalina n. gen., n. sp. *The Journal of Foraminiferal Research, 6*(4), 312-321.

Scott, D.B., & Medioli, F. S. (1980) Quantitative studies of marsh foraminifera distribution in Nova Scotia: implications for sea-level studies, *Journal of Foraminiferal Research*, Special Publication 17, 1-58.

Scott, D. B., Medioli, F. S., & Schafer, C. T. (2001). Monitoring in coastal environments using foraminifera and thecamoebian indicators. Cambridge University Press, London, pp. 175.

Selby, K. (1997). Late Devensian and Holocene relative sea level changes on the Isle of Skye, Scotland. Coventry University.

Selby, K. A., & Smith, D. E. (2007). Late Devensian and Holocene relative sea-level changes on the Isle of Skye, Scotland, UK. *Journal of Quaternary Science, 22*(2), 119-139.

Selby, K. A., & Smith, D. E. (2016). Holocene relative sea-level change on the Isle of Skye, inner hebrides, Scotland. *Scottish Geographical Journal, 132*(1), 42-65.

Shennan, I. (1982). Interpretation of Flandrian sea-level data from the Fenland, England. *Proceedings of the Geologists' Association, 93*(1), 53-63.

Shennan, I., Bradley, S., Milne, G., Brooks, A., Bassett, S., & Hamilton, S. (2006). Relative sea-level changes, glacial isostatic modelling and ice-sheet reconstructions from the British Isles since the Last Glacial Maximum. *Journal of Quaternary Science, 21*(6), 585-599.

Shennan, I., Coulthard, T., Flather, R., Horton, B., Macklin, M., Rees, J., & Wright, M. (2003). Integration of shelf evolution and river basin models to simulate Holocene sediment dynamics of the Humber Estuary during periods of sea-level change and variations in catchment sediment supply. *314*, 737-754.

Shennan, I. (1986). Flandrian sea-level changes in the Fenland. II: Tendencies of sea-level movement, altitudinal changes, and local and regional factors. *Journal of Quaternary Science, 1*(2), 155-179.

Shennan, I., Bradley, S., Milne, G., Brooks, A., Bassett, S., & Hamilton, S. (2006). Relative sea-level changes, glacial isostatic modelling and ice-sheet reconstructions from the British Isles since the Last Glacial Maximum. *Journal of Quaternary Science, 21*(6), 585-599.

Shennan, I., Bradley, S. L., & Edwards, R. (2018). Relative sea-level changes and crustal movements in Britain and Ireland since the Last Glacial Maximum. *Quaternary Science Reviews, 188*, 143-159.

Shennan, I., Hamilton, S., Hillier, C., & Woodroffe, S. (2005). A 16000-year record of near-field relative sea-level changes, northwest Scotland, United Kingdom. *Quaternary International, 133*, 95-106.

Shennan, I., & Horton, B. (2002). Holocene land-and sea-level changes in Great Britain. *Journal of Quaternary science, 17*(5-6), 511-526.

Shennan, I., Innes, J. B., Long, A. J., & Zong, Y. (1994). Late Devensian and Holocene relative sealevel changes at Loch nan Eala, near Arisaig, northwest Scotland. *Journal of Quaternary Science, 9*(3), 261-283.

Shennan, I., Lambeck, K., Flather, R., Horton, B., McArthur, J., Innes, J., Lloyd, J., Rutherford, M., & Wingfield, R. (2000). Modelling western North Sea palaeogeographies and tidal changes during the Holocene. *Geological Society, London, Special Publications, 166*(1), 299-319.

Shennan, I., Long, A. J., & Horton, B. P. (2015). *Handbook of sea-level research*. John Wiley & Sons, Chicester, pp. 600.

Shennan, I., Milne, G., & Bradley, S. (2012). Late Holocene vertical land motion and relative sea-level changes: lessons from the British Isles. *Journal of Quaternary Science, 27*(1), 64-70.

Shennan, I., Peltier, W. R., Drummond, R., & Horton, B. (2002). Global to local scale parameters determining relative sea-level changes and the post-glacial isostatic adjustment of Great Britain. *Quaternary Science Reviews, 21*(1-3), 397-408.

Shennan, I., & Woodworth, P. (1992). A comparison of late Holocene and twentieth-century sea-level trends from the UK and North Sea region. *Geophysical Journal International, 109*(1), 96-105.

Sissons, J. (1966). Relative sea-level changes between 10,300 and 8,300 BP in part of the Carse of Stirling. *Transactions of the Institute of British Geographers*, *39*, 19-29.

Sissons, J. (1967). Glacial stages and radiocarbon dates in Scotland. *Scottish Journal of Geology, 3*(3), 375-381.

Sissons, J. (1983). *Shorelines and isostasy in Scotland Shorelines and isostasy (Vol. 16)*. Academic Press London, pp. 209-225.

Sissons, J., Smith, D., & Cullingford, R. (1966). Late-glacial and post-glacial shorelines in south-east Scotland. *Transactions of the Institute of British Geographers*, *39*, 9-18.

Smith, D., Harrison, S., & Jordan, J. (2013). Sea level rise and submarine mass failures on open continental margins. *Quaternary Science Reviews, 82*, 93-103.

Smith, A. (1959). The Mires Of South Western Westmorland: Stratigraphy And Pollen Analysis. *New Phytologist, 58*(2), 105-127.

Smith, D., Hunt, N., Firth, C., Jordan, J., Fretwell, P., Harman, M., Murdy, J., Orford, J. D. & Burnside, N. G. (2012). Patterns of Holocene relative sea level change in the North of Britain and Ireland. *Quaternary Science Reviews, 54*, 58-76.

Smith, D., Wells, J., Mighall, T., Cullingford, R., Holloway, L., Dawson, S., & Brooks, C. L. (2002). Holocene relative sea levels and coastal changes in the lower Cree valley and estuary, SW Scotland, UK. *Earth and Environmental Science Transactions of The Royal Society of Edinburgh, 93*(4), 301-331.

Smith, D. E., Cullingford, R. A., & Firth, C. R. (2000). Patterns of isostatic land uplift during the Holocene: evidence from mainland Scotland. *The Holocene, 10*(4), 489-501.

Solway Coast AONB, 2010. *Landscape and Seascape Character Assessment*. Edinburgh, pp. 191.

Stéphan, P., Goslin, J., Pailler, Y., Manceau, R., Suanez, S., Vliet-Lanoë, V., Hénaff, F., & Delacourt, C. (2015). Holocene salt-marsh sedimentary infilling and relative sea-level changes in West Brittany (France) using foraminifera-based transfer functions. *Boreas, 44*(1), 153-177.

ter Braak, C. J. (2014). History of canonical correspondence analysis. *Visualization and verbalization of Data*. Chapman and Hall/CRC, London, p. 61-75.

ter Braak, C. J., & Smilauer, P. (2002). CANOCO reference manual and CanoDraw for Windows user's guide: software for canonical community ordination (Version 4.5), www.canoco.com.

Tipping, R. (1995). Holocene evolution of a lowland Scottish landscape: Kirkpatrick Fleming. Part I, peat-and pollen-stratigraphic evidence for raised moss development and climatic change. *The Holocene, 5*(1), 69-81.

Tooley, M. (1974). Sea-level changes during the last 9000 years in north-west England. *Geographical Journal*, *140*, 18-42.

Tooley, M. (1976). Flandrian sea-level changes in west Lancashire and their implications for the 'Hillhouse Coastline'. *Geological Journal, 11*(2), 137-152.

Tooley, M. (1985). Sea-level changes and coastal morphology in north-west England. *The geomorphology of North-west England*. Manchester University Press, Manchester, p. 94-121.

Tooley, M. J. (1987). Quaternary history. In: Robinson, N. A. and Pringle, A. W. (eds), *Morecambe Bay: an Assessment of Present Ecological Knowledge*. Morecambe Bay Study Group in conjunction with Centre for North West Regional Studies, University of Lancaster, Lancaster, p. 25-50.

Tooley, M. J. (1978). Sea-level changes: north-west England during the Flandrian Stage. Oxford University Press, Oxford, pp. 232.

Törnqvist, T. E., De Jong, A. F., Oosterbaan, W. A., & Van Der Borg, K. J. R. (1992). Accurate dating of organic deposits by AMS 14 C measurement of macrofossils. *34*(3), 566-577.

Trotter, F. (1922). *Report from the Cumberland district*. Summary of Progress of the Geological Survey of Great Britain for 1921, p. 46-48.

Trotter, F. (1923). *Report from the Cumberland district*. Summary of Progress of the Geological Survey of Great Britain for 1922, p. 61-63.

Trotter, F., & Hollingworth, S. (1932). The glacial sequence in the North of England. *Geological Magazine,* 69(8), 374-380.

Trotter, F. M. (1929). The glaciation of eastern Edenside, the Alston block, and the Carlisle plain. *Quarterly Journal of the Geological Society, 85*(1-4), 549-612.

Tröels-Smith, J. (1955). Karakterisaring af Løse jordarter. *Danmarks Geologiska Undersoegelsa IV Reakke Bd,* 3, 1-73.

Tsompanoglou, K., Croudace, I. W., Birch, H., & Collins, M. (2011). Geochemical and radiochronological evidence of North Sea storm surges in salt marsh cores from The Wash embayment (UK). *The Holocene, 21*(2), 225-236.

Turner, J. (1979). The environment of northeast England during Roman times as shown by pollen analysis. *Journal of Archaeological Science, 6*(3), 285-290.

Turney, C. S., & Brown, H. (2007). Catastrophic early Holocene sea level rise, human migration and the Neolithic transition in Europe. *Quaternary Science Reviews, 26*(17-18), 2036-2041.

Törnqvist, T. E., & Hijma, M. P. (2012). Links between early Holocene ice-sheet decay, sea-level rise and abrupt climate change. *Nature Geoscience, 5*(9), 601.

Törnqvist, T. E., Wallace, D. J., Storms, J. E., Wallinga, J., Van Dam, R. L., Blaauw, M., Derksen, M. S., Klerks, C. J., Meijneken, C., & Snijders, E. M. (2008). Mississippi Delta subsidence primarily caused by compaction of Holocene strata. *Nature Geoscience, 1*(3), 173.

Van de Plassche, O. (2013). *Sea-level Research: a Manual for the Collection and Evaluation of Data: a Manual for the Collection and Evaluation of Data*: Springer.

Wacker, L., Lippold, J., Molnár, M., & Schulz, H. (2013). Towards radiocarbon dating of single foraminifera with a gas ion source. *Nuclear Instruments and Methods in Physics Research Section B: Beam Interactions with Materials and Atoms, 294*, 307-310.

Walker, D. (1966). The Late Quaternary history of the Cumberland lowland. *Philosophical Transactions of the Royal Society of London B: Biological Sciences, 251*(770), 1-210.

Walker, M. (2004). A Lateglacial pollen record from Hallsenna Moor, near Seascale, Cumbria, NW England, with evidence for arid conditions during the Loch Lomond (Younger Dryas) Stadial and early Holocene. *Proceedings of the Yorkshire Geological Society, 55*(1), 33-42.

Walker, M., Johnsen, S., Rasmussen, S. O., Popp, T., Steffensen, J. P., Gibbard, P., Hoek, W., Lowe, J., Andrews, J., Björck, S., & Cwynar, L. C. (2009). Formal definition and dating of the GSSP (Global Stratotype Section and Point) for the base of the Holocene using the Greenland NGRIP ice core, and selected auxiliary records. *Journal of Quaternary Science, 24*(1), 3-17.

Waller, M. P., & Long, A. J. (2003). Holocene coastal evolution and sea-level change on the southern coast of England: a review. *Journal of Quaternary Science, 18*(3-4), 351-359.

Wells, J. (1997). Holocene RSL changes in Solway Firth, Scotland. Unpublished Ph.D. Thesis. University of Coventry.

Wentworth, C. K. (1922). A scale of grade and class terms for clastic sediments. *The Journal of Geology, 30*(5), 377-392.

Wilson, L. J., Austin, W. E., & Jansen, E. (2002). The last British Ice Sheet: growth, maximum extent and deglaciation. *Polar Research, 21*(2), 243-250.

Wilson, P. (2002). Morphology and significance of some Loch Lomond Stadial moraines in the south-central Lake District, England. *Proceedings of the Geologists' Association, 113*(1), 9-21.

Wilson, P. (2004). Description and implications of valley moraines in upper Eskdale Lake District. *Proceedings of the Geologists' Association, 115*(1), 55-61.

Wilson, P., & Clark, R. (1999). Further glacier and snowbed sites of inferred Loch Lomond Stadial age in the northern Lake District, England. *Proceedings of the Geologists' Association, 110*(4), 321-331.

Wimble, G., Wells, C. E., & Hodgkinson, D. (2000). Human impact on mid-and late Holocene vegetation in south Cumbria, UK. *Vegetation History and Archaeobotany, 9*(1), 17-30.

Woodworth, P., Teferle, F. N., Bingley, R., Shennan, I., & Williams, S. (2009). Trends in UK mean sea level revisited. *Geophysical Journal International, 176*(1), 19-30.

Woodworth, P., Tsimplis, M., Flather, R., & Shennan, I. (1999). A review of the trends observed in British Isles mean sea level data measured by tide gauges. *Geophysical Journal International, 136*(3), 651-670.

Yeloff, D., & Mauquoy, D. (2006). The influence of vegetation composition on peat humification: implications for palaeoclimatic studies. *Boreas, 35*(4), 662-673.

Yu, S. Y., Berglund, B. r. E., Sandgren, P., & Lambeck, K. (2007). Evidence for a rapid sea-level rise 7600 yr ago. *Geology, 35*(10), 891-894.

Zong, Y. (1998). Diatom records and sedimentary responses to sea-level change during the last 8000 years in Roudsea Wood, northwest England. *The Holocene, 8*(2), 219-228.

Zong, Y., & Tooley, M. J. (1996). Holocene sea-level changes and crustal movements in Morecambe Bay, northwest England. *Journal of Quaternary Science, 11*(1), 43-58.